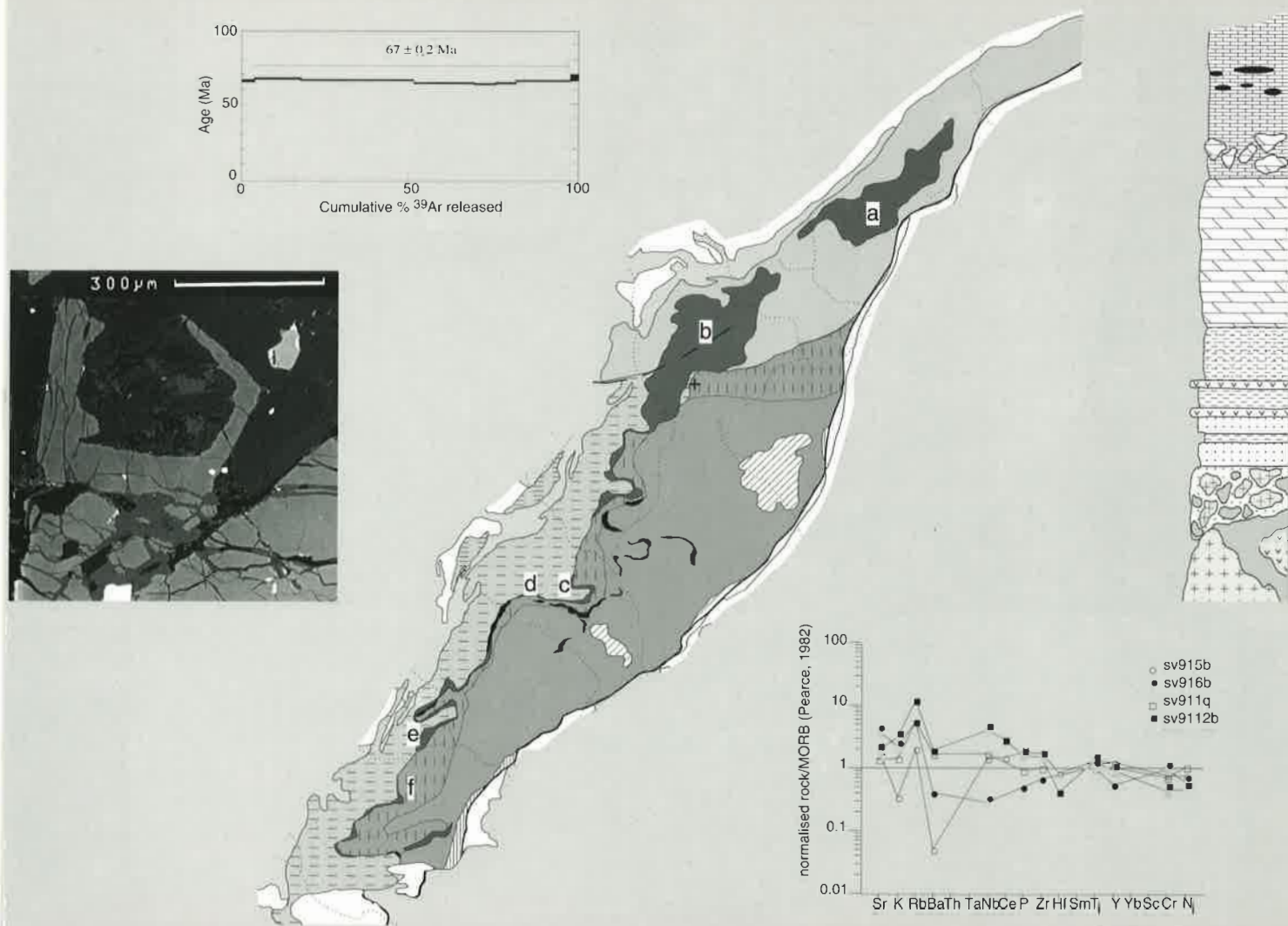


Geology , Geochemistry and Geochronology of the inner central Sesia Zone (Western Alps - Italy)

by Guido Venturini



Mémoires de Géologie (Lausanne)

Section des Sciences de la Terre

Université de Lausanne

BFSH-2, 1015 Lausanne, Suisse



This work is licensed under a Creative Commons
Attribution 4.0 International License
<http://creativecommons.org/licenses/by-nc-nd/4.0/>

25

Memoires de Géologie (Lausanne)

EDITEUR

Jean Guex

Institut de Géologie et Paléontologie
BFSH-2 Université de Lausanne
CH-1015 Lausanne, SUISSE

COMITE EDITORIAL

Clark Blake

U.S. Geological Survey
345 Middlefield Road
94025 Menlo Park, California, U.S.A.

Francis Hirsch

Geological Survey of Israel
30 Malkhe Israel Street
95501 Jerusalem, ISRAEL

Gilles S. Odin

Laboratoire de Géochronologie et Sédimentologie
Université P. et M. Curie, 4 P. Jussieu
75252 Paris Cedex 05, FRANCE

Jean Chaline

Centre des Sciences de la Terre
Université de Bourgogne, 6 bvd. Gabriel
21000 Dijon, FRANCE

Alan R. Lord

Department of Earth Science
University College, Gower Street
WC1E 6BT London, U.K.

José Sandoval

Dpto. Estratigrafía y Paleontología
Universidad de Granada
18002 Granada, ESPAGNE

Jim T.E. Channell

Department of Geology
University of Florida
Gainesville, FL 32611-2036, U.S.A.

Jean Marcoux

Géologie Université de Paris VII et IPGP
Tour 225/24, 2 P. Jussieu
75251 Paris Cedex 05, FRANCE

Rudolph Trümpy

Geologisches Institut, ETH-zentrum
Sonneggstrasse 5
CH-8092 Zürich, SUISSE

Giorgio Martinotti

Dipartimento di Scienze della Terra
Università di Torino, Via Valperga Caluso 37
10125 Torino, ITALIE

Mémoires de Géologie (Lausanne)

Section des Sciences de la Terre
Institut de Géologie et paléontologie
Université de Lausanne
BFSH-2, CH 1015 Lausanne

VENTURINI, Guido

Geology, Geochemistry and Geochronology of the inner central Sesia Zone (Western Alps, Italy)

Mém. Géol. (Lausanne), n°25, 1995, 148 p., 57 fig., 13 pl.

Dépôt légal: 4ème trimestre 1995

ISSN: 1015-3578

Imprimeur: Officine Grafiche Editoriali Zeppegno, Torino, Italie

Cover figure

Computer graphic by Guido Venturini

**Geology, Geochemistry and Geochronology
of the inner central Sesia Zone
(Western Alps, Italy)**

Guido Venturini

Mémoires de Géologie (Lausanne) No. 25, 1995

Thèse de doctorat
présentée à la Faculté des Sciences
de l'Université de Lausanne

par **Guido Venturini**

Jury de thèse:

Johannes C. HUNZIKER, Lausanne (Directeur)
Henri JORIS (Président, Université de Lausanne)
Giorgio V. DAL PIAZ, Padova - Italie
Giorgio MARTINOTTI, Torino - Italie
Henri MASSON, Lausanne - Suisse
Albrecht STECK, Lausanne - Suisse

Author's present address:
Via Garibaldi 5, 10122, Torino, ITALY

*Le Alpi, si sa,
sono un muro
di sassi.....*

Francesco Guccini
(Emilia)

Table of Contents

Abstract	1
Resumé	1
Riassunto	2
Foreword	4

- Chapter 1 -

General Overview	5
1.1. Introduction.....	5
1.2. The Austroalpine System.....	7
1.3. The western Austroalpine System	7
1.3.1. The Dent Blanche System	7
1.3.1a The Dent Blanche Nappe	7
Lower element	9
<i>The polycyclic basement</i>	9
<i>The monometamorphic cover sequences</i>	9
Upper tectonic element	9
<i>The pre-Alpine high grade basement</i>	9
1.3.1b The Mont Mary Klippe	9
Lower Unit	9
<i>The polycyclic basement</i>	9
Intermediate unit	11
<i>The pre-Alpine high grade basement</i>	11
Upper unit	11
<i>The monometamorphic cover sequences</i>	11
<i>The polycyclic basement</i>	11
1.3.1c The etiol-Levaz Slice (lower element).....	11
<i>The polycyclic basement</i>	11
1.3.1d The Pillonet Klippe (lower element).....	11
<i>The polycyclic basement</i>	11
The monometamorphic cover sequences	11
1.3.1e The Grun Slice (lower element).....	11
<i>The polycyclic basement</i>	11
<i>The monometamorphic cover sequences</i>	12
1.3.1f The Mont Emilius Klippe (lower element)	12
<i>The polycyclic basement</i>	12
1.3.1g The Glacier-Rafray Klippe (lower element)	12
<i>The polycyclic basement</i>	12
1.3.1h The Tour Ponton Klippe (lower element)	12
<i>The polycyclic basement</i>	13
1.3.1i The Santanel Klippe (lower element)	13
<i>The polycyclic basement</i>	13
1.3.2. The Sesia Zone	13
1.3.2a The lower element.....	13
<i>The polycyclic basement complex</i>	13
Internal unit	15
Intermediate unit	15

	External unit	15
	<i>The monometamorphic cover complex</i>	17
	The Bonze unit	17
	The Scalaro unit.....	17
1.3.2b	The upper element.....	17
	<i>The pre-Alpine high grade basement complex</i>	17
1.3.3.	Structural outline of the Central Sesia Zone.....	19

- Chapter 2 -

Field and petrographic investigations	21	
2.1. Introduction.....	21	
2.2. Geological mapping and petrography.....	21	
2.2.1. The mapped units.....	21	
2.2.2. Area location.....	23	
2.3. Lithology.....	23	
2.3.1. The polycyclic basement	23	
2.3.1a Internal unit	23	
	Eclogitic Micaschists (passing locally to Micaceous Gneisses).....	23
	Quartz-micaschists with pre-Alpine high grade relics.....	23
	sylvery micaschists with Chloritoid porphyroblasts	25
	Metagranitoids with relics of magmatic texture	25
	Jadeite-poikiloblast orthogneisses	25
	Leucocratic orthogneisses	26
	Eclogitic basic bodies	26
	Impure marbles	26
2.3.2b Intermediate unit	26	
	Albitic gneisses and quartz-micaschists with relics of the high pressure paragenesis	26
	Micaschists with porphyroblast of chloritoid.....	26
	Albite-epidote orthogneisses.....	26
	Metagranitoids with relics of the magmatic textures	27
2.3.1c External unit	28	
	Albitic gneisses	28
	Grn-Ab gneisses and garnet-quartz micaschists	28
	Qtz-micaschists with pre-Alpine relics	28
	Albite-bearing metagranitoids with relics of magmatic textures	28
2.3.2. Monometamorphic covers sequences.....	28	
	Glucophane-eclogites	29
	Quartz-rich metasediments closely related to the glaucophane-eclogites	29
	Blastomylonitic metagabbros.....	29
	Carbonatic rocks.....	30
	Albitic gneisses, quartzites and impure quartzites	32
	Albitic gneisses containing centimeter to meter blocks and/or boudins of epidote-rich metabasites and acid rocks.....	32
2.3.3. Representative Areas	32	
2.3.3a Introduction	32	
2.3.3a Summary of structural data	32	
2.3.3b The Scalaro valley.....	34	

2.3.3c	The Cima di Bonze area	37
2.3.3d	The Succinto valley	37
2.3.3e	The Croix Courma region	37
2.3.3f	The Mombarone lake region	37
2.3.4.	The Pre-Alpine High Grade basement complex - Fert Valley region	39

- Chapter 3 -

Whole rock geochemistry	43
3.1. General Remarks	43
3.2 Chemical composition of micaschists and gneisses	43
3.2.1. Introduction	43
3.1.2. Choice of samples.....	43
3.2.3. Mobility diagrams.....	43
3.2.3. Discriminative diagrams	47
3.2.4. Interpretation	49
3.3. Chemical composition of metagranitoids and orthogneisses.....	49
3.3.1. Introduction	49
3.3.2. Choice of samples.....	50
3.3.3. Mobility diagrams.....	50
3.3.4. Discriminative diagrams	51
3.3.5. Interpretation	55
3.4. Chemical composition of basic rocks	55
3.4.1. Introduction	55
3.4.2. Choice of samples.....	57
3.4.3. Mobility diagrams.....	57
3.4.4. Discriminative diagrams of the mafic rocks.....	57
3.4.5. Discriminative diagrams for basalts	64
3.4.6. The metabasalts of the monometamorphic cover sequences.....	66
3.4.7. The Mg-rich metagabbros related to the monometamorphic cover sequences	71
3.5. The origin of the <i>Gneiss Pipernoides</i> on the basis of the geochemical analyses	72

- Chapter 4-

Mineral chemistry, temperature/pressure estimations and stable isotope investigations	73
4.1 Introduction.....	73
4.2. General remarks	73
4.3. White micas	74
4.4 Amphiboles	78
4.4.1 Calcic amphiboles.....	80
4.4.2 Alkali amphiboles.....	80
4.4.3 Sodic calcic amphiboles	81
4.5. Garnets	83
4.6. Clinopyroxenes	85
4.7. Pressure and temperature estimations.....	88
4.7.1. Introduction	88
4.7.2. Garnet-pyroxene thermobarometry	90
4.7.3. Garnet-amphibole thermometry	91

4.7.4.	Formation conditions for the prograde actinolite	92
4.8.	Oxygen isotope geochemistry	93
4.8.1.	Introduction of techniques	94
4.8.2.	Results	94
4.8.3.	Discussion.....	94
4.9.	Hydrogen isotope geochemistry	95
4.9.1.	Introduction to techniques	96
4.9.2.	Results.	96
4.9.3.	Discussion.....	96

- Chapter 5 -

⁴⁰Ar/³⁹Ar geochronological investigations.....	99
5.1. Introduction.....	99
5.2. Analytical methods	99
5.2.1. Introduction of techniques	99
5.2.2. Sample preparation	100
5.2.3. Experimental procedure.....	100
5.2.4. Presentation of the results.....	102
5.3. ⁴⁰ Ar/ ³⁹ Ar data of phengites	102
5.3.1. Choice of the samples.....	102
Ages younger than 50 ma	105
50-60 Ma ages.....	105
60-70 Ma ages.....	105
70-80 Ma ages.....	105
80-110 Ma ages.....	105
5.3.2. Discussion.....	111
5.3.3. Cooling history of the central Sesia zone	112
5.4. ⁴⁰ Ar/ ³⁹ Ar data of biotites and glaucophane.....	114
5.4.1. Introduction	114
5.4.2. Choice of samples.....	114
5.4.3. Presentation of the results and discussion	114

- Chapter 6 -

Conclusions.....	117
6.1 The monometamorphic cover sequences - introduction.....	117
6.1.1. The monometamorphic cover sequences.....	117
6.1.2. The provenience of the monometamorphic cover sequences.....	117
6.1.3. The lithostratigraphic reconstruction of the cover sequences	117
6.2. The mylonitic metagabbros	120
6.3. Geochronological considerations derived from radiometric data.....	120
6.4. Paleogeographic evolution of the central Sesia zone.....	121
Acknowledgements	126
References.....	127

Annexes

Annex 1.	Legend of lithologic columns and text abbreviations	137
Annex 2.	Whole rock geochemical analyses.....	138
2.1.	Geochemical analyses of acid rocks.....	138
2.2.	Geochemical analyses of acid rocks (litterature)	139
2.3.	Geochemical analyses of basic rocks	140
2.4.	Geochemical analyses of basic rocks (litterature)	141
Annex 4.	Analytical tables of the $^{40}\text{Ar}/^{39}\text{Ar}$ incremental heating age determinations. (phengite, biotite and glaucophane systems)	143

Abstract

This study addresses three broad topics: 1) the metamorphic and tectonic history of the internal central Sesia zone (western Alps, northern Italy), 2) the problem of distinguishing between monometamorphic cover sequences (of supposed Mesozoic age) and polycyclic basement units, 3) the cooling history of the region based on $^{40}\text{Ar}/^{39}\text{Ar}$ age determinations.

We present a new geological map of the region. Detailed mapping indicates the Sesia zone can be divided into three main complexes: 1) a polycyclic basement complex, 2) a monometamorphic cover complex, and 3) a pre-Alpine high-grade basement complex. We subdivide the polycyclic basement complex into three units on the basis of degree of metamorphism. The internal units show HP assemblages only weakly reequilibrated under GS facies conditions. The intermediate units display reequilibration to GS facies conditions with relicts of the HP assemblages. GS facies lithologies dominate the external units, where HP relicts are scattered and rare.

The monometamorphic cover complex crops out between the Gressoney Valley and the Chiussella valley. This complex comprises basic and quartz-rich ribbons, layered on a metric scale. We interpret these rocks as a volcano-sedimentary sequence. The basic rocks show a geochemical within-plate basalt (WPB) signature with tholeiitic affinity. Dolomitic marbles overlie this sequence. Similarities to neighboring sedimentary sequences, whose age is well-constrained by fossil assemblages, allows us to infer an upper Triassic age for the marbles. Mid-ocean ridge (MORB) metabasalts and associated meta-sediments commonly punctuate these marbles, and therefore are probably also of upper Triassic to lower Jurassic age. A calcschist sequence exists in contact with both the metabasalts and dolomitic marbles. These calcschist units contain olistholiths of the rock-types described above and are characterized by high-manganese content typical of near-ridge sediments. We propose, then, that the calcschists were deposited soon after the other units of the monometamorphic cover complex. Decametric-scale mylonitic gabbroic bodies appear dispersed throughout the entire monometamorphic cover complex. These gabbros are magnesium-rich, tholeiitic, and geochemically identical to other Austroalpine gabbros emplaced at the crust-mantle boundary. The gabbros described in this study are not found in association with typical oceanic crustal material (such as serpentinites) and are probably related to the other Austroalpine gabbros. Lower Permian U/Pb age determinations support this hypothesis (Bussy et al., in prep.).

We use mineral chemistry and $^{40}\text{Ar}/^{39}\text{Ar}$ ages to define the P-T-t (pressure-temperature-time) path followed by the monometamorphic cover rocks. Actinolites record a prograde metamorphic path; their compositions indicate temperature conditions between 300 to 500°C and pressure conditions between 4 and 7 Kbars. Cation-exchange equilibria, which are reached in the garnet-pyroxene system at 550°C, reflect metamorphic peak conditions. Cation-exchange equilibria are reached in the garnet-amphibole system at 450°C. Omphacites show a decreasing jadeite component from the core to the rim. We link the latter equilibria and the omphacite zonation to a retrograde pressure path. Stable isotope thermometry applied to eclogite mineral separates (quartz-garnet-rutile) yields temperatures of 570°C, consistent with cation exchange thermometers. Stable isotope thermometry applied to retrograde mineral separates (quartz-albite-omphacite) yields temperatures of 420°C, also consistent with the garnet-amphibole geothermometer. Stable isotope Deuterium investigations of phengitic micas indicate a fluid source linked to deep subduction of the oceanic crust beneath the continental crust. All of the basement and cover units, with the exception of the pre-Alpine high-grade basement complex, reached isotopic equilibrium.

We present incrementally heated $^{40}\text{Ar}/^{39}\text{Ar}$ age spectra from 29 phengites both in the internal HP basement and cover units and the external GS basement units. Cooling ages group at 100-60 Ma for the well-preserved HP units and at 45-50 Ma for the GS units. Ages from the internal units between 70-80 Ma are based on isochrons and reliable plateaux. Our field and isotopic data, combined with published data, support different cooling histories prior to 35 Ma for the internal and external units. These two units follow a common P-T-t path subsequent to 35 Ma.

Resumé

Les trois thèmes majeurs abordés dans ce travail sont: 1) l'histoire tectonique et métamorphique de la région centrale interne de la zone Sesia (Alpes occidentales, Italie du nord, basse vallée d'Aoste), 2) la distinction entre les couvertures monométamorphiques (présusés d'âge Mésozoïque) et les unités de socle polycyclique, 3) l'histoire du refroidissement de la région à partir des âges $^{40}\text{Ar}/^{39}\text{Ar}$.

Des nouvelles données cartographiques conduisent à distinguer trois complexes principaux: 1) un socle polycyclique, 2) des couvertures monométamorphiques, 3) un socle préalpin caractérisé par des faciès de haute température.

Le socle polycyclique est subdivisé en trois unités: une unité interne reconnaissable par des paragenèses HP

faiblement retromorphosées, une unité intermédiaire dominée par des paragéneses GS avec nombreuses reliques HP, une unité externe en faciès GS où les reliques HP sont rares et dispersées.

Le complexe de couverture monométamorphique affleure entre la vallée du Gressoney et le Valchiusella. On y reconnaît une série composée de gneiss mésocrates, de quartzites et de niveaux basiques. Ces roches sont interprétées comme formant une série d'origine volcano-sédimentaire. Les roches basiques montrent une signature géochimique de basalte intraplaque (WPB) et sont d'affinité tholéitique. Cette série est surmontée par des marbres dolomitiques d'âge supposé Trias supérieur à Lias. Des metabasaltes de type MORB et des métasédiments associées s'intercalent dans ces marbres dolomitiques. Une série de calcschistes vient en contact avec ces marbres et metabasaltes. Ces calcschistes contiennent des olistolithes de composition variée (marbres et metabasaltes dominants) et sont caractérisés par de fortes teneurs en manganèse, typiques d'environnements océaniques. Nous proposons donc que ces calcschistes se soient déposés dans le même contexte que les séries du complexe de couverture monométamorphique. Des corps décamétriques de gabbros blastomylonitiques parsèment l'ensemble de ce complexe. Ces gabbros sont riches en Mg, d'affinité tholéitique, et géochimiquement identiques aux autres gabbros austroalpins mis en place à la limite croûte-manteau. Les gabbros décrits ici ne sont pas associés à des produits typiques de croûte océanique (p. ex. serpentinites) et sont probablement liés aux autres gabbros austroalpins. Des âges préliminaires U/Pb indiquant le Permien inférieur soutiennent cette hypothèse (Bussy et al., in prep.)

L'évolution P-T-t (pression, température, temps) enregistrée par le complexe de couverture monométamorphique est définie par la chimie minérale et les âges $^{40}\text{Ar}/^{39}\text{Ar}$. Les actinolites indiquent une évolution prograde du métamorphisme; leurs compositions reflètent des températures comprises entre 300 et 500°C et des pressions comprises entre 4 et 7 Kbars. Les équilibres d'échange cationiques dans la paire grenat-pyroxène sont atteints à 550°C ce qui correspond au pic métamorphique. Les équilibres d'échange cationiques dans la paire grenat-amphibole sont atteints à 450°C. Les profils de microsonde dans les omphacites montrent une décroissance de la molécule jadéitique vers les bords. Cette zonation est interprétée comme étant liée à une diminution de la pression pendant la croissance du pyroxène. La géothermométrie selon la méthode des isotopes stables, appliquée sur les minéraux du faciès éclogite (Qtz, Gr, Rut), donne des températures de l'ordre de 550°C. Ces températures sont cohérentes avec les résultats obtenus par le géothermomètre grenat-omphacite. De même, les minéraux formés lors de la rétro-morphose (Qtz Alb Omph) indiquent des températures de l'ordre de 420°C, en bon accord avec les valeurs déduites par le géothermomètre grenat-amphibole. Les isotopes stables du Deutérium mesurés sur les micas phengitiques suggèrent une source de fluides provenant de la déshydratation d'une croûte océanique en cours de subduction sous la zone de Sesia. L'homogénéité des rapports isotopiques du Deutérium montre que toutes les unités du socle et de la couverture avaient atteint un équilibre isotopique à l'exception du socle préalpin à faciès haute température.

Les spectres d'âges de refroidissement $^{40}\text{Ar}/^{39}\text{Ar}$ sur phengites des unités internes et intermédiaires du socle polymétamorphique en faciès haute pression et couvertures associées sont compris entre 100 et 60 Ma. Les âges dans l'intervalle 80-70 Ma. se distinguent par des isochrones et des plateaux particulièrement fiables. D'autre part, les phengites de l'unité externe en faciès Schiste vert indiquent des âges de refroidissement Ar/Ar compris entre 45 et 50 Ma. Conjointement aux données antérieures, nos âges $^{40}\text{Ar}/^{39}\text{Ar}$ suggèrent des trajectoires de refroidissement distinctes pour les unités internes et externes avant l'Eocène. Les trajectoires de refroidissement de ces unités sont par contre identiques au cours de l'évolution tectonométamorphique post-Eocène.

Riassunto

Il presente studio affronta tre tematiche principali: 1) la ricostruzione dell'evoluzione tettono-metamorfica della zona Sesia (alpi italiane nord-occidentali) con particolare riguardo al suo settore centrale 2) la distinzione tra sequenze monometamorfiche di copertura (di supposta età Mesozoica) e le unità appartenenti al basamento policiclico, 3) la ricostruzione della storia di raffreddamento della zona Sesia sulla base di nuove datazioni radiometriche ottenute con il metodo $^{40}\text{Ar}/^{39}\text{Ar}$.

Nella prima parte di questo studio viene presentata una nuova carta geologica interpretativa del settore centrale della zona Sesia. Rilevamenti di dettaglio, uniti alla rivisitazione critica dei dati della letteratura hanno permesso di suddividere il settore centrale della zona Sesia in tre complessi maggiori: 1) un basamento policiclico 2) un complesso monometamorfico di copertura 3) un complesso di rocce di alto grado metamorfico di età pre-Alpina. Viene inoltre proposta la suddivisione del basamento policiclico in tre unità: a) un unità interna, caratterizzata da litotipi di alta pressione solo debolmente riequilibrati in condizioni di facies scisti verdi; b) un unità intermedia, dove le paragenesi di alta pressione sono in genere

parzialmente sostituite da minerali tipici della facies scisti verdi e, c) un unità esterna costituita da gneiss in facies scisti verdi e con sporadici relitti di alta pressione.

Il complesso monometamorfico di copertura affiora tra la valle di Gressoney e la Valchiusella. È costituito alla base da una alternanza di gneiss mesocratici contenenti al loro interno livelli e blocchi di rocce mafiche ed orizzonti decimetrici-metrici di quarziti più o meno pure. L'insieme di questi litotipi viene interpretato come una sequenza sedimentaria di affinità vulcano-detritica di probabile età Permo-Triassica, come suggerito dalle sue analogie con simili successioni affioranti nelle unità limitrofe. I livelli ed i blocchi basici hanno composizione basaltica con affinità tholeiitica di tipo itraplacca (WPB). Dei marmi dolomitici si trovano al tetto della sequenza vulcano detritica. Tali marmi sono correlati per analogia di facies al Triassico Superiore, benchè nessuna evidenza sicura sulla loro età sia stata rinvenuta nel corso di questa Tesi. Metabasalti tholeiitici, caratterizzati da un pattern geochimico tipico dei basalti di fondo oceanico (MORB), ed associati metasedimenti, sono stati rinvenuti in diretto contatto con i marmi dolomitici. Un'età Triassico superiore-Liassica è proposta per queste metabasiti, vista la loro intima associazione con le rocce dolomitiche. Una sequenza di calcescisti è stata cartografata in diretto contatto sia con i marmi dolomitici che con i metabasalti. I calcescisti contengono al loro interno degli olistoliti delle rocce descritte precedentemente, nonchè livelli estremamente arricchiti in manganese, caratteristica questa che fa supporre per essi un ambiente deposizionale non lontano da un ridge. Sugeriamo pertanto che i calcescisti in questione abbiano una età non dissimile da quella dei marmi dolomitici e dei metabasalti rinvenuti nelle coperture. Corpi decametrici di metagabbri blastomilonitici sono stati infine rinvenuti al contatto tra le coperture monometamorfiche ed il basamento poliociclico, od all'interno delle coperture stesse. Questi corpi basici derivano da Mg-gabbri tholeiitici con caratteristiche geochimiche identiche a quelle dei gabbri sotto crostali ben conosciuti nel sistema Austroalpino. Inoltre, il fatto che i gabbri delle coperture monometamorfiche non siano associati a litotipi di crosta oceanica (serpentiniti) suggerisce che questi corpi basici vadano correlati piuttosto alle intrusioni sottocrostaali Austroalpine. Età U/Pb Permiano inferiori, recentemente ottenute sugli zirconi di alcuni dei gabbri analizzati sembrano convalidare quest'ultima ipotesi (Bussy et al., in prep.).

La ricostruzione delle traiettorie pressione-temperature-tempo, seguite dalle sequenze di copertura e dalle unità di alta pressione del basamento, è stata permessa grazie all'applicazione dei geotermometri basati sui coefficienti di ripartizione e sul frazionamento isotopico tra le diverse fasi minerali analizzate. L'età di raffreddamento delle diverse unità sono state ottenute utilizzando il metodo $^{40}\text{Ar}/^{39}\text{Ar}$ sulle miche fengitiche. Il cammino progrado delle sequenze di copertura è testimoniato dalla presenza di actinoto, che mostra condizioni di formazione comprese tra 300 e 500°C e tra 4 e 7 Kbars. Il geotermometro granato-pirosseno sulle paragenesi di alta pressione indica la temperatura del picco di metamorfismo attorno a 550°. La stima delle temperature di equilibrio della coppia granato-amfibolo ha invece dato valori attorno a 450°C. Lo studio del frazionamento isotopico dell'Ossigeno tra i minerali di alta pressione (quarzo-granato-rutilo) ha permesso di valutare le temperature di equilibrio nell'ordine di 550°C. Lo stesso metodo applicato ai minerali legati alla riequilibrio retrograda ha dato temperature di 420°C. Il rapporto isotopico del Deuterio delle miche fengitiche suggerisce che tutte le unità della zona Sesia, ad eccezione del complesso pre-Alpino di alto grado metamorfico, furono interessate ed isotopicamente equilibrate da una sorgente di fluidi di crosta oceanica durante le diverse fasi del ciclo orogenetico Alpino.

Le età ottenute con il metodo $^{40}\text{Ar}/^{39}\text{Ar}$ sulle fengiti del basamento poliociclico e delle coperture monometamorfiche sono state raggruppate in due intervalli. Le unità interne di alta pressione mostrano età di raffreddamento Ar/Ar comprese fra 100 e 60 Ma, mentre le fengiti dell'unità esterna hanno età di 45-50Ma. I dati particolarmente affidabili delle età di raffreddamento della parte interna si collocano nell'intervallo compreso tra 70 ed 80 Ma. I dati $^{40}\text{Ar}/^{39}\text{Ar}$ ottenuti, combinati con quelli già disponibili, hanno permesso di evidenziare due diverse curve di raffreddamento anteriori all'Eocene per la parte interna e quella esterna del zona Sesia centrale. Tali unità hanno poi registrato la stessa evoluzione tettono-metamorfica a partire dall'Eocene.

Foreword

This work aims to better understand the geology and origin of the monometamorphic cover sequences of the Sesia-Lanzo zone (shorted in Sesia zone in the text). My personal goal in undertaking this thesis was to become familiar with the laboratory methods most suitable to studying geochronology and metamorphic and igneous petrology. This study focuses on the central Sesia zone, which, at the time I began working there, had been rather incompletely studied. In addition, the more robust body of literature on the northern Sesia zone is reviewed, but no new research on this region is presented. The first chapter introduces a brief summary of the geology of the western Austroalpine system in order to compare it to results presented herein. The second chapter presents in detail the field and petrographic work carried out over the past three years. The third chapter contains an analysis and discussion of the geochemistry of the felsic and mafic rocks of both the monometamorphic cover sequences and the polycyclic basement complex. Particular attention is given to the geochemistry of the eclogites and gabbros of the monometamorphic cover sequences. These geochemical analyses serve to distinguish between different rock types when this distinction was impossible in the field. In the fourth chapter, we use stable isotope analyses and the cation exchange equilibria to understand the pressure and temperature conditions of the Alpine metamorphism. Hydrogen isotopes inform our understanding of the fluid reservoirs that affected these rocks during metamorphism. Chapter five outlines the geochronology of the central Sesia zone using the $^{40}\text{Ar}/^{39}\text{Ar}$ method. This allows us to critically review the geochronological work done in the region over the past two decades. Chapter six wraps up and summarizes all of the work presented in the preceding chapters. Microprobe data tables couldn't be listed as annexes because of space limitations of the contribution. People interested to look at the entire data sheets have to require a copy to the Isotope Geochemistry Laboratory of the Institut de Minéralogie of the University of Lausanne, BFSH2, CH1015, UNIL, Lausanne, Switzerland..

- Chapter 1 -

General Overview

1.1. Introduction

Since the middle of 19th century the western Austroalpine system has been the object of several extensive field and laboratory investigations, beginning with the pioneering studies of Gerlach (1869) and Gastaldi (1871), over one hundred contributions have been produced on the western Austroalpine system. As in other metamorphic belts, three main problems characterise this area:

- the origin of the rocks observed in the field (protolith problem);
- the evolution of these lithologies during different metamorphic events, *e.g.* their pressure-temperature-time evolution histories;
- the tectonic setting of the different groups of rocks (units) and their relationships with surrounding Alpine complexes;

Until now, the subdivisions of the western Austroalpine units were mainly achieved on the basis of their different metamorphic signatures, protolith composition and structural position (*e.g.* Dal Piaz et al., 1972; Compagnoni et al., 1977a; Martinotti and Hunziker, 1984; Ballèvre et al., 1986, Dal Piaz, 1993).

In the next paragraphs we will try to summarise the western Austroalpine setting on the basis of the following criteria:

- 1) number and type of metamorphic cycles which recorded by different lithologies and/or units. Following Venturini et al. (1994a), three main distinctions are observed:
 - pre-Alpine high grade basement rocks metamorphosed to the high-temperature granulite-amphibolite facies during a Palaeozoic cycle, only weakly reworked during the Alpine orogeny (Dal Piaz et al., 1972; Hunziker, 1974; Compagnoni et al., 1977a; Dal Piaz, 1993). These rocks preserve pre-Alpine textures and/or mineral assemblages
 - polycyclic basement lithologies, which are related either to the Paleozoic or to the Alpine

orogenic cycle, the latter imprint being predominant. This group of rocks include two types of protoliths: paragneisses¹ with interbedded marbles and mafic rocks, which have experienced a pre-granitic high grade and the monometamorphic late Paleozoic granitoids, only affected by the Alpine metamorphism.

- monometamorphic cover sequences (non fossiliferous), of supposed Permo-Mesozoic age, sedimented after the Variscan orogeny and the onset of the Lower Cretaceous subduction (eo-Alpine orogeny), hence affected only by the Alpine metamorphism.
- 2) the tectonic position of the different Austroalpine units;
 - 3) the P-T conditions of the Alpine metamorphic equilibration;
 - 4) the supposed or measured ages of the different Alpine metamorphic reequilibration.

In this chapter a general overview of the western Austroalpine system will be given on the basis of the parameters reported above; the second part of the section is completely dedicated to a detailed introduction of the geological, structural and petrographic knowledge on the Sesia zone. Some summary tables will be proposed in support of this introduction.

1.2. The Austroalpine System

The Austroalpine System is one of the four main structural domains of the Alpine chain, together with the Penninic, Helvetic-Ultrahelvetic and Southalpine domains (Fig. 1.1.a).

The Austroalpine System represents the uppermost element of the Europe-vergent Alpine nappe pile (Bigi et al. 1990) and it is comprised of

¹ The term gneiss is used following the definition of Bates and Jackson (1987) Gneiss: a foliated rock formed by regional metamorphism, in which bands or lenticles of granular minerals alternate with bands or lenticles in which minerals having flaky or elongate prismatic habits predominate.

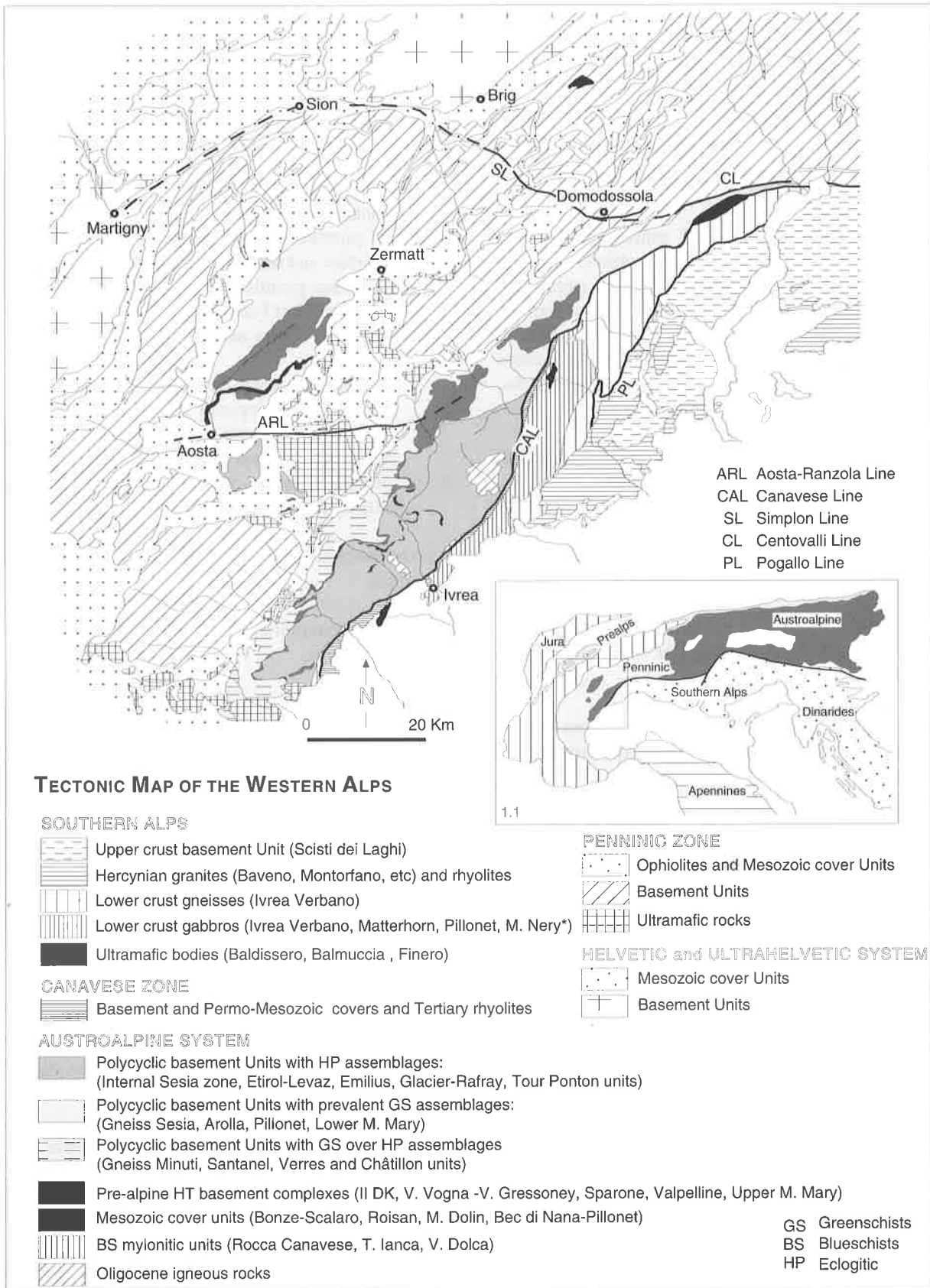


Fig. 1.1 - Tectonic map of the western Alps. The Austroalpine system has been compiled using data of Pognante (1989), Canepa et al., (1990), Pennacchioni and Guermani (1993) and Venturini et al. (1994). The main tectonic map is based on the structural model of the Italian Geological Survey (Bigi et al., 1990).

several polycyclic basement units of pre-Alpine and/or Alpine age, and minor monometamorphic Permo-Mesozoic cover units. The Austroalpine System can be coarsely subdivided into an eastern and a western sector; the former comprises large units in the Valtellina (Italy), Grisons, Alto Adige and in Austria, the latter is recorded only in the Aosta valley and southwestern Valais.

1.3. The western Austroalpine System

The Austroalpine in the western Alps, e.g. the western Austroalpine System, comprises the Sesia zone and the Dent Blanche System and their subunits (Fig. 1.1b). A schematic summary of the general geological and tectonic setting of the western Austroalpine System can be found in Compagnoni et al. (1977a) (Tab. 1.1a).

Both the Sesia zone and the Dent Blanche System contain an upper and a lower tectonic element (Diehl et al., 1952; Carraro et al., 1970). The upper element of the Sesia zone is formed by high grade metamorphic rocks of pre-Alpine age (Second Diorite-Kinzigite zone (II DK), Novarese, 1931, dal Piaz et al., 1971), while the lower element is traditionally subdivided into two main complexes, barically reflecting a different Alpine imprint: the Eclogitic micaschists complex (Stella, 1894) with subduction-induced high pressure assemblages, and the Gneiss Minuti complex (Gastaldi, 1871, 1874) showing a predominant greenschist facies imprint.

The Dent Blanche System (e.g. Dent Blanche s.l. of Argand) is formed by several units: 1) the Dent Blanche Nappe, consisting of an upper tectonic element, the Valpelline series, and a lower tectonic element, the Arolla series; 2) the smaller klippen of Mont Mary, Etirol Levaz, Pillonet, Grun, Châtillon, Monte Emilius, Ponton, Glacier-Rafray, Santanel and Verres, which have been related to the lower element (Compagnoni et al., 1977a, Martinotti and Hunziker, 1984).

The Valpelline series, as its homologous II DK zone in the Sesia zone and the upper element in the Mont Mary klippe, consists of high grade metamorphic rocks of pre-Alpine age, while the Arolla series mainly consists of orthogneisses from late Paleozoic intrusive bodies, also occurring together with high grade parashists in the Pillonet klippen in Châtillon slice and in the external edge of the Sesia zone (Gneiss Minuti unit).

All the other elements of the Dent Blanche System (Etirol Levaz, Mont Emilius, Ponton, Glacier-Rafray

and Santanel Klippen) are made of high pressure lithologies re-equilibrated in greenschist facies, and have been compared to the Eclogitic Micaschists complex of the Sesia zone (Dal Piaz and Nervo, 1971; Dal Piaz et al. 1983; Kienast, 1983, Ballèvre et al., 1986).

Mesozoic cover sequences are known since long time in the Dent Blanche System (Mont Dolin, Roisan zone, and in the Pillonet klippen Elter, 1960. Weimann and Zaninetti, 1974; Dal Piaz and Sacchi, 1969; Dal Piaz, 1976; Canepa et al., 1990). Their occurrence in the NW-Sesia zone were locally suggested (Dal Piaz et al., 1971, Pognante et al, 1987), and lately widely discovered by Venturini et al. (1994a) in the internal Sesia zone

Ballèvre et al. (1986) proposed a new subdivision of the western Austroalpine system on the basis of the tectonic position and lithological features of the different units (Tab. 1c). The Eclogitic southern klippen of the Dent Blanche system and the Etirol-Levaz slice are considered as slices of pre-Alpine lower crust and are grouped in a lower element, because of their Alpine high pressure metamorphism and their superposition over the Zermatt-Saas Zone and southern homologues (high pressure ophiolitic unit). The Gneiss Minuti complex and the northern Austroalpine units are otherwise related to an upper element, because of the absence of eclogitic mineral assemblages and the superposition over the Combin Zone (greenschist ophiolitic unit). The proposed subdivision is not be adopted here on the basis of two main considerations: a) except of the Valpelline series, in the Dent Blanche and Mont Mary nappes and the IIDK zone (granulite-free lower crust), all the other Austroalpine units have been intruded by late Paleozoic calcalkaline granitoids (Callegari et al., 1976; Compagnoni et al., 1977a; Bearth et al., 1980; Oberhänsli et al., 1985; Dal Piaz, 1993) and are interpreted as slices of upper crust at the moment of the intrusion of the Upper Paleozoic granitoids; b) part of the Gneiss Minuti complex shows high pressure relics (Spalla et al., 1991), c) the different structural position of the southern Austroalpine eclogitic klippen (excepting the Tour Pont klippe) in comparison to the Etirol-Levaz slice.

1.3.1. The Dent Blanche System

The aim of these paragraphs is to give a brief overview of the western Austroalpine System from recent contributions, trying to homogenise the available data using the criteria given in the introduction, in order to correlate and discuss the different western Austroalpine System-forming units.

Ref.	Austroalpine sector	Structural position	main subdivisions	Sesia Lanzo zone	Dent Blanche s.l.	lithologies	metamorphism	age of the metamorphism
Compagnoni et al. 1977	Sesia-Lanzo (Dent Blanche)	upper		II DK B1 Gneiss Minuti B2 Arolla Pillonet M. Mary B3	Valpelline	Paragneisses, marbles, metabasites	HT	Prealpine
						Metagranitoids, augengneisses, minor paragneisses, metabasites and marbles	GS	Eoalpine
						Paraschists and paragneisses, minor Metagranitoids metabasites and marbles	GS over HP	Mesoalpine
Martinotti & Hunziker 1984	Sesia-Lanzo Dent Blanche	upper	upper unit	II DK EMS GM	Valpelline	Paragneisses, marbles, metabasites	HT	Prealpine
					Emilius Glacier-Rafay T. Ponton Santanel	Eclogitic micaschists, metagranites, metagranodiorites, basic and ultrabasic bodies, gneiss minuti	HP (BS over HP)	Eoalpine
		lower	basic bodies	Corio Pinter	Arolla Chatillon		GS	Mesoalpine
					Matterhorn-M. Collon Tantañè	olivine gabbros, layer gabbro and less ultramafic rocks	GS	Mesoalpine
Ballevre et al. 1986	Dent Blanche nappe (Sesia-Lanzo)*	upper	Paleozoic basement	Gneiss Minuti	Canavese	Oligocene vulcano-sedimentary cover	post metamorphic	Mesoalpine
					Valpelline	Paragneisses, marbles, metabasites	HT	Prealpine
					Arolla Pillonet covers Dolin Roisan	Eclogitic micaschists, metagranites, metagranodiorites, basic and ultrabasic bodies, gneiss minuti	HP (BS over HP)	Eoalpine
Ballevre et al. 1986	Dent Blanche nappe (Sesia-Lanzo)*	lower	Paleozoic basement	Micaschistes eclogitiques	Emilius Etrol-Levaz Glacier-Rafay T. Ponton	Micaschists, metaplates, metagranulites, eclogitic relics	HP (BS over HP) GS over HP	(?) Eoalpine for EMC
					Valpelline	Paragneisses, marbles, metabasites	HT	Prealpine
					Arolla M. Mary Pillonet covers Dolin Roisan	ortogneisses, paragneisses and gabbros Mesoalpine dolomitic marbles- breccias-calcschists Triassic marbles and Liassic breccias Triassic marbles and calcschists (Lias) Mn-bearing quartzites	GS (GS)	alpine (?)

Tab. 1.1 - Comparative synoptic tables of different intrnal subdivisions proposed for the western Austroalpine system. Each table indicates the structural position of the units, their lithology, the pressure-temperature conditions and the age of metamorphism. Tab. 1.1a (Compagnoni et al., 1977) has been mainly reconstructed for the Sesia zone and lesser extended to the Dent Blanche system; this table correctly summarises the problem of the differences in age and in metamorphic conditions for the Gneiss Minuti complex (external Sesia zone). Tab. 1.1b (Martinotti and Hunziker, 1984) has four main subdivisions for the Austroalpine System, taking into account not only the polycyclic basement units but also the Mesozoic cover sequences and the mafic bodies which are in tectonic contact with the others units. In Tab. 1.1c (Ballevre et al., 1986) the units are grouped in function of their supposed metamorphism and not of their structural position (GS = Greenschists; BS = Blueschists; HP = Eclogitic).

1.3.1A THE DENT BLANCHE NAPPE

The Dent Blanche System is composed of the Dent Blanche Nappe s.s., containing a lower element (=Arolla series, Argand, 1908) and an upper tectonic element (=Valpelline series, Gerlach, 1869), and of several klippen supposedly comprising both tectonic elements (Mont Mary) or the lower element only (Etirol-Levaz, Pillonet, Grun, M: Emilius, Glacier-Rafay, Santanel units and other minor slices). The Arolla series is composed of a polycyclic basement affected by Alpine greenschist facies reequilibration, while the Valpelline series shows a pre-Alpine high-temperature amphibolite-granulite facies basement only partially reworked by the Alpine metamorphism.

The Dent Blanche and the Mont Mary nappes also contains some ophiolite free Mesozoic cover sequences; in the northern sector of the Dent Blanche nappe the monometamorphic cover is exposed at Mont Dolin (Argand, 1908; Hagen, 1948; Wiedmann and Zaninetti, 1974; Ayrton et al., 1982), while in the southern edge of the Arolla series the covers (Roisan zone) mark the contact between the Dent Blanche and the Mont Mary nappes (Diehl et al., 1952; Elter, 1960; Canepa et al., 1990; Pennacchioni and Guermani, 1993). A similar cover also occurs in the Pillonet klippe (Dal Piaz, 1976).

In the eastern and north-eastern sector of the Dent Blanche Nappe large bodies of continental gabbroic rocks (Matterhorn and Mont Collon-Dent de Bertol; Dal Piaz et al., 1977) are included within the Arolla series; their contact is mylonitic.

LOWER ELEMENT

The polycyclic basement

The polycyclic basement is made of several differentiated stocks of diorite-granodiorite to granite, probably late Palaeozoic in age, intruded into paraschists and gneisses (Diehl et al., 1952; Ayrton et al., 1982; Dal Piaz, 1993). The intrusive rocks were transformed during the Alpine orogeny into greenschist (\pm blueschist relics) orthogneisses (Ayrton et al., 1982; Ballèvre et al., 1986; Dal Piaz, 1992b, Pennacchioni and Guermani, 1993). The age of the greenschist Alpine reequilibration is still uncertain; available K/Ar and $^{40}\text{Ar}/^{39}\text{Ar}$ age determinations along the shear contact between the lower tectonic unit (Arolla) and the underlying ophiolitic units, are middle Eocene in age (Hunziker, 1974; Ayrton et al., 1982; Cosca et al., 1993).

The monometamorphic cover sequences

Two main units are classically indicated as the original cover of the Austroalpine basement: the Mont

Dolin series in the Dent Blanche nappe (Argand, 1911, 1934; Hagen, 1948) and the Roisan zone. The former is composed of Triassic and Liassic marbles, overlain by monogenic breccias (upper Lias) (Ayrton et al., 1982), while the latter has been related to the uppermost unit of the Mont Mary klippe (Elter, 1960; Canepa et al. 1990) and it will be described in the next paragraph.

Ballèvre et al., (1986), postulated a monometamorphic origin for the paragneisses of the Arolla series in which the granitoids are intruded. On the other hand Dal Piaz and Guermani, (in Dal Piaz, 1992b), described polycyclic paraschists intruded by magmatic series in the Mont Morion region, Valpelline.

UPPER TECTONIC ELEMENT

The pre-Alpine high grade basement

The pre-Alpine high grade basement consists of granulite to high-temperature amphibolite facies paragneisses (kinzigites), impure marbles and metabasites and rare mantle peridotites (Cesare et al.; 1989). A scattered greenschist reequilibration can be observed near the contact with the polycyclic basement or along internal Alpine shear zones (Dal Piaz, 1992b, 1993; Pennacchioni and Guermani, 1993). Granitoids are lacking, whereas migmatites, anatectic veins and pegmatite dykes are present. Several Rb/Sr, K/Ar and $^{40}\text{Ar}/^{39}\text{Ar}$ age determinations (240 to 180 Ma) are available for the upper tectonic unit (Hunziker, 1974; Cosca et al., 1993).

1.3.1B THE MONT MARY KLIPPE

Generally described as the equivalent of the Dent Blanche Nappe (Diehl et al., 1952), the Mont Mary Klippe has recently been investigated by Canepa et al. (1990) who subdivided the klippe into three main units: a lower unit, made of a polycyclic basement, an intermediate unit, composed of Pre-Alpine high grade basement rocks, and an upper unit comprising a mylonitic crystalline basement and its detached monometamorphic cover, crosscutting the contact between the lower and intermediate units (Tab. 1.2).

LOWER UNIT

The polycyclic basement

The polycyclic basement is mainly represented by paraschists and paragneisses intruded by minor granodiorites and granitoids (Diehl et al., 1952). All lithologies are affected by an Alpine greenschist reequilibration and transformed into fine grained gneisses; some relict green-blue amphiboles have been observed (Canepa et al., 1990). Several mylonitic horizons affect either the orthogneisses or the polycyclic paraschists.

INTERMEDIATE UNIT

The pre-Alpine high grade basement

The pre-Alpine high grade basement is formed by high grade parashists, metabasites and marbles equivalent to the Dent Blanche-Valpelline series. Cesare et al., (1989) discovered a serpentized harzburgite body of upper mantle origin, with similarities to outcrops of ultramafic rocks from the Artogna valley (Artini and Melzi, 1900, Dal Piaz et al., 1971, Beccaluva et al., 1976) and of Baldissero, Balmuccia and Finero in the Ivrea Verbano Zone. The contact between the ultramafic rocks and the lower and intermediate units is marked by a tectonic discontinuity.

UPPER UNIT

The upper unit of Canepa et al. (1990) comprises either the Mesozoic cover sequences of the Roisan Zone or a mylonitic polycyclic basement.

The monometamorphic cover sequences

These are interposed between the southern edge of the Dent Blanche Nappe and the Mont Mary klippen and consist essentially of a Triassic dolomitic sequence on the top of which are Liassic breccias and quartzites followed by calcschists and fine grained schists (Cima Bianca; Polino, unpublished data). Ballèvre and Kienast, have observed some blueschist FeMn-bearing quartzites.

The polycyclic basement

This consists of hectometric pods of layered gabbrodiorites and orthogneisses embodied in greenschist mylonites. The gabbroic bodies are similar to the quartz-diorite and gabbros cropping out in the Comba della Sassa (Diehl et al., 1952; Guermani, 1992, Pennacchioni and Guermani, 1993). All the lithologies are affected by pervasive greenschist reequilibration; no high pressure assemblages have been described.

1.3.1c THE ETIROL-LEVAV SLICE (LOWER ELEMENT)

The Etirol-Levav slice is a small northern Austroalpine unit of polycyclic basement lithologies between the underlying Zermatt Saas zone and the Combin zone (Kienast, 1983; Ballèvre et al., 1986).

The polycyclic basement

The slice consists of parashists and granulitic metagabbros; the former have been transformed in eclogitic micaschists by the eo-Alpine high pressure metamorphism, the latter into eclogites. The metagabbros have been interpreted as lower continental crust intrusions of pre-Alpine age, comparable to the granulitic metagabbros of the Ivrea Verbano zone (Ballèvre et al., 1986)

No monometamorphic cover sequences have been described in the Etirol-Levav slice. Nevertheless, lithologies comparable to the "gneiss pipernoïdes" of the Mont Emilius klippe (Amstutz, 1962) widely occur in the Etirol Levav slice (Kienast, 1983). These lithologies, interpreted by Amstutz as a monometamorphic vulcano-detritic pyroclastic sequence, will be further described and discussed.

1.3.1d. THE PILLONET KLIPPE (LOWER ELEMENT)

The Pillonet Klippe is made of a polycyclic basement and a monometamorphic cover sequence (Dal Piaz and Sacchi, 1969; Dal Piaz, 1976); furthermore, a greenschist gabbroic body similar to the alpine-derivates of the Matterhorn - Mont Collon - Dent de Bertol layered gabbros has been described by the same authors at Mont Tantanè (southern sector of the Pillonet klippe). Its contact with surrounding Arolla gneisses is mylonitic.

The polycyclic basement

It consists of Arolla type paragneisses, granitoids and amphibolites, generally converted by a greenschist Alpine metamorphism to orthogneisses, micaschists and Ab-rich metabasites. This lithological setting is similar to that of the polycyclic basement of the lower unit of the Mont Mary Nappe (and differs from the Arolla series by the dominance of paragneisses and micaschists with respect to the orthogneisses). Relics of aegirine and glaucophane locally occur (Dal Piaz, 1976; Dal Piaz and Martin, 1986).

The monometamorphic cover sequences

A sequence of Mesozoic cover rocks has been described by Dal Piaz (1976) at the Gran Dent-Becca di Nana ridge. It is composed of dolomitic marbles of supposed Lower Triassic age, microbreccias, and calcschists and micaschists of supposed Jurassic age. All the lithologies are strongly deformed and affected by Alpine reequilibration under greenschist facies metamorphism.

1.3.1e THE GRUN SLICE (LOWER ELEMENT)

The Grun slice is the smallest unit of the Austroalpine System. It is located east of St. Vincent, at the contact between the Zermatt Saas zone and the Combin zone along the Aosta-Ranzola fault. It has recently been subdivided into two basement elements showing different metamorphic reequilibration and separated by a narrow horizon of mylonitic marbles (Biino and Compagnoni, 1988).

The polycyclic basement

The polycyclic basement is made of micaschists, orthogneisses, metabasites and metakinzigitites, showing widespread high grade relics only partially

Austroalpine sector	Structural position	Complex	Unit	Lithologies	metamorphism	age of the metamorphism	
Canepa et al. 1990	M.Mary nappe	upper	upper	cover (Roisan) basement	Mesozoic carbonate sequence orthogneisses, gabbrodiorites bodies, mylonites	(GS) GS	Eoalpine (?)
			intermediate	intermediate	Paragneisses, marbles, metabasites, ultrabasic bodies (B. Aveyille)	HT	Prealpine
		lower	lower	lower	Metagranitoids, augengneisses, minor paraschists, metabasic rocks	GS	Eoalpine (?)

Tab. 1.2 - Synoptic table for the Mont Mary nappe (Canepa et al., 1990). The authors propose three main units, separated by sharp tectonic contacts. The upper unit lies in tectonic discordance on the other two units and is composed of either Mesozoic covers or by igneous basement and mylonites. The age of metamorphism has been deduced by Canepa et al. (1990) by analogy with the other similar Austroalpine units.

re-equilibrated under high pressure (lower element) or blueschist (upper element) conditions (Biino and Compagnoni, 1988). The upper element is mainly composed of orthogneisses reworked by a pervasive greenschist foliation.

The Monometamorphic cover sequences

These are supposedly represented by a thin level of white-grey marble with centimeter boudins of chlorite concentrations (Biino and Compagnoni, 1988); the marbles are considered as monometamorphic on the basis of the absence of high grade calc-silicate relict minerals, typical of polymetamorphic carbonates. In any case their belonging to the closer Combin zone cannot be excluded.

1.3.1f THE MONT EMILIUS KLIPPE (LOWER ELEMENT)

The Mont Emilius klippe is the largest of the southern polycyclic basement units of the Dent Blanche system, displaying Alpine metamorphic reactivations, mainly under eclogitic conditions (Compagnoni et al., 1977a; Bearth et al., 1980; Dal Piaz et al., 1983). It is composed of polycyclic basement lithologies (kinzigites, granulites), locally preserving either textures or assemblages of the pre-Alpine high grade metamorphism (Dal Piaz et al., 1983; Pennacchioni, 1989; Benciolini, 1989; Dal Piaz, 1993; Pennacchioni, 1993).

The polycyclic basement

It is represented by eclogitic micaschists or by greenschist facies derivatives. The unit-forming rocks are mainly garnet-quartz micaschist locally containing glaucophane, jadeite and chloritoid, metabasites with minor orthogneisses and meta-aplitic dykes. Relics of granulites crop out in the NW edge of the Mont Emilius klippe and show well-preserved layered textures and primary pre-Alpine assemblages (Benciolini, 1989; Pennacchioni, 1989; Dal Piaz, 1993). Bearth et al. (1980), Dal Piaz et al. (1983) and Dal Piaz (1993) have also recognised and described massive grey gneisses interpreted as strongly transformed late Paleozoic metagranitoids.

In the southern sector of the klippe a narrow zone of Ab-rich micaschists with widespread metabasic boudins has been interpreted by Amstutz (1962) as a monometamorphic volcano-sedimentary pyroclastic level (gneiss pipernoides). These lithologies are widespread in other Austroalpine units (Glacier-Rafraay klippe, (Dal Piaz and Nervo, 1971), Etirol Levaz slice (Ballévre et al., 1986)) and are interpreted as strongly reworked pre-Alpine interlayers of basic and acid levels (Pennacchioni, 1991).

1.3.1g THE GLACIER-RAFRAY KLIPPE (LOWER ELEMENT)

It is made of a polycyclic basement intercalated between the underlying Zermatt Saas zone equivalent (Dal Piaz and Nervo, 1971; Dal Piaz et al., 1979; Dal Piaz, 1992) and the overriding Combin zone, occurring southward (Dondena valley). Neither monometamorphic cover sequences nor pre-Alpine high grade mineral relics have been observed, whereas evident textural relics are present.

The polycyclic basement

It consists of albite-bearing gneisses and minor garnet micaschists \pm glaucophane, chloritoid and Na-rich pyroxene (Micascisti Eclogitici of Dal Piaz and Nervo, 1971); part of the albitic gneisses are probably deriving from Arolla type leucocratic granites, other are retrogressed eclogitic paraschists; greenschist metagabbros layers and garnet-bearing amphibolites have been described, although their appartence to the basement or to the underlying ophiolites is still discussed (Dal Piaz and Nervo, 1971)

1.3.1h THE TOUR PONTON KLIPPE (LOWER ELEMENT)

It is a small slice of Austroalpine polycyclic basement rocks (Nervo and Polino, 1976), reequilibrated under high pressure conditions and later pervasively reworked by the greenschist decompression; the klippe occurs below the structural level of the Monte Emilius and Glacier Rafray klippe, interlayered within Zermatt Saas Zone and Combin equivalents (Dal Piaz, 1993).

Ref.	Complex	Unit	lithologies	metamorphism	age of the metamorphism
Venturini et al. 1994	Polycyclic basement - upper crust	external	Micaschists, orto and paragneisses, Metagranites, metagranodiorites, metabasites and marbles	GS	Mesoalpine
		intern.		GS over HP	Mesoalpine on Eoalpine
		internal		HP (BS over HP)	Eoalpine
	Monometamorphic cover	Scalero Bonze	Dolomitic marbles, calcschists, quartzites, metabasalts and metagabbros	HP (BS over HP)	Eoalpine
Prealpine HG basement - lower crust	II DK zone	Kinzigites, acid and basic granulites, amphibolites, ultramafics and marbles	HG	Prealpine	

Tab 1.3 - Synoptic table for the Sesia zone (Venturini et al., 1994) showing the subdivisions that will be adopted in this paper. The definition of upper and lower crust (Complex subdivisions) correspond to the moment of formation of the polycyclic basement, e.g., to the intrusion of late Variscan granitoids. During the early Permian, the crust that was intruded by the acid stocks was already located in the upper crustal level, while the high grade basement without the granitoid intrusions was positioned in a lower crustal position.

The polycyclic basement

It is made of albitic gneisses, garnet-bearing micaschists and lesser meta-aplites and metabasites, all affected by a pervasive greenschist reequilibration. Scattered relics of early Alpine assemblages can be observed in the metabasites; the age of the high pressure metamorphism and the greenschist reequilibration is unknown.

1.3.1i THE SANTANEL KLIPPE (LOWER ELEMENT)

The Santanel klippe is an elongated klippe tectonically inserted within the Piedmont zone close to the western edge of the Sesia zone; it consists of a polycyclic basement with a pervasive greenschist imprint locally preserving relics of high pressure and pre-Alpine textures (Battiston et al., 1987). It is in tectonic contact with the Combin and underlying Zermatt Saas equivalents.

The polycyclic basement

The polycyclic basement is mainly composed of albitic gneisses and garnet-bearing micaschists showing a pervasive greenschist recrystallization overprinting high pressure mineral assemblages. Omphacite and garnet are visible in the basic levels or boudins. Scattered pre-Alpine paragneiss relics are rare, and no intrusive lithologies have been observed.

1.3.2. The Sesia Zone

The Sesia zone is subdivided into three main complexes, distinguished on the basis of both lithologic and tectonic differences (Venturini et al., 1994a): a po-lycyclic basement complex, a monometamorphic cover complex, and a pre-Alpine high grade basement complex; the first two correspond, as whole, to the lower tectonic element of Compagnoni et al. (1977a), while the third one corresponds to the upper tectonic element of Venturini et al. (1994a), (Tab. 1.3 and Fig. 1.3). The different complexes are composed by lithological associations with different Alpine

metamorphic imprint and/or protoliths and are generally separated by sharp tectonic contacts.

1.3.2.a THE LOWER ELEMENT

THE POLYCYCLIC BASEMENT COMPLEX (PLATE I)

The polycyclic basement complex is derived from pre-Alpine lithologies (mainly high grade paragneisses, granulites and amphibolites, intruded by calcalkaline granitoids locally dated as Lower Permian (Paquette et al., 1989, Bussy et al., in prep.). It has been pervasively affected by the eo-Alpine metamorphism and later retrogression (Dal Piaz et al., 1972; Hunziker, 1974; Compagnoni et al., 1977; Martinotti and Hunziker, 1984). It has been further subdivided into three units based on different Alpine metamorphic characteristics after Passchier et al. (1981) and Venturini et al. (1994a) (Tab. 1.3):

an internal unit with high pressure assemblages underlining the regional foliation (the main part of the eclogitic micaschists complex of Compagnoni et al, 1977),

an intermediate unit where greenschist re-equilibration of the high pressure mineral assemblages is pervasively developed (~B3-zone of Compagnoni et al. (1977a), Unit B of Passchier et al. (1981) or Unit II of Williams and Compagnoni, (1983) (Tab.1.4)

an external unit, composed of rocks where the main foliation is defined by greenschist mineral assemblages (Gneiss Minuti complex or B1 and B2-zones of Compagnoni et al., (1977), Unit D of Passchier et al. 1981 or Unit I of Williams and Compagnoni, 1983) (Tab.1.5).

The terms internal, intermediate and external adopted for these units are referred to the present geographic position of these sectors of the Sesia zone, compared to the western Alpine arc.

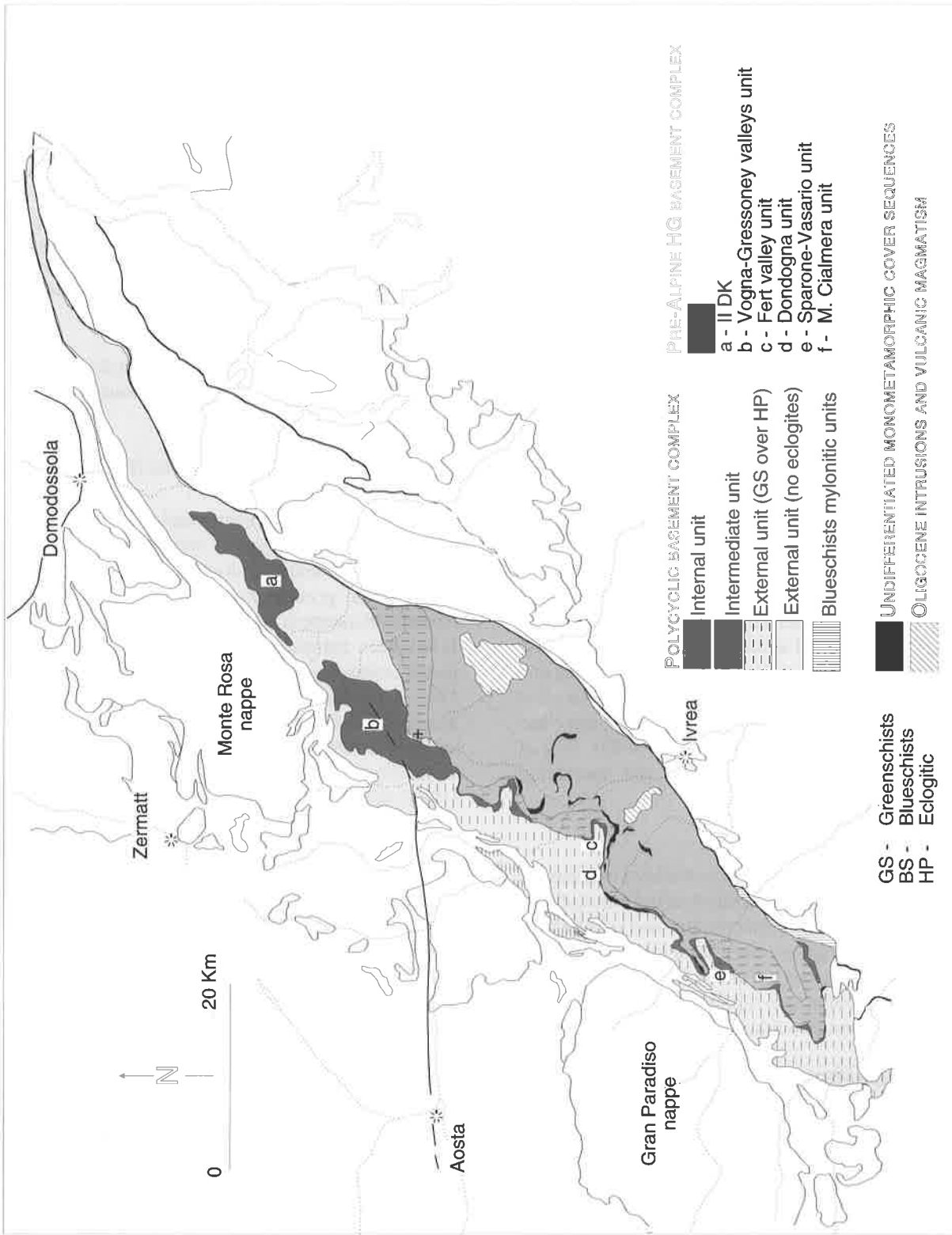


Fig. 1.3 - Tectonic map of the Sesia zone (from Venturini et al., 1994, with ref.). The limits between the different basement units are approximate for the northern and the southern sector, while they have been checked in the central Sesia zone.

Venturini et al. 1994	Compagnoni et al. 1977	pre-Alpine protoliths	alpine lithologies	metamorphic conditions	age of alpine metamorphism
internal unit	Eclogitic Micaschists Complex	HG metapelites HG metabasites marbles granodiorites/granites	phe-gln±omp-grn-cld micaschists omp-grn-gln-ru-czo±phe-qtz metabasites omp-grn-zo±gln marbles jd-zo/czo-phe metagranite and ortogneisses	HP assemblages P=15-17Kb (1) T=550-580 °C (1) (1) Compagnoni, 1977	eoalpine Hunziker, 1974 Hy, 1985 Stöckhert et al., 1987
intermediate unit	Gneiss Minuti Complex (B3)	HG metapelites HG metabasites marbles granodiorites/granites	phe-chl-barr±omp-II-grn-II-cld micaschists omp-II-grn-II-barr-sph-ep-chl±phe-qtz metabasites aegr-grn-II-czo/ep-chl±barr marbles ab-czo/ep-aegr-phe metagranites/ortogneisses	GS over HP(2,3) (2) Passchier et al., 1981 (3) Venturini et al., 1994	eoalpine/mesoalpine Hunziker, 1974
external unit	Gneiss Minuti Complex (B1-B2)	HG metapelites HG metabasites marbles granodiorites/granites	phe-chl-barr-ab±act micaschists/paragneisses ab-barr/act-sph-ep-chl±phe/mu-qtz metabasites ab-ep-chl±tr/act marbles ab-ep-chl-kf±mu metagranites/ortogneisses	pervasive GS assemblages (2) over rare HP relics (4) (2) Passchier et al., 1981 (4) Spalla et al., 1991	mesoalpine Hunziker, 1974

Tab 1.4 - Synoptic comparative table showing the different metamorphic and other characteristics of the lithologies forming the polycyclic basement (Venturini et al., 1994) or Lower Element (Compagnoni et al., 1977).

The polycyclic basement protoliths are mainly high grade metapelites (kinzigites) with minor bodies and masses of metabasic rocks and marbles (Dal Piaz et al., 1971, 1972; Hunziker, 1974; Compagnoni et al., 1977a) metamorphosed under upper granulite facies and later reequilibrated under amphibolite conditions, during continental thinning and Alpine rifting (Lardeaux and Spalla, 1991). This high grade complex has been intruded by kilometer-size bodies of granitoids (quartz-diorites to granites) of lower Permian age (Oberhänsli et al., 1985; Paquette et al., 1989; Bussy et al., in prep.). The Alpine metamorphic cycle transformed these protoliths according to different P-T-t paths followed by the different units.

Internal unit

In this unit the pre-Alpine lithologies have been transformed into omphacite-garnet-bearing micaschists and metabasites, and jadeite-bearing metagranites and orthogneisses. Reddish micaschists are the main lithologies, while the eclogites usually form meter to decameter beds and boudins in the micaschists. Impure marbles with scattered pre-Alpine relics crop out in the central and southern sector of the unit (Compagnoni et al., 1977a). Metapelite and metapegmatites often crosscut either the micaschists or the marbles. In the southern part of the unit, kilometer-sized bodies of eclogitic metagabbros have been described (Bianchi et al., 1964; Spalla et al., 1983) as well as in the central area (Compagnoni and Fiora, 1977; Pognante, 1979). Jadeite-bearing metagranodiorites and metagranites constitute a large part of the north and eastern sector (Dal Piaz et al., 1972; Compagnoni and Maffeo, 1973; Callegari et al., 1976, Dal Piaz et al., 1993). Peak metamorphic conditions have been determined by several authors to be 15-17 Kb and 550-600 °C (Droop et al., 1990 and ref. therein)

Intermediate unit

Lithologically equivalent to the internal unit, this can be distinguished because of a weak to penetrative greenschist re-equilibration of the high pressure mineral assemblages. In the central sector of this unit the metagranodiorites dominate. The age of the greenschist reequilibration is not supported by any specific age determination, but it can probably be still late Cretaceous (Hunziker, 1974; Stöckhert et al., 1986).

External unit

It is mainly built of fine to medium-grained albite-two mica-epidote gneisses (Gneiss Minuti auct.) and to a lesser extent of chlorite and actinolite micaschists. Several interbeddings of calcschists and metabasite bodies occur in the southern sector (Pognante et al., 1987). A characteristic and penetrative greenschist

VENTURINI et al. 1994	STUNITZ 1989	POGNANTE et al. 1987	SPALLA et al. 1983	WILLIAMS & COMPAGNONI 1983
Central Sesia zone	M. Nery area	Orco and Soana valleys	South Sesia zone	Bard and Verale areas
pre -Alpine HG basement complex (kinzigites)	Pre -Alpine kinzigites and strolalites	(gneisses) Vasario -Sparone subunit	Paraderivati prealpini Complesso M. Cialmera	-
pre -Alpine HG basement complex (amphibolites)	Amphibolites	amphibolites Vasario -Sparone subunit	Anfiboliti Complesso M. Cialmera	-
pre -Alpine HG basement complex (kinzigites)	A Meta -kinzigites	gneisses Vasario -Sparone subunit	parascisti (Ponte Cusard)	Unit I
polymetamorphic basement (HG relics)	B	micaschists Eclogitic Micaschists	parascisti	Unit II, Unit III
polymetamorphic basement (external unit)	Ortogneisses and Chlorite schists	gneisses Gneiss Minuti subunit	gneiss albitico -cloritici	Unit I, Ab in
polymetamorphic basement (interm. unit)		gneisses Eclogitic Micaschists	gneiss con relitti di Jd (Pertus)	Unit II, Jd in
-	Metagabbros Gneiss Minuti subunit	Metagabbros (M. Garné)	Metagabbri glaucofanici	-
polymetamorphic basement (metagranitoids)	Metagranitoids	-	-	-
Dykes	Dykes	Dykes	-	-
Monometamorphic cover complex	-	-	-	-
PASSCHIER et al. 1981	COMPAGNONI et al. 1977	GOSSO 1977	DAL PIAZ et al. 1971	NOVARESE 1934
Central Sesia zone	Entire Sesia zone	Val Vogna-Gressoney	Val Vogna-Gressoney	Entire Sesia zone
Unit C (II DK)	II DK upper element	II DK	II DK parascisti	II DK
Unit C (II DK)	II DK upper element	II DK	II DK rocce basiche	II DK
Paraschists Unit C	(II DK)	(II DK)	II DK	-
Micaschists Unit A	Eclogitic Micaschist unit	P. Plaïda subunit (EMC)	Micascisti eclogitici	Micascisti eclogitici
Orthogneiss Unit D (Ab in)	Gneiss Minuti B1 + B2 Chlorite schists	Gneiss Minuti	gneiss minuti (Gneiss Sesia)	Gneiss Minuti
Orthogneiss Unit B (Jd in)	Gneiss Minuti B3	Eclogitic Micaschist unit	gneiss occhiadini	-
Metabasites	Metagabbroids Corio -Monastero M. Pinter	-	metagabbri,	metadioriti
Granitoids	Metagranitoids	Metagranitoids	metagraniti metagranodioriti	-
Dykes	Dykes	Dykes	Filoni	Filoni
Marmi mesozoici Gh. d'Otro, P.Uomo storto	-	-	-	-

Tab 1.5 - Comparative table of different mapping subdivisions proposed for the different sectors of the Sesia zone (modified after Stünitz, 1989).

reequilibration completely obliterates the previous high pressure assemblages. Only few relics of high pressure mineral assemblages are preserved in the central sector of this unit or in its southern area (Lardeaux and Spalla, 1991), while in the northern external unit no eclogitic relics have been reported (Novarese, 1931, Dal Piaz 1976, Dal Piaz et al., 1971, 1972, Compagnoni et al., 1977a; Chabloz, 1990; Halter, 1992; Simic, 1992). The pervasive greenschist foliation is lower Tertiary in age, as shown by the Rb/Sr and K/Ar age determinations of Hunziker (1974) and $^{40}\text{Ar}/^{39}\text{Ar}$ age determinations of Venturini and Hunziker (1992) and Venturini et al. (1994b). It predates the emplacement of lamprophyric dykes date 30-31 Ma (Dal Piaz et al., 1973).

THE MONOMETAMORPHIC COVER COMPLEX (PLATE II - PHOTOS 2.1 & 2.2)

The presence of a para-autochthonous cover of the Sesia zone was postulated by Dal Piaz et al. (1971) on the ridge between the Sesia and the Gressoney valley and by Pognante et al. (1987) in the southern sector of the Sesia zone (external unit). The occurrence of noticeably extended cover sequences was discovered by Venturini et al. (1991) in the lower Aosta valley. The lithostratigraphic setting was later summarised by Venturini et al. (1994a).

The monometamorphic cover complex crops out as a narrow and continuous belt in the central and southern Sesia zone, within the internal unit or at its boundary with the intermediate unit; its presence in the northern sector of the Sesia zone has still to be investigated even if Simic (1992) described some dolomitic horizons as possible monometamorphic covers of the Sesia zone. Two main lithostratigraphic units have been described on the basis of their lithology: 1) the Bonze unit and 2) the Scalero unit (Venturini et al., 1991, 1994a), both with eclogitic imprint.

The Bonze unit

The Bonze unit comprises a sequence of extrusive basic rocks such as metabasalts, pillow breccias and related metasediments (Mn-bearing calcschists and quartzites), locally tectonically associated with hectometer-sized metagabbro slices. The metabasalts are supposed to be upper Triassic-Lower Triassic in age. Metabasalts and related basic rocks show omphacite-garnet-rutile-glaucophane assemblages. This unit mainly crops out between the Aosta valley and the Chiusella valley and it is always located at the limit between the internal and intermediate unit.

The Scalero unit

The Scalero unit is characterised by a terrigenous sequence of supposed Permo-Triassic age overlain by

Triassic dolomitic marbles, a carbonate conglomerate and a second terrigenous formation of quartzites, micaceous quartzites and metapelites (Venturini et al., 1991, 1994a). The terrigenous basal sequences show a penetrative greenschist reequilibration on the high pressure fabric. Eclogitic minerals are mainly preserved in basic levels and boudins inside the metapelites. The Scalero unit occurs either together with the Bonze unit at the western edge of the internal unit or within the internal unit itself. The contact between the Scalero and Bonze unit is marked by intercalations of the metabasalts and dolomitic marbles and by the presence of blocks of metabasalts within the calcschists. Although a pervasive transposition of the sedimentary contacts does not permit the reliable reconstruction of the original lithostratigraphy, the interbedding between the dolomitic marbles and the metabasalts is probably stratigraphic, as testified by the lack of tectonic contacts or boudins of both the lithologies within the other.

1.3.2.b THE UPPER ELEMENT

THE PRE-ALPINE HIGH GRADE BASEMENT COMPLEX (PLATE II - PHOTOS 2.3 & 2.4)

The pre-Alpine high grade basement complex comprises (from north to south): the II DKs.s. (Artini and Melzi, 1900; Franchi, 1905, Novarese, 1929, 1930), the Val Vogna-Valle di Gressoney- klippe (Novarese, 1931; Carraro et al., 1970; Dal Piaz et al., 1971), the unit C of Passchier et al. (1981), the Valle del Fert-Alpe Dondogna slice (Venturini, 1994, this work), the Sparone-Vasario unit (Carraro et al., 1970; Minnigh, 1978; Pognante et al., 1987) and Mont Cialmera unit (De Maria et al. in Spalla et al., 1983), (Fig. 1.3; Tab. 1.6). These elements are located at the boundary between the internal and the external sector of the polycyclic basement (Venturini et al., 1994a) and they are characterised by the preservation of both pre-Alpine textures and assemblages, although Alpine re-equilibration increasing toward the south (Tab. 1.6). All the pre-Alpine units display sharp tectonic contacts with the underlying polycyclic basement units (Carraro et al., 1970, Bigi et al., 1990). The lithologies of this complex are characterised by pre-Alpine high grade mineral assemblages (Dal Piaz et al., 1971; Vuichard 1987). They are mainly represented by kinzigites (biotite-garnet-sillimanite-plagioclase and Kfeldspar-bearing paragneisses), minor metric boudins of mafic granulites /amphibolites within the kinzigites and impure marbles, crosscut by decimeter to meter pegmatitic veins (Dal Piaz et al., 1971; Gosso, 1977). A small body of serpentized harzburgite has been described from the northern part of the IIDK (Artini and Melzi, 1900, Beccaluva et al., 1986).

	UPPER ELEMENT	5	Gneiss Minuti	5	Gneiss Minuti (B3)	5	Eclogitic Micaschists	5	LOWER ELEMENT	5
metamorphic degree	pre-Alpine HT basement complex	14	external unit	14	polymetamorphic basement complex	14	internal unit	14	monometamorphic cover complex	14
PRE-ALPINE HT	II Diorito Kinzigitic zone Val Vogna-Val Gressoney Sparone-Vasario M. Cialmera Unit C	1 2 8 6	Verres unit	11	Rassa Valley M. Cassarello	11 11	L. Microne Val Tesso L. Plaida	4 11 11		
GS	Val Vogna-Val Gressoney Unit C	3 6	Gneiss Minuti B1 sector Gneiss Sesia Settore I Gneiss leucocrate Gneiss mesocrate	1 5 1 4 13 13					Ch. dell' Otro marbles Couverture ophiolitique	3 13
GS over HP			B2 sector	5	B3 sector Unit B Unit II	5 7 6				
BS	Vallone del Fert Alpe Dondogna Colle del Prà	15 15 15	Unit D Unit I	6 7			R. Canavese Trust Sheet Val Dolca	9 14		
HP	Polymetamorphic Paraschist Sparone-Vasario	10 9	Gneiss Minuti subunit	9			Micaschisti Eclogitici Unit A Unit I	1 7 6	Scalero unit Bonze unit	14 14

Tab. 1.6 - Synoptic table of different mapping units proposed for the Sesia zone in relation to the metamorphic degree affecting the unit-forming lithologies. Numbers indicate the related references.

Rb/Sr and K/Ar geochronological data on biotites from the northern sector give ages of around 240-180 Ma interpreted as pre-Alpine cooling (Dal Piaz et al., 1972; Hunziker, 1974, Hunziker et al., 1992). Similar ages have also been obtained for the Valpelline series and for the Ivrea Verbano zone, (Hunziker, 1974; Hunziker and Zingg, 1980).

1.3.3. Structural outline of the Central Sesia Zone

Geological and structural studies were carried out from the beginning of the century in the Sesia zone, but the first organic contribution on the deformation-recrystallisation history for the central Sesia zone is due to Gosso (1977) and Gosso et al. (1979). Tab. 1.7 summarise the main available structural and metamorphic data on the central Sesia zone.

Four main Alpine deformation episodes (F_1 to F_4) are generally described: in Tab. 1.7 only the F_1 to F_3 fold phases are represented, while F_4 (late kilometric open folds associated with vein formation) is omitted; different syn-deformation assemblages are indicated together with the fold style. F_1 folds are generally rootless to isoclinal and they are underlined by eclogitic minerals (high pressure-climax: jadeite, omphacite, and garnet). F_1 folds deform a previous foliation (F_0 of Tab. 1.7) which in some case is clearly a pre-Alpine foliated schistosity (Dal Piaz et al., 1971) in other can be interpreted as an

Alpine prograde foliation preceding the high pressure-climax (Pognante et al., 1980; Venturini et al., 1991). F_2 folds are isoclinal to tight - in some cases open - and they have been related to the blueschists decompression path (Gosso, 1977; Lardeaux et al., 1982). The assemblage underlining this folding episode is characterised by albite, chloritoid and glaucophane with only a retrograde iron-rich clinopyroxene. Fold axes are oriented ESE-WNW and plunge a few degrees in both directions, while axial planes are dispersed. F_3 folds are tight to open with fold axes generally plunging E of 10-15° (Gosso, 1977; Pognante et al., 1980; Williams and Compagnoni, 1983), or E-W with a shallower plunge (Passchier et al., 1981; Venturini et al., 1991); this deformation is related to the greenschist reequilibration, which in some case erases the high pressure assemblages. All the structural studies, on the central and southern sectors of the Sesia zone, summarised in Tab. 1.7, show a good concordance about fold axes of F_2 and F_3 orientations, with the exception of the southern Sesia zone (Spalla et al., 1983), where a diversion in plunge direction for both set of folds occurs. Unfortunately no detailed work on the central and northern external Sesia zone have been published, thus it is not possible to compare the previously reported deformation- stages with this sector of the belt. On the other hand, F_2 and F_3 fold axis orientations are consistent with those described by Halter (1992) in the north-eastern sector of the Sesia zone.

	Gosso 1977 Val Vogna- Gressoney	Pognante et al. 1981 Mombarone area	Passchier et al. 1981 Central Sesia zone	Spalla et al. 1983 Southern Sesia zone	Williams et al. 1983 Bard-Verale areas	Venturini et al. 1991 Scaloro area
F0	# type foliation	X foliation	- foliation	- foliation	- foliation	F0-1 mylonitic foliation
sin	Fe-grn, phe, zo omp, gln, Mg-chl	CaNa amph, gln zo/czo, phe, ru	phe, gln (ru, sph, czo)	zo, grn, Na-pyx, ru, sph, chl	gln, czo, phe, sph, qtz	gln, czo, phe qtz, sph, Mg-chl
F1	# type B1 rootless isoclinal	B1 rootless isoclinal	D1 rootless tight / isoclinal	F1 rootless isoclinal	F2+F3 rootless tight / isoclinal	F1 rootless tight/isoclinal
sin	gln, zo, (omp), Mg-chl, phe, qtz,	omp, grn, jd zo-czo	omp, zo, jd, ru phe, zo, gln	grn, jd, zo, ru, phe, (gln)	jd, omp, grn II, zo, cld, phe, ru	jd, omp, grn, gln, phe, ru, zo/czo
F2	# type B2 isoclinal, tight, open	B2 isoclinal, open	D2 close to tight	F2 isoclinal to tight	F4 isoclinal, open	F2 isoclinal to tight
sin	phe, ab I, crst, czo aegr., sph, cld	phe, cld, gln, sph, qtz	ab, phe, grn II, czo aegr, sph, czo, cld,	phe, gln, ru, aegr	aegr, grn II, czo, gln, phe, sph, barr	aegr, phe, grn II, czo gln, cld, sph, qtz
axis	ESE / 10-30°	ESE / 10-30°	ESE- WNW / 10-30°	S-SW / 5-15°	WNW / 10-30°	ESE- WNW / 10-30°
F3	# type B3 tight, open	B3 tight, open	D3 tight, open	F3 tight to open	F5 tight, open	F3 tight, open
sin	ab II, Mn-grn, phe barr/act, ep, sph	gln/barr, ep, ab, aegr, phe, qtz, sph	ab, bio I, Mn-grn act, czo-ep, sph	green amph, ab Fe-ep, chl, phe	czo-ep, barr-act, phe, sph, ab, chl, bio	qtz, phe, ab, barr, ep sph, ap, chl,
axis	E-W / 10-15°	E / 10-15°	E-W / 5-20°	E-NE / 5-35°	E / 10-15°	E-W / 5-20°

Tab. 1.7 - Synoptic table of different structural and metamorphic studies which have been carried on in the central Sesia zone.

- Chapter 2 -

Field and Petrographic Investigations

2.1. Introduction

Detailed field investigations in the lower Aosta valley, Crabun valley and Chiusella valley (Fig. 2.1) provide new data to the body of geological knowledge on the central Sesia zone (Table 1 and Fig. 2.2).

The aim of the field work was to define: a) the protoliths of different units and b) structural and metamorphic relationships existing between the different units, defined on the basis of the different lithological associations.

New whole rock geochemical analyses has been carried out to better investigate the composition of the protoliths, while mineral chemistry and stable isotope analyses provide new constraints on the metamorphic history of the different Sesia zone units. Timing of the pressure-temperature path reconstructions is defined by over thirty $^{40}\text{Ar}/^{39}\text{Ar}$ incremental heating age determinations. All the results are presented in the next chapters and compared with the literature data summarised in chapter 1. Part of the previous data will be partially re-considered to be compared with our data.

2.2. Geological Mapping and Petrography

2.2.1. The Mapped Units

As previously seen, the investigated area has been subdivided into three main complexes, the polycyclic basement, the monometamorphic cover and the pre-Alpine high grade basement, according to Venturini et al. (1994a) (Par. 1.3.2.).

The polycyclic basement is made of paraschists, paragneisses and subordinate marbles that underwent pre-Alpine high grade metamorphism of upper amphibolite-granulite facies conditions. These lithologies were later intruded by intermediate to acid plutons of supposed Lower Permian age by comparison with the Monte Mucrone body (Bussy et al., in prep.). Paraschists, paragneisses and granitoids finally underwent different metamorphic conditions during the Alpine orogenic cycle. The different Alpine metamorphic conditions recorded by the Sesia basement entail further subdivisions of the polycyclic group into:

- a) an internal unit, characterised by well preserved high pressure metamorphic assemblages;
- b) an intermediate unit, where the high pressure imprint is partially erased by the greenschist re-equilibration;
- c) an external unit consisting of rocks with a pervasive greenschist foliation.

The monometamorphic cover sequences crop out in the central Sesia zone along a narrow but continuous band and are often interposed between the internal and the intermediate unit of the polycyclic basement or within the intermediate unit itself (Fig. 2.3). According to Venturini et al. (1991, 1994) the monometamorphic cover is defined as a group of lithologies of sedimentary and basic volcanic origin which underwent only the Alpine metamorphic cycle. Although no indisputable evidence has been found yet, the post-Paleozoic age of these sequences is postulated by the following considerations:

- a) both the carbonatic and terrigenous lithologies and the basic rocks differ in aspect from the basement-forming lithologies. The paraschists and paragneisses always alternate with dolomitic marbles, impure marbles and calcschists, quartzites and basic levels. The basic rocks are laterally continuous for several kilometers and show homogeneous lithostratigraphic relationships with the carbonatic sequence.
- b) no relics of the high grade pre-Alpine metamorphism have been found either in the carbonatic and terrigenous lithologies or in the basic rocks;
- c) the transition between the carbonatic sequences and the basic rocks is often marked by interbedded dolomitic marbles and metabasalts; such associations have been described in the Eastern Alps (De Zanche et al., 1972; Rossi et al., 1980; Castellarin et al., 1980, 1988; De Zanche, 1990 with ref.) in the upper Ladinian;
- d) calcschists and impure marbles locally contain decimeter to meter blocks of either basement paraschists or basic rocks and quartzites (Col Fenêtre, Venturini et al., 1994a) (Fig. 2.8); the

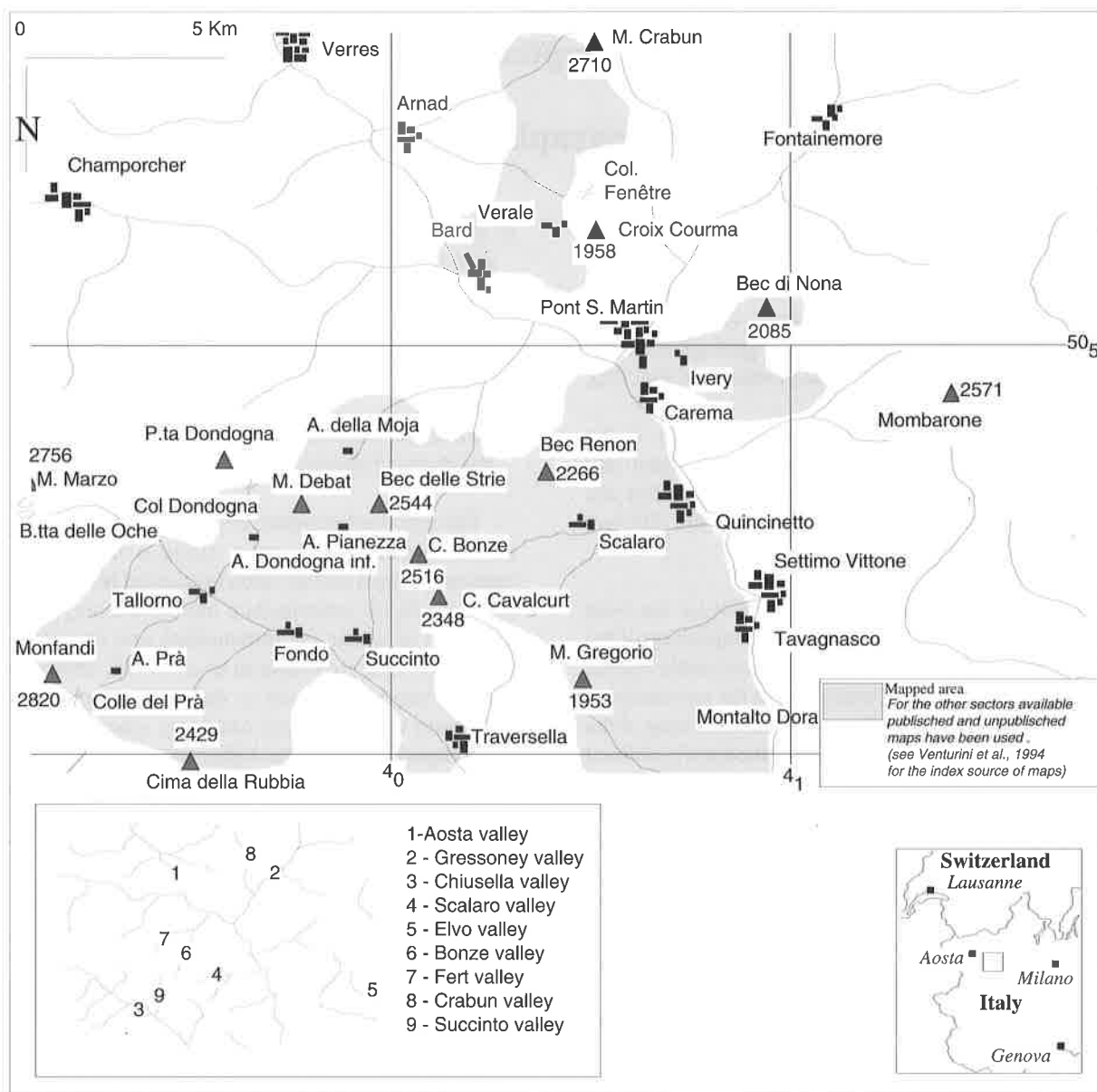


Fig. 2.1 - Geographical sketch of lower Aosta valley and of the middle Chiusella valley.

presence of the blocks within the calcschists does not seem to be the consequence of a tectonic melange, because the calcschists show progressive and not tectonized interbeddings with other lithological horizons (e.g. dolomitic marbles and quartz-rich marbles).

e) the lithologic association in this complex is unknown in the preserved pre-Alpine basement belts of the western Alps (Ivrea-Verbano zone, Valpelline series and intermediate unit of the Mont Mary klippe). Even if dolomitic marbles have been reported in the Ivrea zone, these rocks and their lithostratigraphic relationships with the basic rocks are different in the Sesia zone.

f) the calcschists and the dolomitic marbles of the monometamorphic cover sequences display a strong analogy with some impure marbles and calcschists of the «ophiolitic sequences» of the western Alps.

The significance of the mylonitic metagabbros associated with the monometamorphic cover sequences, doubtfully interpreted by Venturini et al. (1991, 1994) as an «ophiolitic» sequence together with the other basic rocks, have to be reconsidered on the basis of new field and geochemical investigations and on comparison with other gabbros described by the literature in the Western Austroalpine system.

The pre-Alpine high grade basement is composed of paragneisses, impure marbles, mafic and felsic granulites and high temperature amphibolites, which early underwent lower crustal pressure and temperature granulitic conditions (Variscan or older) and they were affected by late-Paleozoic-Mesozoic amphibolite decompressive re-equilibration (Lardeaux and Spalla, 1991).

These lithologies have locally more or less re-equilibrated under different metamorphic conditions during the Alpine orogenic cycle. In this chapter new field and petrographic data on this complex indicate Alpine blueschists re-equilibration conditions (Lardeaux, 1981; Pognante et al., 1987; Ridley, 1989).

As pointed out elsewhere (e.g. Valpelline Serie, II diorito-kinzigitic zone), the pre-Alpine high grade basement can also be distinguished from the polycyclic basement because of the absence of intrusive granitoids. The contact between the pre-Alpine high grade basement and the other complexes is always marked by mylonites.

In the next paragraphs mesoscopic and microscopic descriptions of the different unit-forming lithologies are given. Numerous representative maps and lithologic columns are used to illustrate the more representative outcrops.

2.2.2. Area Location

The investigated area extends from the northern side of the Aosta valley to the Chiusella valley (north western Italy; Fig. 2.1a). The Scalero valley, the central sector of the Chiusella valley, the Fert valley, the upper Bonze valley and the Cima Courma region have been mapped at 1: 5.000 scale (Fig. 2.1b). Additional, field studies have been carried out in the Elvo, Gressoney, Crabun, Savenca, Châmporcher, Soana valleys and in the Lanzo and Pont regions to check the available geological maps. The topographic maps at the scale of 1:10.000 of the Regione Piemonte and Regione Valle d'Aosta have been used as cartographic support.

The field area is limited to the Sesia zone. The predominant lithologic types represented by garnet-omphacite-bearing paraschists (eclogitic micaschists) of the polycyclic basement. The monometamorphic cover sequences mostly crop out in the central sector of the investigated zone, while the pre-Alpine high grade basement unit is mainly located in the northern part of the studied region, although it can be discontinually followed throughout the entire Sesia zone (Table 1).

2.3. Lithology

2.3.1. The Polycyclic basement

2.3.1A THE INTERNAL UNIT

The internal unit of the polycyclic basement is mainly composed of omphacite-garnet-glaucophane bearing micaschists and micaceous gneisses, and of minor chloritoid-porphyroblasts micaschists, eclogitic basic bodies within the micaschists, metagranodiorites to metagranite bodies, jadeite-poikiloblasts orthogneisses and impure marbles. Quartz-micaschists with pre-Alpine relics have been observed in several places.

ECLOGITIC MICASCHISTS (PASSING LOCALLY TO MICACEOUS GNEISSES)

They are composed of millimeter to centimeter phengitic white mica underlining the main foliation together with quartz, glaucophane, zoisite/clinozoisite and rutile; omphacite and garnet are generally surrounded by the main schistosity. Garnet locally preserves relics of a previous foliation (upper Scalero valley; Pian del Gallo). The greenschist re-equilibration is generally very weak or absent. These rocks are characterised by a centimeter quartz bedding alternating with white mica-rich levels and by a reddish weathering. Centimetric to decimeter pre-Alpine leucocratic veins and dykes, locally not completely parallelled to the main foliation, have been observed in the upper part of the Scalero valley as well as in the Albard area and in the central Chiusella valley.

QUARTZ-MICASCHISTS WITH PRE-ALPINE HIGH GRADE RELICS

They generally show quartz-phengite-kyanite-omphacite-garnet-zoisite/clinozoisite-rutile \pm sphene-chlorite-opaques assemblages with relics of pre-Alpine garnet, biotite and kyanite on previous sillimanite. These micaschists are characterised by white-brownish surface and by partially or completely preserved pre-Alpine textures as crosscutting aplitic veins or dark quartz ribbons. The relics of pre-Alpine mineral assemblages are mostly exposed in the Monte Mucrone area (Martinotti, 1970; Dal Piaz et al., 1972; Hy, 1984; Lardeaux and Spalla, 1991) and on the ridge between the Savenca and the Sacra valleys (Barbero, 1992; Venturini et al., 1994a). The last outcrop displays well preserved biotite-sillimanite-garnet-quartz-K-feldspar-ilmenite micaschists and gneisses (kinzigites), together with centimeter K-feldspar-albite-quartz dykes and brown hornblende-amphibolites. As in the Monte Mucrone area, all the pre-Alpine minerals are more or less re-equilibrated under high pressure conditions; jadeite-rich

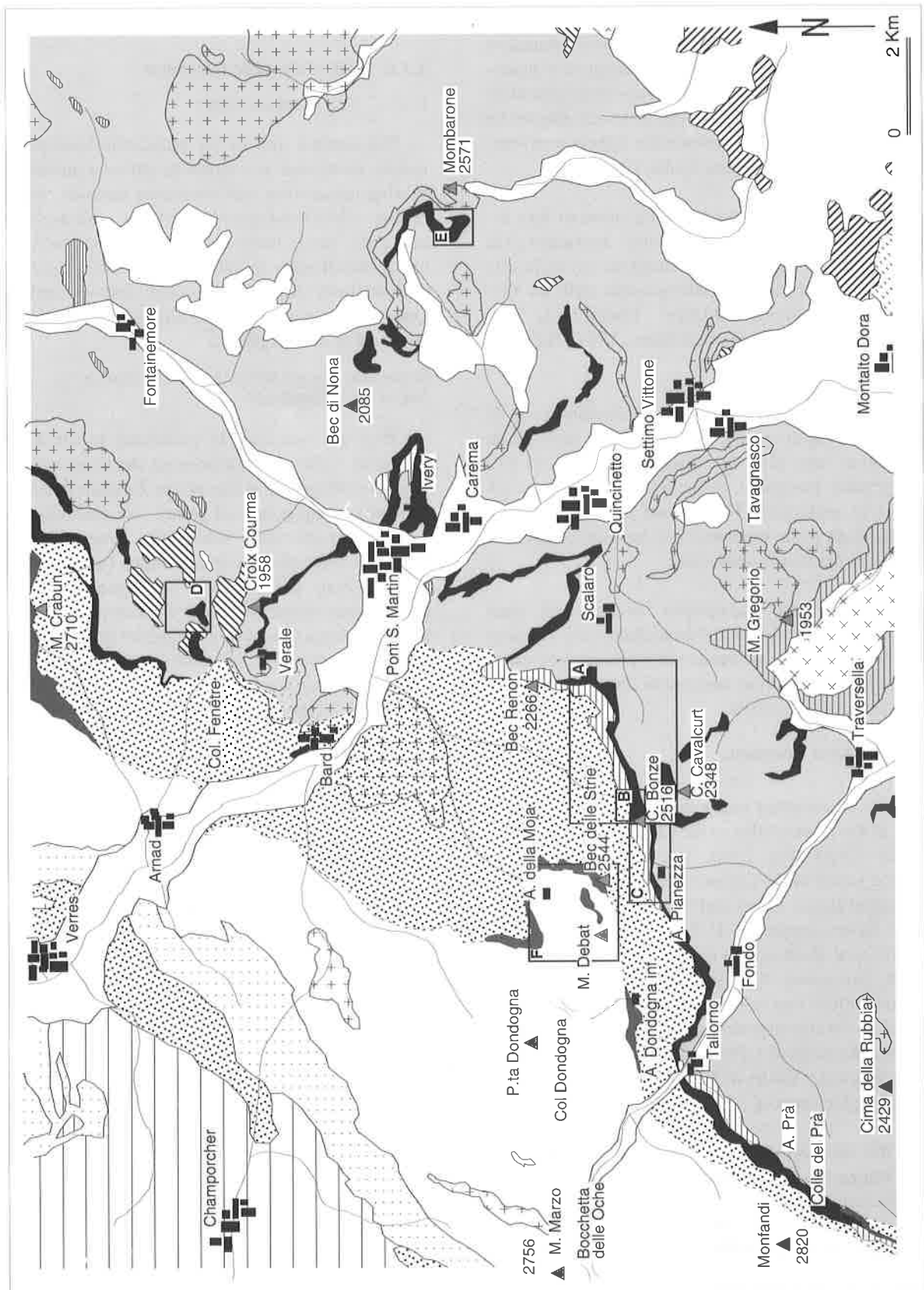


Fig. 2.2- Geological interpretative map of the lower Aosta Valley and of the Chiusella valley (particular from the interpretative Map of Plate 1). Squares indicate the location of the geological maps reported from Fig. 2.5 to Fig. 2.10 (A = Fig. 2.5; B = Fig. 2.6; C = Fig. 2.7; D = Fig. 2.8; E = Fig. 2.9 F = Fig. 2.10). For the legend see next page.

clinopyroxene grows on plagioclase, garnet II \pm phengites replaces biotite as well as kyanite develops on sillimanite and rutile on ilmenite (Barbero, 1992). The evolution of kinzigites to omphacite-garnet-glaucophane micaschists is progressive; no tectonic contacts or mylonic layers have been observed in between.

Lesser well preserved pre-Alpine high grade textures and mineral assemblages have been observed even in the upper sector of the Scalero Valley and in the Arnad region. In the latter case the pre-Alpine assemblage seems to be directly replaced by albite-clinozoisite/epidote-phengite-quartz-chlorite greenschist assemblage. Brown hornblende and plagioclase of the pre-Alpine mafic rocks are replaced by a fine grained actinolite-barroisite-epidote assemblage. Also in this case the passage to the homogeneous greenschist paragneisses is progressive.

SYLVERY MICASCHISTS WITH CHLORITOID PORPHYROBLASTS

They are generally composed of quartz-phengite-chloritoid-garnet-glaucophane-Na-clinopyroxene \pm chlorite-riebeckite assemblages. The chloritoid forms centimetre-sized dark green porphyroblasts which post-date the eclogitic climax and they grow in equilibrium with glaucophane, phengite and garnet II. In the field they are generally characterised by a silvery colour. Whereas no pre-Alpine relics are present in these lithologies, they are commonly referred to the polycyclic basement because of their progressive passages to micaschists with pre-Alpine high grade

relics. The main chloritoid-bearing micaschist occurrences of the internal unit are in the Tavagnasco, St. Maria and Cavalcurt regions, as well as in the northern side of the lower Aosta valley (Pognante, 1979, Pognante et al., 1980).

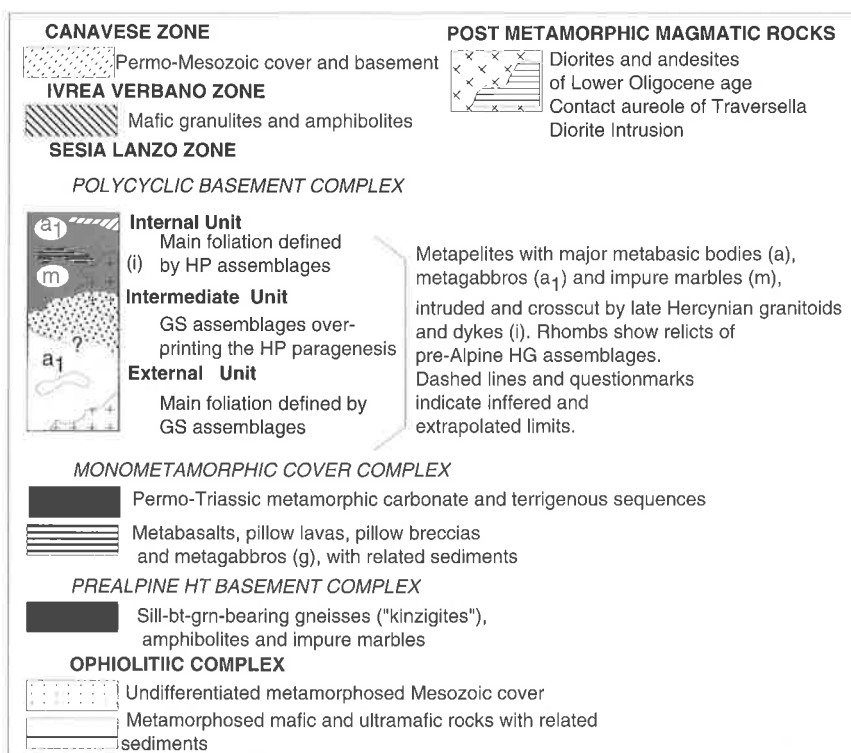
METAGRANITOIDS WITH RELICS OF MAGMATIC TEXTURE

The metagranitoids from the internal unit are characterised by an eclogitic assemblage (quartz-phengite-jadeite-garnet-zoisite/clinozoisite-rutile) replacing the magmatic minerals. Quartz and biotite and pseudomorphs on plagioclase are often the only visible relics of the original protolith. The main foliation is generally underlined by phengitic flakes surrounding jadeite-poikiloblasts, while the greenschist re-equilibration is generally recorded by the substitution of jadeite in albite. The size of magmatic stocks can vary from a few hundred metres (Succinto valley) to kilometer (Mont Gregorio, Tavagnasco) (Fig. 2.2); the more internal bodies generally show a more acid composition with respect to the granodioritic outcrops of the intermediate unit. In the Elvo valley Armando (1992) and Venturini et al. (1994a) have observed granodiorites crosscut by leucogranite dykes. Granodioritic textures are generally recognisable by the presence of millimeter to centimeter-size quartz flattered crystals, while the metagranites are generally greenish. A few basic eclogitised bodies within the metagranitic stocks have been observed in the Palit region or the Mont Gregorio. In the Elvo valley several basic bodies have been mapped at the edge of the granite stocks (Armando, 1992; Venturini et al.,

1994a); these lithologies could be interpreted as reworked gabbroic bodies related to the first stage of intrusions, whereas neither magmatic textures or relics are preserved within the mafic bodies.

JADEITE-POIKILOBLAST ORTHOGNEISSES

These lithologies have been observed in several zone of the lower Aosta and Chiusella valleys. They generally form decameter dykes or sub-parallel leucocratic layers within the omphacite-garnet-glaucophane micaschists. In the southern sector of Mont Cavallaria and in the southeast face of Cima La Rubbia the jadeite-orthogneisses form hundred meter-size outcrops. In thin section quartz-jadeite-



phengite-garnet-zoisite/clinozoisite-rutile±sphene-ilmenite mineral assemblages are generally observed; centimeter-size jadeites contain small granoblasts of quartz together with big flakes of phengitic white mica and zoisite nematoblasts; the jadeite is only partially and locally replaced by albite pseudomorphs and by a rim of acmitic clinopyroxene. A magmatic origin of these lithologies was postulated by Andreoli et al., (1976), Compagnoni et al. (1977a), and Lombardo et al. (1977). In the field no magmatic textural relics have been found, so that further laboratory analysis have been required to confirm the magmatic origin of these lithologies. The geochemical results are given in Chapter 3.

LEUCOCRATIC ORTHOGNEISSES

These rocks are common in the internal unit within the micaschists and the micaceous gneisses; they generally consist of decimeter to meter dykes sub parallel to the eclogitic foliation. Quartz, albite after jadeite, phengite, clinozoisite/epidote, microcline±garnet and cloromelanite form the main foliation. The protolith of these leucocratic orthogneisses is probably a pre-Alpine pegmatite related to the high grade metamorphic cycle.

ECLOGITIC BASIC BODIES

Layers and boudins of mafic eclogites are very common within the omphacite-garnet-glaucophane micaschists and micaceous gneisses; they are formed by well preserved eclogitic assemblages. Glaucophane, zoisite/clinozoisite, rutile and pyrite are present together with omphacite and garnet, while quartz, chlorite, sphene represent minor phases. Observed pre-Alpine mineral relics are very rare (colourless amphibole and pseudomorphs on biotite). The eclogitic boudins, generally decimeter to meter in size, are particularly concentrated north-east of Scalero village, in the Tour Promotton region, and in the lower Bonze valley. Three hundred meters above Quincinetto a few characteristic eclogitic dykes crosscut the omphacite-garnet micaschists. Centimeter euhedral omphacite and garnet constitute the metamorphic assemblages of the rock together with phengite and a Mg-rich biotite. The biotite seems to grow in equilibrium with the high pressure minerals. These rocks have been analysed by X-ray fluorescence while microprobe investigations have been carried on the Mg-rich biotite.

IMPURE MARBLES

They are characterised by a pale green colour, a granoblastic texture and by the presence of several basic boudins. Several impure carbonate outcrops have been mapped in the Crabun valley. The marbles form a narrow and discontinuous band which extends from the Cima Courma to Fontainemore. Stable mineral assemblages are formed by calcite-clino-zoisite-

apatite-white mica±quartz-ankerite; a clino-pyroxene of supposed pre-Alpine age is often observed (Castelli, 1991). Similar occurrences have been mapped in the Marine area as well as at Tour Promotton. These morbles are present only within the poly-cyclic basement omphacite-garnet micaschists (Fig. 2.2).

2.3.2B INTERMEDIATE UNIT

The intermediate unit corresponds to unit B3 of Compagnoni et al. (1977a). It consists of the same lithologies of the internal unit, excepting for the higher degree of re-equilibration under greenschist conditions. Indeed, in the intermediate unit the high pressure mineral assemblages are partially or completely substituted by greenschist assemblages, although relics of jadeite and omphacite can be still preserved.

ALBITIC GNEISSES AND QUARTZ-MICASCHISTS WITH RELICS OF THE HIGH PRESSURE PARAGENESIS

This group of rocks represents the product of a pervasive greenschist re-equilibration of original omphacite-garnet micaschists and micaceous gneisses of the internal unit. The main foliation is composed of phengite, clinozoisite and quartz and it envelops relics of garnet, omphacite and glaucophane. The albitic gneisses and quartz-micaschists generally show a fine grained texture and are easily recognisable even in the field by the presence of albite porphyroblasts and garnet, the latter more or less replaced by fine chlorite. The albite-quartz micaschists are the main constituents of the Sesia zone between Quincinetto and Donnaz in the Aosta Valley and in the lower Fert Valley. They crop out in the Chiusella valley, between Tallorno and Pasquere, and in the Crabun valley between Fei and Prà (Fig. 2.2). On the southern side of the lower Aosta valley they occur between the monometamorphic cover sequences, to the south-east, and the external unit to the north-west.

MICASCHISTS WITH PORPHYROBLAST OF CHLORITOID

Some small outcrops of chloritoid-bearing albitic gneisses have been mapped at Cima Dondogna, along the ridge between the Chiusella and the Aosta valleys. They have the same mineral assemblages as the previous albite-quartz-micaschists, but also display centimeter porphyroblasts of dark green chloritoid growing in equilibrium with the phengite-clinozoisite foliation. Relics of garnet and glaucophane have also been observed in these outcrops. The same rock type can be observed on the other side of Chiusella valley, along the ridge between Buffa lakes and the Prà valley (Fig. 2.2).

ALBITE-EPIDOTE ORTHOGNEISSES

They are made of fine grained albite-clinozoisite-quartz±phengite and constitute decimeter to meter

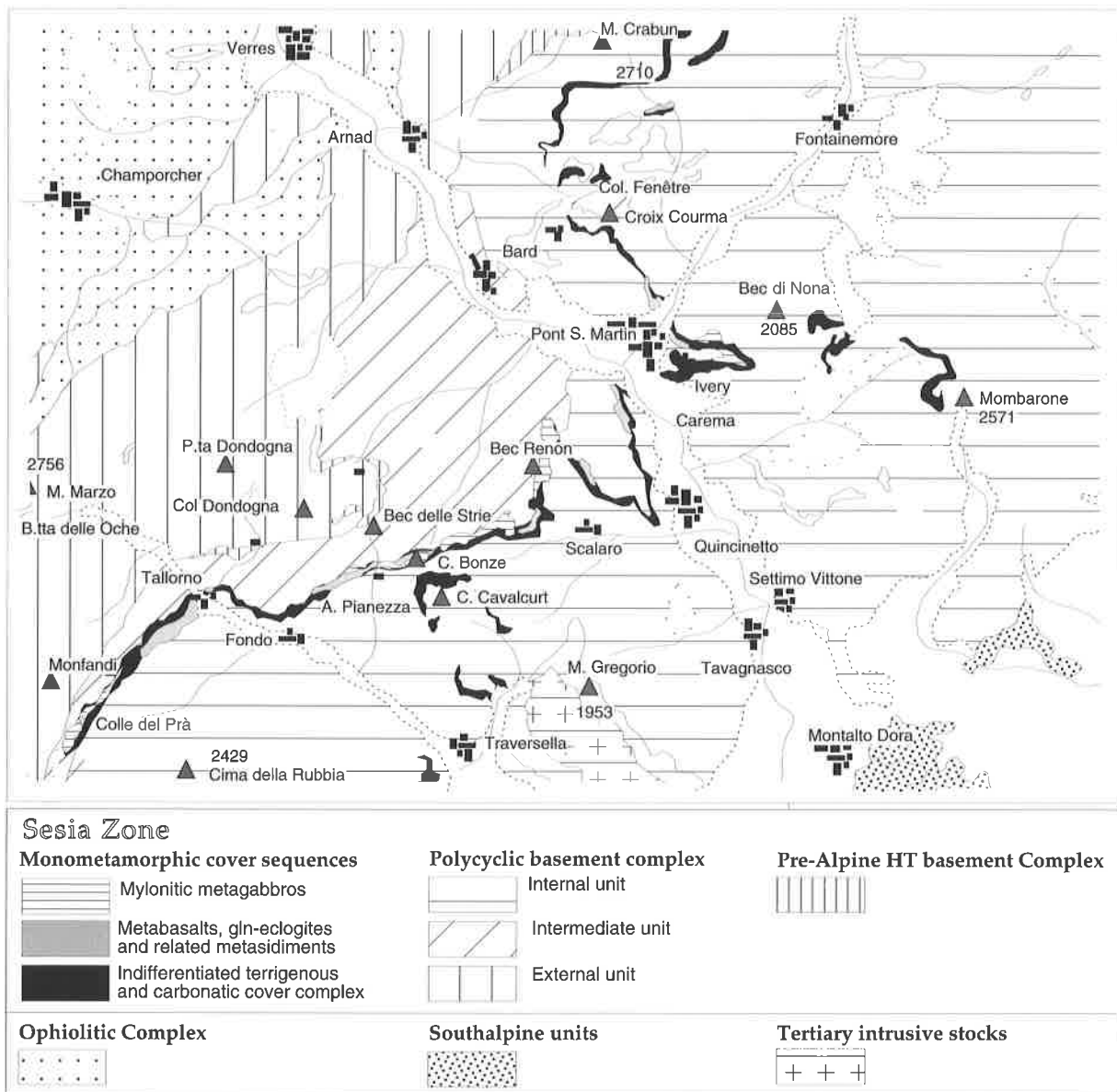


Fig. 2.3 - The monometamorphic cover sequences in the lower Aosta valley. The mafic eclogitic rocks (gln-eclogites, metabasalts and related metasediments) outcrop along a narrow band between the internal and the intermediate unit of the polycyclic basement, while the terrigenous and carbonatic lithologies are distributed either within the internal unit or at the boundary with the intermediate unit. The gabbroic bodies are located mainly in the southern side of lower Aosta valley within the monometamorphic cover sequences or at the boundary between the covers and the polycyclic basement. An outcrop of metagabbros was mapped also above Ivery, in the northern side of the Aosta valley.

levels sub-parallel to the main foliation. They are generally interpreted as transposed dykes and associated with the quartz-micaschists.

METAGRANITOIDS WITH RELICS OF THE MAGMATIC TEXTURES

These rocks constitute a kilometer-size body extending between the Albard-Verale area and the Brenve valley (Châmporcher). Several small bodies have also been mapped in the upper Bonze unit. They differ from

the metagranitoids of the internal unit because of the stability of albite (instead of jadeite) and some differences in bulk compositions of the intrusive rocks which mainly show granodioritic compositions. The paragenesis is constituted by quartz, phengite, albite, microcline, clinozoisite/epidote, rutile, riebeckite \pm chlorite; relics of garnet and glaucophane can locally be observed while Na-rich clinopyroxene are completely replaced by fine white mica, clinozoisite and feldspars. In the Chiusella valley the metagranodiorites are less frequent and mostly localised north-west of Prà.

2.3.1c THE EXTERNAL UNIT

The external unit is composed of rocks where the main foliation is defined by greenschist mineral assemblages (Gneiss Minuti complex or B1 and B2-zones of Compagnoni et al., 1977a). Albite-rich leucocratic and mesocratic banded gneisses represent the more widespread lithologies. Metagranites and micaschists crop out in the Aosta valley and in the northern region, while in the southern sector of the External unit several marbles crop out, interbedded to micaschists and gneisses.

ALBITIC GNEISSES

They are made of quartz-white mica (phengite)-clinozoisite/epidote-chlorite-albite \pm rutile-sphene; the foliation is defined by alternating ribbons of quartz and albite and white mica-clinozoisite. Relics of Na-amphibole have been found, although they are completely replaced by a new pale green amphibole (barroisite-actinolite). The albitic gneisses of the external unit are commonly known as gneiss minuti because of their mesoscopic fine grained texture. They represent the main lithology of the external unit of the central Sesia zone, forming the steep cliffs between Arnad and Hône in the Aosta valley. Representative outcrops of albite gneisses can be seen along the ridge of Machaby and Tête du Cou (Fig. 2.2). Within these lithologies are strongly mylonitised fine grained gneisses with similar greenschist assemblages; these mylonitic levels are parallel to the main gneiss foliation. More to the south the albite gneisses are located towards the external edge of the Sesia zone in the Champorcher valley and in the upper Chiusella valley.

GRN-AB GNEISSES AND GARNET-QUARTZ MICASCHISTS

These lithologies crop out in the central part of the Fert Valley. They are very similar to the albitic-gneisses with exception of small granoblasts of pink garnet. The paragenesis is white mica (phengite)-quartz-garnet-epidote-albite \pm chlorite-sphene-pyrite; Na-rich clinopyroxene has been never observed while glaucophane relics are surrounded by the main foliation and partially substituted by green amphiboles. The only mesoscopic difference between these lithologies with the albitic gneisses is the presence of euhedral pink garnet. The garnet-bearing gneisses crop out also in the upper Chiusella valley north of the Buffa lakes.

QTZ-MICASCHISTS WITH PRE-ALPINE RELICS

A small outcrop of pre-Alpine high grade paragneisses partially reworked by the Alpine greenschist metamorphism has been found on the road to Bonavesse, near Arnad. The main foliation is underlined by white mica-quartz-clinozoisite/epidote-

chlorite-green biotite and porphyroclasts of albite, growing on pre-Alpine kinzigitic assemblages. Only the habits of the previous high grade minerals are preserved; no high pressure minerals have been observed. These lithologies do not seem to have undergone high pressure conditions between the pre-Alpine high grade metamorphism and the greenschist reworking. Not far from this area, metakinzigites and transformed high grade amphibolites have been observed. In the same region some well preserved «eclogitised granulites» have been described by Lardeaux and Spalla (1991); The transition from granulitic facies to the eclogitic conditions was not observed in any of the collected samples.

ALBITE-BEARING METAGRANITOIDS WITH RELICS OF MAGMATIC TEXTURES

Some well preserved metagranitoid outcrops have been observed close to Anoié (Arnad region). Although the textures are perfectly preserved, the metamorphic mineral assemblages are completely re-equilibrated under greenschist conditions. Also in this case these lithologies do not show any high pressure relics; on the other hand the greenschist re-equilibration seems to have directly reworked the original protoliths. The pressure-temperature path could thus show basic differences from the other paths followed by the lithologies of the internal and intermediate units.

2.3.2. Monometamorphic cover sequences

The monometamorphic cover sequences are composed of different lithologies which have been previously grouped in two main units: a) the Scalero unit, made essentially of terrigenous and carbonatic metasediments, and b) the Bonze unit composed of mafic rocks and subordinate quartz-rich metasediments (Venturini et al., 1991). According to Venturini et al. (1994a), the former unit is interpreted as a Permo-Triassic cover while the latter represents a basaltic sequence partially interbedded with the supposed upper Triassic dolomitic marbles. Although the adopted subdivision is a helpful tool for the field mapping, we prefer to lay down this subdivision which does not always reflect the field observations and relationships.

The monometamorphic cover sequences crop out in the central Sesia zone, forming a narrow but continuous band, often interposed between the internal and the intermediate unit of the polycyclic basement or within the intermediate unit itself (Fig. 2.3).

The main mapped lithologies are:

- a) eclogitic mafic rocks, which have been subdivided into phengite-glaucophane eclogites, phengite-glaucophanites, partially or completely reequilibrated eclogites and epidote-rich metabasic rocks,
- b) quartzitic metasediments closely related to the previous metabasic lithologies,
- c) mylonitic metagabbro bodies, generally outcropping together with metabasites,
- e) carbonatic rocks, comprising yellow dolomitic marbles, white mica-rich metalimestones, quartz-rich marbles and calcschists, Mn-bearing calcschists and meta-conglomerate marbles,
- f) mesocratic paragneisses, impure quartzites, graphitic micaschists, mesocratic to leucocratic gneisses containing centimeter to meter blocks and/or boudins of epidote-rich metabasites and acid rocks.
- g) centimeter levels of epidote-rich metabasites interbedded with leucocratic gneisses and thin levels of carbonatic rocks.

GLAUCOPHANE-ECLOGITES (PLATES III & IV)

These rocks crop out in the upper sector of the Scalario valley, in the upper Succinto valley, between Tallorno and Fumà in the middle Chiusella valley, and at Alpe Prà; some isolated outcrops have been mapped in the Crabun valley and between Carema and Ivery (Fig. 2.3).

The predominant occurrences are meter to decameter-thick dark blue to green blue massive glaucophane eclogites, made of glaucophane-Na-rich clinopyroxene-jadeite-zoisite/clinozoisite-Mg chlorite-rutile±phengite-epidote-NaCa amphibole. These mafic eclogites mafic show different metamorphic assemblages depending on the distribution of different rock-forming minerals or by the greenschist re-equilibration products. The main foliation is generally underlined by glaucophane and locally is crosscut by veins of omphacite-garnet-clinozoisite. In thin section two foliations can be recognised: the former is generally preserved within the jadeite, omphacite and garnet and is made of Mg-chlorite, a first generation of blue amphibole, zoisite/clinozoisite and sphene; the latter is surrounding the high pressure mineral and is mainly underlined by glaucophane and clinozoisite. Phengite is generally concentrated in thin levels. In a few samples a prograde Ca-amphibole has been observed within the garnet (MB24) or surrounded by the

eclogitic foliation; microprobe investigations indicate it to be a Ca-actinolite.

The glaucophane-eclogites can be weakly reequilibrated under greenschist conditions, with new assemblages growing as pseudomorphs on the high pressure relics. The reequilibrated lithologies can be recognised in the field by a lighter colour due to the growth of epidote and chlorite. The eclogitic mafic rocks have been interpreted as the result of metamorphic Alpine transformations of basalt protoliths (Venturini et al., 1991, 1994). The field evidence for their origin are: 1) the presence of pillow breccias textures; 2) the alternance of thin Mn-rich quartzitic levels within these mafic rocks; 3) the absence of gabbroic textures which permit to distinguish the glaucophane-eclogites from the mylonitic metagabbros. Bulk rock geochemical investigations have been carried on in order to confirm the basaltic origin of the glaucophane-eclogites and of the reequilibrated metabasites; the results are given in Chapter 3.

QUARTZ-RICH METASEDIMENTS CLOSELY RELATED TO THE GLAUCOPHANE-ECLOGITES (PLATE III)

The quartz metasediments, characterised by a silvery colour, generally form centimeter to decimeter levels within the glaucophane-eclogites; locally they form the matrix of eclogitic mafic breccias. In some cases these metasediments show centimeter-thick alternations of quartz-rich levels and glaucophane-rich levels. In the field small pink garnet and glaucophane nematoblasts can be recognised together with big flakes of phengite. In some cases quartz constitutes 60-70 % of the whole rock; the more representative outcrops occur at Cima Bonze, in the Succinto valley and near Tallorno. (fig. 2.4, 2.5 and 2.6).

BLASTOMYLONITIC METAGABBROS (PLATE V)

The metagabbros can be distinguished from the other mafic rocks by relics of magmatic textures and/or by the alternance of zoisite/clinozoisite-rich leucocratic layers and glaucophane-rich mafic layers. They form stretched decameter to hectometer-size masses which are adjacent either to the glaucophane-eclogites (Balma Nera, Pianezza, Cima Bonze, Ivery), or to the other monometamorphic sediments, as dolomitic marbles (upper sector of the Bonze valley, Pianezza) and quartz-calcschists (Cima Bonze, A. Colletto, A. Prà, Cima Prà) (Fig. 2.3 and detail maps). Smaller metagabbro outcrops have also been mapped on the northern ridge of the Chiusella valley at Cima Dondogna and between the Cima Dondogna and the Monte Marzo within the intermediate unit of the polycyclic basement (Accotto, 1992).

The metagabbros always show a pervasive mylonitic texture underlined by oriented nematoblasts of glaucophane and zoisite/clinozoisite. In thin section they display an eclogitic mineral assemblage developing on a previous prograde blueschist foliation, which is made of glaucophane-zoisite-Mg chlorite-sphene±white mica-quartz. Several structural relics of the magmatic assemblage can already be seen; discoloured hornblende constitute pre-kinematic porphyroblasts partially substituted by glaucophane.; the plagioclase-sites have been replaced by zoisite and fine white mica. The high pressure minerals (garnet-omphacite-rutile) grow on the prograde foliation, which is generally preserved within the garnet porphyroblasts. A second generation of blue amphibole underlines the retrograde blueschist foliation, together with clinozoisite-epidote, phengite and sphene II. The greenschist re-equilibration is generally not present or very weak; only close to the intermediate unit the mylonitic metagabbros show a scattered greenschist re-equilibrations with chlorite growing on garnet and green amphibole on glaucophane: these paragenesis are never related to a new pervasive foliation.

The mylonitic metagabbros were initially correlated to the metabasaltic glaucophane-eclogites (Venturini et al., 1991, 1994) as part of an «ophiolitic slice». During further investigations they have been compared to other masses of similar lithologies observed in the Sesia zone, as the Corio and Monastero metagabbros (Bianchi et al., 1964), the Cima Bossola metagabbros (Compagnoni and Fiora, 1977) and the other gabbro bodies (Mont Nery, Cima Pianone and Mont Pinter (Dal Piaz 1976; Gosso et al., 1979; Stünitz, 1989; Chabloz, 1991). The mylonitic metagabbros of the Bonze region show field similarities with the Mont Nery and Cima Pianone metagabbros, because of their coarse size and of the alternance of leucocratic and mafic layers, while they are quite dissimilar from the Cima Bossola and Corio and Monastero metagabbros, which are small grain glaucophanites and homogeneous eclogites, progressively passing to the eclogitic micaschists of the polycyclic basement. These differences have also been confirmed by geochemical data and will be further discussed.

CARBONATIC ROCKS (PLATES VI, VII & VIII)

The carbonatic lithologies comprise yellow dolomitic marbles, white mica-rich meta-limestones, quartz-rich marbles and calcschists, Mn-bearing calcschists and metamorphosed polygenic breccias. The quartz-rich marbles and calcschists are the most common lithologies together with the yellow dolomitic marbles, and can be found along all the

extension of the monometamorphic cover complex from the Crabun valley to the Cima Prà (Fig. 2.3).

The dolomitic marbles (Plate VI) are characterised by a light brown-yellow colour and crop out either as meter to decameter-thick lenses and boudins within the glaucophane-eclogites or as continuous levels together with the calcschists and the quartz-rich marbles. The more important outcrop of dolomitic marbles occurs in the Mombarone lake area (Fig. 2.9), where they are over 50 meters thick. Other important dolomitic marble outcrops have been mapped in the Crabun area as well as in the Cavalcourt region and the Bersella valley. They are generally characterised by a weak foliation underlined by stretched dolomite, calcite and big flakes of white mica, which can be concentrated in thin levels. Some levels of yellow dolomitic marbles have been folded and boudinaged within the glaucophane-eclogites (Cima Bonze, Pianezza, B. Renon); unfortunately, no evidence of primary contacts has been found. At the same time they do not represent a particular or continuous tectonic sheet.

The quartz-rich marbles and calcschists (Paate VII) form meter to decameter-thick continuous outcrops, are generally characterised by dark grey to brownish weathered colour, and crop out over the entire monometamorphic complex: in the Mombarone area as well as in the Bersella valley they are closely associated with the dolomitic marbles. The calcschists locally pass to polygenic breccias containing decimeter to meter stretched blocks of dolomitic marbles, glaucophane-eclogites, quartzites and basement rocks; in some cases they show a conglomeratic facies with original bedding not completely transposed (Col Fenêtre, Cima Bonze and Pianezza, see detail maps Fig. 2.4-2.7). They contain quartz and less frequent phengite that underline the main foliation; the quartz is homogeneously distributed in the rocks and in some cases a compositional grading is observable. The carbonates (mainly calcite with subordinated dolomite and ankerite) occur as euhedral crystals; zoisite/clinozoisite, sphene and garnet represent minor phases.

The Mn-rich calcschists are closely related to the quartz marbles and calcschists (Plate VIII). They are characterised by a dark grey colour, pervasive foliation underlined by phengite and zoisite, and centimeter to decimeter marble lens and spessartine-rich fels. The Mn-rich levels are particularly abundant at Cima Bonze, in the Scalero valley and at Alpe Prà, where both carbonatic lithologies and mafic rocks compose the monometamorphic cover sequences.

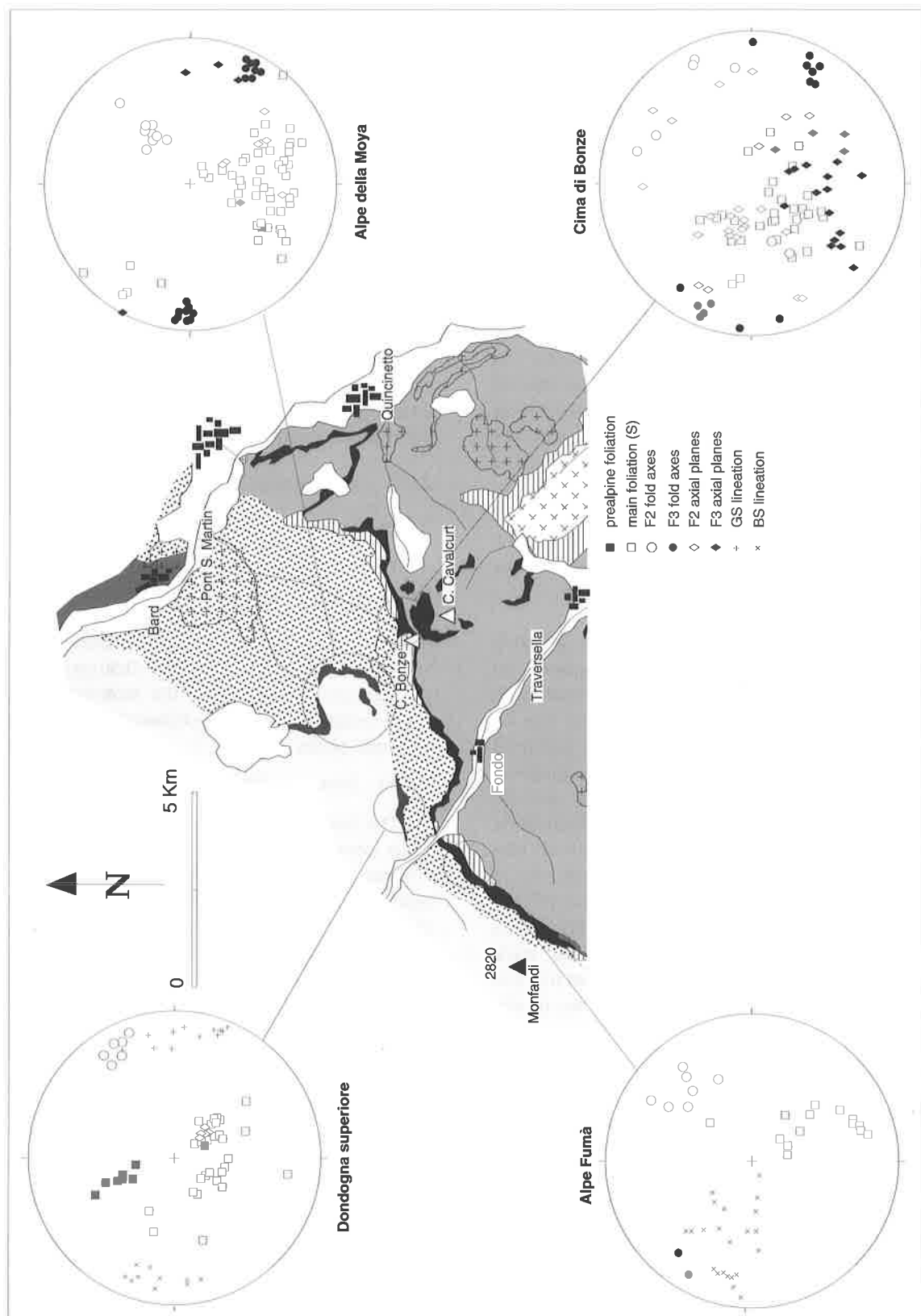


Fig. 2.4 - Stereograms of the different fold phases and lineation observed in the lower Aosta valley and in the Chiusella valley. The main foliation is generally plunging to the north of few degree. F2 fold axes are oriented north-east, while F3 fold are oriented WNW-ESE, plunging of few degree in both directions. F2 axes fold show a certain deviation to the north in comparison to the F2 direction reported in literature.

ALBITIC GNEISSES, QUARTZITES AND IMPURE QUARTZITES (PLATE IX)

These rock-types crop out in the upper Scalario valley, in the Succinto valley and locally in the Mombarone lake area and in the Tallorno region. They are closely interbedded and make up continuous meter-thick horizons. The mesocratic gneisses, made of quartz, albite, phengite, chlorite, clinozoisite/epidote±glaucophane and sphene, are interbedded with the impure quartzites, which normally display concordant sharp contacts; phengite and quartz underline the main foliation. The impure quartzites can be over ten meters thick (A. Giacotto, Scalario valley); quartz and phengite represent the main mineral together with subordinate albite, chlorite and green biotite; albite grows both in the matrix or as porphyroblasts (Cima Bonze). The impure quartzites occur as massive white-grey horizons. Within the impure quartzites are generally centimeter to decimeter horizons of pure quartzites with thin phengite-rich levels. The impure quartzites can show progressive passages to quartz-rich marbles (Cima Bonze and Cavalcurt).

Both impure quartzites and mesocratic gneisses show similarities with the mylonitic polycyclic basement: impure quartzites can be confused with transposed meta-dykes while the gneisses can be indistinguishable from the strongly foliated metakinzigites. Because of this, the main arguments used to associate the impure quartzites and the mesocratic gneisses with the monometamorphic cover are their progressive passages to the calcschists, the complete absence of pre-Alpine textures and paragenesis and the presence of thin levels of carbonatic lithologies and mafic rocks (Cavalcurt, Mombarone lake). Whole rock geochemical analyses have been carried out to try to distinguish between the different protoliths; results are presented in the geochemical section.

ALBITIC GNEISSES CONTAINING CENTIMETER TO METER BLOCKS AND/OR BOUDINS OF EPIDOTE-RICH METABASITES AND ACID ROCKS (PLATE IX)

The mesocratic gneisses are closely related to the mesocratic leucogneisses and the impure quartzites and, in some cases, to the yellow dolomitic marbles (Cavalcurt). They are characterised by a silver-grey colour and foliated aspect and they are made of albite porphyroclasts, quartz, clinozoisite/epidote, phengite±garnet, cloromelanite, microcline, chlorite, sphene. The mesocratic gneisses and the albitic quartz-micaschists often contain decimeter to meter blocks of epidote-rich mafic rocks, which suggests their similarity with the Gneiss Pipernoides of the Mont Emilius and of the Etirol Levaz slice (Amstutz, 1962;

Bearth et al., 1980; Ballèvre et al., 1986); in some cases thin basic levels within these gneisses were recognised (Cavalcurt). These gneisses locally contain decimeter blocks of acid rocks (Rif. Chiaromonte).

These lithologies present the same convergence aspect problems with the mylonitised polycyclic basement as the impure quartzites and the mesocratic gneisses; because of this, in some cases it has not been possible to define with certitude their association with the monometamorphic cover; for the same reason several samples of the albite-micaschist matrix and of the acid and basic blocks and levels have been sampled and analysed with X-ray fluorescence, to try to define possible geochemical differences with the mylonitised polycyclic basement.

2.3.3. Representative Areas

2.3.3A INTRODUCTION

The description of some representative areas has been included; in these areas the analytic description of the monometamorphic cover sequences, which are particularly well exposed, has permitted to deduce some conclusions about the stratigraphic and paleogeographic setting of the monometamorphic cover complex between the Paleozoic and the Alpine orogenic cycles.

2.3.3A SUMMARY OF STRUCTURAL DATA

The field investigations carried on during this study permitted to acquire new data relative to the structural setting of the analysed units. Figure 2.4 reports the stereographic projection of the structural elements recognised. The structural data were mainly collected in the Bonze area, in the upper Scalario valley, in the Fert valley and in the middle Chiusella valley. Detail structural studies were also effectuated in the Chiusella valley by Postelwhite (1992). Exhaustive structural geology investigations of the northern side of the Aosta valley (Mombarone area) and in the Croix Courma area were carried out by Pognante et al. (1980) and Passchier et al. (1981). A brief summary of the structural data acquired on the field during this study is given below.

Four main Alpine folding phases have been recognised during the field mapping and the microscopic analysis. Furthermore, several relics of pre-Alpine fold phases crosscut by acid dykes, have been observed in the upper Scalario valley. The first Alpine folding phase (F1) is characterised by millimeter to centimeter rootless isoclinal folds which are mainly preserved within the garnet-omphacite-micaschists. In thin section phengite, a first generation

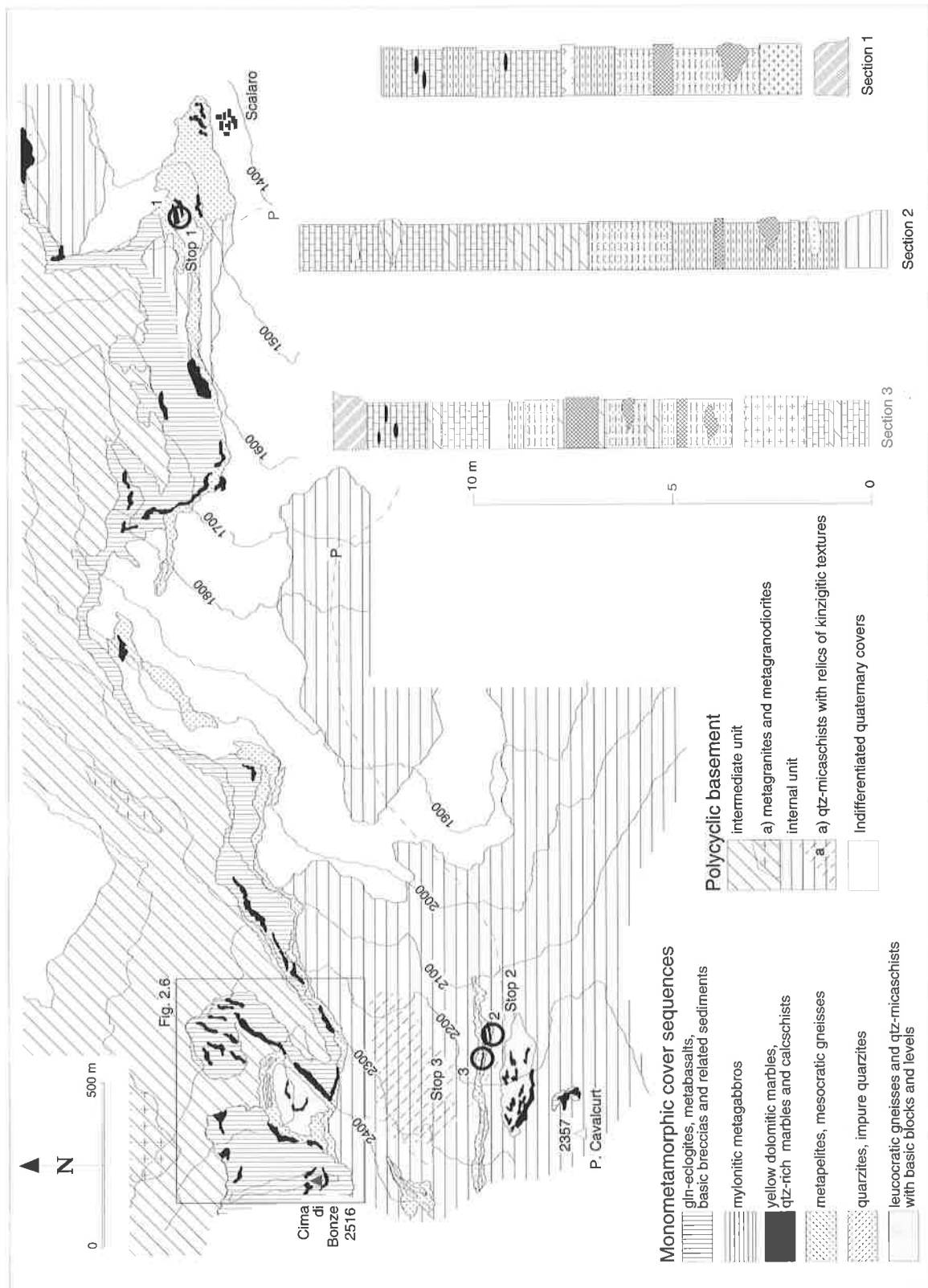


Fig. 2.5 - Geological map and lithological sections of the Scalaro valley. Square indicates location of Fig. 2.7. The monometamorphic cover sequences crop out in the northern side of the valley and are particularly well exposed in its upper sector. P letters indicate the starting places to visit the sections described in the text. (Par. 2.1.5.a). Circles indicate the position of the lithologic sections. Legend of the lithologic columns is reported in annex 1, together with all abbreviations used in the text.

of glaucophane, zoisite and sphene underline this first fold generation.

F2 folds are isoclinal to tight and with axes generally plunging 20-30° to E-NE and only locally to W-SW (Bonze region). The eclogitic assemblages seem to be syn- or pre-kinematic to F2 folds. In the external unit of the polycyclic basement the axial plane S2 schistosity contains glaucophane, garnet clinozoisite and phengite.

F3 folds are tight to open and are generally oriented E-SE or W-NW, with a dip of a few degrees; the folding episode post-dates the high pressure climax phase and the axial plane S3 schistosity is generally underlined by phengite, clinozoisite, glaucophane/riebeckite and chloromelanite. The F3 folding episode is responsible for the mesoscopic and macroscopic fold structures which can be observed both at the outcrop scale and at the unit-mapping scale.

F4 folds are open and normally related to the weak greenschist re-equilibration. F4 axes are oriented N-S, plunging in both directions a few degrees. The weak greenschist re-equilibration characterising the internal basement unit and the monometamorphic cover sequences is related to this phase.

In the Chiusella valley two generation of lineations have been evidenced at the passage between the internal and the intermediate unit and at the contact between the internal unit and the pre-Alpine high grade basement unit. A first lineation, related to the S2 schistosity is underlined by blue amphibole and plunges E with a certain dispersion (Dondogna superiore; Alpe Fumà) while a second lineation generation, contained in the S2 schistosity plunges a few degrees to east, have been observed only in Dondogna superiore and is underlined by clinozoisite/epidote, phengite, paragonite and chlorite. The folding phases recognised in the investigated area are coherent with those described by the previous authors in the central Sesia zone (Par. 1.3.3a and Tab 1.7). Moreover a F0 deformation phase has been recognised in the textures of the mylonitic metagabbros and can be related to the F0 phase of Pognante (1979); this phase will be further described and analysed in the mineral chemistry chapter.

2.3.3B THE SCALARO VALLEY (FIG. 2.5)

The Scalero valley is located on the southern side of the lower Aosta valley; it can be reached with a road starting from Quincinetto to S. Maria and Scalero (after S. Maria a private road begins: ask for the key and permission in Quincinetto).

The Scalero valley is limited to the north by the steep faces of the B. Renon an Cima Battaglia and to the south by the divide with the Chiusella valley. The Monometamorphic cover sequences crop out on the northern side of the Scalero valley. They are macroscopically defined by an alternance of light levels (quartzites, mesocratic gneisses and calcschists) with dark green horizons (glaucophane-eclogites and mylonitic metagabbros). The first representative lithologic section is exposed one hundred meters to north-west of the Scalero village (Section 1); it is composed of five meters of leucocratic gneisses and impure quartzites containing decimeter levels and blocks of epidote-rich mafic rocks. At the top of the sequence the impure quartzites grades to graphitic metapelites (one meter) and are followed by three meters of Mn-rich calcschists. Within the calcschists a level of metapelites occurs. This leucogneiss-impure quartzite-Mn-rich calcschists association crops out also in the upper sector of the Scalero valley (sections 2 and 3). To reach this area follow the road in the central part of the valley to 1710 meter altitude, then walk west and keep the left side of the upper Scalero valley north-east to Cima Cavalcourt (stop 2 - see path on Fig. 2.5). The sections 2 and 3 have been reconstructed at 2220 m of altitude on the northern cliff, constituted of a metric alternance of mesocratic gneisses, metapelites and impure quartzites containing boudins and levels of epidote-rich mafic rocks. Decimeter horizons of dolomitic marbles are interbedded with the metapelites and basic levels. At the top of this sequence the calcschists and quartz-rich marbles contain thin levels of spessartine and calcite boudins and meter blocks of yellow dolomitic marbles. The calcschists are overridden by omphacite-garnet micaschists of the polycyclic basement.

The cliff presents two small steep channels which can be climbed to reach the Cima Bonze area; between the cliff and the Bonze sector the polycyclic basement is particularly well preserved (stop 3). In this zone several pre-Alpine high grade textures are preserved.

2.3.3C. THE CIMA DI BONZE AREA (FIG. 2.6)

The Cima Bonze area is located between the Scalero and the Bonze valley. This sector can be reached directly from the Scalero valley (see previous itinerary) or from the Rif. Chiaromonte, which is located in the upper Bersella valley (the refuge is actually closed and probably out of service; if you want to use it, ask for the key in Traversella).

In the Cima Bonze area the monometamorphic cover sequences and the polycyclic basement crop out in direct geometric contact. The carbonatic cover

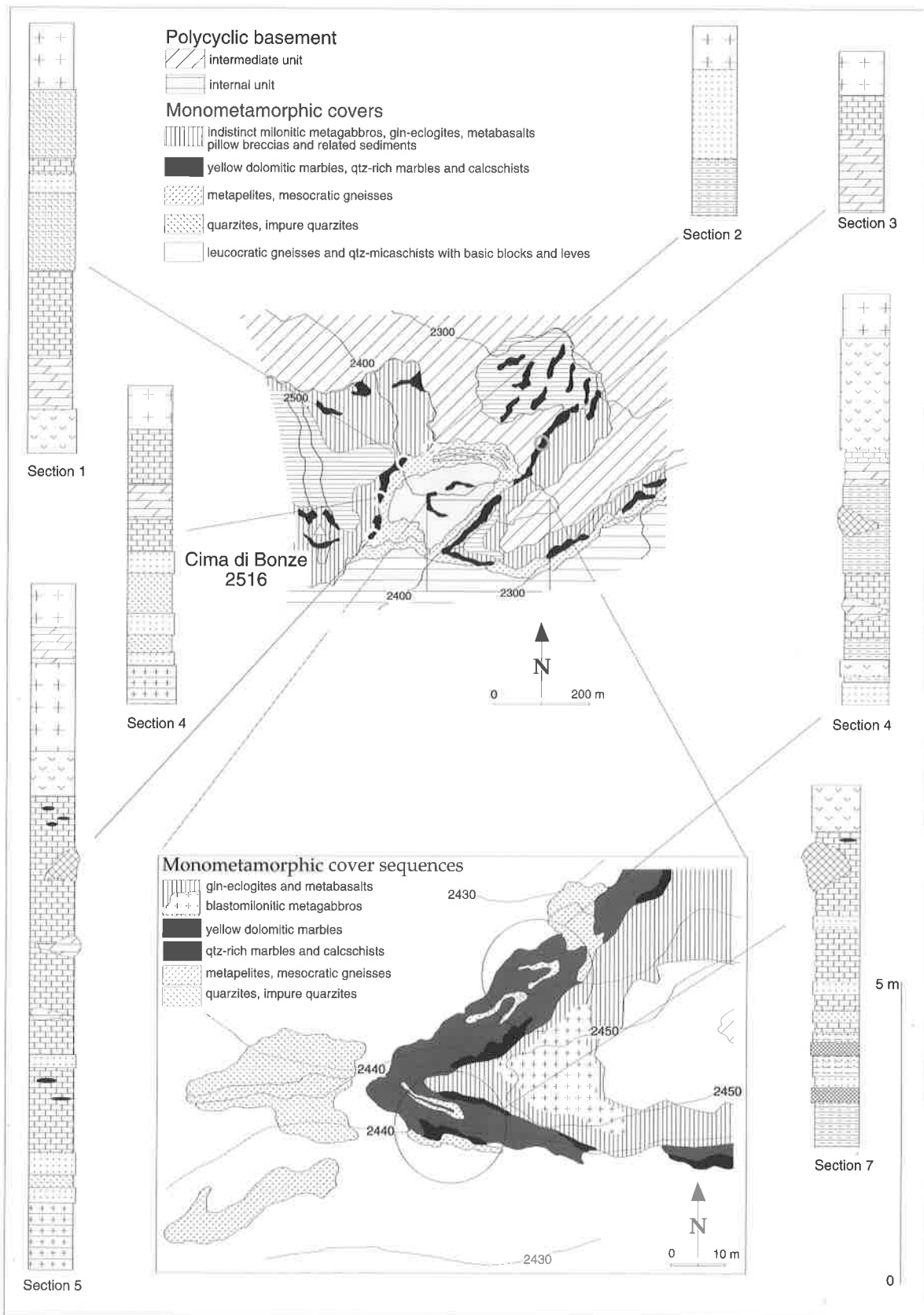


Fig. 2.6 - Detailed geological map and lithologic sections of the Cima Bonze region. The area was mapped at 1:1000 scale (Venturini, 1991). Circles locate of the lithologic sections.

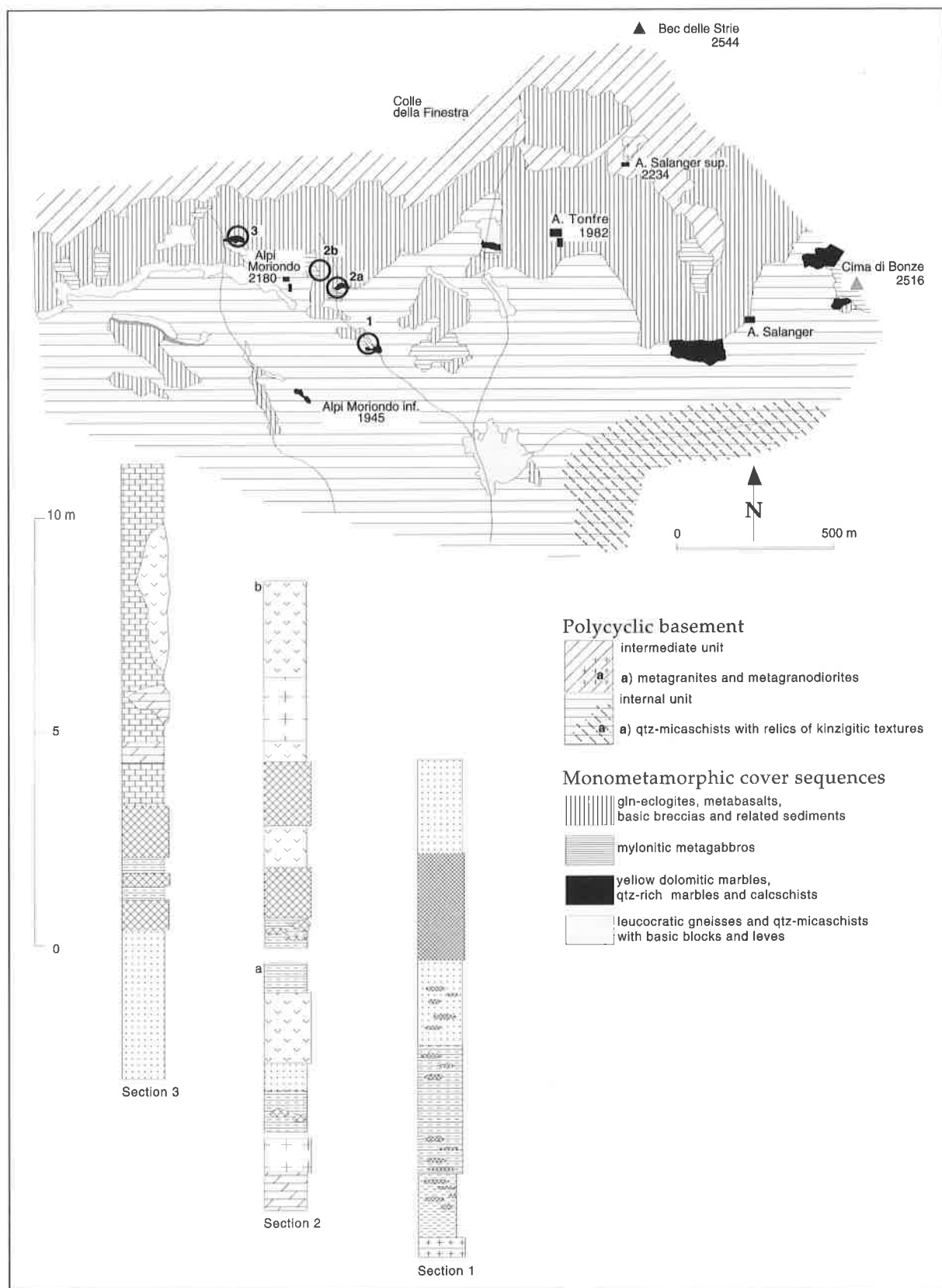


Fig. 2.7 - Geological map and lithologic sections of the upper Succinto valley (Modified after Danieli, 1993). Circles indicate the position of the lithologic sections described in Par. 2.3.3d. The monometamorphic cover sequences cropping out in this area are in contact with those of the exposed to the Cima di Bonze. The area can be reached either from the Chiusella valley (Succinto) or from the Cima di Bonze.

sequences comprise the base of the cliffs countering a small central depression. These lithologies are overridden by the metabasalts (glaucophane-eclogites) and related sediments. Coming from the underling sector (Fig. 2.5) several blocks of beautiful massive eclogites and glaucophanites, which constitute part of a land slide, can be observed. The outcrops at 2400 meter altitude show the first lithologic section (section 7) which is made of few meters of brown calcschists containing Mn-rich levels and decimeter quartz-rich horizons. The calcschists are overridden by massive eclogitic metabasalts (glaucophane-eclogites). This succession is repeated also in the other lithologic section of the area (sections 1-7 of Fig. 2.6). In section 5, which can be reached from section 7 moving horizontally to west, the calcschists contain decimeter blocs of dolomitic marbles, meter boudins of metabasalts and several small levels of impure quartzites and deformed Mn-rich boudins. In the section as in all the region, the calcschists overlay meter-thick impure and pure quartzites, locally interbedded with metapelites. This terrigenous sequence locally contains thin levels and blocks of epidote-rich mafic rocks (section 6). The mylonitic metagabbros locally overlay the cover sequences; even if always strongly deformed, they show relics of magmatic textures. The mylonitic foliation of the metagabbros probably predates the F1 fold phase. The contact between metagabbros and metabasalts is often marked by meter levels of folded yellow dolomitic marbles, which can also be observed within the metabasalts themselves. All the rocks described in the lithologic sections can be observed even in the detritus that fills the depression situated north of the Cima Bonze

2.3.3D THE SUCCINTO VALLEY (FIG. 2.7)

The monometamorphic cover sequences cropping out in the Bonze region can be followed westward; up to the upper sector of the Succinto valley. The area can be reached either from the Scalero valley (long and dangerous) or from the Chiusella valley. In the second case, park the car after Chiara and take the path to Succinto and Alpe Pianezza. From Alpe Pianezza walk east-north to east, in direction of Alpe Moriondo inferiore; go beyond the Alpe and reach the first small stream. Whereas the monometamorphic cover sequences occur in all the upper Succinto valley region, the Alpe Moriondo region contains the more representative sections. Section 1 (1845 m alt.) is made of a thick-terrigenous sequences with impure quartzites and metapelites containing several small boudins of basic rocks. A thick horizon of epidote-rich and mafic rocks characterises the upper part of this section. Section 2 (2005 m. alt.) is reached following the north side of the stream. It is composed of a meter

level of yellow dolomitic marbles interbedded with mylonitic metagabbros; the sequence continues with 3 meters of metabasalts and related sediments and is overridden by another few meters of Mn-rich metasediments, pillow breccias and impure quartzites locally interbedded with metabasalt and metagabbro slices.

The top of the lithologic section is located in correspondence of the path for Alpe Molera. (2145 m alt.) Above the houses some outcrops show the lithologies of section 3. This section is mainly composed of calcschists containing meter to decameter blocks of metabasalts and yellow dolomitic marbles overriding a metric alternance of metasediments intimately related to the metabasalts.

All the lithologies of this sector of the Succinto valley are characterised by well-developed high pressure mineral assemblages; along the ridge with the Fert valley jadeite is replaced by albite and epidote while glaucophane and the garnet remain stable mineral phases (intermediate unit of the polycyclic basement).

2.3.3E THE CROIX COURMA REGION (FIG. 2.8)

The Croix Courma region is located along the north side of the lower Aosta valley between Bard and Pont St. Martin . It has been mapped in detail by Passchier et al., (1981), Williams and Compagnoni (1983) and Venturini (this work). This area exposes the internal and intermediate unit of the polycyclic basement and the monometamorphic cover sequences (Fig. 2.8) The polycyclic basement comprises more or less eclogitized micaschists with hectometer bodies of mafic rocks. In these bodies pre-Alpine granulitic and amphibolitic textures can be seen.

The monometamorphic cover sequences crop out at the Col Fenêtre and along the southern ridge of the Mont Crabun; they can also be observed in the Crabun valley and in the southern side of the Croix Courma, a hundred meter NW of Verale.

At the Col Fenêtre the cover sequences are made up of calcschists with minor horizons of impure quartzites (Fig. 2.8 - section 1). The calcschists include several blocks of dolomitic marbles, mafic rocks and basement rocks. At the top of the section these lithologies grades to a polygenic breccia with a grey carbonatic matrix. The Col Fenêtre section is the only place where blocks of basement lithologies were observed within the calcschists.

2.3.3F THE MOMBARONE LAKE (FIG. 2.9)

The Mombarone area is located on the north side

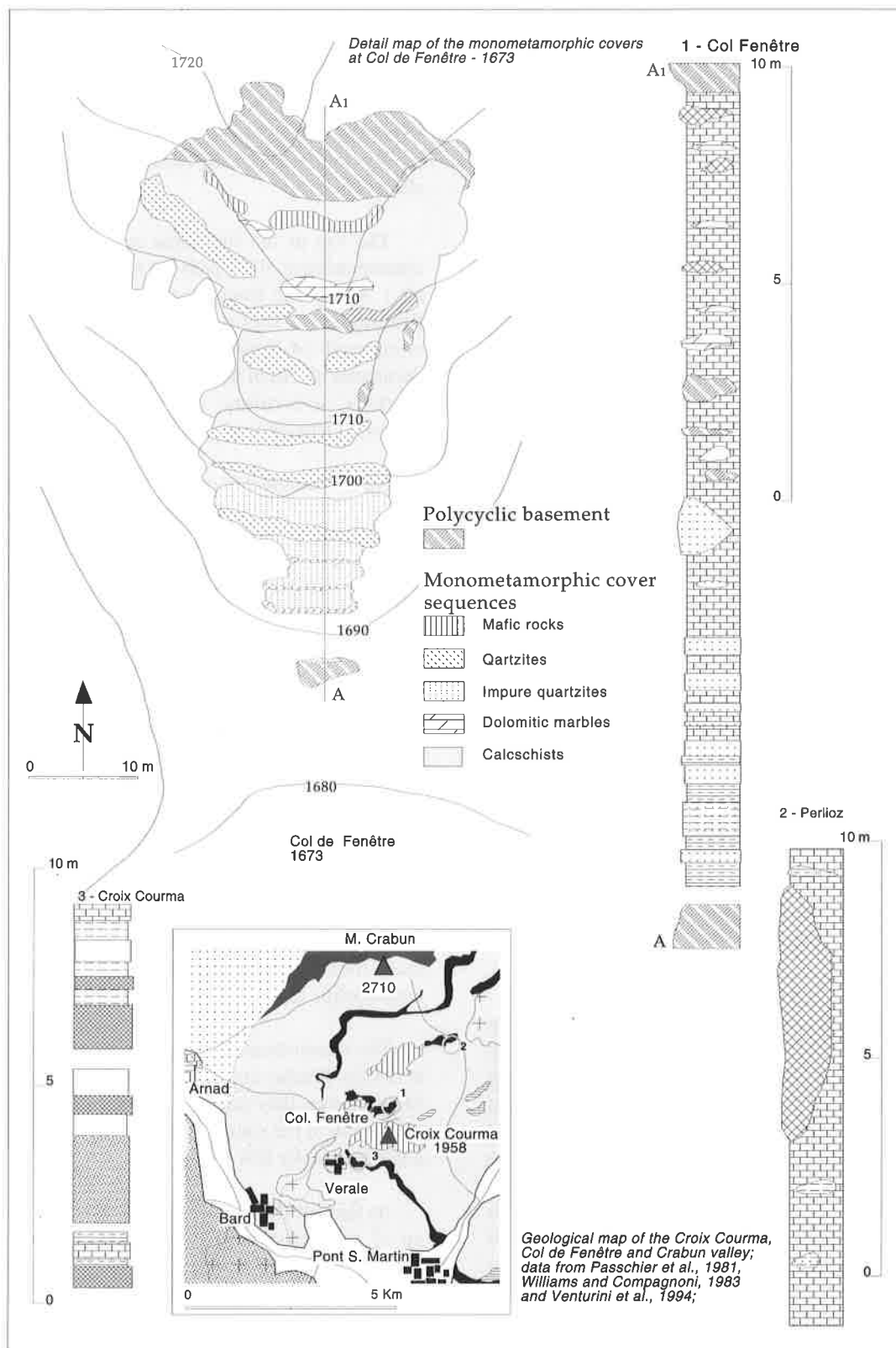


Fig. 2.8 - Detail Geological map and lithologic sections of the Col Fenêtre and Croix Courma region. The quartz-rich marbles and calcschists cropping out at the Col Fênêtre can be followed northerward along on the ridge of the M. Crabun (map modified after Passchier et al., 1981). Profile a-a1 is relative to the lithologic section I (Col Fênêtre). Circles indicate the position of the lithologic sections discussed in Par. 2.3.3e.

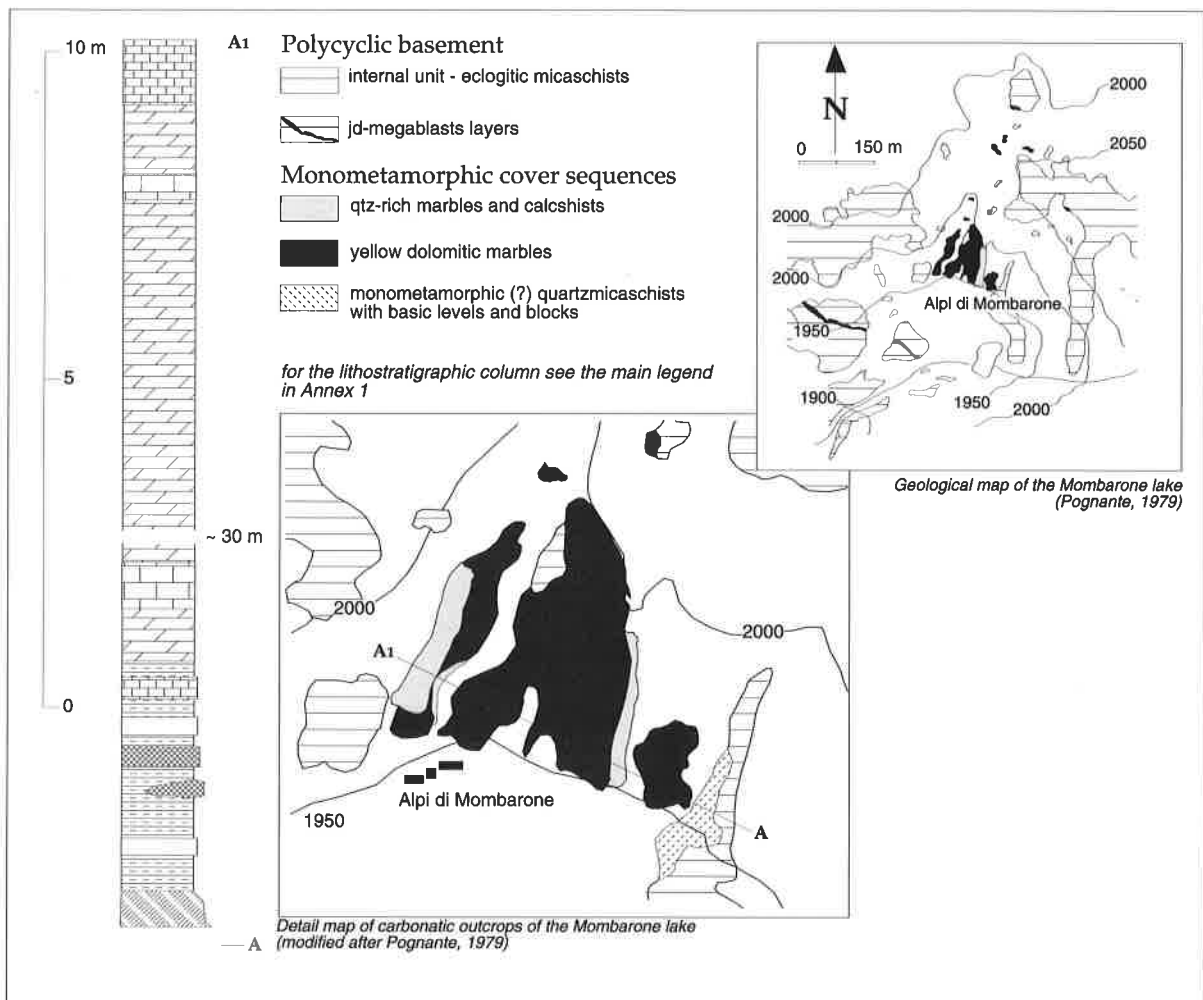


Fig. 2.9 - Detailed Geological map and lithologic section of the Mombarone lake region (modified after Pognante, 1979). Profile a-a1 represents the trace of the lithologic section. (crf.. Par. 2.3.3f).

of the lower Aosta valley, north of Settimo Vittone and Carema. This zone can be reached by car from Settimo Vittone to Trovinasse and Maletto and walking from the parking place to the Mombarone lake. In this sector it is possible to observe the most extensive outcrops of dolomitic marble, which can be followed from the lake to the Bec di Nana. The marbles are coarse grained and massive and are characterised by a weak foliation underlined by rare white mica. Within the dolomitic marbles there are meter horizons of calcshists and quartz-rich marbles. A meter alternance of impure quartzites and gneisses containing blocks and levels of epidote-rich mafic rocks underlies the dolomitic marbles.

2.3.4. The pre-Alpine high temperature basement complex

Two slices of the pre-Alpine high grade basement complex have been mapped at the transition between

the intermediate unit and the external unit of the polymetamorphic basement in the Chiusella valley and in the Fert valley (Fig.2.10).

In the first locality the pre-Alpine high grade basement crops out as an hectometer well-preserved body of high grade paragneisses (kinzigites) with subordinate amphibolites; this slice shows sharp tectonic contacts with eclogitic micaschists below and with glaucophane-chloritoid gneisses above. The pre-Alpine assemblage (biotite-garnet-sillimanite-K-feldspar-ilmenite) is well preserved in the core of the slice while it is partially or completely reequilibrated under blueschist conditions close to the tectonic contact. The pre-Alpine lithologies locally preserve the primary schistosity. The pre-Alpine high grade basement complex is laterally thinning; only the textures are preserved there, while the mineral assemblages are completely erased by the new Alpine assemblages. The tectonic contact is marked by the growth of glaucophane on pre-Alpine hornblende and

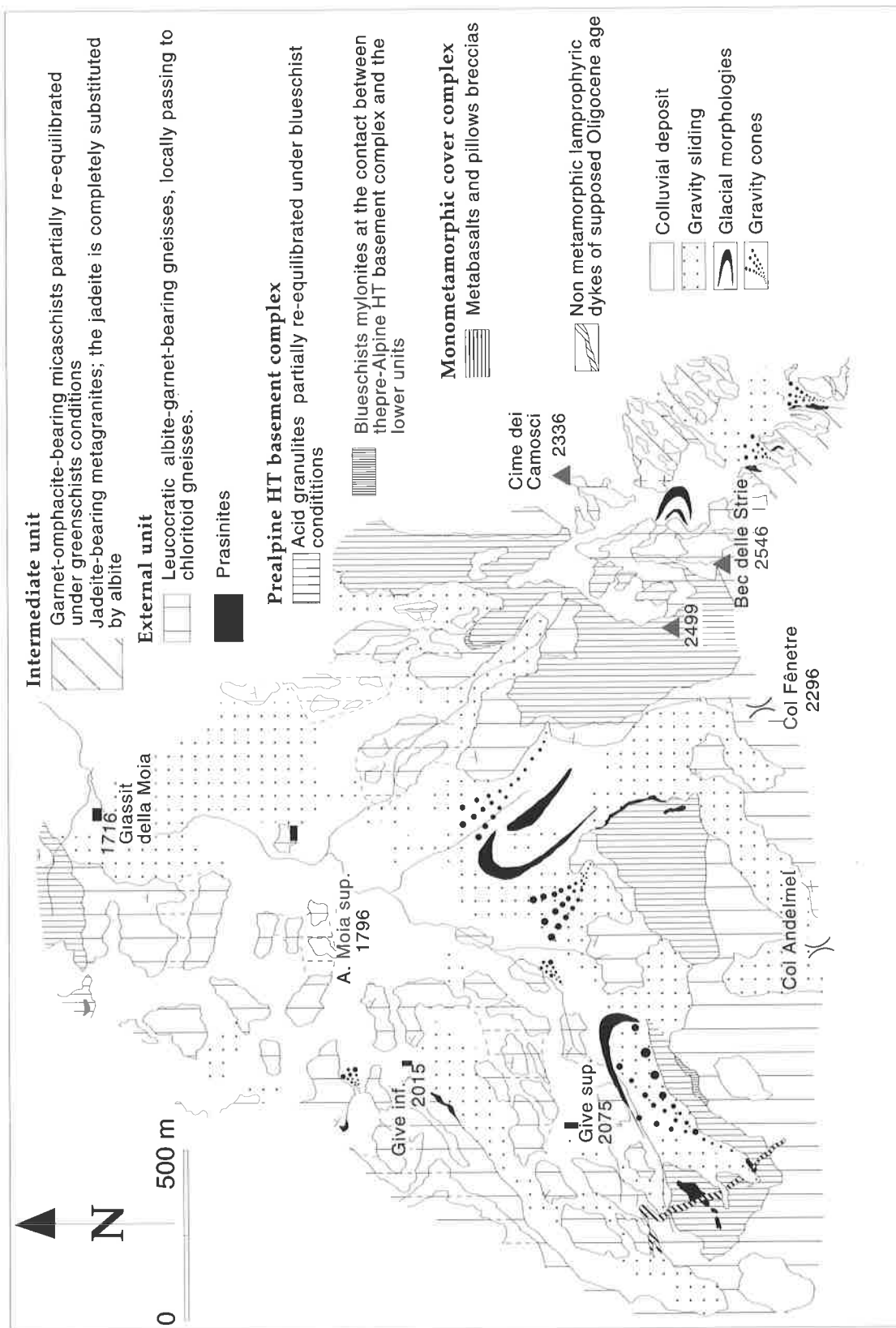


Fig. 2.10 - Geological interpretative map of the upper sector of the Fert Valley. The pre-Alpine high grade basement complex is particularly well exposed north of Col Fênêtre. It is mainly constituted by partially transformed garnet-bearing granulites and by minor kinzigites. These latter crop out in the Dondagna unit of the pre-Alpine high grade basement, south-west of the figured area.

by the presence of a second generation of garnet; no jadeite has been observed on the pre-Alpine plagioclase, which is replaced by clinozoisite, white mica and albite.

In the Fert valley the pre-Alpine high grade basement comprises paragneisses with centimeter to decimeter porphyroblasts of reddish garnet. These lithologies are only rarely interbedded with mesocratic paragneisses. The mafic rocks are very rare or absent. In thin section the pre-Alpine garnet is partially replaced by a new generation of Fe-rich garnet or by chlorite. The main foliation is generally

underlined by white mica, phengite, albite, clinozoisite/epidote, small euhedral garnet and small glaucophane. The schistosity is generally surrounding the first generation of poikiloblastic garnet relics. Kyanite on a previous sillimanite has been recognised, as well as a saussuritic aggregate on plagioclase relics. The underlying greenschist gneisses have been related to the external unit of the polycyclic basement and are constituted by albite, clinozoisite, glaucophane /barroisite and garnet; in these lithologies no Na clinopyroxene have been observed. Orthogneisses with rare relics of jadeite represent the overriding lithologies and comprise part of the intermediate unit.

- Chapter 3 -

Whole Rock Geochemistry

3.1. General Remarks

The field and microscopic investigations presented in Chapter 2 have been integrated by over sixty whole rock analyses. The analysed samples come from both the polycyclic basement, the monometamorphic covers and the mylonitic metagabbros. They were selected as follows:

- gneisses and micaschists (19 samples), whose protolith is unknown
- metagranitoids and orthogneisses (14 samples)
- mafic rocks of the polycyclic basement (13 samples) and the monometamorphic covers (15 samples).

The geochemical analyses were addressed to:

- a) differentiate the gneisses and micaschists in ortho- and paraderivates, in order to better define their attribution to the monometamorphic cover or to the polycyclic basement, with particular regard to the *gneiss pipernoïdes* (crf. Par. 1.3.1f);
- b) characterise the geochemical pattern and the geotectonic affinity of metagranitoids and orthogneisses and to find, as far as possible, potential differences between the granitoid bodies and the orthogneiss layers;
- c) specify the geochemical affinity of protoliths of the glaucophane-eclogites from the monometamorphic cover sequences, as well as to compare them to the mafic rocks of the polycyclic basement.
- d) investigate the geochemical characteristics of the mylonitic metagabbros closely related to the monometamorphic cover sequences.
- e) in addition, the results were compared to those reported by the earlier contributions on the Sesia zone and on the western Austroalpine system.

The Centre d'Analyse Minérale of the University of Lausanne, provided the facilities for these rock analyses. The methods applied correspond to those described by Pfeifer et al. (1989, 1991). Major and trace elements were measured with a Philips PW 1400 spectrometer, using a combined Mo-Sc tube. FeO/Fe₂O₃ ratio was determined with a Metrohm

photometer ($2\sigma = 3-7$ relative %), using the method of Hermann and Knacke (1973). Coulometer analyses (Ströhlein) permitted CO₂ determination ($2\sigma=1-2$ relative %). H₂O was calculated from loss on ignition and FeO-analyses. Standard error (2σ) for the major elements was 2-6% relative (0.8 absolute % for the SiO₂) with a detection limit of 0.01 wt.%. For the trace elements, it was 5-10 ppm (10-30% relative), the detection limit varying between 2 and 5 ppm.

3.2 Chemical composition of Gneisses and Micaschists

3.2.1. Introduction

The aim of this research is to find geochemical discriminants which permit us to differentiate the gneisses and micaschists of the polycyclic basement from those of the monometamorphic covers.

3.1.2. Choice of Samples

Most of the gneiss and micaschist samples come from the monometamorphic cover sequences, with exception of few samples collected in the internal and the external units of the polycyclic basement. The lithologies comprise massive leucocratic gneisses, jadeite-poikiloblast gneisses, chloritoid-gneisses and micaschists (Tab. 3.1). In the upper Scalero valley, two samples of mesocratic gneiss pipernoïdes (par.2.6b) and a leucocratic boudin, comprised into these lithologies, were collected. A sample of metasediment related to the metabasalts of the monometamorphic cover sequences completes the group of analysed samples.

Five to eight kilograms of material were taken for each sample, according to the grain size of the rock-forming minerals. Weathered samples were systematically eliminated.

3.2.3. Mobility Diagrams

All analysed lithologies record high pressure metamorphic conditions. Some samples also record pre-Alpine granulite to upper amphibolite facies conditions. As a result, considerable changes in the rock bulk chemistry are expected because of both the different nature of the protoliths and the element

lithology - sample - locality	Sesia unit	macroscopic aspect	main assemblage
<i>leucogneisses of uncertain origin</i>			
sv911a - Arnad	external unit	albitic gneiss with stretched qtz levels or pebbles	qtz-ab-czo/ep-phe-sph±pyr-ru
sv912a - Arnad	external unit	brownish gneiss with centimetric porphyroblasts of albite; it is locally associated with mafic boudins	ab-qtz-wm/phe-mc-czo/ep-sph±amph
sv912b - Bonze	internal unit	qtz-albitic gneiss within basement paraschists	ab-qtz-czo-phe-mc±ru-ep
sv9110b - Bonze	internal unit	decimetric horizon of massive gneiss within the micaschists	ab-qtz-czo-phe-gln-ru±mc-ep-grn
sv9128c - Cavalcurt	internal unit	decametric outcrop of leucocratic gneiss containing blocks of mafic rocks	ab-qtz-czo-phe-glnru±ep (jd)
sv9131c - Cavalcurt	internal unit	metric repetition of leucocratic gneisses and micaschists	ab-qtz-czo-phe-mc-±ru-ep
<i>jadeite-gneisses of uncertain origin</i>			
sv9119c - Cavalcurt	monometamorphic cover sequences	jadeite-bearing micaschist closely related to the <i>Gneiss pipernoïdes</i>	jd(ab)-phe-qtz-grn-zo/czo-ru±gln-sph
sv919m - Mombarone	internal unit	green massive gneiss with centimetric porphyroblasts of pale-green jadeite	jd-phe-qtz-zo-ru±gln-ab-sph
sv9110m - Mombarone	internal unit	green massive gneiss with centimetric porphyroblasts of pale-green jadeite	jd-phe-qtz-zo-ru±gln-ab-sph
<i>leucogneiss boudin comprised within the mesocratic gneisses (Gneiss Pipernoïdes)</i>			
sv9113c - Cavalcurt	monometamorphic cover sequences	decimetric boudin of grey gneiss comprise within the <i>Gneiss pipernoïdes</i> (sv9114c and sv9115c)	ab(jd)-qtz-czo-phe-ru±mc-ep
<i>mesocratic gneisses containing levels and boudins of mafic and acid rocks (gneiss pipernoïdes)</i>			
sv9114c - Cavalcurt	monometamorphic cover sequences	albite-epidote gneiss containing several centimetric and decimetric blocks of acid and mafic rocks	phe-ab-qtz-czo/ep-gln-grn-ru±mc-ep
sv9115c - Cavalcurt	monometamorphic cover sequences	albite-epidote gneiss containing several centimetric and decimetric blocks of acid and mafic rocks	phe-ab-qtz-czo/ep-ru±ep-gln
<i>chloritoid-gneisses</i>			
sv9129c - Cavalcurt	internal unit	silvery gneiss with centimetric-porphyroblasts of cld, gln and small grn	qtz-phe-grn-cld-gln-ru±ab-sph-czo
sv911t - Tavagnasco	internal unit	silvery gneiss with millimetric euhedral grn and cld	qtz-phe-cld-grn-czo-ru±sph-czo
sv913t - Tavagnasco	internal unit	silvery grn gneiss with centimetric porphyroblasts of cld	qtz-phe-cld-grn-czo-ru±sph-czo
<i>mesocratic gneiss interbedded with the glaucophane-eclogites</i>			
sv9111b - Bonze	monometamorphic cover sequences	mesocratic layer within the gln-eclogites containing centimetric boudins of mafic lithologies	gln-grn-zo/czo-qtz-phe±sph-ilm?
<i>metakinzigites</i>			
mb1k/91 - Savenca	internal unit	preserved pre-Alpine HG mesocratic gneiss crosscut by thin leucocratic dykes	bt-grn-sill-kf-qtz±ilm-wm-zo
126/91 - Savenca	internal unit	preserved pre-Alpine HG mesocratic gneiss crosscut by thin leucocratic dykes	bt-grn-sill-kf-qtz±ilm-wm-zo
sv937lz - Cantoir	southern internal unit	transformed pre-Alpine gneiss with HG paragenesis substituted by GS assemblages	ab-czo/ep-qtz-green amph-sph±grn-bt

Tab. 3.1 - Main macroscopic and petrographic characteristics of the analysed gneisses and micaschists.

movements during metamorphism. The mobility diagrams indicate those elements that can be considered more stable and those that can be considered more mobile with respect to a reference element. Fig. 3.1a and 3.1b shows the trend of the main major and trace elements with respect to TiO₂ (represented in weight percentage). A good

correlation exists for Si, Al, Fe²⁺, Fe³⁺, Mg, Zr, Y, Nd and V, with the exception of sample sv9119c (jadeite-gneiss) which consistently plots outside of the correlation trend. The alkali elements are partially mobile when compared to Ti. Ca and Ba do not correlate meaningfully with either Ti or Zr (other traditionally immobile element). The mobility

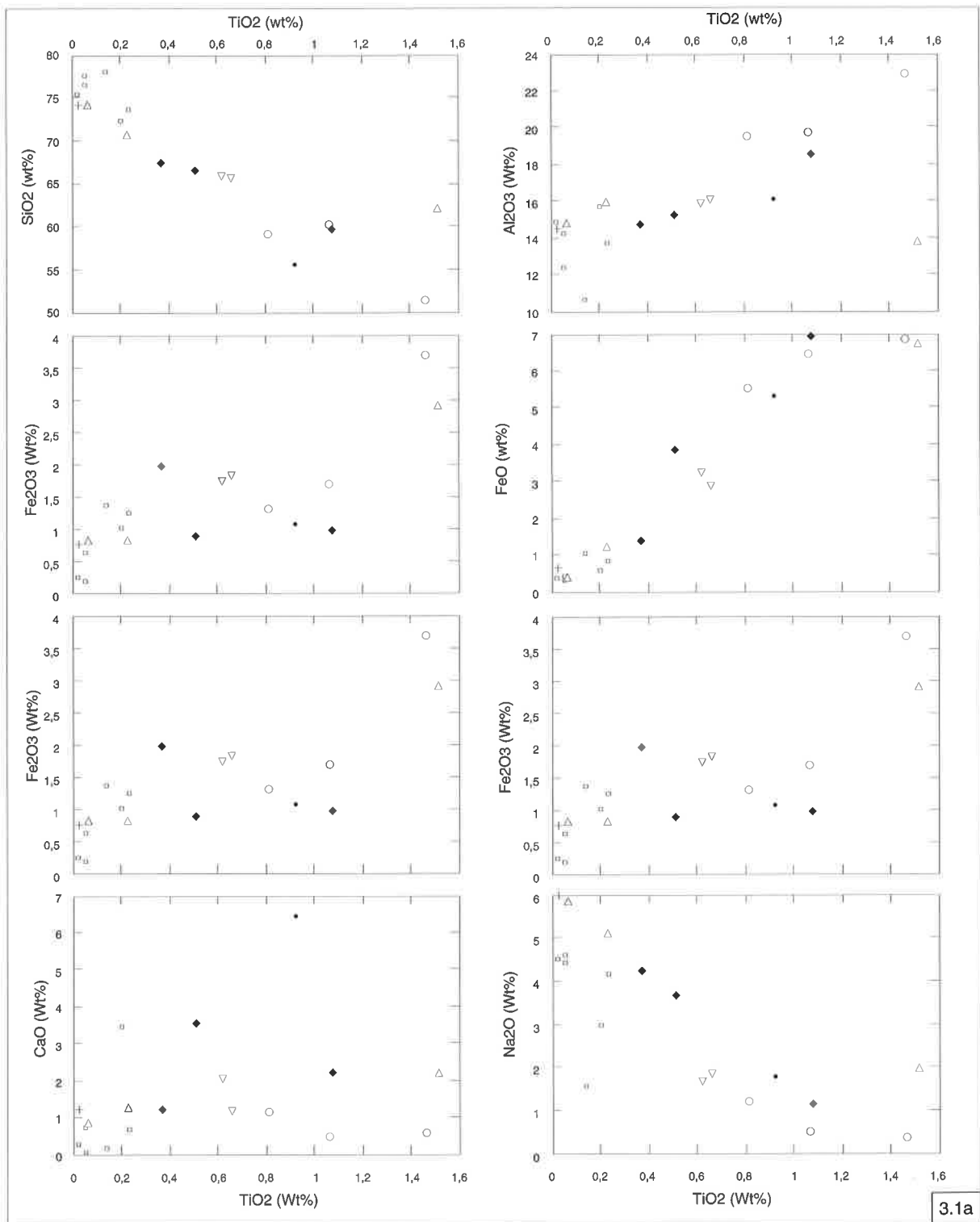
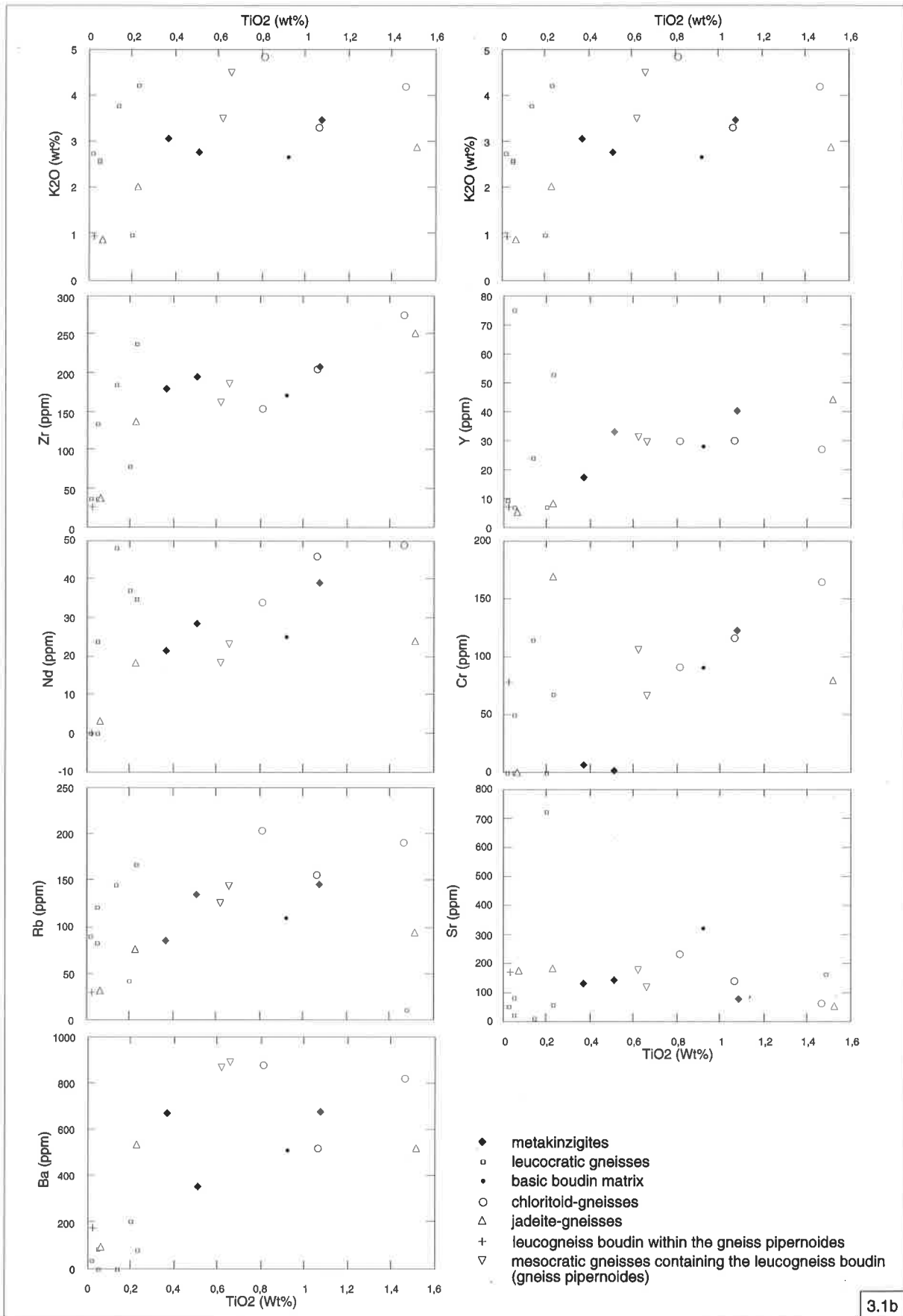


Fig. 3.1- Mobility diagrams for indistinct gneisses and micaschists. In Fig 3.1a major elements are compared to TiO₂. Traces elements, reported in Fig. 3.1b, are partially dispersed although the different lithological groups plotted in the graphics show a certain homogeneity. Sample sv9119c (jadeite-gneiss) is systematically out of range in comparison with other similar lithologies.

- ◆ metakinzigites
- ◻ leucocratic gneisses
- basic boudin matrix
- chloritoid-gneisses
- △ jadeite-gneisses
- + leucogneiss boudin within the gneiss pipernoïdes
- ▽ mesocratic gneisses containing the leucogneiss boudin (gneiss pipernoïdes)



3.1b

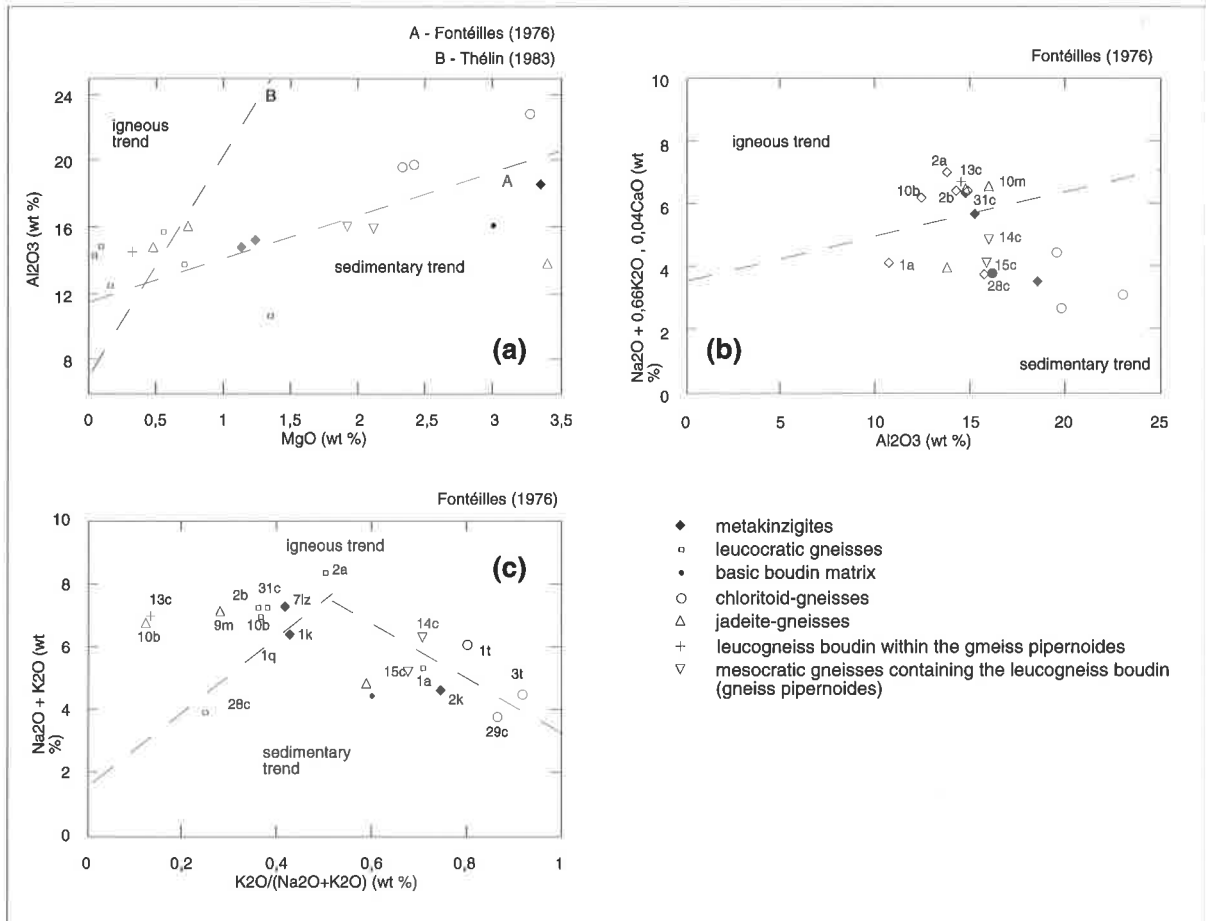


Fig. 3.2 - Discriminative diagrams for the indistinct gneisses and micaschists. Most of the analysed leucogneisses (sv912a, sv912b, sv9110b, sv9131c) constantly fall in the igneous-affinity field as well as two jadeite-gneisses and the leucogneiss boudin contained into the mesocratic gneisses (gneiss pipernoïdes). The mesocratic gneisses display instead a sedimentary affinity.

majority of the leucogneisses (sv912b, sv9110b and sv9131c) as well as for the leucocratic boudin (sv9113c) and two of the jadeite-gneisses. The eclogitized kinzigites, the mesocratic boudin matrix (gneiss pipernoïdes) and the mesocratic gneiss interbedded within the eclogitic glaucophanites indicate a sedimentary affinity.

Fig. 3.2b plots alkalis and CaO against Al_2O_3 content (Fontéilles, 1976); whereas both the alkalis and the Ca can be considered mobile elements, a certain coherence with the previous diagram has been found. Four leucogneisses (sv912b, sv9110b, sv9113c and sv9131c) fall in the igneous field, while the gneiss pipernoïdes, the chloritoid-gneisses (which are particularly enriched in MgO) and the qtz-rich leucogneiss of the external unit (sv911a) indicate a sedimentary origin.

The same relations can be observed in Fig. 3.2c in the alkali diagrams (Fontéilles, 1976): leucogneiss

diagrams also show that different lithological groups are reasonably homogeneous, with the exception of the leucogneisses (samples sv912b-sv9110b and sv9131c show a reasonable chemical similarity, but the others are quite dispersed).

3.2.3. Discriminative Diagrams

A variety of discriminative diagrams (De la Roche, 1972; Fontéilles, 1976; Thélin, 1983; Taylor and McLemman, 1988) allow determination of an igneous or sedimentary origin for the analysed gneisses and micaschists.

The Al_2O_3 -MgO diagram (Fig. 3.2a; Fontéilles, 1976) delimits two areas of igneous or sedimentary affinity as a function of Al_2O_3 concentration (line B). Thélin (1983) re-evaluated the field subdivisions of this diagram and proposed a partition depending on both of the elements (line B). The use of this diagram suggests an igneous protolith for the

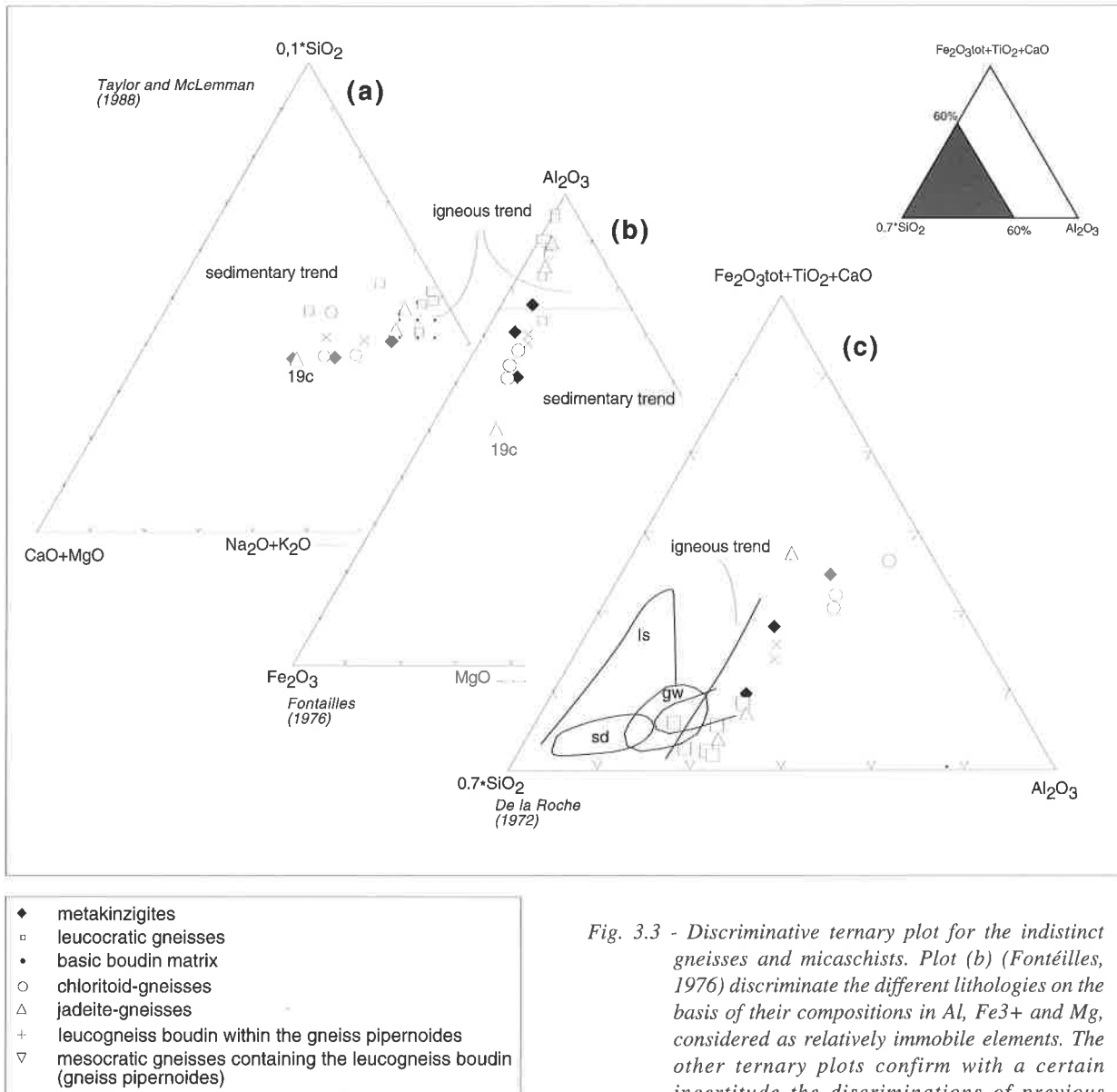


Fig. 3.3 - Discriminative ternary plot for the indistinct gneisses and micaschists. Plot (b) (Fontéilles, 1976) discriminates the different lithologies on the basis of their compositions in Al, Fe³⁺ and Mg, considered as relatively immobile elements. The other ternary plots confirm with a certain uncertainty the discriminations of previous diagrams.

samples sv912b, sv9110b, sv9113c and sv9131c show a clear igneous origin. Either these lithologies or the jadeite gneisses show a high content of Na₂O in comparison with the K₂O, which explains the presence of sodium rich pyroxenes and porphyroblastic albite. On the other hand, the chloritoid-gneisses are characterised by a relative enrichment of K₂O, which is mainly contained in the phengites (these samples show also a high content in Al₂O₃, Fig. 3.2b).

The ternary plots of Fig. 3.3 support the observations discussed above. The magmatic affinity of the four leucogneisses and the jadeite-gneisses as well as the metakinzigite sv912k is clear. The Al₂O₃-Fe₂O₃-Alkali diagram (Fontéilles,

1976) shows a particularly clear split between magmatic and sedimentary lithologies. The ternary plot in Fig. 3.3c (De la Roche, 1972) does constrain the previous observations, although a remarkable enrichment in Al₂O₃ compared with SiO₂ can be observed. Halter (1992) describes the same phenomenon for similar rocks of the northern external Sesia zone. This Al₂O₃ enrichment may be due to Si loss during metamorphism. If so, SiO₂ should be considered mobile (Halter, 1992).

Because these diagrams use mobile elements as geochemical indicators to discriminate between paragneisses and orthogneisses (Fontéilles, 1976; Taylor and McLemman, 1988), these results should be interpreted with care. Their agreement with other

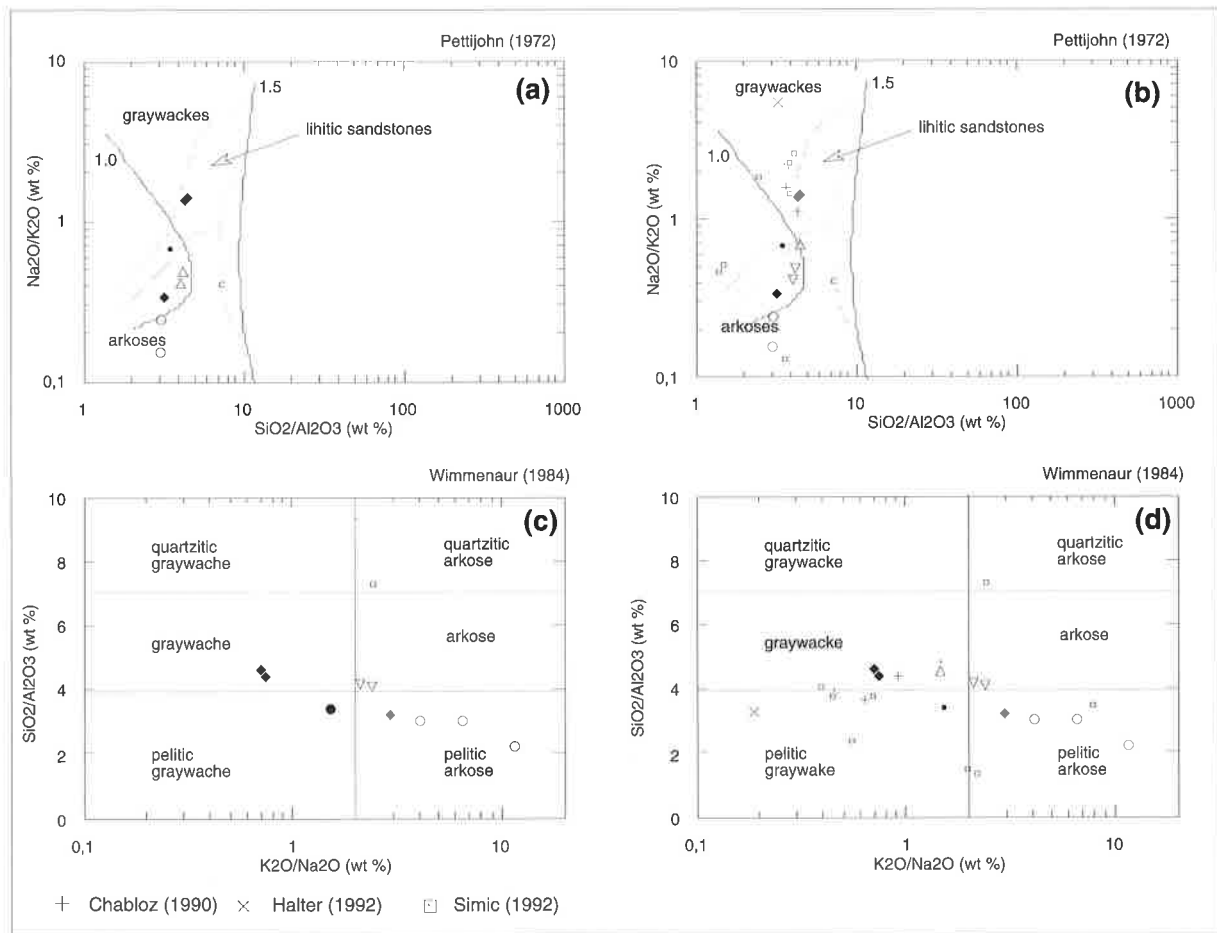


Fig. 3.4 - Classification of the gneisses and micaschists with sedimentary affinity. The samples analysed in the studied area were compared with samples collected in the northern Sesia zone (Chabloz, 1990; Halter, 1992; Simic, 1992). Legend as in figure 3.3.

plots, however, reinforces the reliability of the conclusions summarised in Tab. 3.2.

3.2.4. Interpretation

Four leucogneisses (samples sv912a, sv912b, sv91-10b and sv9131c), as well as the leucocratic boudin within the mesocratic gneisses and two of the jadeite-gneisses, are characterised by igneous protoliths; the gneiss pipernoïdes (sv9114c and sv9115c), one of the leucocratic gneisses of the external zone (1a), the chloritoid-gneisses, and two of the metakinzigites show a sedimentary affinity. Sample sv9119c, collected as a jadeite-gneiss, consistently shows a different geochemical composition with respect to the other similar samples, and its origin is probably sedimentary rock. Although several diagrams using trace elements have been proposed by Thèlin (1982) to differentiate igneous and sedimentary rocks, they were not used because of their incertitude (Halter, 1992). In addition, the meta-sedimentary lithologies are plotted

in the classification diagrams of Pettijohn (1972) and Wimmenaur (1984), to define the sedimentary protolith. Most of the lithologies fall in the quartzitic or pelitic arkose fields, depending to the Si/Al ratio; the metakinzigites, and the jadeite-bearing paragneisses show instead a graywacke composition (Fig. 3.4). The studied samples were also compared to other paragneisses previously investigated in the northern Sesia zone (Fig. 3.4b, Fig. 3.4d; Chabloz, 1990; Halter, 1992 and Simic, 1992). The metakinzigites of this study show similarities with the samples of Simic (1992), collected in the pre-Alpine HG basement complex (IIDK in Val Mastallone, and with the mesocratic gneisses of Chabloz (1990) and Halter (1992).

3.3. Chemical composition of Metagranitoids and Orthogneisses

3.3.1. Introduction

Six samples of metagranitoids and orthogneisses were collected in order to define their geochemical and

lithology group	(SV)	Na+K+Ca	K+Na	Al	Al	Si-Ca+Mg	Al-Fe3+tot	Conclusions	Si/Al-k	Na/K
		Al	K/(k+Na)	Mg	Mg	Na+K	Mg		Na	Si/Al
		(Wt%)	(Wt%)	(Wt%)	(Wt%)					
		Fonteilles	Fonteilles	Fonteilles	Thelin	Taylor	Fonteilles		Wimmenauer	Pettijohn
		1976	1976	1976	1982	1985	1976		1984	1972
leucogneisses	911a	sedim.	sedim.	?	sedim.	sedim.	sedim.	sedim.	quartzitic arkose	arkose
leucogneisses	912a	igneous	igneous	igneous	igneous	igneous	igneous	igneous		
leucogneisses	912b	igneous	igneous	igneous	igneous	igneous	igneous	igneous		
leucogneisses	9110b	igneous	igneous	igneous	igneous	igneous	igneous	igneous		
leucogneisses	9128c	sedim.	sedim.	igneous	igneous	igneous	igneous	igneous?		
leucogneisses	9131c	igneous	igneous	igneous	igneous	igneous	igneous	igneous		
jadeite-gneisses	9119c	sedim.	sedim.	sedim.	sedim.	sedim.	sedim.	sedim.	graywacke	lithic arenite
jadeite-gneisses	919m	igneous	igneous	igneous	igneous	igneous	igneous	igneous		
jadeite-gneisses	9110m	igneous	igneous	igneous	igneous	igneous	igneous	igneous		
leucogneiss boudin	9113c	igneous	igneous	igneous	igneous	igneous	igneous	igneous		
chloritoid - gneisses	9129c	sedim.	sedim.	igneous	sedim.	sedim.	sedim.	sedim.	pelitic arkose	arkose
chloritoid - gneisses	911t	sedim.	igneous	igneous	sedim.	sedim.	sedim.	sedim.	pelitic arkose	arkose
chloritoid - gneisses	913t	sedim.	igneous	igneous	sedim.	sedim.	sedim.	sedim.	pelitic arkose	arkose
acid boudin matrix	9114c	sedim.	igneous	sedim.	sedim.	sedim.	sedim.	sedim.	arkose	arkose
acid boudin matrix	9115c	sedim.	sedim.	sedim.	sedim.	sedim.	sedim.	sedim.	arkose	arkose
basic boudin matrix	9111b	sedim.	sedim.	sedim.	sedim.			sedim.	pelitic graywacke	lithic arenite
metakinzigites	911k	sedim.	sedim.	sedim.	sedim.	sedim.	sedim.	sedim.	graywacke	lithic arenite
metakinzigites	912k	sedim.	sedim.	sedim.	sedim.	sedim.	igneous	sedim.	pelitic arkose	lithic arenite
metakinzigites	917lz	igneous	igneous	sedim.	sedim.	igneous	sedim.	?		

Tab. 3.2 - Summaring table of the results obtained with the discriminative diagrams for gneisses and micaschists (sedim. = sedimentary).

geotectonic characteristics. In addition, the leucogneisses and the jadeite-gneisses with igneous affinity, analysed in the previous chapter, were included in the investigated samples. Finally, we reconsider several geochemical analyses of orthogneisses and metagranitoids previously published in the literature (Callegari et al., 1976; Dal Piaz et al., 1977; Lombardo et al., 1977; Oberhänsli et al., 1985; Halter, 1992) in comparison with our samples.

3.3.2. Choice Of Samples

All the metagranitoids come from the internal unit of the polycyclic basement, with the exception of sv925a, which was sampled in the external unit. Two samples came from the Elvo valley side of Monte Mucrone (Armando, 1991; Venturini et al., 1994a - crf. Fig. 1b). The samples represent the metagranodioritic main stock (sv913e) and the leucocratic metagranitic dykes (sv914e) crosscutting the granodiorites. Sample sv921dz comes from the

granodiorite outcrops of the intermediate unit (Donnaz-Clapey); sv921mt is representative of the decametric-thick leucocratic horizons that can be observed in the cliffs above Ivozio and Tavagnasco, while sv912t is a phengitic leucogranite outcropping between Li Piani and M. Gregorio (Tavagnasco sector). Tab. 3.3 provides further informations on the analysed lithologies. The geochemical composition of the metakinzigites is moreover slightly different from those of the gneiss pipernoides, whereas these differences are only displayed by the alkali-diagrams.

3.3.3. Mobility Diagrams

The chemical elements used below in the geochemical and geotectonic discriminative diagrams for the igneous rocks were tested with the mobility diagrams (Fig. 3.5a and 3.5b). As for the indistinct gneisses and micaschists, the major and trace elements were plotted against both TiO_2 and Zr. Ti, which is generally considered to be an immobile

<i>lithology - sample - locality</i>	<i>Sesia unit</i>	<i>macroscopic aspect</i>	<i>main assemblage</i>
<i>metagranitoids</i>			
913e - Elvo valley	internal unit	partially reequilibrated granodiorite with relics of magmatic bt	qtz-ab(jd)-zo/czo-phe-grn-ru±bt-zr
914e - Elvo valley	internal unit	leucocratic metagranite with several relics of magmatic bt	qtz-ab(jd)-zo/czo-phe-grn-ru±mc-bt-zr
921dz - Donnaz-Clapey	internal unit	Strongly deformed greenish orthogneiss with scattered relics of the magmatic texture	phe-qtz-gln/bar-czo(ep)-ab-aegr-grn±chl
925a - Arnad	external unit	decimetric horizon of massive gneiss within the micaschists	ab-mc-phe-zo/czo-qtz±green bt-chl
912t - Tavagnasco	internal unit	leucocratic metagranite with big flakes of green phe and jadeite	jd(ab)-qtz-phe-zo/czo-aegr±gm-mc-chl
921mt - Montestrutto	internal unit	leucocratic porphyroblastic metagranite	jd(ab)-qtz-phe-czo-phe-ru±mc-ep
<i>leucocratic orthogneisses</i>			
912a - Arnad	external unit	brownish gneiss with centimetric porphyroblasts of albite; it is locally associated to mafic boudins	ab-qtz-wm/phe-mc-czo/ep-sph±amph
912b - Bonze	internal unit	qtz-albitic gneiss within basement paraschists	ab-qtz-czo-phe-mc±ru-ep
9110b - Bonze	internal unit	decimetric horizon of massive gneiss within the micaschists	ab-qtz-czo-phe-gln-ru±mc-ep-grn
9128c - Cavalcurt	internal unit	decametric outcrop of leucocratic gneiss containing blocks of mafic rocks	ab-qtz-czo-phe-glnru±ep (jd)
9131c - Cavalcurt	internal unit	metric repetition of leucocratic gneisses and micaschists	ab-qtz-czo-phe-mc±ru-ep
<i>jadeite-orthogneisses</i>			
919m - Mombarone	internal unit	green massive gneiss with centimetric porphyroblasts of pale-green jadeite	jd-phe-qtz-zo-ru±gln-ab-sph
9110m - Mombarone	internal unit	green massive gneiss with centimetric porphyroblasts of pale-green jadeite	jd-phe-qtz-zo-ru±gln-ab-sph
<i>leuco-orthogneiss boudin</i>			
9113c - Cavalcurt	monometamorphic cover sequences	decimetric boudin of grey gneiss comprise within the <i>Gneiss pipernooides</i> (sv9114c and sv9115c)	ab(jd)-qtz-czo-phe-ru±mc-ep

Tab. 3.3 - Main macroscopic and petrographic characteristics of the analysed orthogneisses and metagranitoids.

element, shows a good correlation with Si, Fe³⁺, Fe²⁺, FeO_{tot}, MgO, CaO and V, while Y, Sr, and Zr are partially mobile (Fig. 3.5b). The alkalis are strongly dispersed. Thus, the interpretation of the following discriminative diagrams must take in account both the strong mobility of such elements and of the shortage of the available analyses.

3.3.4. Discriminative Diagrams

We can infer the main geochemical patterns and geotectonic setting of the orthogneisses and metagranitoids from major element comparisons, diagrams of Pearce et al. (1984), AFM ternary plot, and spider diagram (Fig. 3.7 and 3.8). As with the

mobility diagrams, the results are difficult to interpret unequivocally.

The analysed samples were compared with metagranodioritic and metagranitic samples coming from the lower Aosta valley and the Gressoney valley (Callegari et al., 1976); other geochemical analyses of jadeite-bearing gneisses and metagranitoids were published by Lombardo et al. (1977). Oberhänsli et al. (1985) furnished a clear geochemical picture of the M. Mucrone metagranitoids; these data have been included in our graphic as well as the geochemical analyses of Chabloz (1990) and Halter (1992), who investigated the geotectonic origin of the mesocratic gneisses of the northern external unit of the polycyclic base-

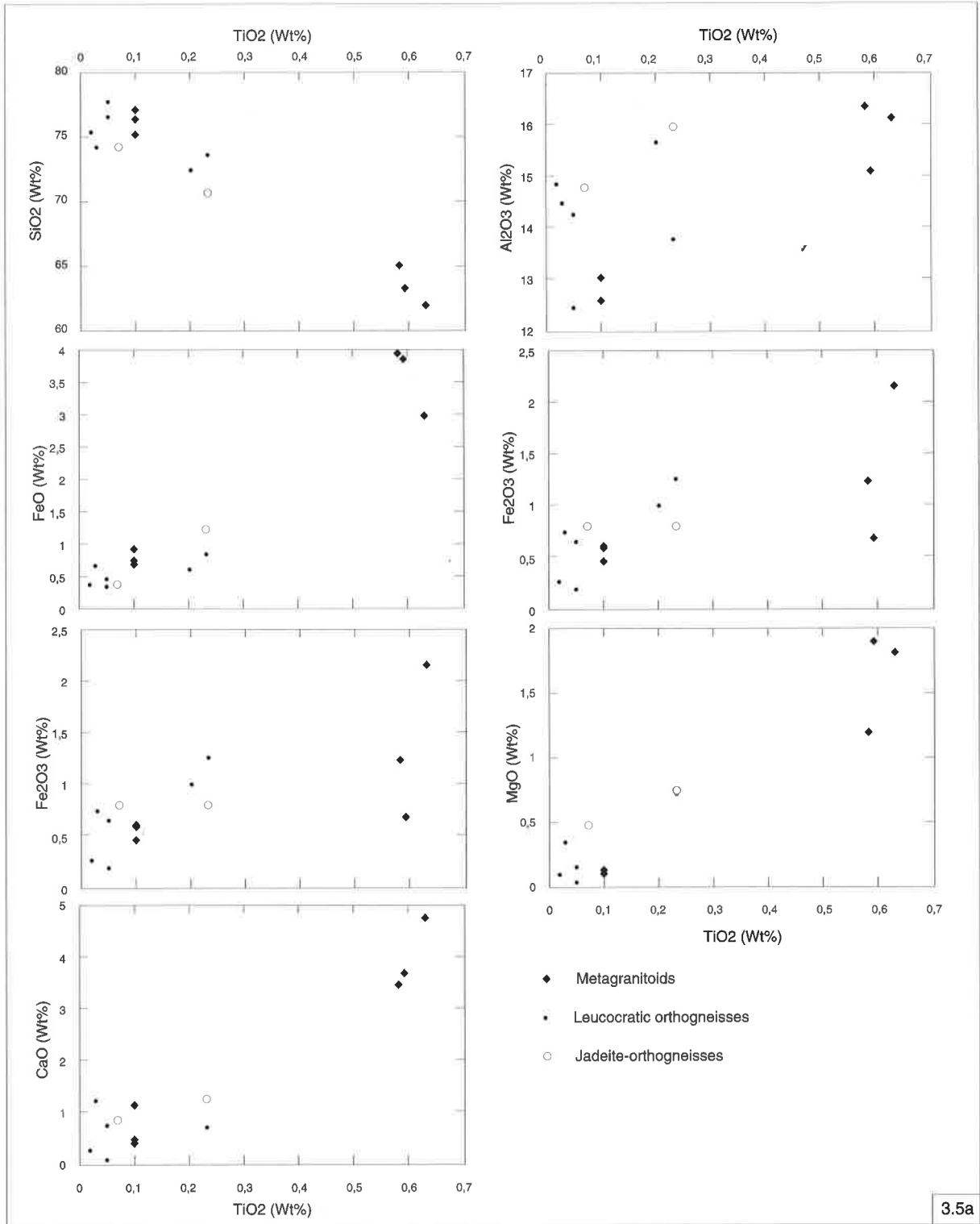
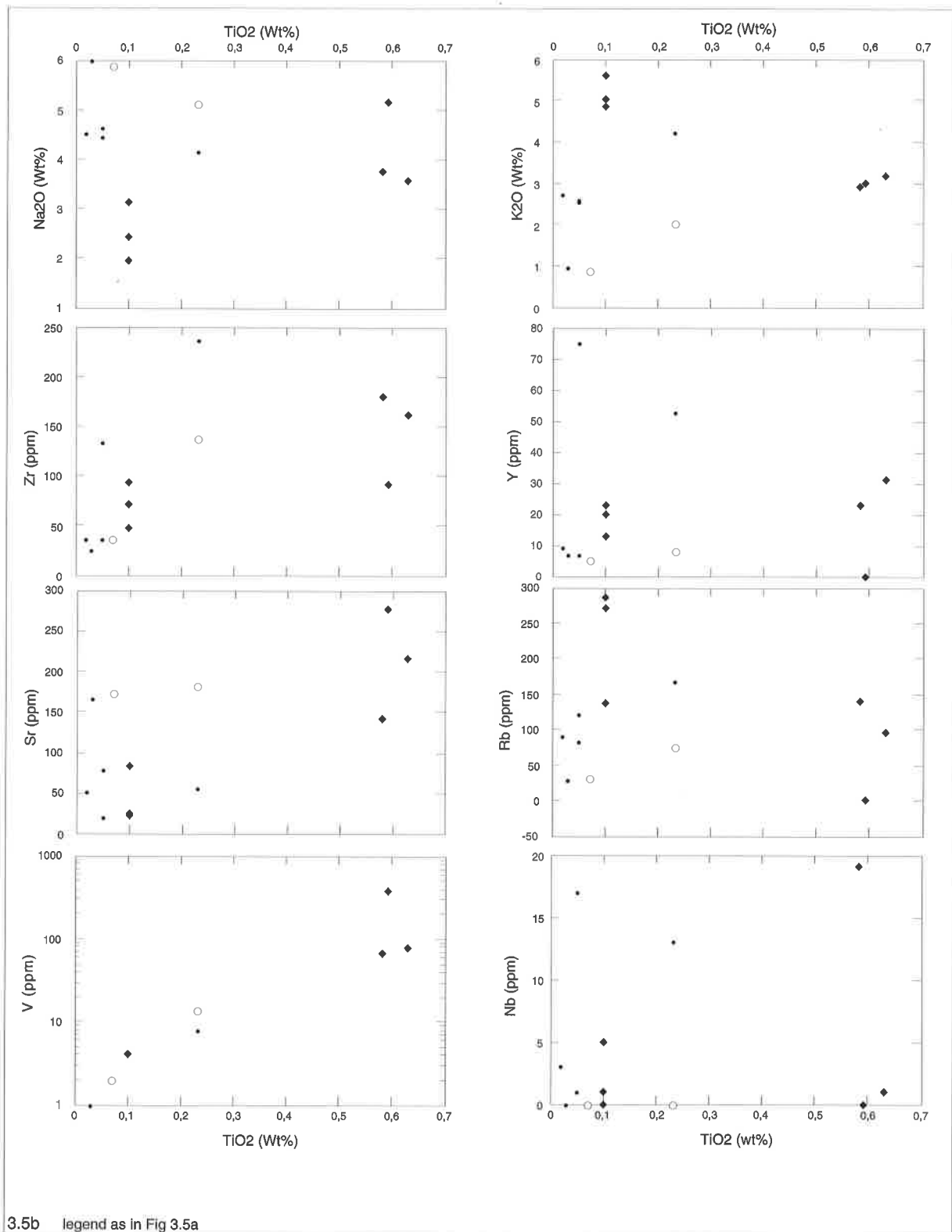


Fig. 3.5 - Mobility diagrams relative to the orthogneisses and metagranitoids. Major elements (Fig. 3.5a) compared to TiO₂ display a reasonable correlation. Trace elements (Fig. 3.5b) are more dispersed, with exception for V and Sr. Nb, Rb and Y do not show any reliable correlation. Results of discriminative and classificative diagrams that will be further used have to be carefully interpreted.



ment. In addition, the analyses of the acid dykes of the Matterhorn gabbroic stock (Dal Piaz et al., 1977) are included in the comparative diagrams (Fig. 3.6).

Fig. 3.6 shows SiO_2 , Al_2O_3 , FeO_{tot} and MgO vs.

TiO_2 for all of the available samples of the Sesia zone and the western Austroalpine system. These diagrams allow us to discriminate two main lithological groups:

a) Ti-rich samples ($\text{TiO}_2 = 0.5-1\%$), represented by the

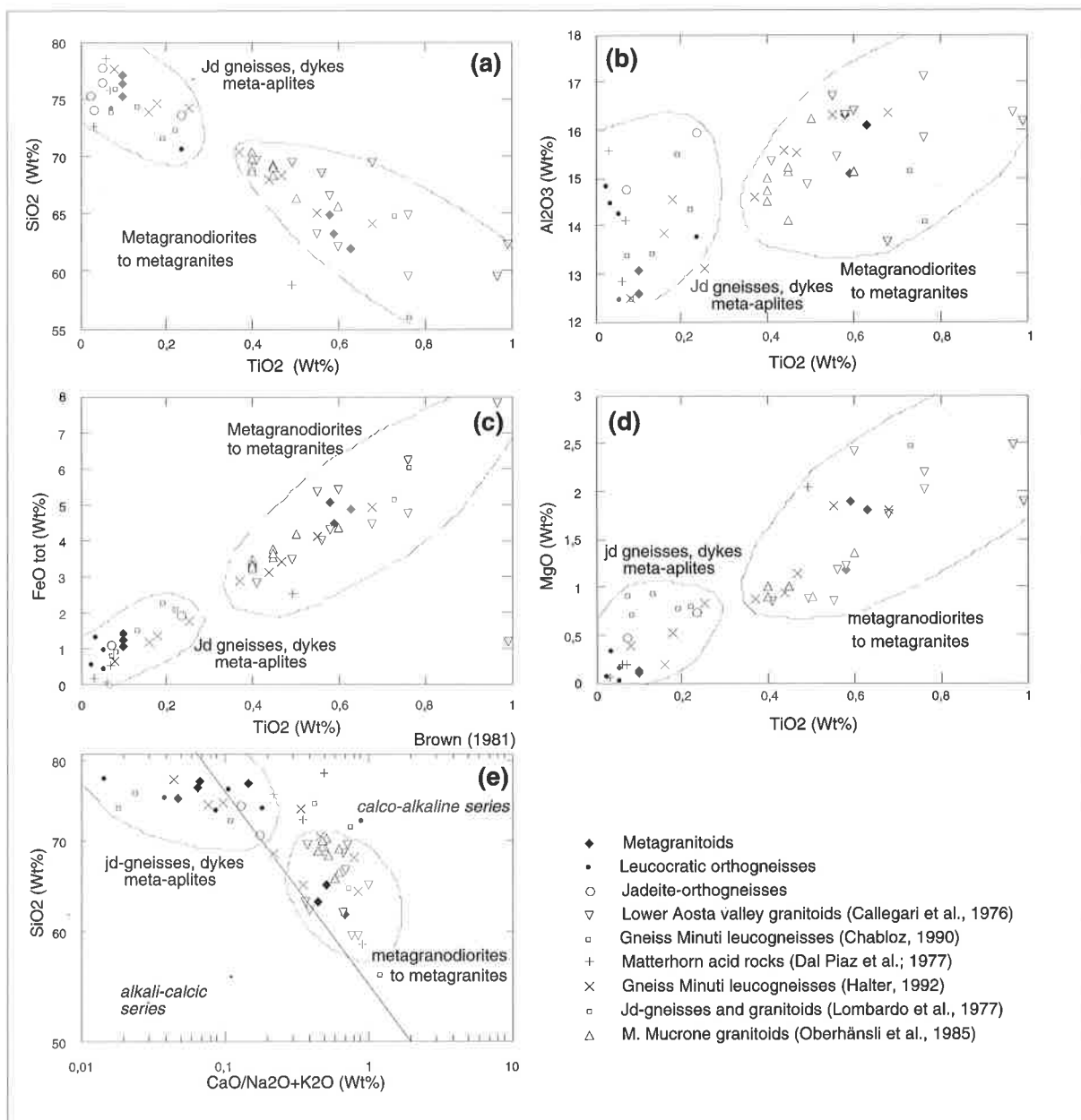


Fig. 3.6 - Comparison of some main elements (Si-Al-Fe-Mg) against TiO₂. Available data from the literature for the Sesia zone are plotted together with the samples analysed in this work. The jadeite-orthogneisses, dikes and meta-aplites constantly show a lower TiO₂ content and lower FeO_{tot} and MgO concentrations (Fig. 3.6c and d). The same lithologies displays an alkali-calcic affinity (Fig. 3.6e).

lower Aosta valley - M. Mucrone metagranodiorites and metagranites, by part of the mesocratic gneisses of the external zone, and by samples sv913e (Elvo-Mucrone), sv921dz (Donnaz) and sv925a (Arnad).

b) very low Ti samples characterised by high Si and alkali values, including jadeite-gneisses (Lombardo et al., 1977), part of the mesocratic gneisses of the external unit, and samples sv912a, sv912b, sv9110b, sv9131c (ortho-leucogneisses), sv919m,

sv9110m (jadeite-gneisses) and sv914e, sv912t and sv921mt (leucogneisses).

Fig. 3.6e allows to compare the different lithologies to the alkali-calcic or calco-alkaline evolutionary series. A distinction between the two groups can be observed: the lithological group a) (granodiorites and granites) shows a calco-alkalic affinity, while the group b) shows an alkali-calcic tendency. The AFM ternary plot of Fig. 3.7b confirms the distin-

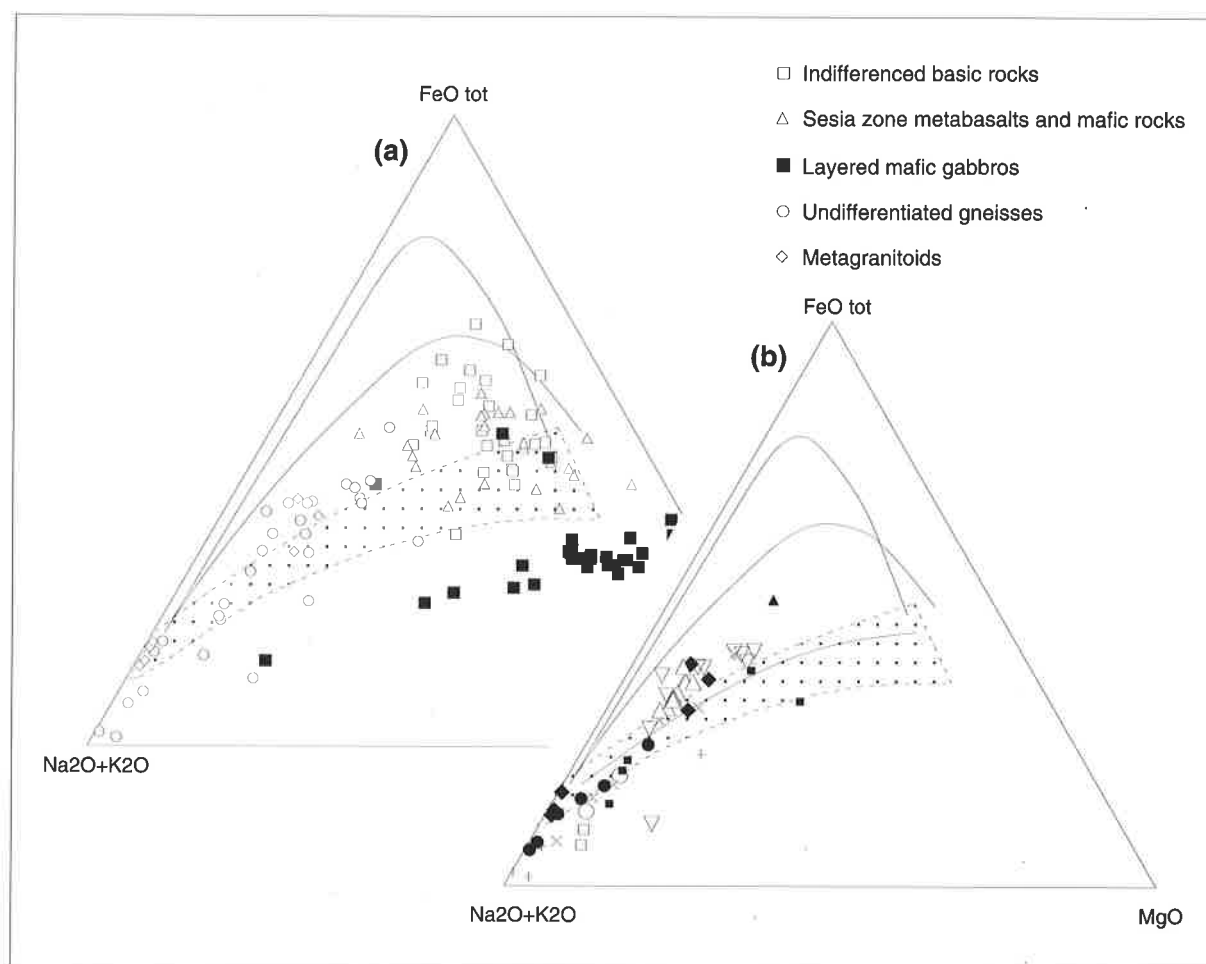


Fig. 3.7 - AFM ternary plot reporting all the available whole rock data of mafic and acidic rocks from the Sesia zone (a). In plot (b) jadeite-orthogneisses, dikes and meta-aplites are closed to the alkali corner. The metagranitoids display a calc-alkaline evolutionary trend (Evolutionary fields from Morse, 1988).

ction between the granitic and granodioritic lithologies, characterised by a calco-alkalic trend and the other more evolved acid dykes and layers.

3.3.5 Interpretation

Fig. 3.8 shows five discriminative diagrams used to infer the geotectonic emplacement origin of igneous rocks (Pearce et al., 1984). Although the mobility diagrams showed the partial reliability of the trace elements, the reproducibility of the results permits us to deduce some preliminary conclusions, summarised in Tab. 3.4.

1) the metagranodioritic and metagranitic bodies of the central Sesia zone and part of the orthogneisses of the northern-external unit indicate a calco-alkaline Island Arc affinity, according to Oberhänsli et al. (1985) and Halter (1992).

2) the leucogranites sv914e and sv912t, as well as the leucogneisses sv912a, sv9110b and sv9131c and the

orthogneiss sv921mt could be related to an alkali-calcic evolutionary series and to a «within plate» geotectonic context (sv914e, sv912a, sv9110b and sv9131c) or to a «collisional» affinity (sv912t and sv921mt).

These preliminary conclusions, however, are speculative for three reasons. First, we made only few analyses. Second, the results were deduced by graphs that use partially mobile elements as plot parameters. Third, the analysed samples are strongly deformed, metamorphosed and reworked rocks. Only further and careful analyses will allow to confirm or deny the presence of two different acid evolutionary series in the Sesia zone.

3.4. Chemical composition of basic rocks

3.4.1. Introduction

The polycyclic basement and the monometa-

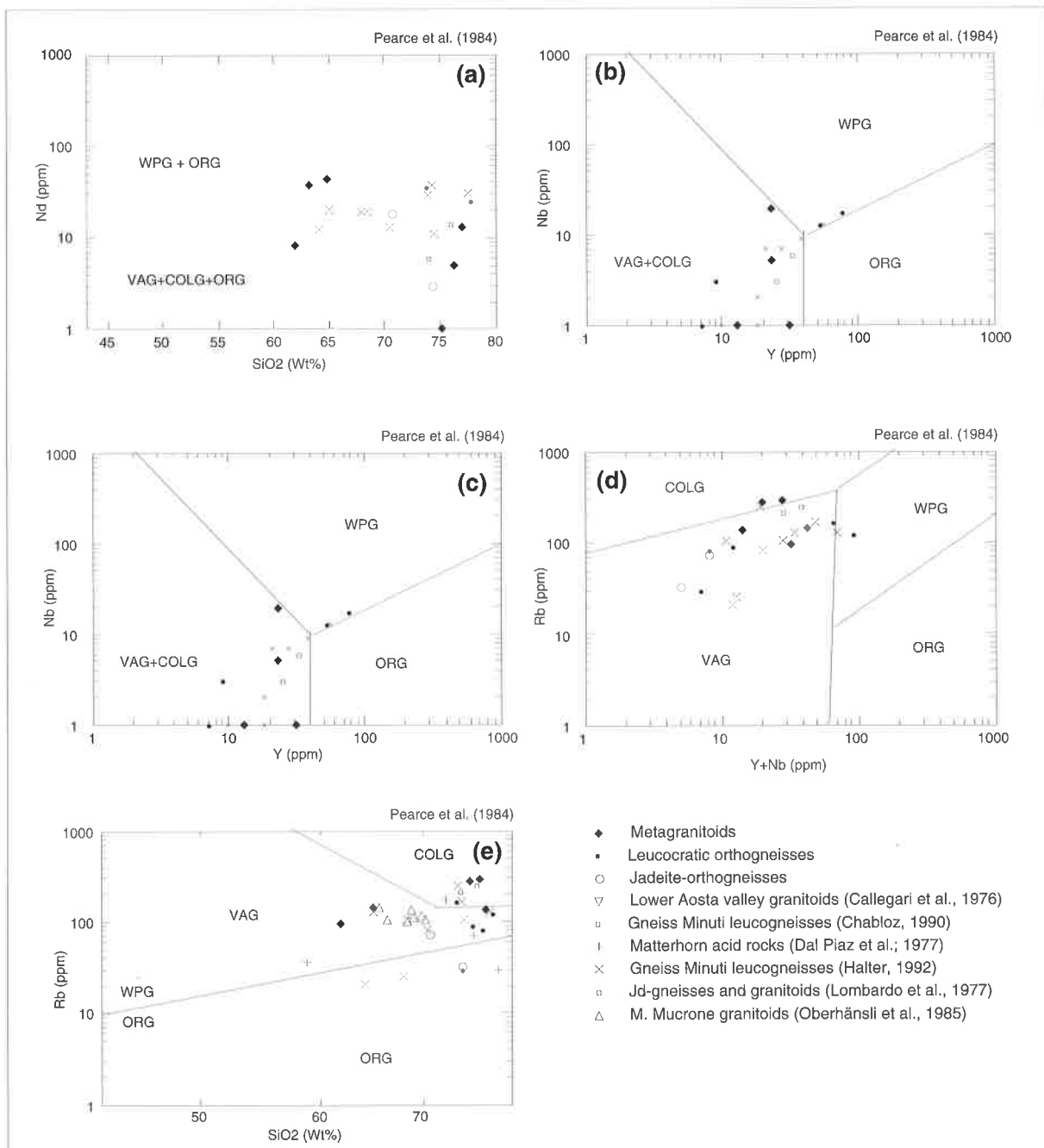


Fig. 3.8. - Conventional discriminative diagrams proposed by Pearce et al. (1984). Results of these diagrams are highly approximate because of the mobility of the plotting parameters (WPG = Within Plate Granites; ORG = Oceanic Ridge Granites; VAG = Volcanic Arc Granites; COLG = Collisional Granites)

morphic cover sequences contain several kinds of mafic rocks. All the metabasites of the central Sesia zone underwent high pressure metamorphism and/or GS metamorphism during the Alpine orogenic cycle. In the absence of relics of pre-Alpine textures, any distinction between different types of eclogites and/or amphibolites is difficult. Geochemistry plays an important role to reconstruct chemical composition of the mafic protoliths and to carefully envisage their

original geotectonic patterns. The geochemical analyses of the mafic rocks were addressed to:

- 1) differentiate the basic lithologies of the monometamorphic cover sequences from those of the polycyclic basement;
- 2) investigate the potential correlation between the glaucophane-eclogites of the monometamorphic

rock type	(SV)	locality	SiO2 TiO2	Al2O3 TiO2	MgO TiO2	FeOtot TiO2	Nd SiO2 *	Nb Y *	Rb Y-Nb *	Rb Si *	SiO2 CaO/Alkali Brown 1981	Conclusions
m-granodiorite	3e	V. Elvo	1	1	1	1	wpg-org	vag	vag	vag	calc-alkaline	vag
m-leucogranite	4e	V. Elvo	2	2	2	2	vag-org-colg	vag-colg	vag	vag	alkali-calcic	wpg?
m-granodiorite	1dz	Montey	1	1	1	1	wpg-org	vag-colg	vag	vag	calc-alkaline	vag
m-granite	5a	Arnad	1	1	1	1	vag-org-colg	vag-colg	vag	vag	calc-alkaline	vag
m-granite	2t	Tavagnasco	2	2	2	2	vag-org-colg	vag-colg	colg	colg	alkali-calcic	colg
m-granite	1mt	Montestrutto	2	2	2	2	vag-org-colg	vag-colg	colg	colg	alkali-calcic	colg
leucogneiss	2a	Arnad	2	2	2	2	wpg-org	wpg	wpg	colg	alkali-calcic	wpg?
leucogneiss	2b	Bonze	2	2	2	2	vag-org-colg	vag-colg	vag	vag-wpg	calc-alkaline	vag
leucogneiss	10b	Bonze	2	2	2	2	wpg	wpg	wpg	vag-wpg	alkali-calcic	wpg?
leucogneiss	13c	Cavalcurt	2	2	2	2	vag-org-colg	vag-colg	vag	org	calc-alkaline	vag
leucogneiss	28c	Cavalcurt	2	2	2	2	vag-org-colg	vag-colg	vag	vag-wpg	calc-alkaline	vag
leucogneiss	31c	Cavalcurt	2	2	2	2	vag-org-colg	vag-colg	vag	vag-wpg	alkali-calcic	wpg?
jadeite-gneiss	9m	Mombarone	2	2	2	2	vag-org-colg	vag-colg	vag	vag	trans	?
jadeite-gneiss	10m	Mombarone	2	2	2	2	vag-org-colg	vag-colg	vag	org	trans	?
<i>1 = Granodiorites to granites</i>							VAG - Volcanic Arc Granites					
<i>2 = Jd gneisses, dykes, phengite-rich gneisses, meta-aplites</i>							ORG - Orogenic Granites					
<i>m - metamorphic</i>							Colg - Collisional Granites					
<i>* = Pearce et al., 1984</i>							WPG - Within Plate Granites					

Tab. 3.4 - Summarizing table of the results obtained with the discriminative diagrams for the orthogneisses and metagranitoids.

cover sequences and the mylonitic metagabbros;

- 3) compare these lithologies with the other mafic bodies of the western Austroalpine system,
- 4) explore similarities between the monometamorphic mafic rocks, the Middle Triassic mafic volcanic rocks of the eastern Alps (Ladinian extrusive units), and the ophiolitic metabasalts of the western Alps, in order to propose some potential correlations.

3.4.2. Choice of Samples

Ten samples, representing the glaucophane-eclogites, basic breccias apparently related to the glaucophane-eclogites, and basic layers and blocks contained within the gneiss pipernoïdes, were selected from the monometamorphic cover sequences while the mylonitic metagabbros provided six samples. Thirteen samples were collected from the polycyclic basement. These samples represent the basic granulites, the massive gabbroic glaucophanites, the phlogopite-eclogites and other mafic rocks. Tab. 3.5a and 3.5b summarise the lithological characteristics of the sampled rocks.

3.4.3. Mobility Diagrams

These diagrams display the relationships between the major and trace elements and Zr, which is generally an immobile element (Beccaluva et al., 1984, Pfeifer et al., 1989). Many of the main elements do not show a linear correlation with Zr, although they can be correlated within each lithological group (Fig. 3.9a). There are two possible explanations for this dispersion: a) the rocks were affected by a strong pervasive mobility of the elements during the metamorphism or b) the different origin of the mafic rocks may render Zr-concentration a weak tool for direct comparison. The trace elements, on the other hand, show a good correlation in comparison to Zr (Fig. 3.9b).

3.4.4. Discriminative Diagrams of the Mafic Rocks

The eclogitised mafic rocks of the Sesia zone have been generally interpreted as deriving from pre-Alpine HG amphibolites and/or basic granulites (Dal Piaz et al., 1972; Lardeaux and Spalla, 1991). On the other hand, the basic lithologies of the monometamorphic

<i>lithology - sample</i>	<i>Sesia unit</i>	<i>macroscopic aspect</i>	<i>main assemblage</i>
<i>Bonze-type metagabbros*</i>			
912az - Sermenza	internal unit	hbl-layer gabbro showing preserved magmatic textures crosscut by metric pegmatitic acid veins	pl-hbl-cpx-mg±zo - wm-chl
913az - Sermenza	internal unit	hbl-layer gabbro showing preserved magmatic textures and crosscut by metric pegmatitic acid veins	pl-hbl-cpx-mg±zo - wm-chl
914b - Bonze	monometamorphic cover sequences	metagabbro with main foliation underlined by alternances of zo/czo and gln-grn layers	gln-czo-Mg chl - wm-grn±omp-ru - spe-qtz
919b - Bonze	monometamorphic cover sequences	brownish eclogite with rare relics of gabbroic textures; the foliation is marked by alternances of grn and gln	gln-zo-grn-phe±ru - qtz-sph
9115vc - C. del Prà	monometamorphic cover sequences	metagabbro with main foliation underlined by alternances of zo/czo and gln-grn layers	gln-czo-Mg chl - wm-grn±omp-ru - spe-qtz
912i - Ivery	internal unit	gln-eclogite with local relics of magmatic textures	omp-grn-zo/czo - gln-wm±hbl relics
<i>glaucophane-eclogites</i>			
915b - Bonze	monometamorphic cover sequences	foliated blue eclogite with foliation underlined by cm porphyroblast of gln and partially crosscut by porphyroblasts of omph and grn	omp-grn-gln - zo/czo-ru±Mg chl - sph
916b - Bonze	monometamorphic cover sequences	massive eclogite with weak foliation underlined by cm porphyroblast of gln and partially crosscut by porphyroblasts of omph and grn	omp-grn-gln - zo/czo-ru±Mg chl - sph
9112b - Bonze	monometamorphic cover sequences	decimetric block of gln-eclogite within a wm-rich metasediment related to the mafic rocks	omp-grn-gln - zo/czo-ru±Mg chl - sph
911q - Quincinetto	monometamorphic cover sequences	metric massive horizon of gln-eclogites associated to stretched levels and blocks of mafic rocks and wm-rich metasediments	omp-grn-gln - zo/czo-ru±Mg chl - sph
<i>basic breccias relate to the glaucophane eclogites</i>			
9118b - Bonze	monometamorphic cover sequences	decimetric block of eclogite included in a qtz-wm matrix and closely related to the gln-eclogite	qtz-phe-cc-grn-gln - chl-sph±czo
9120c - Cavalcurt	monometamorphic cover sequences ?	decimetric block of eclogite included in a qtz-wm-gln matrix	ab-qtz-czo-phe - ru±mc-ep
<i>basic layer and blocks</i>			
9112c - Cavalcurt	monometamorphic cover sequences	mafic block or boudin contained within a leucocratic gneiss; in the same outcrop are also acid blocks or boudins (13c)	omp-grn-phe-zo - cc-gln-sph
9116c - Cavalcurt	monometamorphic cover sequences	eclogitic levels interbedded with the leucocratic gneisses in those sample 12c is contained	gln-grn-czo-phe - qtz-omp±ab-cc
9126c - Cavalcurt	monometamorphic cover sequences	mafic boudin comprises within a ab-ep rich matrix (<i>gneiss pipernoides</i>) which is locally interbedded with carbonatic levels.	ab-phe-qtz - gln±grn-czo
9115c - Cavalcurt	monometamorphic cover sequences	mafic boudin comprises within a ab-ep rich matrix (<i>gneiss pipernoides</i>) which is locally interbedded with carbonatic levels.	cross-(gln)-grn - chl±qtz

Tab. 3.5a - Geological location, macroscopic and microscopic characteristics of the analysed basic rocks. The Bonze-Type metagabbros comprise the mylonitic metagabbros of the monometamorphic cover sequences and two samples of cumulitic gabros collected in the northern Sesia zone (Sermenza valley).

<i>lithology - sample</i>	<i>Sesia unit</i>	<i>macroscopic aspect</i>	<i>main assemblage</i>
<i>hbl-amphibolites</i>			
911v - Verale	intermediate unit	HG amphibolite with preserved pre-Alpine hbl and saussuritized pl	gln-grn-czo - phe±hbl
931v - Verale	internal unit	glucophanite with millimetric porphyroblasts of grn a rare omp	gln-grn-czo±hbl
932v - Verale	internal unit	glucophanite with millimetric porphyroblasts of grn a rare omp	gln-grn-czo - phe±hbl
933v - Verale	internal unit	glucophanite with millimetric porphyroblasts of grn a rare omp	gln-grn-czo - phe±hbl
934v - Verale	internal unit	glucophanite with millimetric porphyroblasts of grn a rare omp	gln-grn-czo - phe±hbl-ru
923i - Ivery	internal unit	massive glaucophanic eclogite	grn-omp-gln - ru±pre-Alpin hbl - czo/ep
<i>phl - eclogites</i>			
914q - Quincinetto	internal unit	metric dyke of black mica-eclogites crosscutting a body of orthogneisses	omph-grn-gln-phl - phe-ru±czo-chl
915q - Quincinetto	internal unit	metric dyke of black mica-eclogites crosscutting a body of orthogneisses	omph-grn-gln-phl - phe-ru±czo-chl
<i>metagabbroic glaucophanites</i>			
9311lz - Corio	southern internal unit	massive and homogeneous glaucophanites locally interbedded with gln-eclogites	gln-grn-czo - phe±ab-
9312lz - Corio	southern internal unit	massive and homogeneous glaucophanites locally interbedded with gln-eclogites	gln-grn-czo - phe±ab
<i>indistinct mafic rocks</i>			
9311ft - Fert valley	intermediate unit	massive grn-glaucophanite interbedded with layered gln-eclogites; it is probably deriving from a pre-Alpine amphibolite	phe-gln-grn porphyroblasts - zo/czo-ru±qtz
9313lz - Rocca C.se	RCTS*	massive glaucophanite interbedded with metakinzigites preserving pre-Alpine layers	
913a - Arnad	external unit	metric boudin of mafic composition included within the leucocratic gneisses	czo/ep-ab-green bt chl-bar(gln)±qtz-ru

* Rocca Canavese Trust Sheet (Pognante, 1989)

Tab. 3.5b - Geological location, macroscopic and microscopic characteristics of the analysed basic rocks.

morphic cover sequences could derive either from basaltic lava flows and/or from mafic volcano-detritic sequences (Par. 2.2.4.) (Venturini et al., 1991, 1994a). The following discriminative diagrams attempt to:

- 1) differentiate the rocks of sedimentary origin from those of igneous affinity;
- 2) differentiate the basic rocks on the basis of geochemical parameters;
- 3) attribute a specific evolutionary trend to the different lithological groups, and
- 4) define their geotectonic affinity.

Figure 3.11 permits us to make preliminary hypotheses about the protoliths of the different analysed mafic rocks. The content of Cr (in ppm) in used in graphic 3.10a to differentiate mafic rocks of sedimentary origin (low-Cr concentration) from those of magmatic origin (Fröhlisch, 1960). The mylonitic metagabbros, the pre-Alpine amphibolites and the glaucophane-eclogites show a magmatic trend or fall at the boundary between the magmatic and the intermediate field. A similar geochemical pattern is shown also by the basic levels contained within the mesocratic gneisses, whereas the low-Cr content of the samples collected from the Corio and Monastero gabbroic massif and two of the basic boudins contained in the polycyclic micaschists are plotted at the limit between the sedimentary and the

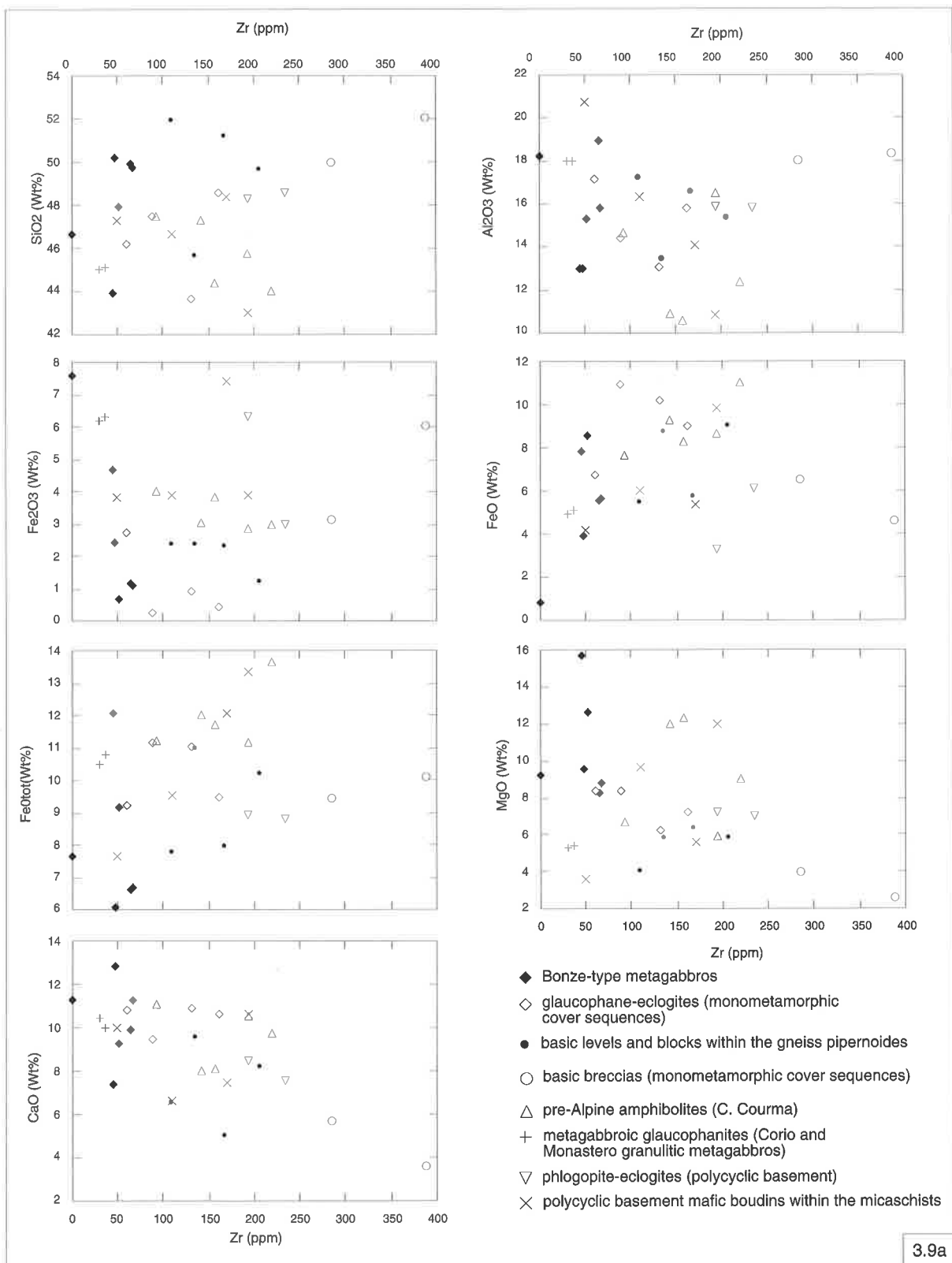
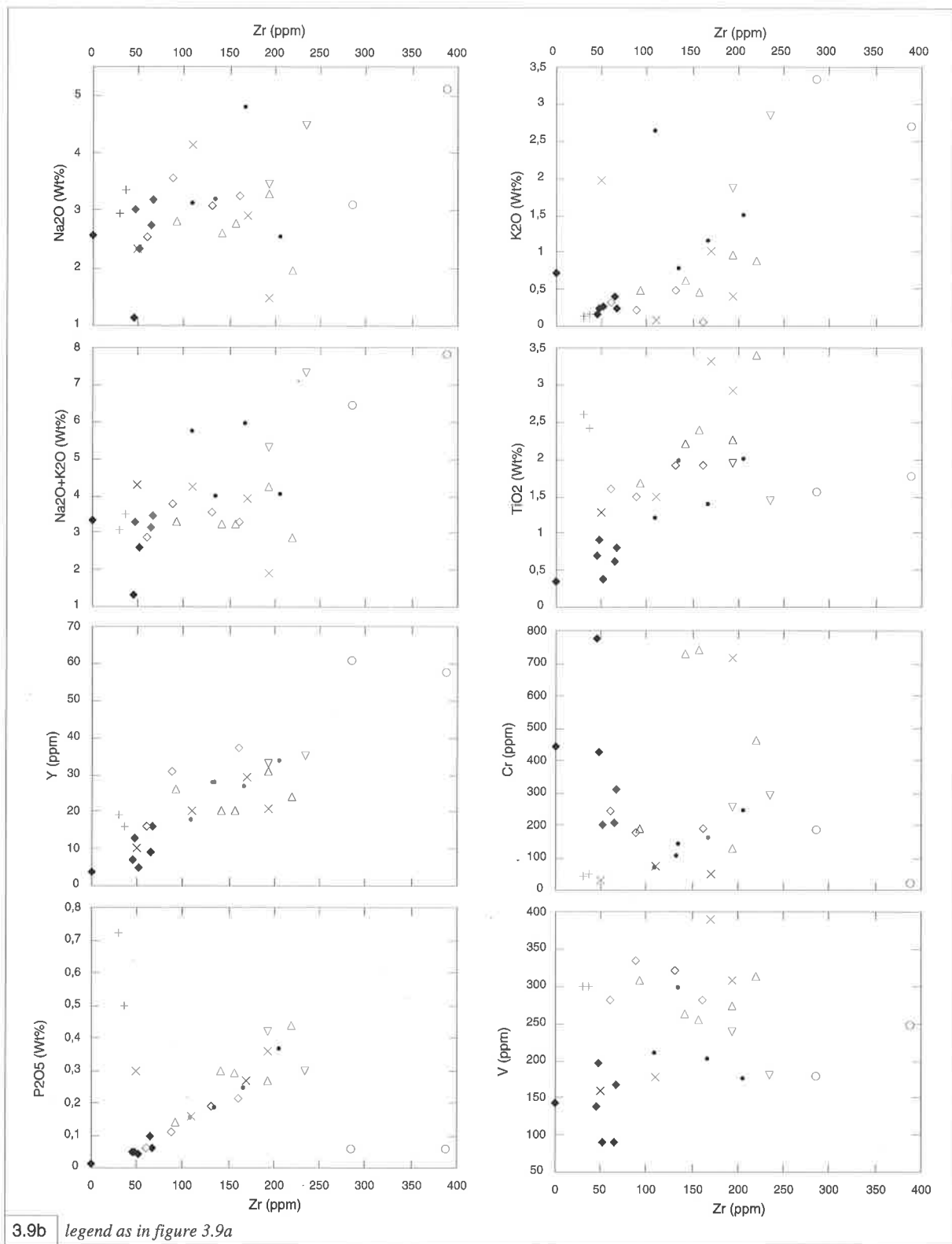
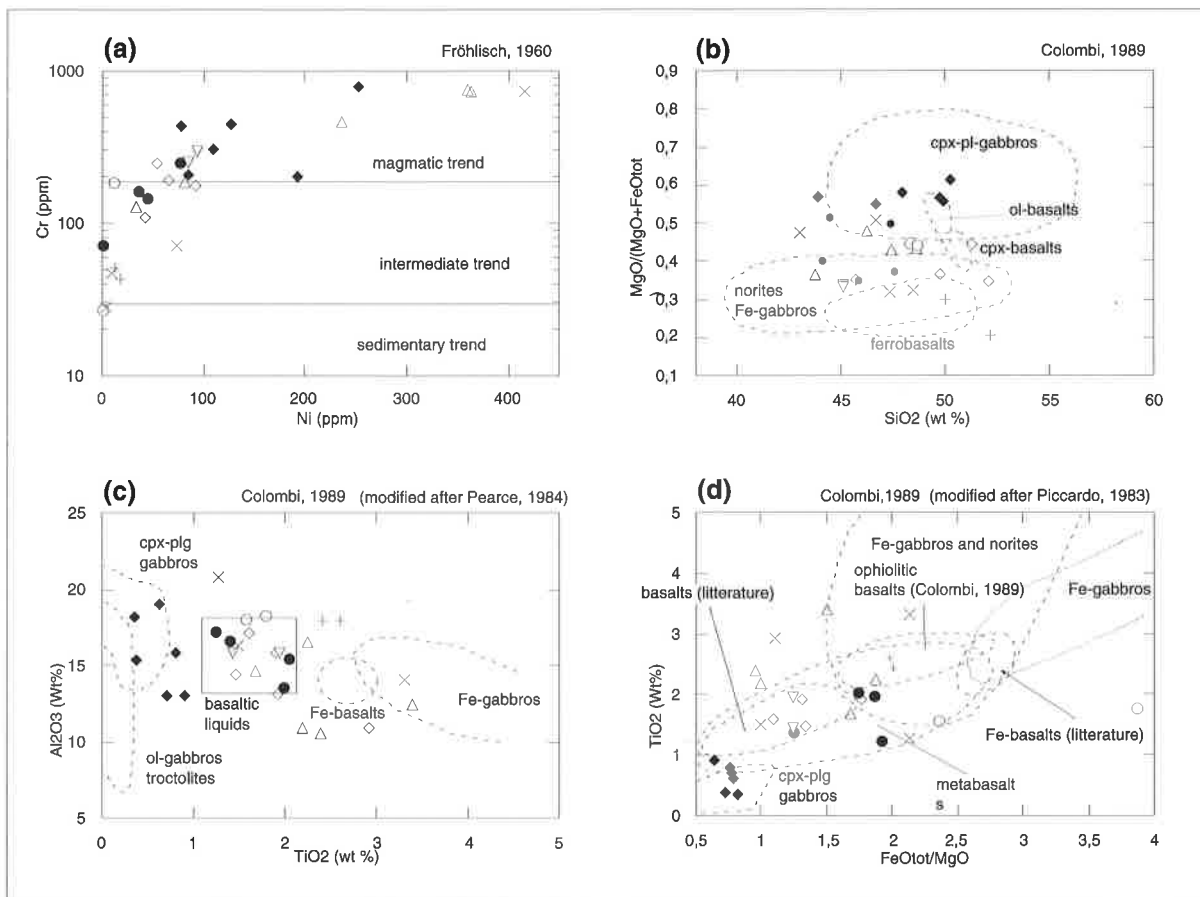


Fig. 3.9 - Mobility diagrams of the mafic rocks. Major and trace elements were compared to Zr (Beccaluva *et al.*, 1984; Colombi and Pfeifer, 1989; Simic, 1992). Although no general correlations are shown by these diagrams, a certain homogeneity of data distributions for each set of data can be observed. Data relative to the mafic boudins within the polycyclic basèment micaschists are instead partially dispersed.



intermediate trend. Figures 3.10b, 3.10c and 3.10d provide instead helpful information about the magmatic protolith of the studied lithologies. These graphics clearly show the presence of different sets of mafic rocks. The first group of data comprises the

mylonitic metagabbros, which constantly fall in the field of the Mg-rich gabbros (clinopyroxene-plagioclase gabbros); the glaucophane-eclogites of the monometamorphic show the same composition of the basaltic liquid (Colombi, 1989; modified after



- ◆ Bonze-type metagabbros
- ◇ glaucophane-eclogites (monometamorphic cover sequences)
- basic levels and blocks within the gneiss pipernoides
- basic breccias (monometamorphic cover sequences)
- △ pre-Alpine amphibolites (C. Courma)
- + metagabbroic glaucophanites (Corio and Monastero granulitic metagabbros)
- ▽ phlogopite-eclogites (polycyclic basement)
- × polycyclic basement mafic boudins within the micaschists

Pearce, 1984). The basic extrusive affinity of these rocks is also confirmed by graphic 3.10d (Colombi, 1989; modified after Piccardo, 1983). Most of the other analysed samples present moreover similar chemical compositions, although a certain enrichment in iron content characterises the pre-Alpine amphibolites, the gabbroic glaucophanites of Corio and Monastero and two of the basic boudins in the polycyclic micaschists.

The ternary plots in Fig. 3.11 provide further preliminary information about both the protolith and the possible geotectonic affinity of those samples characterised by a basaltic composition. The field subdivisions of the AFM ternary graphic of Fig. 3.11a

Fig. 3.10 - Discriminative diagrams for mafic rocks. In graphic (c) the Bonze-type metagabbros constantly fall in the field of the Mg-gabbros while the glaucophane-eclogites of the monometamorphic cover sequences show compositions typical of basaltic liquids (Colombi, 1989, modified after Pearce, 1984). Pre-Alpine amphibolites, as well as the metagabbro glaucophanites of Corio (southern Sesia zone) display Fe-rich basaltic compositions.

(Morse, 1988, modified by Colombi and Pfeifer, 1989) confirm the presence of both Mg-gabbros (corresponding to the mylonitic metagabbros of the monometamorphic cover complex) and «ophiolitic» basalts (glaucophane-eclogites). Moreover, this graphic underlines the high-alkali content of some of the analysed samples, with particular regard to the basic breccias, the phlogopite-eclogites and the basic levels and boudins present into the gneiss pipernoides. Figures 3.11b and 3.11c suggest the geotectonic emplacement origin of those samples characterised by a basaltic protolith. Plot 3.11b (Mullen, 1983) evidentiates a set of samples relatively high in Mn, comprising the eclogite-metabasalts and the basic levels of the gneiss pipernoides, and a group low in

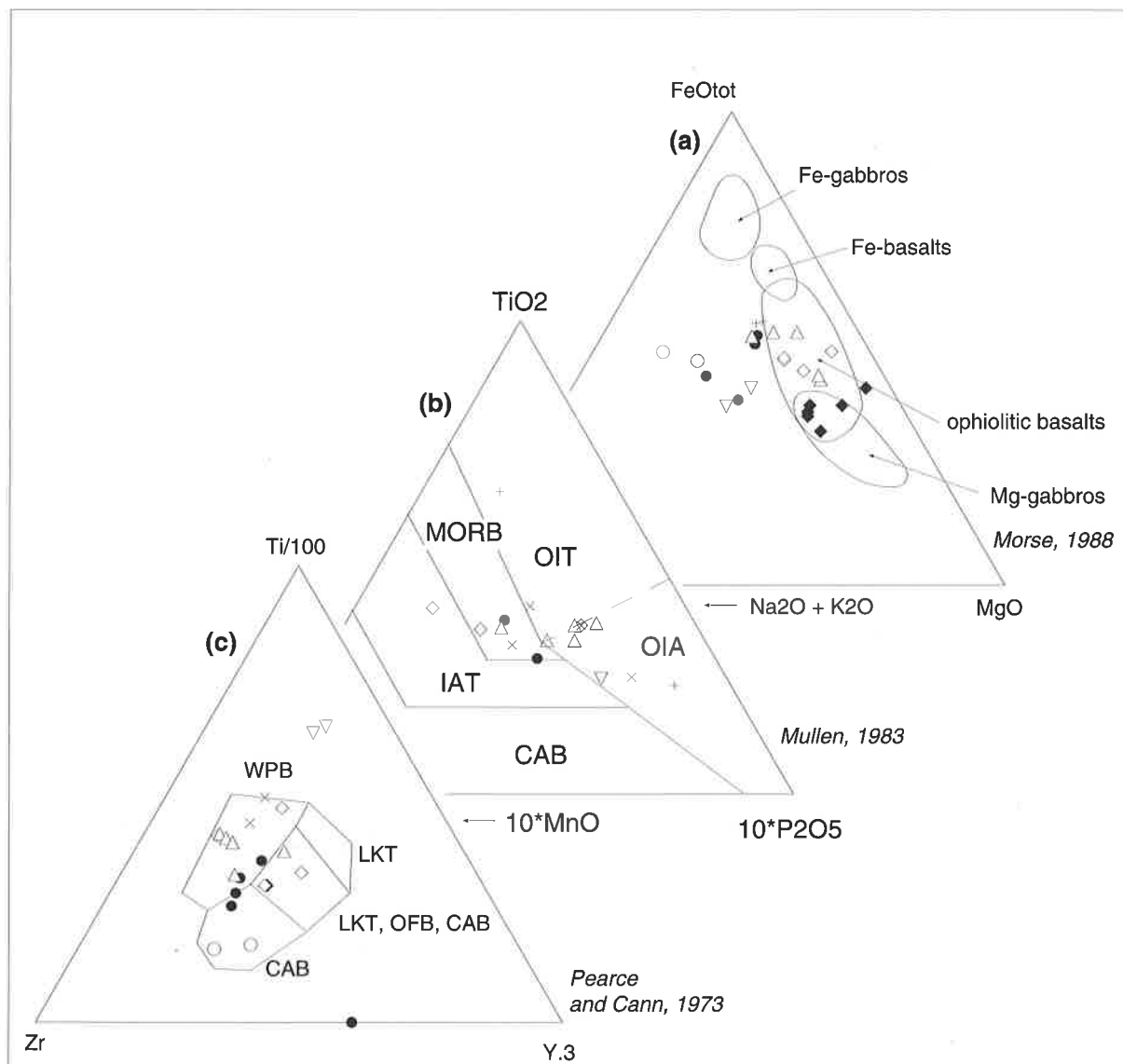


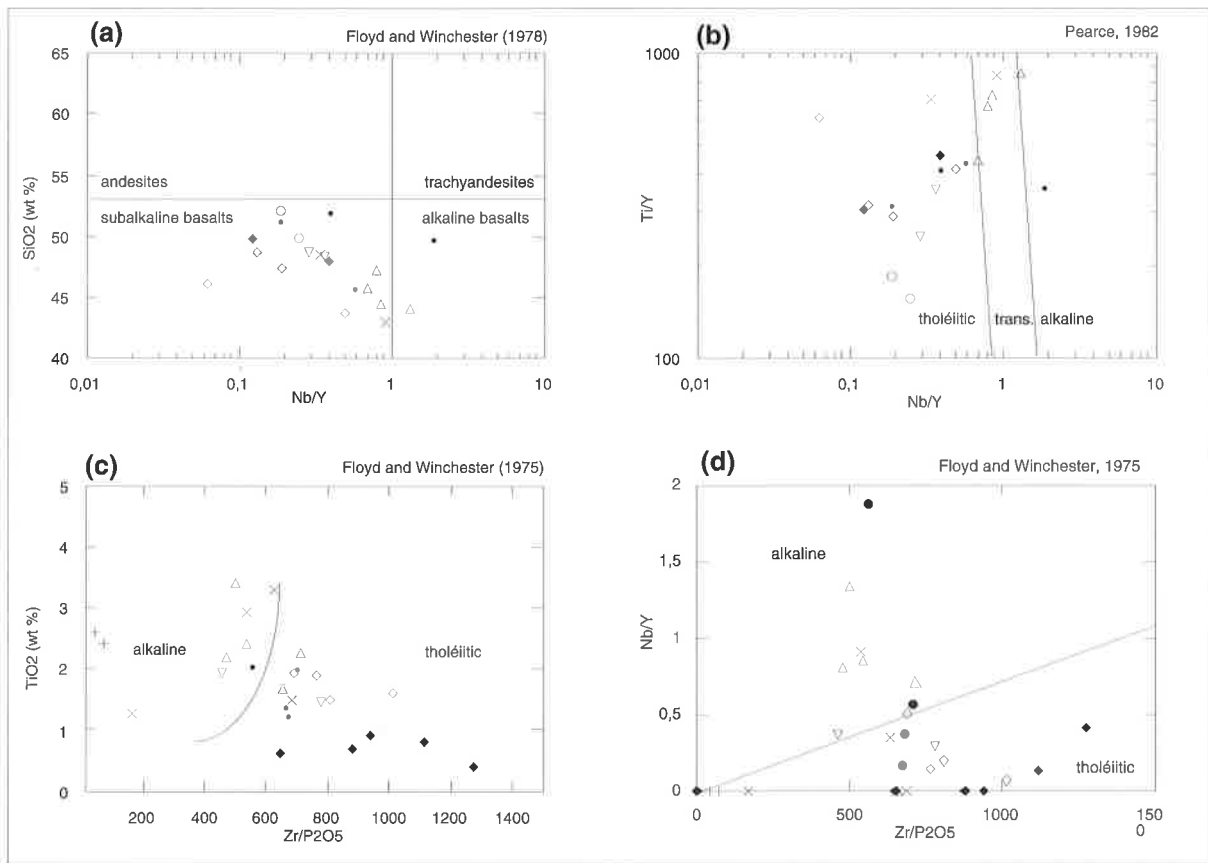
Fig. 3.11 - Discriminative ternary plots for the mafic rocks. AFM plot (c) (Morse, 1988, with compositional field proposed by Pfeifer and Colombi, 1989) permits to distinguish the Mg gabbros (Bonze-type metagabbros) from the rocks with a basaltic composition. The basic levels contained within the mesocratic gneisses, the phlogopite-bearing eclogites, and the basic breccias of the monometamorphic cover sequences display a certain enrichment in alkali. Legend as in Figure 3.10

Mn (pre-Alpine amphibolites, boudins comprised within the polycyclic basement). The former shows a middle ocean ridge basalts (MORB) affinity, while the latter fall in the within plate basalts (WPB) field. These observations are confirmed by plot 3.12c, in which the glaucophane-eclogites indicate an ocean floor basalt trend while the other samples display a WPB resemblance.

The diagrams of Fig. 3.13 discriminate between alkaline and sub-alkaline or tholeiitic series. Graphic 3.13a indicates a sub-alkaline basalt affinity for almost all the analysed samples. In Plot 3.13b and 3.13c most of the samples show tholeiitic affinity with the

exception of some pre-Alpine amphibolites and the mafic boudins in the polycyclic micaschists, which constantly fall in the alkaline field, close to the boundary with the tholeiitic field (3.13c). The mylonitic metagabbros and the glaucophane-eclogites of the monometamorphic cover sequences fall in the tholeiitic field. Sample sv9127c, a mafic boudin from the gneiss pipernoïdes, is instead characterised by an alkaline affinity. The previous graphics permit us to propose a first pre-liminary classification system to analysed mafic rocks:

- 1) the Bonze-type metagabbros are *tholeiitic clinopyroxene-plagioclase gabbros*; they are chara-



- ◆ Bonze-type metagabbros
- ◇ glaucophane-eclogites (monometamorphic cover sequences)
- basic levels and blocks within the gneiss pipernoides
- basic breccias (monometamorphic cover sequences)
- △ pre-Alpine amphibolites (C. Courma)
- + metagabbroic glaucophanites (Corio and Monastero granulitic metagabbros)
- ▽ phlogopite-eclogites (polycyclic basement)
- × polycyclic basement mafic boudins within the micaschists

Fig. 3.12 - Evolutionary diagrams for the mafic rocks. Two main sets of lithologies can be defined: the rocks characterised by tholeiitic affinity (glaucophane eclogites of the monometamorphic cover sequences, Bonze-type Mg-gabbros and mafic levels within the mesocratic gneisses) and those with an alkaline affinity (pre-Alpine amphibolites, glaucophanitic metagabbro and mafic boudins collected within the polycyclic basement micaschists).

cterised by low-Ti and relatively high-Mg contents;

- 2) the glaucophane-eclogites derive from *tholeiitic basalts*; their MORB affinity, according to conventional ternary plots of Mullen (1983) and Pearce and Cann, (1973), has to be tested with further discriminative diagrams (Par. 3.4.5);
- 3) the blocks and basic levels contained in the gneiss pipernoides have a *tholeiitic affinity* and they are characterised by a WPB geotectonic emplacement environment. Sample sv9127c differs from the other similar samples because of its alkaline affinity. The correct compositions of these lithologies must be further investigated;

4) the mafic breccias have *basaltic composition* and are particularly enriched in alkalis;

5) the pre-Alpine amphibolites are *WPB basalts and norites* with a relatively high Fe- and Mg-content; their evolutionary affinity changes from tholeiitic to alkaline series.

Other lithologies (mafic boudin within the polycyclic micaschists and gabbroic glaucophanites) are mainly *Fe-rich basalts* doubtfully related to the WPB geotectonic emplacement environment.

3.4.5. Discriminative Diagrams For Basalts

We discriminate above between the gabbroic

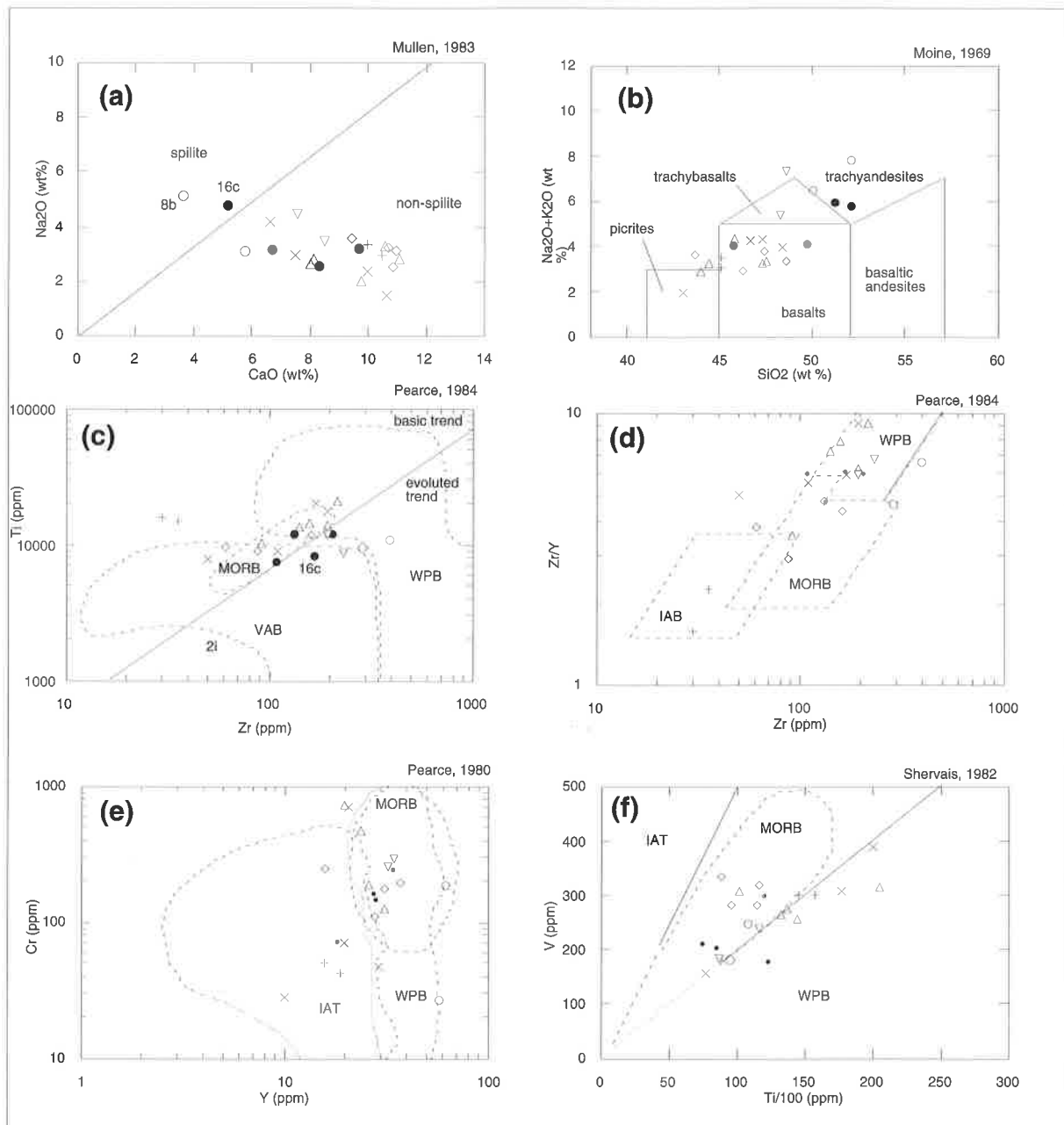


Fig. 3.13 - Discriminative diagrams for the mafic rocks of basaltic composition. The analysed rocks range from picrites to trachyandesites (plot 3.14b). The more evolved lithologies are partially spilitized (plot 3.14a). Plots 3.14c-f gives some indications about the geotectonic origin of the basaltic rocks. The metabasalts of the monometamorphic cover sequences (glaucophane-eclogites) are characterised by a MORB affinity, while the pre-Alpine amphibolites, the mafic levels within the gneiss pipernoïdes, and the phlogopite bearing-eclogites fall generally in the WPB field. Legend as in Figure 3.12.

mafic rocks and the lithologies with basaltic protoliths. In this section some diagrams for rocks with basaltic composition are used to further distinguish within this group of rocks. Figure 3.14 provides information about the original composition of the extrusive mafic rocks, the influence of oceanic spilitisation, and further indicators relative to the

geotectonic and evolutionary affinity of the investigated rocks. Figure 3.13a provides an idea of the possible spilitic alteration affecting the rocks during the emplacement. A basic breccia (sv918b) and a basic boudin (sv9116c) from the gneiss pipernoïdes display an enrichment of alkalis in comparison to the CaO content (Mullen, 1983), while other samples fall

in the field of non-spilites. The basic breccias of the monometamorphic cover sequences represent the more evolved rocks in plot 3.13b proposed by Moine (1969). Most of other samples falls in the basalts field, except for the two phlogopite-eclogites (trachybasalts) and other picritic samples.

According to the Ti-Zr plot (Pearce, 1984) (Fig. 3.13c), most of the metabasalts and metagabbros fall in the MORB and/or WPB field. The basic breccias, and the phlogopite-eclogites, as well as two of the basic levels of the gneiss pipernoïdes, fall in the evolved trend and cannot be geotectonically characterised (Pearce, 1984). Figures 3.13d and 3.13e further characterise the analysed lithologies in order to search a proper geotectonic emplacement environment. The basaltic glaucophane-eclogites show a MORB affinity, while the basic blocks and levels of the gneiss pipernoïdes are characterised by a WPB geotectonic setting as well as the pre-Alpine amphibolites. The other lithological groups are ambiguous. Figure 3.13f (Shervais, 1982) confirms the MORB affinity of the basaltic glaucophane-eclogites of the monometamorphic cover sequences while the pre-Alpine amphibolites and the basic levels and boudins of the gneiss pipernoïdes fall at the boundary between the MORB and the WPB fields.

The spider diagrams of figure 3.14 allow us to compare the trace element content of the different basaltic samples normalised to MORB (Pearce, 1984). Two main trends are represented by the spider diagrams (fig. 3.14a): the basaltic glaucophane-eclogites of the monometamorphic cover sequences display a MORB-type basalt profile, while the other diagrams show more or less disturbed WPB profiles. Samples collected in the southern Sesia zone (gabbroic glaucophanites of Corio and Monastero) exhibit disturbed profiles, while three of the pre-Alpine amphibolites and a basic boudin of the polycyclic micaschists present an anomalous enrichment in light trace elements (Cr and Ni).

Based on the discussion above, we can tentatively advance some main conclusions:

- a) the glaucophane-eclogites of the monometamorphic cover sequences are derived from *tholeiitic middle ocean ridge basalts (MORB)*. They differ from the pre-Alpine mafic lithologies in both their bulk chemical composition and their geotectonic affinity.
- b) the basic blocks and levels contained in the gneiss pipernoïdes are *tholeiitic WPB Fe-basalts and trachyandesites*, more evolved in comparison to the pre-Alpine amphibolites. They moreover differ from the amphibolites of the pre-Alpine basement because of a relative enrichment in heavy trace elements and depletion in light trace elements
- c) the mafic breccias represent intermediate tholeiitic *trachybasalts/ trachyandesites* that have been partially altered by oceanic metamorphism. They cannot be considered as directly deriving from metabasalts of the monometamorphic cover sequences.
- d) a certain compositional correspondence exists between the pre-Alpine amphibolites and the gabbroic glaucophanites of Corio and Monastero. Similar analogies can be seen with the basic boudins in the polycyclic micaschists, with particular regard to sample sv923i.

Tab. 3.6.a and b summarise the discriminative diagrams discussed above.

3.4.6. The Metabasalts of the Monometamorphic Cover Sequences

In the previous paragraphs, we have pointed out the MORB tholeiitic origin of the metabasalts (glaucophane-eclogites) of the Sesia zone monometamorphic covers (Venturini et al., 1994a).

Until now, such kinds of mafic lithologies were described only by Simic (1992) in the pre-Alpine HG basement complex of Val Mastallone (northern Sesia zone). There, the metabasalts were closely related to other HG pre-Alpine rocks (IIDK_{auct}) such as garnet-sillimanite-biotite metapelites and felsic granulites.

In the central Sesia zone, the metabasalts are generally associated with dolomitic marbles, Mn-rich calcschists, and other metasediments (par. 2.1.4). In addition, they display scattered relics of the original textures, such as pillow breccias or intercalations of Mn-rich quartzitic levels. Field relationships with the surrounding monometamorphic lithologies reasonably exclude any correlation of these metabasalts to those described in the II DK by Simic (1992). Until now, no basaltic lithologies were described in the monometamorphic cover sequences of the western Austroalpine system, neither in the Mont Dolin series nor in the Pillonet and in the Roisan covers. The interbedding whereas trasposed relationship of these metabasalts with the yellow dolomitic marbles as well as the presence of blocks of the same lithologies within the calcschists suggests an Upper Triassic-Early Jurassic emplacement age for these mafic rocks, if we admit that the dolomitic

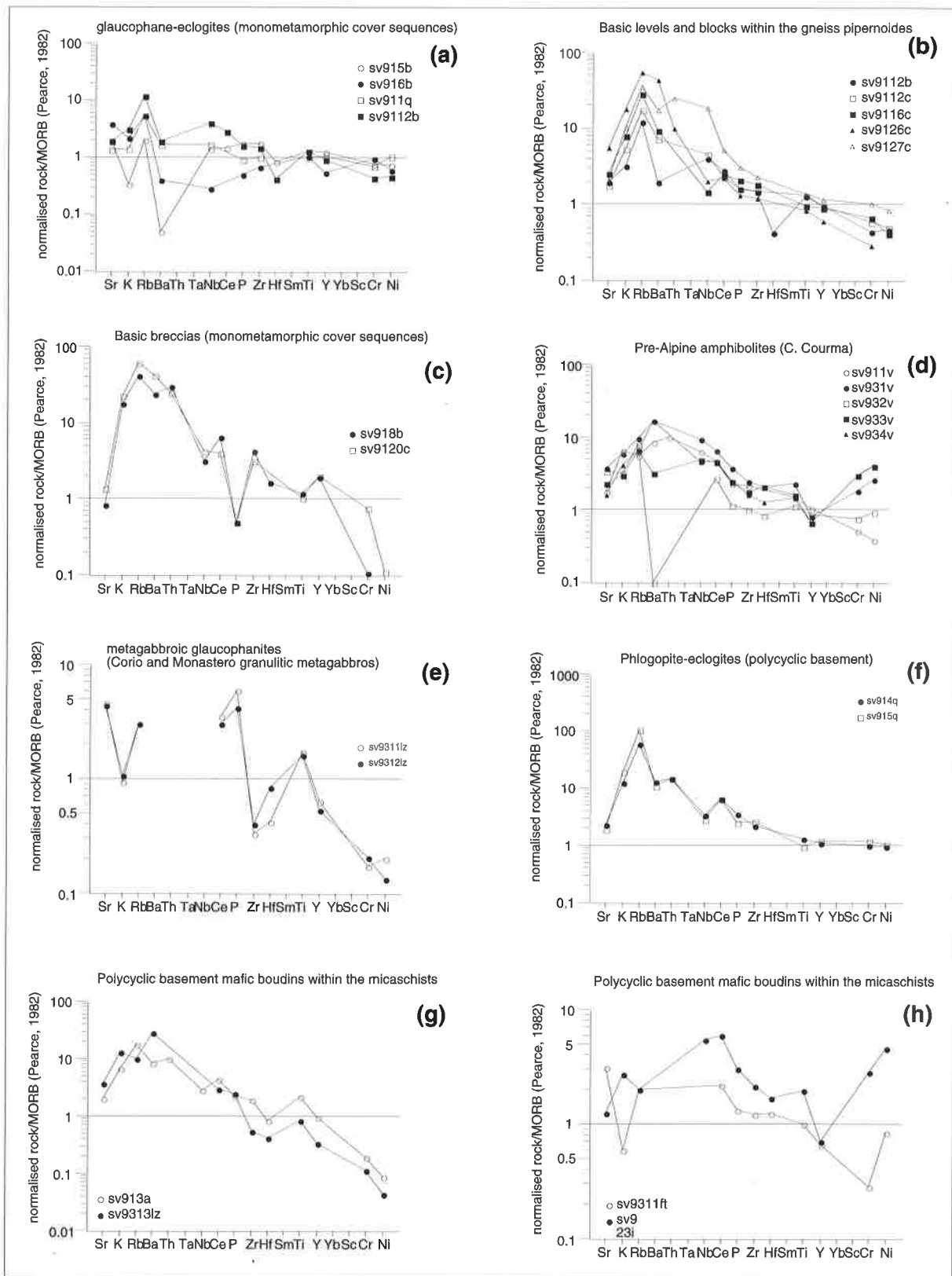


Fig. 3.14 - Spider diagrams for the basaltic lithologies analysed in this study. The metabasalts of the monometamorphic cover sequences display a good MORB-type profile, while the other rocks are generally characterised by WPB-type profiles. Rock values were normalised to N-MORB (Pearce, 1982).

rock type	(SV 91)	locality	Cr Ni	Na ₂ O+K ₂ O SiO ₂	Al ₂ O ₃ TiO ₂	MgO/(MgO+FeOtot) SiO ₂	TiO ₂ FeOtot/MgO	SiO ₂ Nb/Y	Ti/Y Nb/Y	TiO ₂ Zr/P ₂ O ₅	Nb/Y Zr/P ₂ O ₅
			<i>Frölich</i> 1960	<i>Le Maitre</i> 1969	<i>Colombi & Pfeifer</i> 1989	<i>Colombi & Pfeifer</i> 1989	<i>Colombi & Pfeifer</i> 1989	<i>Floyd & Winchester</i> 1978	<i>Pearce</i> 1982	<i>Floyd & Winchester</i> 1975	<i>Floyd & Winchester</i> 1975
metagabbro	4b	Bonze	magmatic	basalt	Mg-gabbros	cpx-pl-gabbro	Mg-gabbros	subalk. basalts	tholeiitic	tholeiitic	tholeiitic
metagabbro	9b	Bonze	magmatic	picrite	Mg-gabbros	cpx-pl-gabbro	Mg-gabbros	-	-	tholeiitic	tholeiitic
metagabbro	15vc	C. del Prà	magmatic	basalt	Mg-gabbros	cpx-pl-gabbro	Mg-gabbros	-	-	tholeiitic	tholeiitic
metagabbro	2i	Ivery	magmatic	basalt	Mg-gabbros	cpx-pl-gabbro	Mg-gabbros	-	-	-	-
metagabbro	2az	Sermenza	magmatic	basalt	Mg-gabbros	cpx-pl-gabbro	Mg-gabbros	-	-	tholeiitic	tholeiitic
metagabbro	3az	Sermenza	magmatic	basalt	Mg-gabbros	cpx-pl-gabbro	Mg-gabbros	subalk. basalts	tholeiitic	tholeiitic	tholeiitic
gln-eclogite	5b	Bonze	magmatic	basalt	basaltic liquid	cpx-pl-gabbro	basalts	subalk. basalts	tholeiitic	tholeiitic	tholeiitic
gln-eclogite	6b	Bonze	magmatic	basalt	basaltic liquid	cpx-pl-gabbro	metabasalts	subalk. basalts	tholeiitic	tholeiitic	tholeiitic
gln-eclogite	12b	Bonze	magmatic	basalt	basaltic liquid	cpx-pl-gabbro	basalts	subalk. basalts	tholeiitic	tholeiitic	tholeiitic
gln-eclogite	1q	Quincinetto	magmatic	basalt	basaltic liquid	cpx-pl-gabbro	basalts	subalk. basalts	tholeiitic	tholeiitic	tholeiitic
basic block	12c	Cavalcurt	intermed.	basalt	basaltic liquid	Fe-norite	metabasalts	subalk. basalts	tholeiitic	tholeiitic	tholeiitic
basic level	16c	Cavalcurt	intermed.	trachyandesite	basaltic liquid	Fe-norite	metabasalts	subalk. basalts	tholeiitic	tholeiitic	tholeiitic
basic block	26c	Cavalcurt	intermed.	trachyandesite	basaltic liquid	Fe-norite	metabasalts	subalk. basalts	tholeiitic	tholeiitic	tholeiitic
basic block	27c	Cavalcurt	intermed.	trachyandesite	basaltic liquid	Fe-norite	metabasalts	alkaline basalts	alkaline	alkaline	alkaline
mafic breccia	8b	Bonze	sedim.	trachyandesite	basaltic liquid	?	?	subalk. basalts	tholeiitic	tholeiitic	tholeiitic
mafic breccia	20c	Cavalcurt	intermed.	trachybasalt	basaltic liquid	Fe-norite	Fe-norites	subalk. basalts	tholeiitic	tholeiitic	tholeiitic
glaucophanite	911v	C. Courma	intermed.	basalt	basaltic liquid	Fe-norite	basalt	subalk. basalts	trans.	tholeiitic	tholeiitic
glaucophanite	931v	C. Courma	magmatic	picrite	Fe-gabbro	Fe-norite	Fe-norite	alkaline basalts	alkaline	alkaline	alkaline
glaucophanite	2v	C. Courma	magmatic	picrite	Fe-basalt	Fe-norite	Fe-norite	subalk. basalts	trans.	tholeiitic	tholeiitic
glaucophanite	3v	C. Courma	magmatic	basalt	Fe-basalt	cpx-pl-gabbro	?	subalk. basalts	trans.	alkaline	tholeiitic
glaucophanite	4v	C. Courma	magmatic	basalt	Fe-basalt	cpx-pl-gabbro	?	subalk. basalts	trans.	alkaline	tholeiitic
phl-eclogites	4q	Quincinetto	magmatic	trachybasalt	basalt	cpx-pl-gabbro	basalt	subalk. basalts	tholeiitic	alkaline	tholeiitic
phl-eclogites	5q	Quincinetto	magmatic	trachybasalt	basalt	cpx-pl-gabbro	basalt	subalk. basalts	tholeiitic	tholeiitic	tholeiitic
glaucophanite	111z	Corio	intermed.	basalt	Fe-basalt?	Fe-norite	Fe-basalt	?	?	alkaline	alkaline?
glaucophanite	121z	Corio	intermed.	basalt	Fe-basalt?	Fe-norite	Fe-basalt	?	?	alkaline	alkaline?
glaucophanite	11ft	Fert	intermed.	basalt	basaltic liquid	cpx-pl-gabbro	metabasalts	?	?	tholeiitic	tholeiitic?
eclogite	3i	Ivery	magmatic	picrite	Fe-basalt?	cpx-pl-gabbro?	?	subalk. basalts	trans.	alkaline	tholeiitic?
amphibolite	3a	Arnad	intermed.	basalt	Fe-gabbro	Fe-norite	Fe-norite	subalk. basalts	tholeiitic	trans.	tholeiitic
gln-eclogite	131z	Rocca C.se	sed.	basalt	?	Fe-norite	metabasalts	?	?	trans.	tholeiitic

Tab. 3.6a - Summarizing table of the results obtained with the discriminative diagrams for the mafic rocks.

rock type	(SV 91)	locality	Ti Zr	Cr Y	Ti/Y Nb/Y	Zr/Y Zr	V Ti/100	Ti/100-Zr Y*3	TiO ₂ -10*MnO 10*P ₂ O ₅	Ti/100-Zr Sr/2	Spider rock/MORB	Conclusion
metagabbro	4b	Bonze	Pearce	Pearce	Pearce	Pearce	Shervais	Pearce & Cann	Pearce & Cann	Pearce & Cann	Pearce	
metagabbro	9b	Bonze	VAB	IAT	VAB	?	?	WPB	IAT	CAB	VAB?	tholeiitic Mg-gabbro (VAB?)
metagabbro	15vc	C. del Prà	VAB	(IAT)	?	?	?	WPB	?	OFB	VAB?	tholeiitic Mg-gabbro (VAB?)
metagabbro	2i	Ivery	-	(IAT)	?	?	?	WPB	OIA	LKT	VAB?	tholeiitic Mg-gabbro (VAB?)
metagabbro	2az	Sermenza	VAB	IAT	WPB	?	?	WPB	?	CAB	VAB?	tholeiitic Mg-gabbro (VAB?)
metagabbro	3az	Sermenza	VAB	IAT	WPB	?	?	WPB	CAB	CAB	VAB?	tholeiitic Mg-gabbro (VAB?)
gln-eclogite	5b	Bonze	MORB	MORB	MORB	MORB	MORB	LKT, OFB, CAB	MORB	OFB	MORB	tholeiitic Ti-basalts - MORB
gln-eclogite	12b	Bonze	MORB	IAT	MORB	MORB	MORB	LKT, OFB, CAB	OIT	OFB	MORB	tholeiitic Ti-basalts - MORB
gln-eclogite	12b	Bonze	MORB	MORB	MORB	MORB	MORB	LKT, OFB, CAB	OFB	OFB	MORB	tholeiitic Ti-basalts - MORB
gln-eclogite	1q	Quincinetto	MORB	MORB	MORB	MORB	MORB	LKT, OFB, CAB	OFB	OFB	MORB	tholeiitic Ti-basalts - MORB
basic block	12c	Cavalcurt	MORB	MORB	WPB	WPB	WPB	WPB	OFB	OFB	WPB	tholeiitic Fe-norite - WPB
basic level	16c	Cavalcurt	VAB	MORB	WPB	WPB	WPB	WPB	OFB	OFB	WPB	tholeiitic trachyandesite - WPB
basic block	26c	Cavalcurt	MORB	IAT	WPB	WPB	WPB	WPB	CAB	CAB	WPB	tholeiitic trachyandesite - WPB
basic block	27c	Cavalcurt	WPB	MORB	WPB	WPB	WPB	WPB	OFB	OFB	WPB	alkaline Fe-norite - WPB
mafic breccia	8b	Bonze	WPB	WPB	?	IAT	MORB	CAB	?	?	WPB?	tholeiitic trachyandesite - WPB
mafic breccia	20c	Cavalcurt	WPB	WPB	?	IAT	WPB	CAB	?	?	WPB?	tholeiitic trachybasalt - WPB
glaucophanite	911v	C. Courma	WPB	WPB	WPB	WPB	WPB	WPB	OFB	OFB	WPB	tholeiitic Fe-norite - WPB
glaucophanite	931v	C. Courma	WPB	WPB	WPB	WPB	WPB	WPB	OFB	OFB	?	alkaline Fe-norite - WPB?
glaucophanite	2v	C. Courma	VAB?	WPB	WPB	WPB	WPB	WPB	OFB	OFB	WPB	tholeiitic Fe-norite - WPB
glaucophanite	3v	C. Courma	WPB?	WPB	WPB	WPB	WPB	WPB	OFB	OFB	WPB	trans. Fe-basalt-WPB
glaucophanite	4v	C. Courma	WPB?	WPB	WPB	WPB	WPB	WPB	OFB	OFB	WPB	trans. Fe-basalt-WPB
phl-eclogites	4q	Quincinetto	WPB	WPB	WPB	WPB	MORB?	?	OIA	OFB	WPB?	tholeiitic trachybasalt - WPB?
phl-eclogites	5q	Quincinetto	WPB	WPB	VAB	MORB?	MORB?	?	OIA	?	WPB?	tholeiitic trachybasalt - WPB?
glaucophanite	11lz	Corio	VAB?	IAT	?	IAT	WPB	?	OIA	?	?	trans. Fe-norite - WPB?
glaucophanite	12lz	Corio	VAB?	IAT	?	IAT	WPB	?	OIA	?	?	trans. Fe-norite - WPB?
glaucophanite	11ft	Fert	MORB?	IAT	?	MORB	MORB?	?	OIA	?	?	tholeiitic Ti-basalts - MORB??
eclogite	3i	Ivery	WPB	WPB	WPB	WPB	WPB	WPB	LKT	LKT	?	trans. picrite-WPB
amphibolite	3a	Arnad	WPB	WPB	WPB?	?	WPB	?	?	?	WPB	tholeiitic Fe-norite - WPB
gln-eclogite	13lz	Rocca C.se	VAB	IAT	?	?	WPB?	WPB	OFB	OFB	WPB	alkaline Fe-norite - WPB?

Tab. 3.6b - Summarizing table of the results obtained with the discriminative diagrams for the mafic rocks.

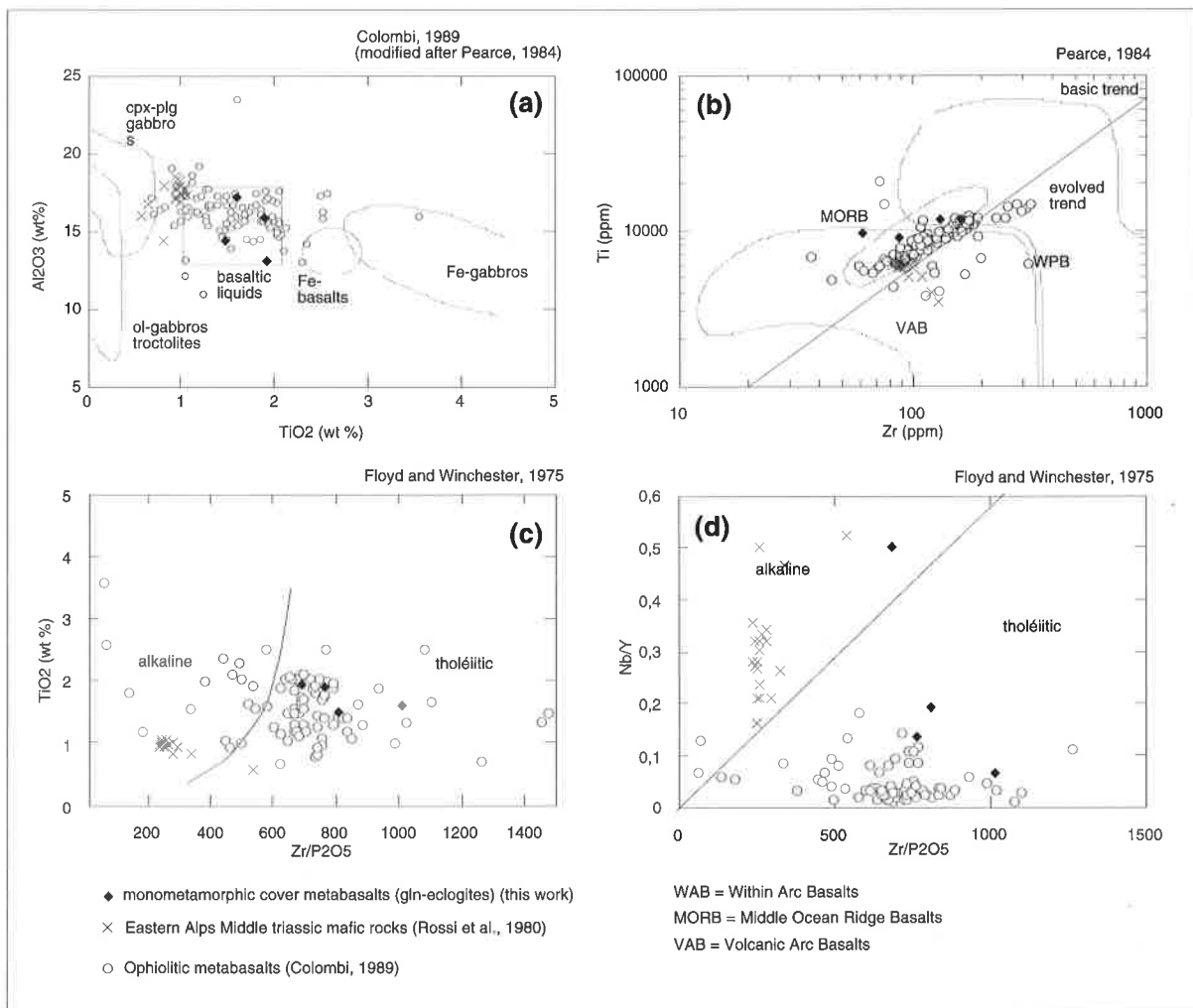


Fig. 3.15 - Comparative diagrams relative to the metabasalts of the monometamorphic cover sequences, the Penninic ophiolitic metabasalts (Colombi, 1989) and the mafic volcanic rocks of the middle Triassic (Ladinian) outcropping in the Eastern Alps (Rossi et al., 1980). The Ladinian mafic rocks are characterised by alkaline affinity and by a lower-Ti content, which permit us to distinguish them from the monometamorphic cover metabasalts and the ophiolitic basalts. Marked similarities exist instead between the monometamorphic cover metabasalts and the ophiolitic metabasalts.

marbles are Upper Triassic and the contacts with the metabasalts are only locally and partially transposed. In the Eastern Alps, several dykes of andesites and basaltic andesites crosscutting the dolomitic marbles of the Middle Triassic have been described (De Zanche and Sedeo, 1972; Rossi et al., 1980; Castellarin et al., 1980, 1988; De Zanche, 1990 with ref.). The Ladinian (Middle Triassic) magmatism of the Eastern Alps is mainly characterised by intercalations of trachyandesites with volcanic arc calc-alkaline origin (Rossi et al., 1980; Castellarin et al., 1988), preventing any potential correlation. The geochemical pattern of metabasalts of the monometamorphic cover sequences of the Sesia zone suggests, on the other hand, a close affinity with the eclogitic metabasalts of the Zermatt-Saas zone derived from Jurassic MORB (Dal Piaz et al., 1981; Piccardo, 1983;

Beccaluva et al., 1984; Colombi 1989). The analysed metabasalts of the mono-metamorphic cover sequences are plotted in some discriminate diagrams together with the Middle Triassic mafic rocks of the eastern Alps (data from Rossi et al., 1980) and the Penninic ophiolitic basalts analysed by Colombi (1989) and Pfeifer et al. (1989) (Fig. 3.15). Two distinct compositional fields can be recognised; the Middle Triassic mafic volcanics of the Eastern Alps have a low-Ti content in comparison to the ophiolitic basalts and the metabasalts of the monometamorphic cover sequences (3.15a). Graphic 3.15b shows the inferred the volcanic arc basalts (VAB) affinity of the Ladinian mafic rocks, contrary to the MORB signature of the ophiolitic basalts and the monometamorphic cover metabasalts. In addition, the calc-alkaline to shoshonitic affinity of

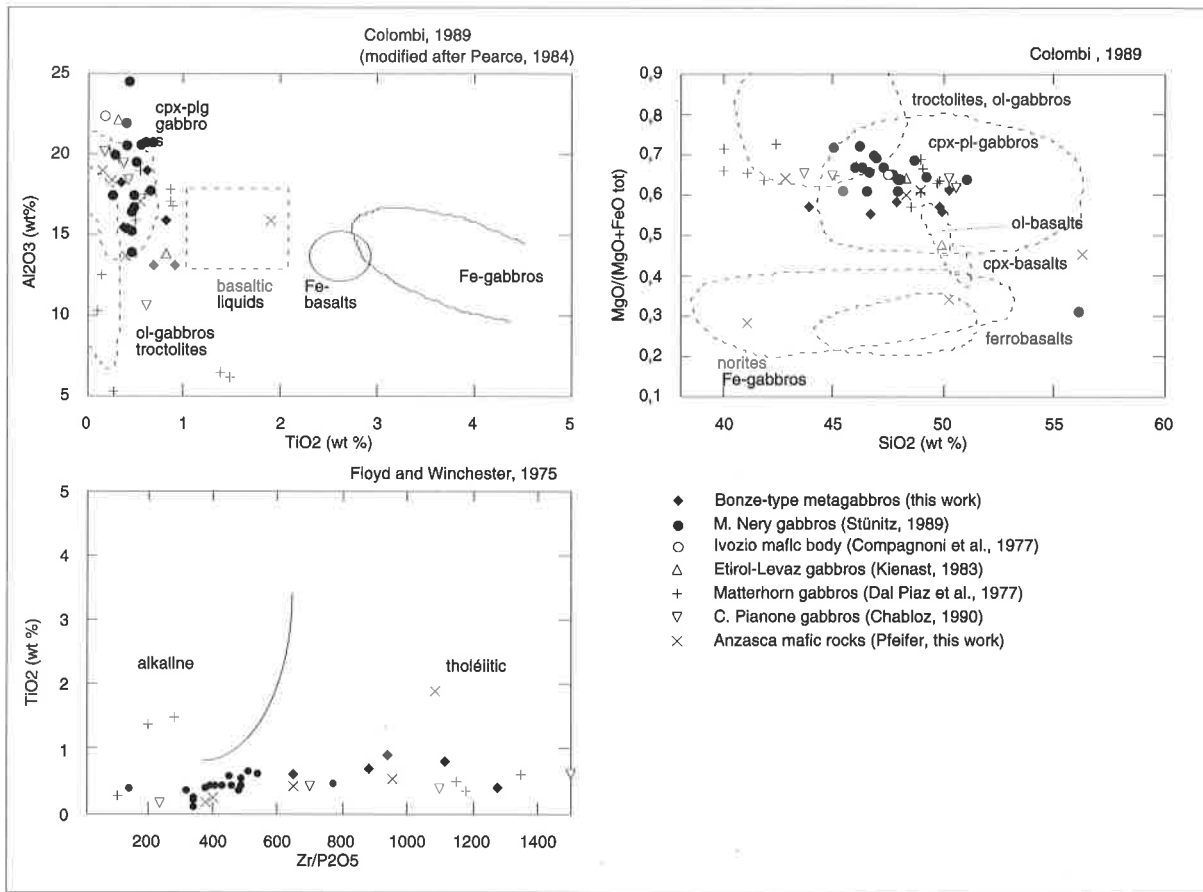


Fig. 3.16 - Comparative diagrams relatives to the Bonze-type metagabbros and the available data of the literature for the western Austroalpine mafic intrusions. The different diagrams display a strong chemical and evolutionary convergence between the different compared mafic lithologies.

the Middle Triassic extrusive rocks permits us to distinguish them from samples of tholeiitic affinity (Fig. 3.15d).

The original chemistry and the geotectonic characterisation of the Ladinian mafic rocks exclude therefore any possible correlation with metabasalts of the monometamorphic cover sequences of the Sesia zone. The hypothesis of a Ladinian effusive magmatism in the Sesia zone, postulated by Venturini et al. (1994a), similar to the volcanic activity in the Eastern Alps cover sequences, must be abandoned. The only geochemical difference between the metabasalts of the monometamorphic cover sequences and the ophiolitic metabasalts is the higher TiO₂ content and V concentration of the former. The chemical similarity of the metabasalts of the Sesia monometamorphic covers with the ophiolitic metabasalts of the Penninic domain does not univocally prove that the Sesia «cover sequences» are a slice of Alpine ophiolitic units. Some fundamental features distinguish the metabasalts of the Sesia monometamorphic cover

from those of the classic ophiolitic sequences. These features are: 1) the absence of the ultramafic components of an ophiolitic sequence (serpentinites²); 2) the presence of dolomitic marbles interbedded within the metabasalts. There are two explanations for the lack of serpentinites. First, a thin but already continental crust may have existed at the time of the emplacement of the MORB basalts of the Sesia cover sequences. The extrusive mafic rocks could have followed existing crustal fractures opened in a pull-apart context. Second, the emplacement of these volcanics could have also taken place at the foot of the margin and/or as dolerites in the carbonatic sequence.

3.4.7. The Mg-rich Metagabbros related to the Monometamorphic Cover Sequences

² No ultramafic lithologies were found in contact or close to the metabasalts, whereas few outcrops of ultramafic bodies were signaled in the lower Aosta valley (Ivozio, Compagnoni et al., 1977b; Pognante et al., 1980) and in the southern Sesia zone (Spalla et al., 1983; Pognante, 1989a)

The gabbroic bodies associated to the monometamorphic cover sequences (Venturini et al., 1991; 1994) were compared to other mafic intrusive bodies of the Sesia zone and Dent Blanche system. The main investigated basic stocks are: the Mont Nery gabbro (Stünitz, 1989), the Cima del Pianone cumulate gabbro (Chabloz, 1990), the Sermenza valley gabbroic and dioritic masses (Pfeifer, pers. comm.), the Ivozio mafic outcrops (Compagnoni et al., 1977b), the Corio and Monostero metagabbro (Bianchi et al., 1964), the gabbroic stock of the Matterhorn (Dal Piaz et al., 1977) and the metagabbro of the Etirol Levaz slice (Kienast, 1983). Unfortunately no geochemical data for the Testa Grigia gabbros (Dal Piaz et al., 1971) or the Sparone-region gabbro (Pognante et al., 1987) are available. Figure 3.16 reports some of the main discriminative diagrams which uses all the data from the mafic stocks mapped in the Sesia zone and in the western Austroalpine klippen. All samples are characterised by low-Ti content and fall in field of Mg-gabbros and/or olivine-gabbros and troctolites (Fig. 3.16a and 3.16b). The low-Ti content of the layered metagabbros is due to the fractionated crystallisation of magnetite, during the initial phases of accumulation (Stünitz, 1989). This genetic evolution could also explain the high-Ti concentrations shown by the some ultramafic samples of the Matterhorn and Sermenza gabbroic stocks. The analysed data show moreover a tholeiitic evolutionary affinity, with exception of the acid dykes of the Matterhorn gabbroic intrusion. The geochemical and emplacement characteristics of the Matterhorn gabbroic stock have been described in detail by Dal Piaz et al. (1977), who interpret this mafic intrusion as cumulate gabbros intruded at the upper mantle-lower crust boundary during the beginning of the post-Paleozoic opening phase (Dal Piaz and Ernst, 1978). Some Rb/Sr and K/Ar work on intercumulus phlogopites of the Matterhorn and Collon gabbros indicate an approximate cooling age of 260 Ma, *i.e.* Triassic-Permian boundary.

The similarities between the Bonze-type metagabbros and the other layered mafic intrusions of the western Austroalpine system suggest an analogous genesis and evolution. In this case the Bonze gabbros could represent an under-crustal intrusion of Permian age (Dal Piaz et al., 1977). During the Cretaceous accretion/subduction phase, these basic stocks could have been juxtaposed to the monometamorphic covers. This interpretation could explain the presence in the monometamorphic covers of the gabbroic bodies without other mafic rocks (Col del Prà, Bec Renon) or, vice versa, the absence of the mylonitic metagabbros in contact

with other mafic rocks in the Chiusella valley and in the Aosta and Crabun valleys.

3.5. The origin of the Gneiss Pipernoides on the basis of the whole rock geochemical analyses

Two possible explanations exist at least for these metric to decametric horizons of massive gneisses containing blocks and thin levels of acid and mafic rocks: a) they are strongly deformed polycyclic paraschists in which the pre-Alpine meta-aplites and the amphibolitic bodies have been highly stretched and boudinaged; b) they represent a monometamorphic volcano-detritic series of probable Permo-Triassic age (Venturini et al., 1994a); The geochemical analyses of both acid and basic rocks constituting the gneiss pipernoides are summarised below:

- a) the mesocratic gneisses containing basic levels and boudins, leucogneiss boudins and the carbonatic horizons are of sedimentary origin; their composition is slightly different from that of the a few analysed eclogitised kinzigites, the main protolith of the polycyclic basement-forming lithologies;
- b) the leucocratic boudin contained within the mesocratic gneisses derives from a magmatic protolith; it is chemically equivalent to the meta-aplites of the polycyclic basement. In the field, it is impossible to assign a detritic or tectonic origin to this enclave. The meta-aplites of the strongly deformed portions of polycyclic basement, however, are never boudinaged but only stretched. Field observation suggests a «clastic» origin for the leucocratic boudins.
- c) the basic levels and boudins interbedded with the mesocratic gneisses derive from Within Plate Tholeiitic basalts to trachyandesites. They slightly differ from the pre-Alpine amphibolites by a lower Ti content, a more pronounced concentration in lithophile trace elements and a relative depletion in Cr and Ni. They generally show a tholeiitic evolutionary tendency (except for sample sv9127c that has an alkaline affinity). Their tholeiitic affinity distinguishes them from the pre-Alpine amphibolites, which are preferentially alkaline. The compositional differences between the gneiss pipernoides-forming lithologies and the polycyclic basement rocks - although weak and preliminary - support the hypothesis that the gneiss pipernoides constitute an independent lithological sequence and they not represent the result of a strong and pervasive mylonitization of the polycyclic basement, as probably occurring in other cases.

- Chapter 4-

Mineral Chemistry, Temperature/Pressure Estimations and Stable Isotope Investigations

4.1 Introduction

Numerous petrologic studies involving mineral chemistry of the Sesia zone have been carried out in the last twenty years (Callegari and Viterbo, 1966; Dal Piaz et al., 1972, Hunziker, 1974, Lattard, 1974, Desmons and O'Neil, 1978; Liebeaux, 1975; Andreoli et al., 1976; Desmons and Ghent, 1977; Lombardo et al., 1977; Reinsch, 1979; Minnigh, 1978, Lardeaux, 1981; Lardeaux et al., 1982; Hy, 1984; Rubie, 1984; Oberhänsli et al., 1985; Stöckhert, 1985; Stöckhert et al., 1986; Pognante et al., 1987; Pognante, 1989a; Stünitz, 1989, Lardeaux and Spalla, 1991, Gosso et al., 1994; see Droop et al. (1990) and dal Piaz et al. (1993) for a review). The main goal of these studies was to estimate the peak of pressure and temperature expected by the eclogitic lithologies of the Sesia zone during the Alpine metamorphic cycle. Lattard (1974) characterised the greenschist metamorphism of the external unit, while, recently, Lardeaux and Spalla (1991) provided new refining informations of the evolution of the polycyclic basement. Several specific contributions were dedicated to the mineral chemistry of high pressure minerals (Fiorentini Potenza and Morelli, 1968; Callegari and Viterbo, 1966; Andreoli et al., 1976; Lombardo et al., 1977; Reinsch, 1979; Ungaretti et al., 1983; Stöckhert, 1985; Stöckhert et al., 1986).

The mineral chemical analyses carried out during this study provide some new information of the pressure-temperature path followed by the monometamorphic cover sequences of the central Sesia zone during the Alpine cycle, and are compared them to previous data of the literature described above. White micas, amphiboles, garnets and pyroxenes have been analysed in order to define:

- 1) the phengites used for geochronological investigations;
- 2) the different generation of amphiboles of the monometamorphic cover sequences, with particular regard to the amphiboles of the pre-eclogitic prograde foliation;
- 3) describe the chemical variation of garnets and Na-rich pyroxenes, in order to constrain pressure and temperature for both monometamorphic cover and basement lithologies.

4.2. General remarks

Six marbles, eight basic rocks (mainly meta-gabbros and metabasalts of the monometamorphic cover sequences) and fourteen eclogitic micaschists and albitic gneisses were analysed. Samples were prepared as polished sections of 30 μ . Thirty samples of phengite, separated and cleaned for the $^{40}\text{Ar}/^{36}\text{Ar}$ incremental heating method were also analysed. The phengitic mineral separated were assembled on a Teflon® support and polished (some difficulties were found during the microprobe analyses because of the material used for their assemblage).

A CAMECA SX50 microprobe at the University of Lausanne, equipped with five wavelength dispersive spectrometers (WDS) coupled to an energy dispersive spectrometer (EDS) provided the analyses. Either simple point determinations or profile determinations were obtained with a focused beam.

The follow analysis parameters and standards were used for the different minerals:

<i>mineral</i>	<i>beam current (nA)</i>	<i>voltage (HV)</i>	<i>magnification</i>
white micas	15	15	40000
amphiboles	15	15	40000
garnets	20	15	200000
pyroxenes	20	15	20000

	white mica	amphibole	garnet	pyroxene
<i>element</i>	<i>standard</i>	<i>standard</i>	<i>standard</i>	<i>standard</i>
Si	Dio1	Dio1	Pyp1	Dio1
Ti	MnTi	MnTi	MnTi	MnTi
Cr	Cr2O	Cr2O	Cr2O	Cr2O
Al	Anda	Anda	Pyp1	Jad1
Fe	Bio1	And2	And2	Hed1
Mn	MnTi	-	MnTi	MnTi
Mg	Fph2	Dio1	Pyp1	Dio1
Ca	Wol1	Wol1	Gro1	Wol1
Na	Alb4	Jad1	-	Jad1
K	Ort2	Ort2	-	Ort2
F	Fph2	Top1	-	-

Chlorine was initially measured on some amphiboles and was found to be too small. Counting time ranged between 20 and 80 sec., depending of the element.

The data were acquired with QUANTIVIEW™ 2.0 of the CAMECA Co. (SUN version) and collected as stoichiometric values. The precision required for the calibrations was 0.1%. The calibrations were repeated every day of analysis or in case of variation of the physical parameters (filament, current, etc.). The analyses were successively treated by MINFILE program, which manipulated the data to obtain the structural formula analyses for each mineral. White micas were calculated on the basis of 14 cations and 24 oxygens. Calcic amphiboles were calculated on the basis of 13 cations and 23 oxygens while the Na amphiboles formulas were determined on the basis of 15 cations. The garnets and the pyroxenes were calculate an the basis of 12 and 6 oxygens respectively: The iron content of white micas was calculate has Fe^{2+}_{tot} for a better charge equilibrium³.

Samples with defect or excess of charge were systematically rejected as well as the samples with a sum oxides <97% for the micas and sum oxides <99% for the amphiboles, garnets and pyroxenes.

4.3. White Micas

White micas occur very commonly in many of the rock-types of the Sesia zone. They are generally represented by different generations of phengites, although both muscovite and paragonite are represented in minor amounts. White micas are generally present in both the primary high pressure and retrograde mineral assemblages. Stöckhert et al. (1986) found three generation of phengites: a first generation, represented by millimetric to centimetric flakes, in equilibrium with jadeite + quartz, a second generation in equilibrium with

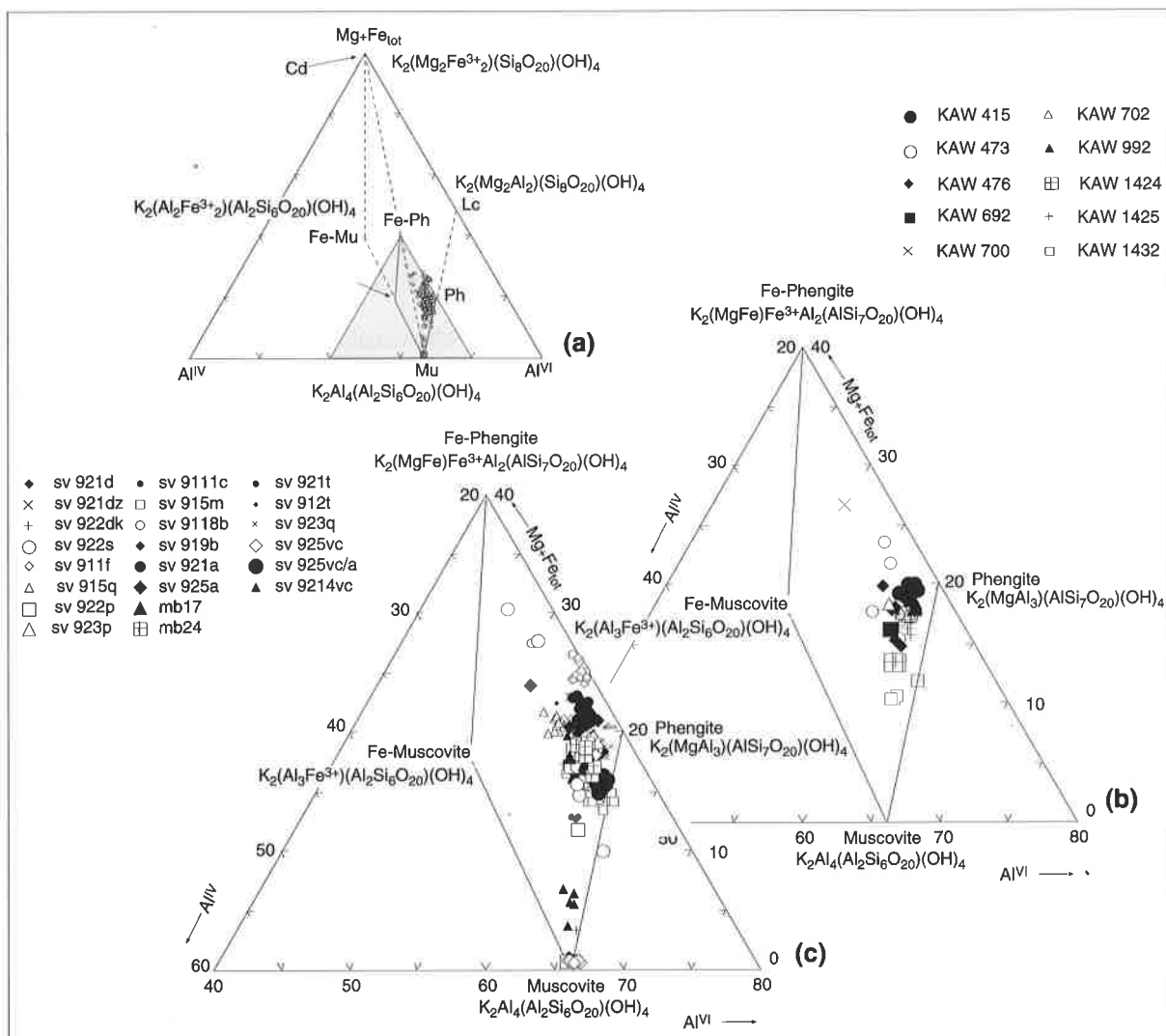


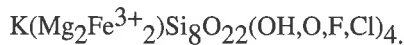
Fig. 4.1 - Ternary classificative diagrams for the white micas (Guidotti, 1984). The analysed samples fall clustered to the phengite end-member, excepting for a few muscovitic and paragonitic population.

³ A measure of the FeO/Fe_2O_3 ratio of the KAW 415 phengites was determined by colorimetry using a modified WILSON method (1960). In this sample all the iron was represented by FeO .

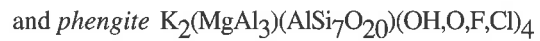
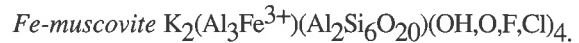
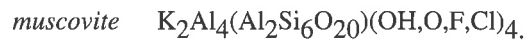
albite and a third small grained generation, which is the product of the destabilisation of high pressure minerals.

Chemical analyses were carried out the white micas in this contribution to investigate possible relationships between the composition of these minerals and their distributions in the different units of the central Sesia zone, in particular, the chemical variations of the white micas in the polycyclic basement samples and the monometamorphic cover lithologies.

White micas have been classified with the ternary diagram of Guidotti (1984) (Fig. 4.1a), in which Al^{IV} , Al^{VI} and $Mg+Fe^{tot}$ represent the axes of the plot. Structural formulas are calculated on the basis of 24 oxygens and 14 cations (K, Mg, Fe, Al, Si). The $(Mg+Fe^{tot})$ corner represents the ideal celadonite end-member :



Other micas reported in the diagram are:



Representative analyses of white micas are listed in Tab 4.1;

Analysed samples were subdivided into two groups; the former consists of the KAW samples from the polycyclic basement lithologies (Fig. 4.1b), the latter is composed of SV samples which were mainly collected in the monometamorphic cover sequences (Fig. 4.1c). All KAW samples are clustered near the phengite corner, except few populations which fall close to the muscovite corner. Silica generally ranges from 6.6 to 7.05 atoms per formula unit (p.f.u.) (per 24 oxygens) in both the KAW samples (Fig. 4.2a) and SV samples (Fig 4.2b). A certain paragonite component is generally present in the eclogitic phengites, where the Na content (per 24 oxygens) normally ranges from 0.8 to 0.24 atoms p.f.u.. Calcium component is generally

Sample	phengites								Muscovites		Paragonites	
	basic rocks				marbles				9114vc	9114vc	925vc	922dk
	919b	MB24	MB24	MB17	911f	913p	9118b	9119b				
SiO2	50.54	50.48	51.06	50.42	52.22	50.83	50.97	52.03	46.58	46.43	46.31	47.39
TiO2	0.37	0.22	0.28	0.05	0.24	0.19	0.12	0.16	0.02	0.08	0.05	0.01
Al2O3	25.88	26.86	26.68	27.55	23.84	26.55	22.34	22.55	34.72	34.47	38.79	39.27
Cr2O3	0.07	0.03	0	0.04	0.01	0	0	0.01	0.02	0	0.02	0
FeOtot	3.303	1.998	1.899	1.575	0.549	1.818	4.347	4.095	1.755	1.503	0.09	0.198
MnO	0	0	0	0.02	0	0.05	0.14	0.14	0	0.01	0	0
MgO	3.32	3.73	3.86	3.6	5.84	3.95	3.79	4.22	0.68	0.75	0.14	0.11
CaO	0.02	0.01	0.02	0.03	0.02	0	0	0	0	0	0.18	0.09
Na2O	0.39	0.57	0.58	0.35	0.16	0.32	0	0.01	0.44	0.46	7.05	7.23
K2O	10.69	10.7	10.8	11.12	11.31	10.56	10.96	11.48	11.02	10.84	0.53	0.76
H2O	4.48	4.51	4.51	4.5	4.46	4.39	4.45	4.42	4.5	4.5	4.71	4.71
F	0	0	0	0.02	0.16	0.28	0	0.04	0	0.02	0.02	0
O=F	0	0	0	0.01	0.07	0.12	0	0.02	0	0.01	0.01	0
Total	99.06	99.11	99.69	99.29	98.88	99.06	97.12	99.18	99.74	99.07	97.90	99.77
SiIV	6.81	6.76	6.8	6.75	6.99	6.8	7.05	7.05	6.21	6.23	6.02	6.05
AlIV	1.19	1.24	1.2	1.25	1.01	1.2	0.95	0.95	1.79	1.77	1.98	1.95
FeIV	0	0	0	0	0	0	0	0	0	0	0	0
TiIV	0	0	0	0	0	0	0	0	0	0	0	0
T-site	8	8	8	8	8	8	8	8	8	8	8	8
AlVI	2.92	3.01	2.99	3.09	2.75	2.98	2.69	2.65	3.66	3.67	3.95	3.96
TiVI	0.04	0.02	0.03	0.01	0.02	0.02	0.01	0.02	0	0.01	0	0
Cr	0.01	0	0	0	0	0	0	0	0	0	0	0
Fetot	0.37	0.22	0.21	0.18	0.06	0.2	0.5	0.46	0.2	0.17	0.01	0.02
Mn+2	0	0	0	0	0	0.01	0.02	0.02	0	0	0	0
Mg	0.67	0.74	0.77	0.72	1.16	0.79	0.78	0.85	0.14	0.15	0.03	0.02
O-site	4.01	3.99	4	4	3.99	4	4	4	4	4	3.99	4
Ca	0	0	0	0	0	0	0	0	0	0	0.03	0.01
Na	0.1	0.15	0.15	0.09	0.04	0.08	0	0	0.11	0.12	1.78	1.79
K	1.84	1.83	1.84	1.9	1.93	1.8	1.93	1.98	1.87	1.85	0.09	0.12
A-site	1.94	1.98	1.99	1.99	1.98	1.89	1.93	1.99	1.99	1.97	1.89	1.92
O	20	20	20	20	20	20	20	20	20	20	20	20
OH	4	4	4	3.99	3.93	3.88	4	3.98	4	3.99	3.99	4
F	0	0	0	0.01	0.07	0.12	0	0.02	0	0.01	0.01	0

Tab. 4.1 - Representative analyses of white micas. Structural formulae are on the basis of 24 oxygens and 14 cations.

below or near the limit of detection (<0.003 atoms p.f.u.)

The ternary plot of Guidotti (1984) can not be used to distinguish between muscovite and paragonite. Four samples with a very low amount in $Mg+Fe^{tot}$ (Fig. 4.2c and d) were thus plotted in the alkali diagram, in order to distinguish the Narich white micas from the muscovites (Fig. 4.2e). Samples sv915vc and sv923q (monometamorphic marble) have both phengite and paragonite components, while sv9111c is composed of phengite and muscovite (Fig. 4.1c). Sv9114c (metagranite) is a muscovite with low amount of celadonic molecule.

In Fig. 4.3a and 4.3b, white micas are plotted in

the Al_{tot} -Mg-Fe ternary diagram. The distribution displayed by the different phengites in this plot is consistent with the data of Stöckhert et al. (1986). A first group, composed of muscovites and the paragonites, falls close to the Al_{tot} pole. A second group, clustered along the Al_{tot} -Fe tie-line, consists of Fe-rich phengites of two metagranites (sv912t and KAW 1425) and of the monometamorphic calcschists (sv925vc). This group corresponds to the distribution of the field of the phengites in equilibrium with jadeite and quartz (Stöckhert et al., 1986). The third group of micas is distributed in the centre of the plot and corresponds to the eclogitic micaschists field of Stöckhert et al. (1986). In particular, KAW samples of the polycyclic basement fall exactly in the same area of the samples of the

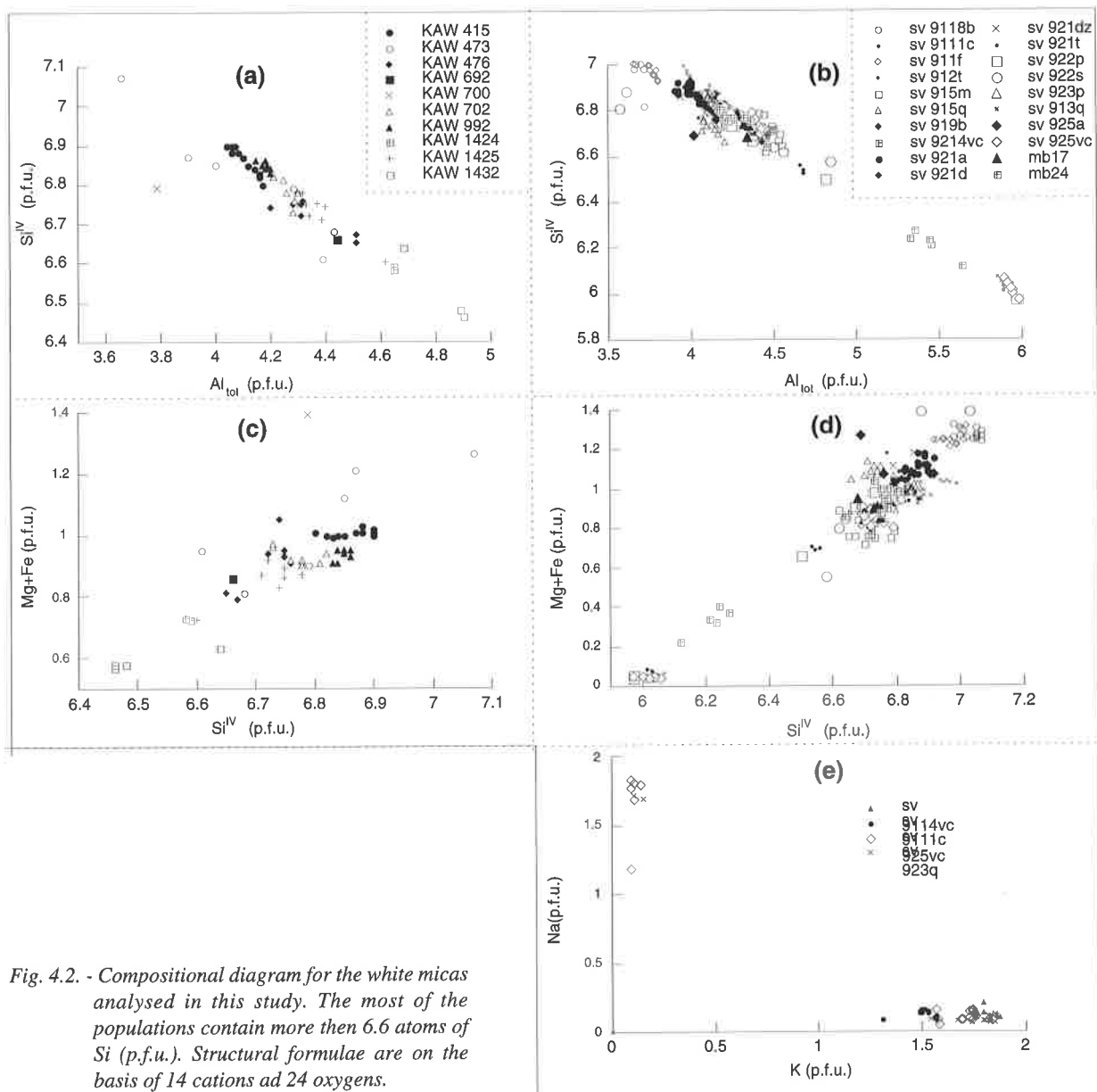


Fig. 4.2. - Compositional diagram for the white micas analysed in this study. The most of the populations contain more than 6.6 atoms of Si (p.f.u.). Structural formulae are on the basis of 14 cations and 24 oxygens.

previous authors. The fourth group is mainly represented by phengites of the monometamorphic cover marbles and it is located close to the Al_{tot} -Mg tie-line. Some samples show a low Al_{tot} content in comparison with the other samples. The Al_{tot} -Mg-Fe ternary diagram suggests that host rock composition and buffering assemblage can control the chemical composition of the phengite. The monometamorphic marbles, generally rich in dolomite, develop Mg-white micas, while metagranitoids permit the growth of an iron-rich phengite. All the other populations show intermediate Mg/Fe_{tot} compositions, whereas phengites from the external unit have relatively low Al_{tot} content.

Summarising, three types of white micas were recognised in both the polycyclic basement lithologies and the monometamorphic cover rocks of the central Sesia zone: a) Mg-rich phengites, found in all the analysed lithologies, b) a population of muscovite, represented only in a metagranitoid sample (sv91114c), and c) a paragonite type, generally found in the monometamorphic marbles. The phengites are generally low Fe-phengites with a certain component of paragonite molecule. The marbles of the monometamorphic cover have Mg-rich phengites. All the populations chosen for the $^{40}Ar/^{36}Ar$ incremental heating age determinations are Mg-phengites, with the exception of samples KAW1425 and sv925vc, which are iron-rich phengites.

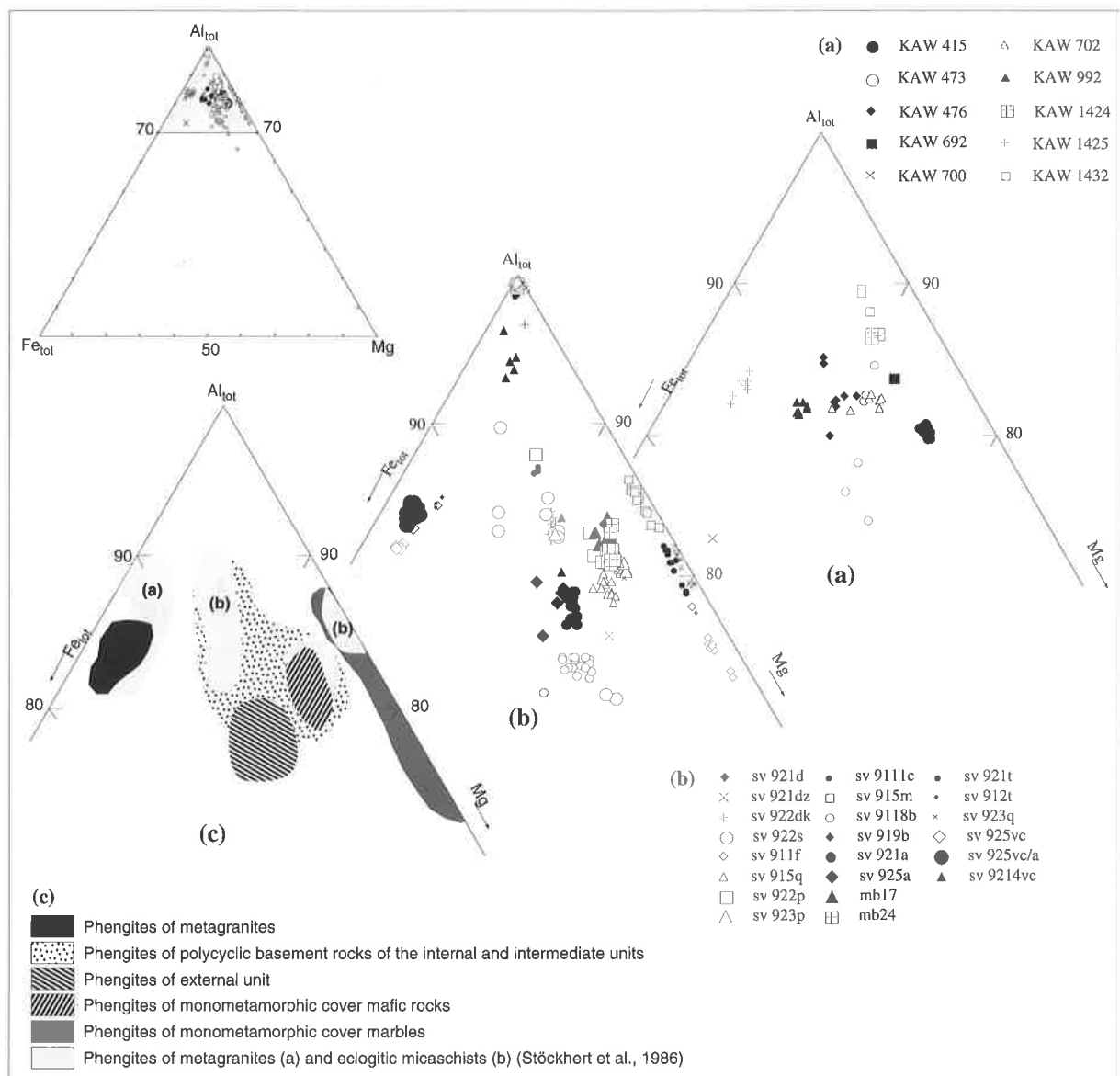


Fig. 4.3 - Compositional ternary plots for the phengites (Stöckhert et al., 1986). The chemical compositions of the phengites is directly dependent from the lithology where white micas develop and by the buffering assemblage in equilibrium with the phengite.

4.4 Amphiboles

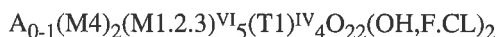
Amphiboles are the main constituent of several mafic lithologies of the Sesia zone. In the internal zone Na-amphiboles are part of the eclogitic paragenesis and are partially replaced by blue-green amphiboles (Franchi, 1902; Bianchi et al., 1964; Dal Piaz et al., 1972; Compagnoni et al., 1977a). In the external unit of the polycyclic basement actinolite and lesser tremolite form the greenschist paragenesis together with albite, clinozoisite, epidote, quartz and phengite (Lattard, 1974). In several localities, pre-Alpine hornblende was observed in the polycyclic metabasites (Bianchi et al., 1963; Compagnoni, 1977; Compagnoni et al., 1977; Compagnoni and Fiora, 1977; Lardeaux, 1981; Pognante et al., 1980; Lardeaux and Spalla, 1991; Accotto, 1992; Gosso et al., 1994).

Pognante (1979) and Pognante et al. (1980) described a CaNa-rich amphibole related to a prograde Alpine assemblage and preserved within the eclogitic garnets. A similar paragenesis was recognised by Venturini et al. (1991) in the monometamorphic cover sequences of the Sesia zone. The aim of the mineral chemistry investigations was to determinate the composition of this «prograde» amphibole and to determinate the chemical proprieties of blue amphiboles in equilibrium with garnet, in order to estimate their cation exchange temperature. All data acquired with the microprobe were initially converted in crystallographic formulas on the basis of 13 cations, excluding K, Na and Ca. The Na-amphiboles were successively recalculated on the basis of 15 cations, according to Hawthorne (1983). Representative analyses of amphiboles are given in Tab. 4.2. The general

sample	Ca-actinolite				actinolitic hornblende		Fe-actinolite	
	MB16	MB16	MB17	MB17	MB16	MB16	MB24	MB24
SiO ₂	52.96	54.51	54.47	54.22	53.1	52.69	52.54	53.87
TiO ₂	0.08	0.09	0.04	0.07	0.08	0.11	1.74	0.02
Al ₂ O ₃	6.58	4.78	5.92	5.96	6.51	7.19	3.83	3.74
Cr ₂ O ₃	0.05	0.05	0.06	0	0.07	0.12	-	0.03
Fe ₂ O ₃	3.09	2.78	2.93	3.9	3.16	2.66	-	3.46
FeO	5.72	4.17	4.74	4.36	4.92	5.26	12	9.07
MnO	0.15	-	0	0	0.02	0.02	-	0.05
MgO	16.19	18.29	17.26	17.3	16.86	16.54	14.54	15.33
CaO	9.69	10.43	9.51	9.52	9.61	9.5	11.25	10.45
Na ₂ O	2.45	2	2.58	2.61	2.67	2.82	1.8	1.72
K ₂ O	0.12	0.07	0.08	0.1	0.15	0.18	0.1	0.07
H ₂ O	2.13	2.15	2.13	2.14	2.13	2.13	2.08	2.11
F	-	-	0.05	0.05	-	-	-	-
O=F	-	-	0.02	0.02	-	-	-	-
Total	99.21	99.31	99.75	100.2	99.3	99.22	99.88	99.92
#Si-IV	7.47	7.61	7.58	7.53	7.46	7.41	7.58	7.66
#Al-IV	0.53	0.39	0.42	0.47	0.54	0.59	0.42	0.34
#Fe+3	-	-	0	0	-	-	-	-
#Ti-IV	-	-	0	0	-	-	-	-
T-site	8	8	8	8	8	8	8	8
#Al-VI	0.56	0.4	0.55	0.5	0.54	0.6	0.23	0.29
#Fe+3	0.33	0.29	0.31	0.41	0.33	0.28	-	0.37
#Ti	0.01	0.01	0	0.01	0.01	0.01	0.19	-
#Cr	0.01	0.01	0.01	0	0.01	0.01	-	-
#Mg	3.4	3.81	3.58	3.58	3.53	3.47	3.13	3.25
#Fe+2	0.67	0.49	0.55	0.51	0.58	0.62	1.45	1.08
#Mn	0.02	-	0	0	-	-	-	0.01
#Ca	-	-	0	0	-	-	-	-
M1,2,3	5	5	5	5	5	5	5	5
#Mg	-	-	0	0	-	-	-	-
#Fe+2	-	-	0	0	-	-	-	-
#Mn	-	-	0	0	-	-	-	-
#Ca	1.46	1.56	1.42	1.42	1.45	1.43	1.74	1.59
#Na	0.54	0.44	0.58	0.58	0.55	0.57	0.26	0.41
M4-site	2	2	2	2	2	2	2	2
#Ca	-	-	0	0	-	-	-	-
#Na	0.13	0.1	0.11	0.12	0.17	0.2	0.24	0.07
#K	0.02	0.01	0.01	0.02	0.03	0.03	0.02	0.01
A-site	0.16	0.12	0.13	0.14	0.2	0.24	0.26	0.08
#O	22	22	22	22	22	22	22	22
#OH	2	2	1.98	1.98	2	2	2	2
#F	-	-	0.02	0.02	-	-	-	-

Tab. 4.2a - Representative analyses of Calcic amphiboles. Structural formulae are on the basis of 13 cations.

crystallographic formula for the amphiboles is:



where A, M1- 4 and T are respectively the cubic, octahedral and tetrahedral sites. The crystallographic structure of the amphiboles is strictly determined by some restrictions which are based on the charge balance and on site allocations (Robinson et al., 1982). A general assumption is that vacancies are not present in any site other than A site. The elements are strictly related to the different sites as shown below.

The analysed amphiboles have been subdivided following Leake (1978). Three groups have been determined on the basis of Na and Ca contents as follow:

element	A	M4	M3	M2	M1	T
K	x					
Na	x	x				
Ca		x				
Mn		x	x	x	x	
Fe ²⁺		x	x	x	x	
Mg		x	x	x	x	
Fe ³⁺			x	x	x	
Ti				x		
Al				x		x
Si						x

Sodic calcic amphiboles

$$(Na+Ca)_{M4} \geq 1.34$$

and

$$0.67 < Na_{M4} < 0.67$$

Alkali amphiboles

$$Na_{M4} > 1.34$$

Chemical variation and possible zonation within each amphiboles have been investigated with profile analysis. The distance between each analysis varied in function of the dimension of the crystal and of its optical characteristics.

Fig. 4.4 report Mg and Fe²⁺ against Na_{M4} amounts of the calcic and alkali amphiboles analysed to the microprobe. The data fall into two distinct groups; the Na-poor amphiboles for which the (Mg/Fe)_{M1-3} ratio is approximately 4:1, and an alkali-rich amphiboles, which have a (Mg/Fe)_{M1-3} ratio ranging from 2:1 (glaucophane) to 1:2 (crossite).

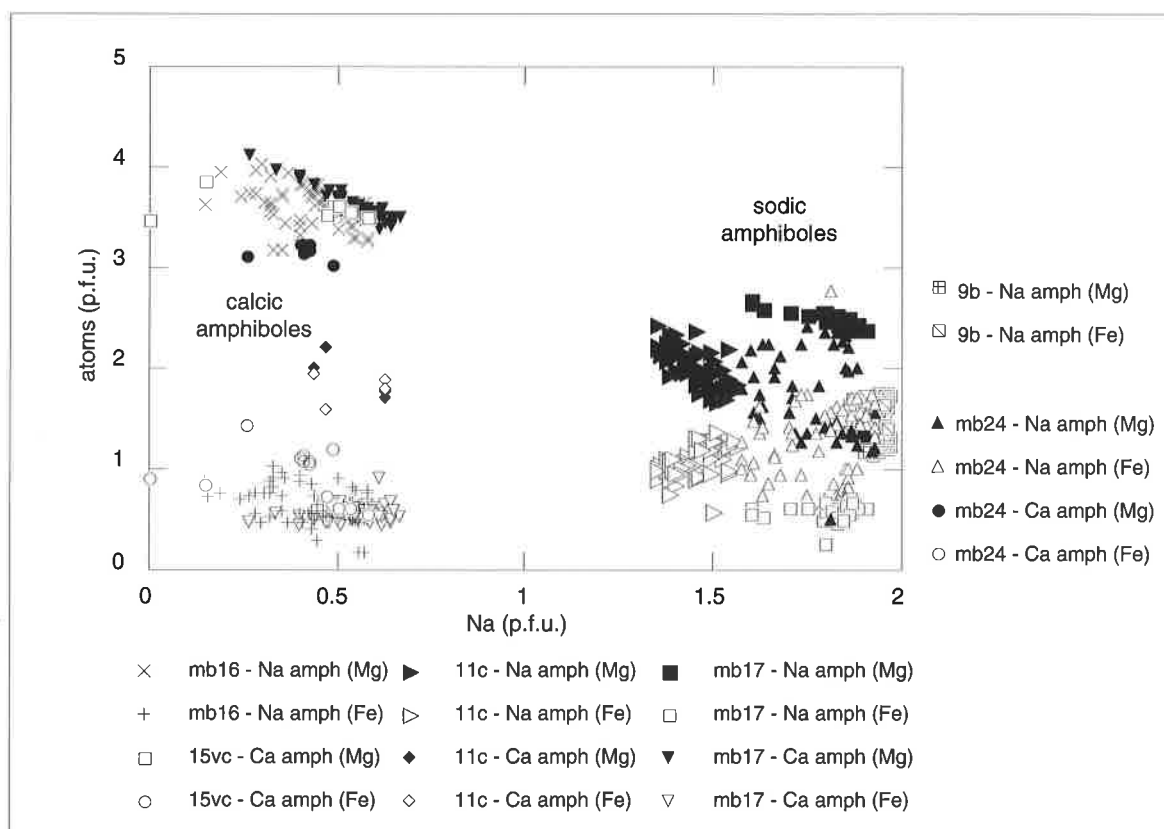


Fig. 4.4 - Sodium vs. Mg and Fe²⁺ diagram for the Alpine amphiboles of the monometamorphic cover sequences. Sodium-poor amphiboles are mainly actinolites.

4.4.1 CALCIC AMPHIBOLES (Plate X - Fig. 10.2).

Calcic amphiboles have been found in the metabasalts of the monometamorphic cover sequences and in the mylonitic metagabbros, in which they appear to replace a magmatic hornblende. Lepidoblasts of calcic amphibole were also found into the garnets of the monometamorphic metabasalts (MB24), where they define a prograde foliation with zoisite, white mica, quartz, Mg-chlorite and glaucophane. In thin section they are characterised by a pale green colour, $\delta_{\max} = 0.010-0.012$, $2V\alpha = 70-90^\circ$ and $\gamma = 27^\circ$. Because of the optical characteristic, they were initially classified as Na-pargasites.

Four of these amphiboles were analysed; the data are plotted in the diagram for the Calcic amphiboles proposed by Leake (1978) (Fig. 5). The amphiboles of samples MB17 and sv9115vc fall at the Ca-rich actinolite-actinolitic hornblende boundary. In MB16, a certain variation of $Mg/Mg+Fe^{2+}$ from the rim to the core is observed. The profiles through calcic amphiboles of MB16 display decreasing trend of Mg/Fe rate from the core to the rim of the crystals. This variation defines a weak zonation from actinolitic hornblende to Fe-actinolite (Fig. 4.7b). Calcic amphiboles of samples MB17 and sv9215vc are more homogeneous, although MB17 displays a certain variation in the Si content. MB24 is instead characterised by a higher Fe^{2+} content that increases from the core to the rim of the amphibole. In summary, the calcic amphiboles are actinolites or actinolitic hornblendes. They show a weak zonation from calcic actinolite to iron actinolites going from the core to the rim.

The calcic amphiboles of the basic monometamorphic

cover lithologies differ from the pre-Alpine amphiboles of the acid and basic granulites studied by Lardeaux and Spalla (1991) on the basis of their higher contents of Si and lower Al and Ti contents. The pre-Alpine amphiboles were classified by the authors as magnesio hornblendes and tschermakitic hornblendes (Leake, 1978, modified by Howthorne, 1983).

4.4.2 ALKALI AMPHIBOLES (PLATE X - FIG. 10.1).

Alkali amphiboles are widespread in different lithologies of both the polycyclic basement and the monometamorphic covers. Sodic amphiboles from four samples of the monometamorphic cover sequences and two mylonites of the pre-Alpine HT basement complex have been investigated.

The Fe^{3+}/Al^{VI} vs. Mg/Fe^{2+} diagram of Leake (1978) was used to classify the alkali amphiboles of this study. Two specimens were recognised: glaucophane, present in all the analysed samples and crossite, found only in sample sv911vc (Fig. 4.6). In the basic rocks of the monometamorphic cover sequence (MB17, MB24 and 919b), glaucophane generally grows as large rhombic-shaped crystals underlining the main foliation together with zoisite/clinozoisite, phengite and lesser rutile; it can also be observed as relict within the garnet. The main eclogitic foliation surrounds millimetric lepidoblasts of actinolite. Glaucophanes of MB17 and MB24 are homogeneous and do not show any marked chemical zonation from the core to the rim. In sample 919b a zonation from glaucophane in the core to Fe-glaucophane in the rim, was observed.

Sodic amphiboles of sample sv9111vc (dark amphibolite related to the metabasalts of the

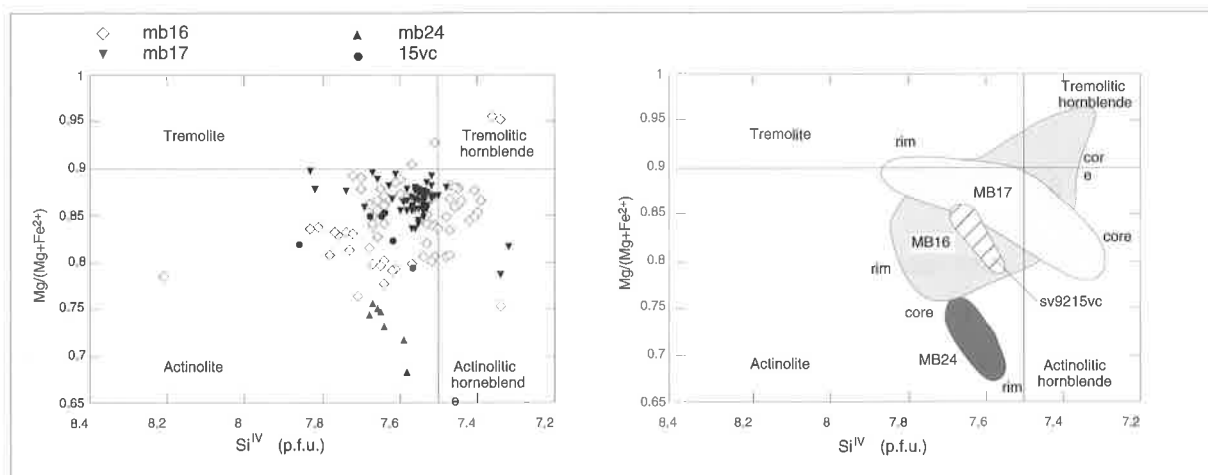


Fig. 4.5 - Classificative diagram of Leake (1978) for the calcic amphiboles. Structural formulae are on the basis of 13 cations.

monometamorphic cover sequences) form centimetric size crystals and represents more than 50% of the rock. In thin section, the amphibole is characterised by strong blue-violet pleochroic colours and by the presence of many opaque inclusions. In the diagram of Leake (1978) for the alkali amphiboles this phase fall in the field of the high magnesium crossite (Fig. 4.6). Profiles through the pleochroic amphiboles display the presence of weak zonation from crossite-Mg riebeckite in the core to glaucophane in the rim. In some profiles, relics of Ca amphiboles (tremolite and

tremolitic hornblende) were found.

4.4.3 SODIC CALCIC AMPHIBOLES

Sodic calcic amphiboles are characterised by intense blue-green pleochroic colours; in the internal unit of the polycyclic basement they coexist with the retrograde greenschist assemblage (albite, epidote, white mica, chlorite and quartz), generally rimming the alkali amphiboles of the eclogitic mineral assemblages. In the external unit these amphiboles

mineral	Fe-glaucophane		Crossite		Mg-riebeckite		Wincherite		Barroisite	
	919b	919b	9211vc	9211vc	9211vc	9211vc	MB17	9211vc	9211vc	9211vc
SiO ₂	56.67	55.87	52.55	52.21	51.62	51.31	55.52	52.1	47.32	47.4
TiO ₂	0.01	0.02	0.35	0.13	0.28	0.87	0.03	0.19	0.17	0.21
Al ₂ O ₃	11.4	7.78	7.41	6.4	7.21	6.44	5.5	6.44	5.39	5.58
Cr ₂ O ₃	0.05	0	0.05	0.02	0.03	0.01	0.04	0.06	0.07	-
Fe ₂ O ₃	2.74	5.26	9.68	9.11	14.61	11.04	2.9	9.54	10.73	11.49
FeO	12.91	12.18	12.21	9.62	6.37	8.25	5.04	8.24	14.55	13.86
MnO	0	0	0.21	0.1	0.14	0.22	0	0.12	0.43	0.37
MgO	6.98	8.02	7.24	10.11	9.08	10.24	17.05	10.84	7.61	7.68
CaO	0.31	0.84	2.5	4.47	2.81	4.22	8.86	4.31	8	7.75
Na ₂ O	7.27	6.96	5.85	4.86	4.96	4.97	2.86	5.1	2.68	2.75
K ₂ O	0.05	0.03	0.12	0.24	0.13	0.23	0.09	0.28	0.22	0.19
H ₂ O	2.15	2.1	2.07	2.03	2.05	1.99	2.15	2.01	1.98	1.95
F	0	0	0.02	0.1	0.06	0.19	0.02	0.15	-	0.07
O=F	0	0	0.01	0.04	0.03	0.08	0.01	0.06	-	0.03
Total	100.53	99.06	100.23	99.36	99.32	99.89	100.1	99.31	99.15	99.27
#Si _{IV}	7.89	7.97	7.59	7.55	7.43	7.39	7.69	7.51	7.17	7.15
#Al _{IV}	0.11	0.03	0.41	0.45	0.57	0.61	0.31	0.49	0.83	0.85
#Fe ₊₃	0	0	-	-	-	-	-	-	-	-
#Ti _{IV}	0	0	-	-	-	-	-	-	-	-
T ₀ site	8	8	8	8	8	8	8	8	8	8
#Al _{IV}	1.76	1.28	0.85	0.64	0.65	0.49	0.59	0.6	0.13	0.15
#Fe ₊₃	0.29	0.56	1.05	0.99	1.58	1.2	0.3	1.03	1.22	1.31
#Ti	0	0	0.04	0.01	0.03	0.09	-	0.02	0.02	0.02
#Cr	0.01	0	0.01	-	-	-	-	0.01	0.01	-
#Mg	1.45	1.71	1.56	2.18	1.95	2.2	3.52	2.33	1.72	1.73
#Fe ₊₂	1.5	1.45	1.47	1.16	0.77	0.99	0.58	0.99	1.84	1.75
#Mn	0	0	0.03	0.01	0.02	0.03	-	0.01	0.06	0.05
#Ca	0	0	-	-	-	-	-	-	-	-
M _{1,2,3}	5	5	5	5	5	5	5	5	5	5
#Mg	0	0	-	-	-	-	-	-	-	-
#Fe ₊₂	0	0	-	-	-	-	-	-	-	-
#Mn	0	0	-	-	-	-	-	-	-	-
#Ca	0.05	0.13	0.39	0.69	0.43	0.65	1.31	0.67	1.3	1.25
#Na	1.95	1.87	1.61	1.31	1.38	1.35	0.69	1.33	0.7	0.75
M ₄₀ site	2	2	2	2	1.82	2	2	2	2	2
#Ca	0	0	-	-	-	-	-	-	-	-
#Na	0.01	0.05	0.02	0.05	-	0.04	0.08	0.09	0.09	0.06
#K	0.01	0.01	0.02	0.05	0.02	0.04	0.02	0.05	0.04	0.04
A ₀ site	0.02	0.06	0.05	0.1	0.02	0.08	0.1	0.14	0.13	0.09
#O	22	22	22	22	22	22	22	22	22	22
#OH	2	2	1.99	1.95	1.97	1.91	1.99	1.93	2	1.97
#F	0	0	0.01	0.05	0.03	0.09	0.01	0.07	-	0.03

Tab. 4.2b - Representative analyses of sodic-calcic amphiboles. Structural formulae are on the basis of 15 cations.

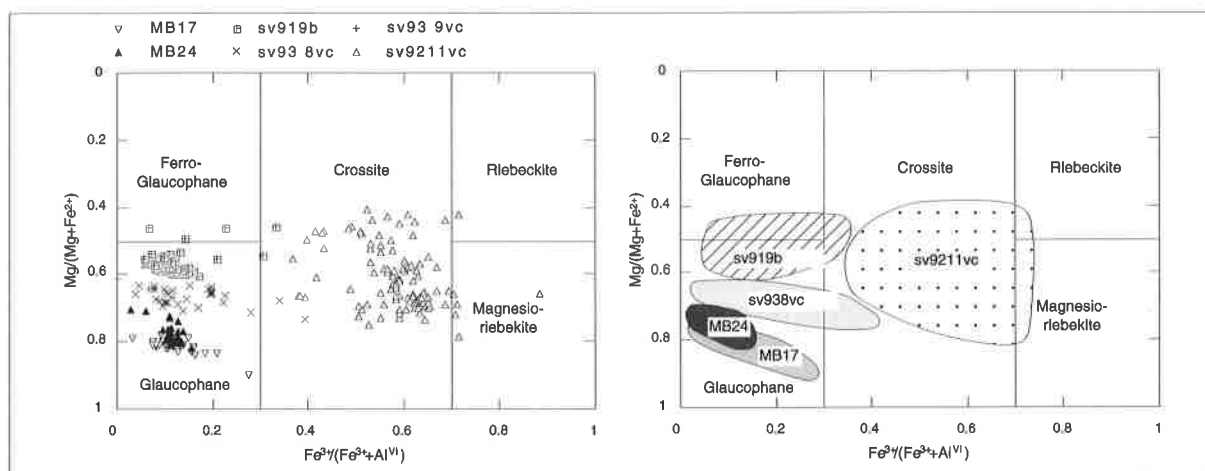


Fig. 4.6 - Classificative diagram of Leake (1978) for sodic amphiboles. Structural formulae are on the basis of 15 cations

	Glaucophane				Glaucophane		Glaucophane		Glaucophane	
sample	sv919b				MB17		MB24		sv938vc	
SiO ₂	57.28	56.93	57.03	57	58.22	57.81	57.61	57.7	57.41	57.9
TiO ₂	0.01	0.02	0	0.09	0.07	0.04	0.13	0.01	0.02	0.03
Al ₂ O ₃	11.54	11.41	11.25	11.36	11.77	11.27	11.54	11.53	11.38	11.42
Cr ₂ O ₃	0	0	0	0	0.02	0.04	0.04	-	0.04	0.06
Fe ₂ O ₃	2.17	2.26	1.84	1.81	0.62	3.6	1.06	2.48	1.42	1.57
FeO	10.79	10.69	11.02	11.55	5.88	4.43	7.98	5.83	9.42	8.6
MnO	0	0	0	0	0	0	-	0.05	0.05	0.07
MgO	8.46	8.26	8.5	8.25	12.23	12.68	10.77	11.65	9.58	10.08
CaO	0.33	0.27	0.29	0.37	1.37	1.46	0.93	1.07	0.65	0.56
Na ₂ O	7.37	7.21	7.49	7.5	6.96	6.98	7.25	7.06	7.26	7.33
K ₂ O	0.04	0.03	0.05	0.04	0.03	0.04	0.03	0.01	0.01	0.02
H ₂ O	2.16	2.15	2.16	2.16	2.2	2.22	2.19	2.2	2.17	2.19
F	0.02	0	0	0	0.03	0	-	-	-	-
O=F	0.01	0	0	0	0.01	0	-	-	-	-
Total	100.17	99.24	99.64	100.15	99.37	100.6	99.52	99.59	99.41	99.83
#SiIV	7.91	7.93	7.92	7.9	7.9	7.79	7.9	7.86	7.93	7.93
#AlIV	0.09	0.07	0.08	0.1	0.1	0.21	0.1	0.14	0.07	0.07
#Fe+3	0	0	0	0	0	0	-	-	-	-
#TiIV	0	0	0	0	0	0	-	-	-	-
Tsite	8	8	8	8	8	8	8	8	8	8
#AlVI	1.79	1.8	1.77	1.76	1.78	1.58	1.76	1.71	1.78	1.78
#Fe+3	0.23	0.24	0.19	0.19	0.06	0.36	0.11	0.25	0.15	0.16
#Ti	0	0	0	0.01	0.01	0	0.01	-	0	0
#Cr	0	0	0	0	0	0	-	-	0	0.01
#Mg	1.74	1.72	1.76	1.71	2.48	2.55	2.2	2.37	1.97	2.06
#Fe+2	1.25	1.25	1.28	1.34	0.67	0.5	0.91	0.66	1.09	0.99
#Mn	0	0	0	0	0	0	-	0.01	0.01	0.01
#Ca	0	0	0	0	0	0	-	-	-	-
M1,2,3	5	5	5	5	5	5	5	5	5	5
#Mg	0	0	0	0	0	0	-	-	-	-
#Fe+2	0	0	0	0	0	0	-	-	-	-
#Mn	0	0	0	0	0	0	-	-	0	0
#Ca	0.05	0.04	0.04	0.06	0.2	0.21	0.14	0.16	0.1	0.08
#Na	1.95	1.95	1.96	1.94	1.8	1.79	1.86	1.84	1.9	1.92
M4site	2	1.99	2	2	2	2	2	2	2	2
#Ca	0	0	0	0	0	0	-	-	-	-
#Na	0.02	0	0.06	0.07	0.03	0.04	0.06	0.02	0.04	0.03
#K	0.01	0	0.01	0.01	0.01	0.01	0.01	-	0	0
Asite	0.03	0	0.07	0.08	0.03	0.04	0.07	0.02	0.04	0.03
#O	22	22	22	22	22	22	22	22	22	22
#OH	1.99	2	2	2	1.99	2	2	2	2	2
#F	0.01	0	0	0	0.01	0	-	-	-	-

Tab. 4.2c - representative analyses of sodic amphiboles. Structural formulae on the basis of 13 cations

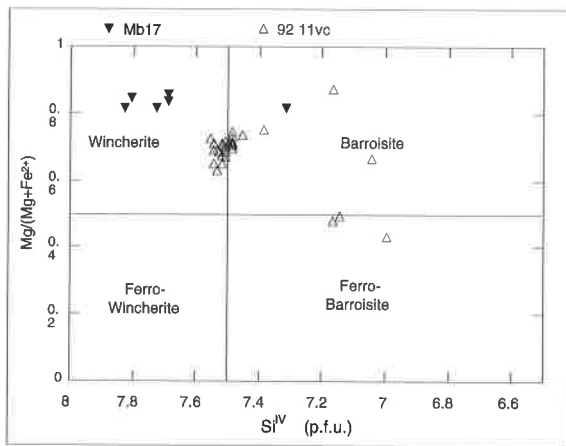


Fig. 4.7 - Classificative diagram of Leake (1978) for Sodic-Calcic amphiboles. Structural formulae are on the basis of 15 cations

completely replace the Na amphiboles. Data of Fig. 4.9 (Leake, 1978) are given for two samples, in which the blue green amphibole partially replaces the primary glaucophane. Structural formulae of the sodic calcic amphiboles are calculated on the basis of 15 cation. The diagram of Leake (1978) (Fig. 4.7) displays two different population of NaCa-amphibole. Amphiboles from MB17, partially replacing the actinolite, fall in the field of the wincherite, while amphibole rimming the crossite of sv9111vc shows a wider range of compositions, comprising wincherite, barroisite and Fe-barroisite.

4.5. Garnets (Plate X - Fig. 10.3).

Garnets are widely distributed in both the polycyclic basement lithologies and in the

monometamorphic cover sequences. In the mafic rocks of the internal unit garnet constitutes the main component together with clinopyroxene, Na-rich amphibole and rutile. In the eclogitic micaschists of the polycyclic basement, they generally replace pre-Alpine biotites (Dal Piaz et al., 1972, 1973; Compagnoni, 1977), while in the monometamorphic cover sequences they do not seem to grow on any pre-Alpine relict. Two generation of garnet were recognised in the central Sesia zone (Desmons and Ghent, 1977; Venturini et al., 1991): a first coarse grained garnet (garnet I), generally rich in sagenitic rutile inclusions, and a second smaller, clean idioblastic generation, growing around garnet I. The mineral chemistry of garnets of the central Sesia zone were investigated by Callegari and Viterbo (1966), Velde and Kienast (1973), Lattard (1974), Liebeaux (1975), Lardeaux (1981), Oberhänsli et al. (1985) Pognante et al. (1987), Battiston et al. (1987) and Pognante (1989), evidencing two main chemical groups: the pyrope-rich garnets, corresponding to the pre-Alpine garnets, and the almandine-grossular garnets, showing an Alpine normal zonation. The former are mainly present in the pre-Alpine high grade basement complex in the southern sector of the Sesia zone (Pognante, 1989), while the latter are homogeneously distributed either in the polycyclic basement or in the monometamorphic cover sequences. Garnets were investigated with clustered-point

	MB24		sv919b		sv915q		sv922i		sv9124c	
sample	core	rim	core	rim	core	rim	core	rim	core	rim
SiO ₂	37.65	37.06	36.6	37.25	37.4	38.09	38	38.41	36.68	36.7
TiO ₂	0.11	0.13	0	0.05	-	0.48	0.1	0.01	0.24	0.1
Al ₂ O ₃	21.57	21.24	20.86	21.23	21.37	21.62	21.37	21.9	20.64	20.75
Cr ₂ O ₃	0.05	-	0.03	-	-	0	0.12	0.1	0.02	0.05
Fe ₂ O ₃	1.07	1.23	0.79	0.73	0.98	0.33	0.38	0.91	0.98	0.51
FeO	26.11	27.2	33.4	30.14	29.15	26.14	23.98	24.88	10.4	11.73
MnO	0.45	0.2	2.62	0.99	1	0.46	2.63	0.28	28.12	26.3
MgO	3.54	2.28	2.12	1.49	5.17	3.71	3.54	5.85	0.86	1.26
CaO	10.17	10.78	3.52	8.82	4.72	10.01	9.92	8.61	3.15	2.83
Total	100.7	100.1	99.93	100.7	99.8	100.84	100.05	100.96	101.08	100.23
#SiIV	5.88	5.87	5.92	5.94	5.92	5.94	5.98	5.92	5.92	5.95
#AlIV	0.12	0.13	0.08	0.08	0.1	0.08	0.04	0.1	0.08	0.05
T site	6	6	6	6	6	6	6	6	6	6
#AlVI	1.93	1.92	1.95	1.96	1.94	1.95	1.97	1.94	1.925	1.96
#TiVI	0.005	0.01	0	0.01	0	0.03	0.01	0	0.015	0.005
#Cr	0.005	0	0	0	0	0	0.01	0.01	0	0.005
#Fe+3	0.065	0.075	0.05	0.05	0.06	0.02	0.03	0.06	0.06	0.03
O site	2	2	2	2	2	2	2	2	2	2
#Fe+2	1.705	1.8	2.26	2.01	1.93	1.71	1.6	1.66	0.7	0.795
#Mn+2	0.03	0.015	0.18	0.07	0.07	0.03	0.18	0.02	1.92	1.805
#Mg	0.41	0.27	0.26	0.18	0.61	0.43	0.42	0.67	0.105	0.15
#Ca	0.85	0.915	0.31	0.75	0.4	0.84	0.84	0.71	0.275	0.245
A site	3	3	3	3	3	3	3	3	3	3
#O	11.98	11.97	11.98	11.99	11.98	12.00	12.00	11.98	11.99	11.99

Tab. 4.3 - Representative analyses of garnets. Structural formulae are on the basis of 12 oxygens

profiles, in order to highlight possible chemical variability from the core to the rim. Structural formulae were calculated on the basis of 12 oxygens.

In this study two main group of garnets characterise the investigated lithologies: almandine-rich garnets, with a chemical composition similar to those of the literature, and spessartine-rich garnets, which represent the main silicate constituents of the Mn-rich lithologies of the monometamorphic cover sequences. Representative analyses are reported in Tab. 4.3.

All acquired data are shown in two classificative ternary plots of Fig. 4.8 (Oberhänsli et al., 1985). The spessartine-grossular-(almandine+pyrope) diagram is

used to differentiate the Mn-rich garnet of the monometamorphic cover sequences (sv9124c) from the other specimens (Fig. 4.8a). The same data are plotted in the pyrope-almandine-(grossular+spessartine) ternary plot (Fig. 4.8b), in which analysed populations fall not far from the Almandine end-member, except for the spessartine-rich sample (sv9124c).

Regarding in detail the single populations of data, some differences appear in the zonation characteristics of the garnets. Sample MB24 (metabasalt of the monometamorphic covers) does not show any particular zonation, with all points clustered within $\text{alm}_{0.60-0.65}\text{gr}_{0.30-0.25}\text{PYP}_{0.05-0.015}$ compositions. Garnets of samples sv919b (monometamorphic

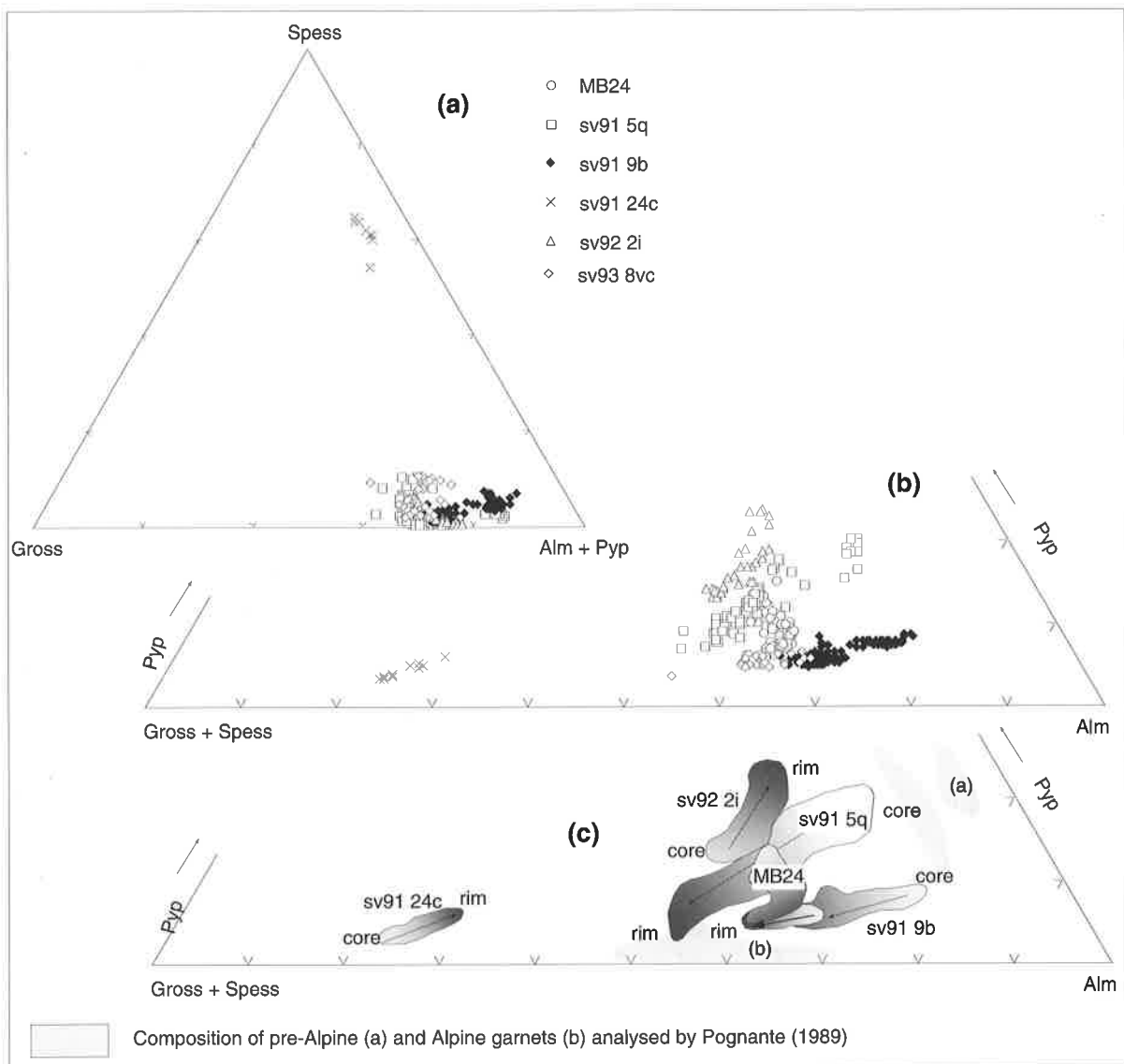


Fig. 4.8 - Classificative ternary plots for garnets. Plot (a) permits the distinction of Spessartine-rich garnets while in plots (b) and (c) the inverted zonation affecting the garnets are shown. (See text for discussion).

morphic cover sequences), sv915q (polycyclic basement) and sv938vc (pre-Alpine high grade complex) show a marked zonation from almandine in the core to grossular at the edge, which can be classified as an «inverted» zonation, *e.g.* a compositional trend inverted in comparison to the *normal* zonation of Banno et al. (1986) and Spear (1989, 1993) (Fig. 4.9). Whereas hardly interpretable, the inverted zonation displayed by some of analysed garnets could indicate an increasing temperature path from the core to the rim, using the method of Spears and Silverstone, (1983). A normal zonation is instead present in sample sv922i, in which an increase in

pyrope molecule and a decrease in grossular content is observed toward the rim. The partial enrichment in pyrope molecule in the core of the garnets of sample sv915q is probably due to the fact that the centre of the garnet grew in equilibrium with a Mg-rich biotite. The chemical composition of the core of this garnet is not far from the composition of the garnet of the pre-Alpine high grade basement complex studied by Pognante (1989). The composition of the alpine garnets of sample 938vc (mylonitised high grade paraschist) corresponds to those of alpine garnets of the pre-Alpine high grade basement complex (Pognante et al., 1987, Pognante, 1989) (Fig. 4.8c) and

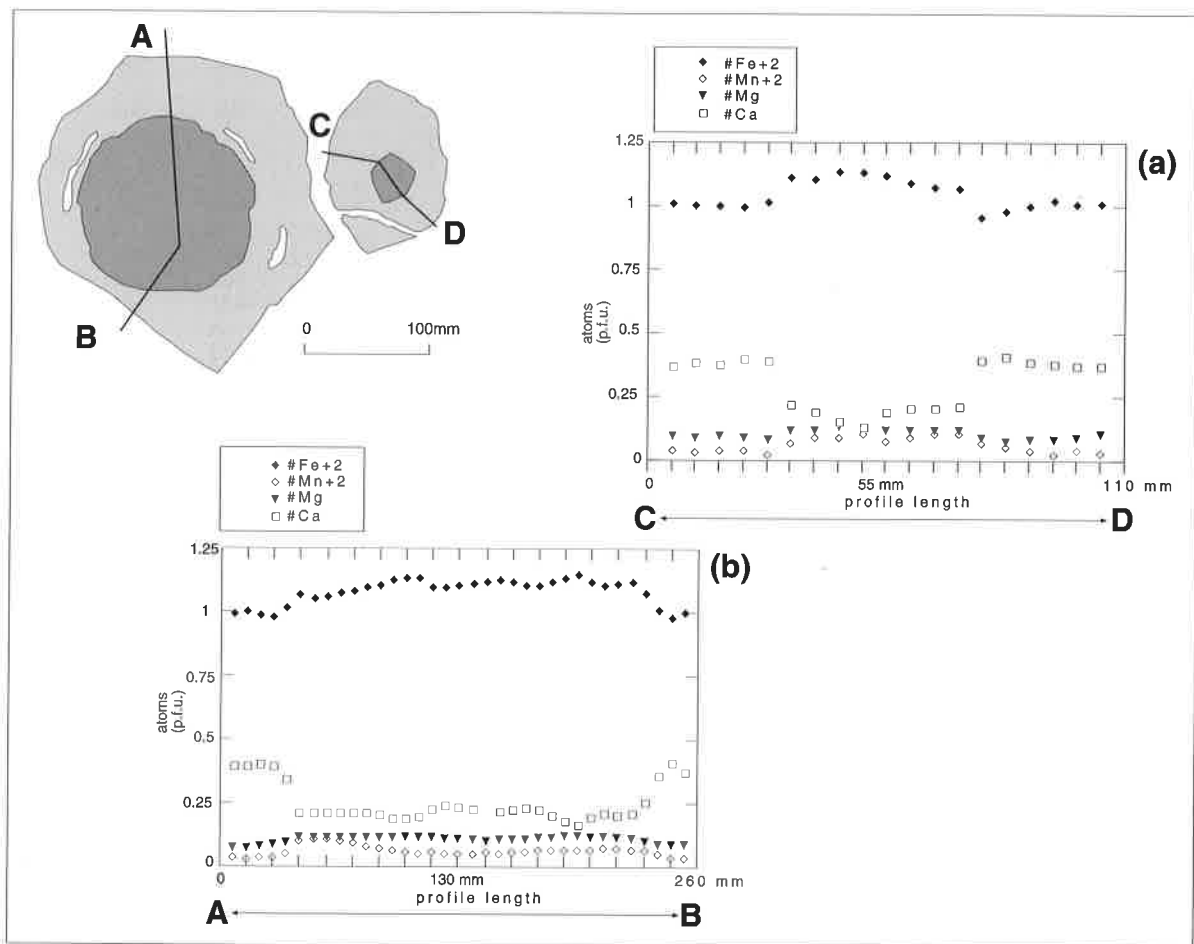


Fig. 4.9 - Representative profiles of inverted zonation in sv919b garnets. Structural formulae are calculated on the basis of 12 oxygens.

to the composition of the alpine garnets replacing granulitic facies garnets (Lardeaux and Spalla, 1991).

4.6. Clinopyroxenes (Plate X - Fig. 10.4).

Clinopyroxenes occur generally as eclogitic phases together with garnet, rutile, and Na-rich amphibole in many lithologies of the central Sesia

zone. Secondary Fe-rich pyroxenes, related to the retrograde destabilisation of the high pressure assemblages, rim the first generation of clinopyroxenes (Callegari and Viterbo, 1966; Dal Piaz et al., 1972; Andreoli et al., 1976; Lombardo et al., 1977; Compagnoni, 1977; Compagnoni et al., 1977a, Lardeaux, 1981, Ober-hänsli et al., 1985). Microscopic investigations permitted us to define at least three different types of clinopyroxene, rarely

sample	MB24		sv915q		sv921t		sv922i	
	omphacite core	rim	omphacite core	rim	jadeite		chloromelanite	
SiO ₂	56.51	55.54	57.06	56.38	58.92	58.66	53.09	53.52
TiO ₂	0.04	0.06	0.1	0.07	0.07	0.02	-	0.09
Al ₂ O ₃	10.31	8.53	14.17	11.28	22.61	22.65	2.35	3.6
Cr ₂ O ₃	0.08	0.02	0.03	0.05	0.03	0.03	0.05	0.01
Fe ₂ O ₃	1.97	2.05	2.45	1.17	-	1.1	21.59	17.44
FeO	3.37	3.56	2.09	2.6	2.57	1.72	1.89	3.96
MnO	0.01	-	0.01	0.06	0.04	0.07	0.13	0.09
MgO	8.08	9.09	5.73	8.4	0.54	0.58	3.83	3.64
CaO	13.14	14.8	9.16	13.45	1.43	1.47	6.44	6.81
Na ₂ O	7.11	5.98	9.53	7.02	13.97	14.12	10	9.65
K ₂ O	0	-	0.02	0.02	0	-	0.01	0.02
Total	100.62	99.63	100.36	100.51	100.18	100.41	99.36	98.82
#SiIV	2	2	2	1.99	2.01	2	2.01	2.02
#AlIV	-	0	0	0.01	-	0	-	-
T site	2	2	2	2	2.01	2	2.01	2.02
#AlVI	0.43	0.36	0.58	0.46	0.91	0.91	0.26	0.16
#Ti	0	0	0	0	0	0	-	0
#Cr	0	0	0	0	0	0	0	0
#Fe+3	0.05	0.06	0.06	0.03	-	0.03	0.61	0.5
#Fe+2	0.1	0.11	0.06	0.08	0.07	0.05	0.06	0.13
#Mn+2	0	-	0	0	0	0	0	0
#Mg	0.43	0.49	0.3	0.44	-	-	0.22	0.21
#Ca	0.5	0.57	0.34	0.51	0.03	0.03	0.26	0.28
#Na	0.49	0.42	0.65	0.48	0.05	0.05	0.73	0.71
#K	0	-	0	0	0.92	0.93	0	0
M1,M2	2	2	2	2	2	2	2	2
#O	6	6	6	6	6	6	6	6

Tab. 4.4 - representative analyses of pyroxenes. Structural formulae are on the basis of 6 oxygens

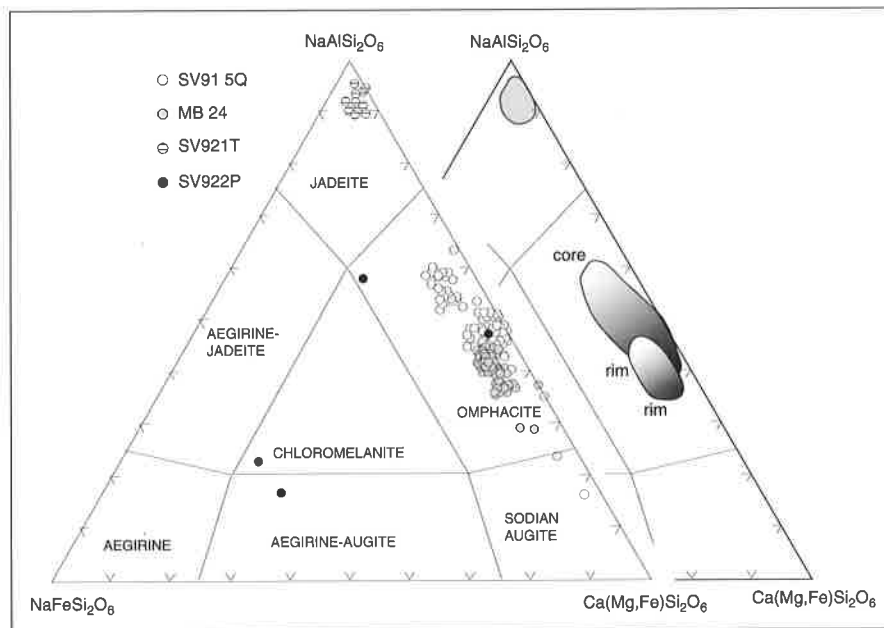


Fig. 4.10 - Ternary classificative diagrams for the Na-rich pyroxenes (Essene and Fyfe, 1967). Two main populations can be distinguished: a) pure jadeitic pyroxenes, and b) zoned omphacites. Formulae are on the basis of 6 oxygens.

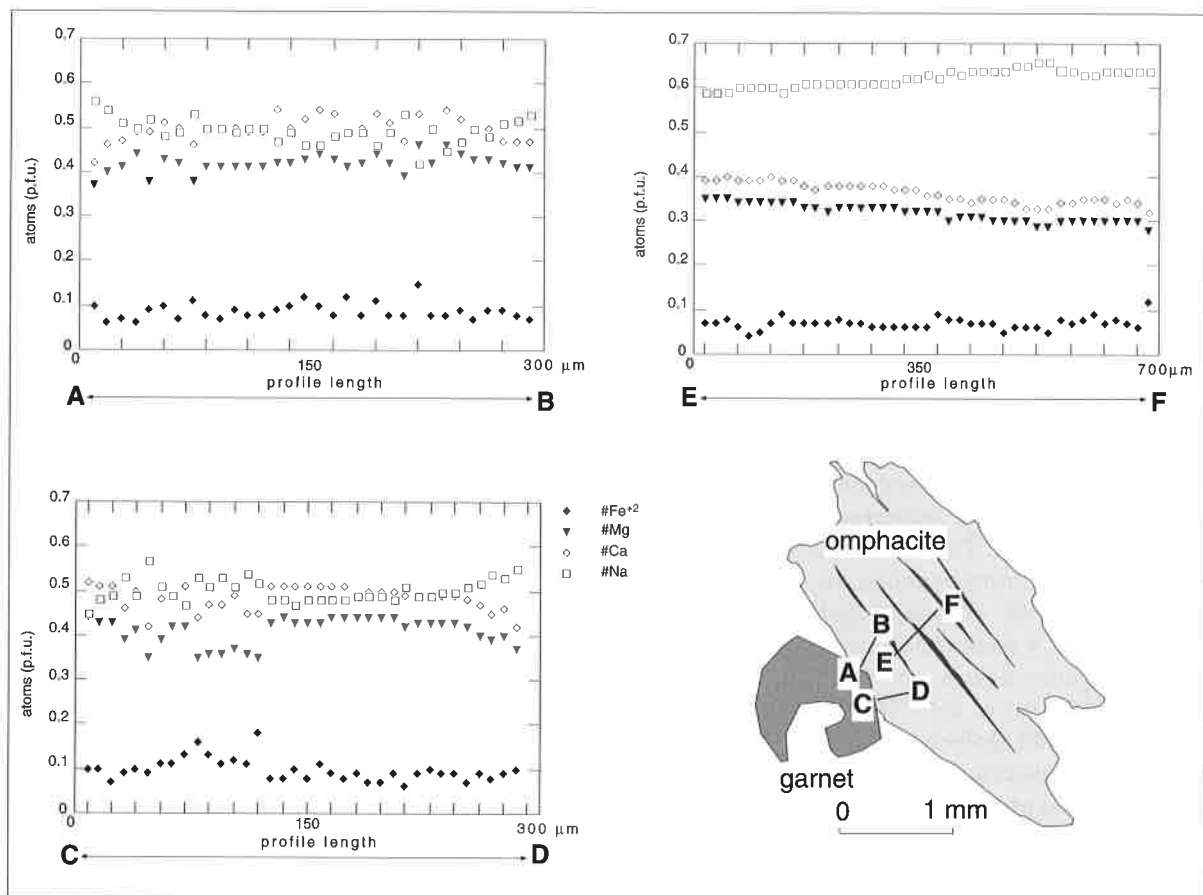


Fig. 4.11 - Representative profile of a zoned omphacites in sample sv915q. The core shows 60 molecular % of jadeite while the rims is depleted in Na-molecule. Structural formulae are on the basis of 6 oxygens.

existing in the same lithology. A first pyroxene is represented by pale green poikiloblastic jadeite, preferentially developing in acid rocks. The jadeite, investigated in detail by Compagnoni and Maffeo (1973), Andreoli et al. (1976) and Lombardo et al. (1977) is generally partially replaced by albite, although well preserved jadeite can be seen in leucocratic metadiques of the internal Sesia unit. This Na-pyroxene has never been described in external unit north to the Soana valley, or in the northern Sesia zone. A second and widely distributed clinopyroxene is represented by omphacite, crystallising as idioblastic deep green forms. This pyroxene grows in both acid and basic rocks; in the internal unit it is widely preserved, while in the external unit of the Sesia zone it was described as relict within the basic boudins of leucocratic gneisses (Spalla et al., 1991). The later apparition of omphacite was signalled in the Sesia valley, while field investigations in the north of the Sesia zone (Dal Piaz et al., 1971; Gosso et al., 1979; Chabloz, 1990; Halter, 1992; Simic, 1992) pointed out the absence of this Na-rich clinopyroxene. Omphacite occurs commonly in the southern Sesia zone. The third observed clinopyroxene is related to the metamorphic

history followed by the lithologies of the Sesia zone during their retrograde path. It is represented by a deep green pleochroic Fe-rich sodic pyroxene, commonly called chloromelanite (Compagnoni, 1977; Compagnoni et al., 1977a). It generally rims the jadeitic pyroxenes, although it was observed also around the omphacite.

Mineral chemistry investigations on some samples of both polycyclic basement and monometamorphic cover samples were carried out in order to investigate the jadeitic content of the clinopyroxene and consequentially to give an estimation of the pressure conditions reached by the lithologies of the central Sesia zone. Clinopyroxenes coexisting with garnet were also analysed to determinate the equilibrium temperature of cation exchange. Profiles through omphacite blasts furnished an idea of the variation of the jadeite content from the core to the rim of crystals. Normalisation was done on the base of 4 cation and 6 oxygens. Analyses without neutral charge were systematically eliminated as well as data with defective oxide sums. Representative analyses of

investigated pyroxenes are given in Tab. 4.4.

The analysed pyroxenes were plotted in the diagram jadeite-aegirine (acmite)-augite (Essene and Fyfe, 1967) for the sodic pyroxenes (Fig 4.10). Three distinct populations of pyroxenes were observed. Pure jadeites, with a augite+aegirine content < 10 molecular %, were analysed in a polycyclic leucocratic meta-aplitite collected in the southern side of the lower Aosta valley. All the analyses provided by samples sv915q (polycyclic basement) and MB24 (metabasalt of the monometamorphic cover sequences) fall in the field of the omphacite. The aegirine content of the pyroxenes of these sample is constantly lower than 10 molecular % when augite+aegirine+jadeite is calculated to 100%. The molecular jadeite/augite ratio is quite homogeneous in MB24, with decreasing of 10% of jadeite molecule from the core to the rim. A marked decreasing of the jadeitic molecule is instead observed in sv915q, where the jadeite content varies from 60-65 molecular % in the core to 45-50 molecular % at the edge of the crystal. This zonation could be explained in terms of decreasing of pressure, although Lombardo et al. (1977) postulated that the composition of the jadeitic and omphacitic clinopyroxenes not in equilibrium with the albite is controlled by the whole rock composition and not by pressure and temperature. Taking in account these considerations, another explanation for the compositional variation of clinopyroxene of sample sv915q is furnished by the grow of a new Na-rich phase (glaucophane) contemporaneous to the developing of the rim of the omphacite.

Chloromelanite-aegirine-augite constitute the third population of analysed pyroxenes. According to Lombardo et al. (1977) these clinopyroxenes are in equilibrium with the albite and represent the retrograde product of the high pressure jadeite-rich pyroxene. The low Na-content of these phases and their coexistence with the albite would indicate low pressure conditions of formation (Lombardo et al., 1977).

4.7. Pressure and Temperature Estimations

4.7.1. INTRODUCTION

Since the early seventies, several contributions have permitted to estimate the retrograde P-T path for the central and southern Sesia zone (Fig. 4.12). Microscopic analyses of equilibrium assemblages as well as cation exchange analyses of garnet-clinopyroxene and garnet-hornblende pair minerals

yielded reasonable P-T constraints.

Three stages characterise the retrograde path followed by the polycyclic basement:

- 1) an high pressure climax, characterised by the stability of the jadeite and by temperatures on the order of 550 °C (Dal Piaz et al., 1972; Compagnoni et al., 1977a; Desmons and O'Neil, 1978; Reinsch, 1979; Lardeaux, 1981; Lardeaux et al., 1982; Oberhänsli et al., 1985; Pognante et al., 1987; Pognante, 1989; Vuichard and Ballèvre, 1988). Williams and Compagnoni (1983) and Ridley (1989) observed a difference in the high pressure climax between the central Sesia zone, the external sector, and the pre-Alpine high grade basement complex (jadeite-out/albite-in).
- 2) a high temperature blueschist stage where the stable clinopyroxene has a reduced jadeite content and the Na-amphibole represents the dominant phase together with phengite and chloritoid.
- 3) a greenschist stage characterised by the stability of albite and green amphibole (mainly barroisite).

Fig. 4.12 summarises the different stability fields proposed for the central and southern Sesia zone. The metamorphic climax proposed by Reinsch (1979), Lardeaux et al.(1982) Rubie (1984) and Vuichard and Ballèvre (1989) seems to correspond to the maximum relative of both pressure and temperature. The different retrograde P-T paths represented in the graphic (Reinsch, 1979; Lardeaux et al., 1982; Ridley, 1989) indicate an initial decompression path followed by a cooling trend. On the basis of these observations, a temperature increasing during the decompression path as previously proposed by various authors (Hunziker, 1974; Compagnoni et al., 1977a; Oberhänsli et al., 1985) does not seem justifiable. The southern Sesia zone, studied by Spalla et al. (1983), Pognante et al. (1987) and Pognante (1989) records different retrograde P-T trajectories, characterised by an initial cooling followed by the decompression stage.

Although the prograde path is often approximately defined, no constraints have been furnished in support of any trajectory except for the stability of prograde Na-rich amphibole, sphene and a first generation of white mica (Pognante et al., 1980; Venturini et al., 1991). The mineral chemistry investigations carried out in this study provided some new constraints for the pressure-temperature reconstructions of the central Sesia zone, with

particular regards to the monometamorphic cover sequences. Some cation exchange calibrations on the garnet-clinopyroxene and garnet-amphibole pairs from monometamorphic cover lithologies permitted quantitative determinations of the equilibrium temperatures. The jadeite molecule content in the

clinopyroxene were used for the minimal estimation of the pressure. Finally, the calcic amphiboles were tentatively used to characterise the prograde pressure and temperature conditions. The data presented were produced taking into account the useful precautions suggested by Essene (1989).

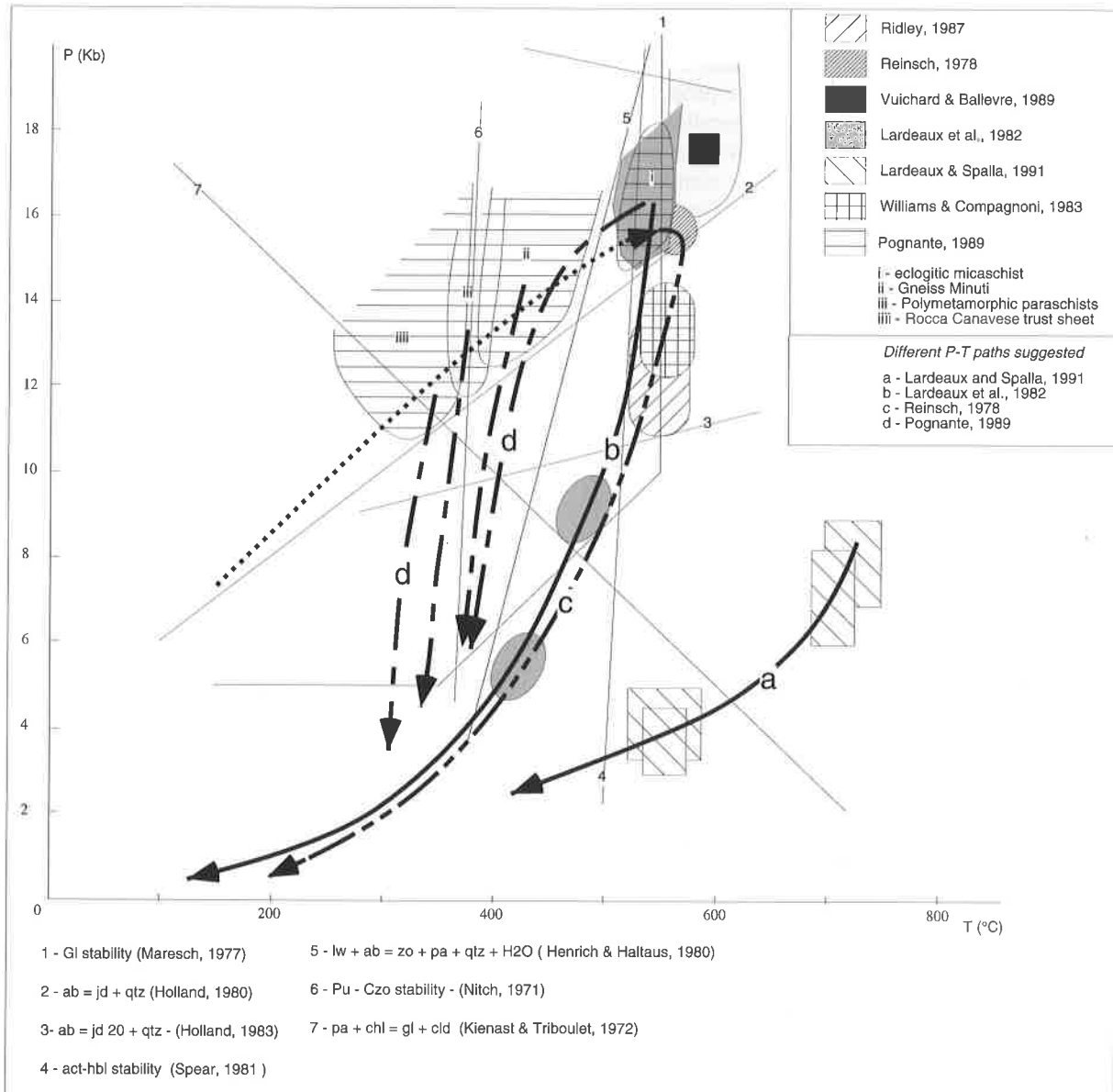


Fig. 4.12 - Summary pressure-temperature diagram for the central and southern Sesia zone. Two different high pressure climaxes have been recognised by several authors: the first is relative to the internal unit of polycyclic basement at 16 Kb and 570 °C (Eclogitic climax), while the second is characterised by lower pressure (Jd out) and similar temperature (Williams and Compagnoni, 1983; Ridley, 1987). The second field (blueschist climax) is related to the external unit of the polycyclic basement and to the mylonitic boundary between the intermediate unit and the pre-Alpine high grade basement complex. The diagram shows two different retrograde paths: the first one (b,c), reconstructed for the central Sesia zone, is characterised by a decompression trend followed by a cooling path, while the second (d), related to the southern sector of the Sesia zone begins with a cooling trajectory followed by decompression (Pognante, 1989). Curve a) (Lardeaux and Spalla, 1991; Dal Piaz et al., 1983) is relative to the cooling path followed by the former high grade lithologies during the Variscan orogenic cycle. No reliable prograde pressure-temperature paths have yet been correctly defined.

4.7.2. GARNET-PYROXENE THERMOBAROMETRY

Garnet and omphacite are primary mineral phases of the eclogitic mineral assemblages in the internal Sesia zone; the mineral pair was successfully used for the temperature estimations of the central and southern Sesia zone. The garnet-clinopyroxene geobarometer is based on the Fe-Mg exchange equilibrium between these two mineral phases. Several different calibrations were proposed to evaluate the temperature values depending to the chemical composition of an equilibrium garnet-clinopyroxene pair for rocks of basaltic compositions (Råheim and Green, 1974; Ellis and Green, 1979; Koons, 1984; Powell, 1985; Krogh, 1988, Ganguly, 1979). Some other calibrations, not suitable for rocks of basaltic composition affected by eclogitic facies conditions, were proposed by Saxena (1979), Dahl (1980) and Pattison and Newton (1989). All these geothermometers were reviewed in detail by Carswell and Harley (1990).

For the garnet-omphacite calibrations of the monometamorphic cover samples of the central Sesia zone, we used both the geothermometer for the basaltic eclogites proposed by Ellis and Green (1979) and those

partially modified by Powell (1985). This calibration takes in account the grossular component in the garnet

The equation proposed by Ellis and Green (1979) to estimate the equilibrium temperature for the garnet-omphacite pair is the following:

$$T (K) = \frac{3030 + 10.86P + 3104X_{Gm}^{Ca}}{1.9034 + \ln Kd}$$

while the modified geothermometer of Powell (1985) is :

$$T (K) = \frac{2790 + 10P + 3140X_{Gm}^{Ca}}{1.735 + \ln Kd}$$

where:

T = temperature in Kelvin degrees,

P = pressure in Kbars

X_{Gm}^{Ca} = grossular component in the garnet

$$Kd = \frac{\left(\frac{X_{Fe^{2+}}^{Gt}}{X_{Mg}^{Gt}}\right)}{\left(\frac{X_{Fe^{2+}}^{Cpx}}{X_{Mg}^{Cpx}}\right)}$$

These geothermometers were applied to different

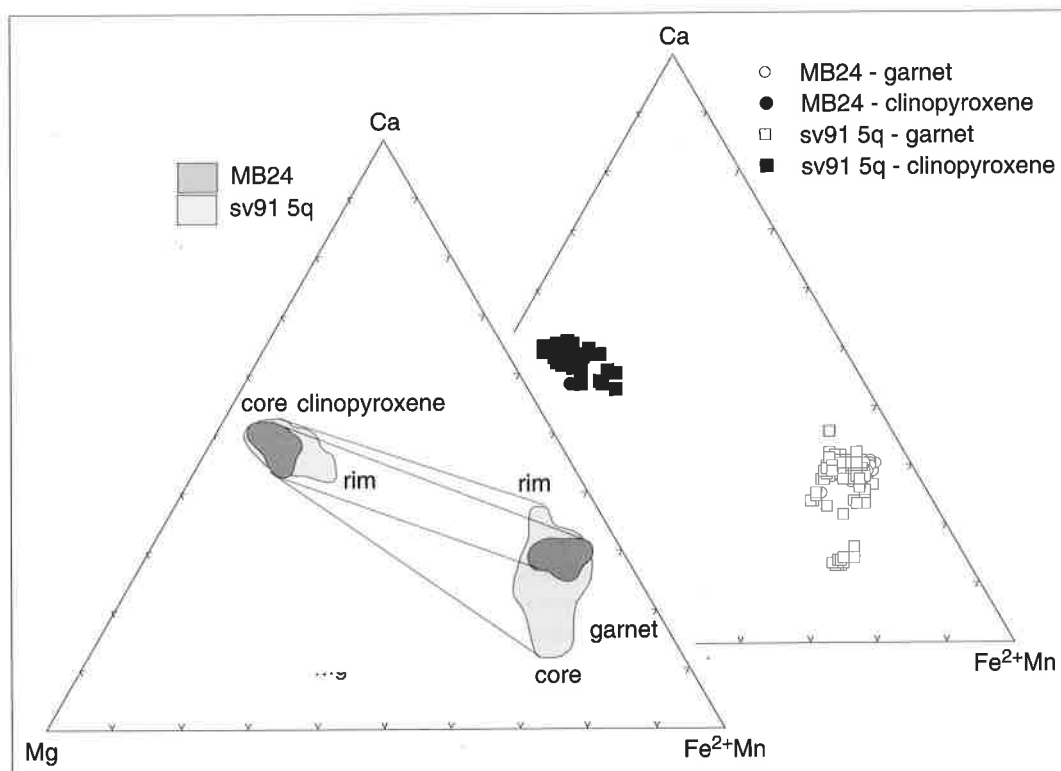


Fig. 4.13 - Comparative diagrams of Coleman et al. (1965) where coexisting omphacite and garnet are plotted. Compositional variation of both omphacite and garnet of sample sv915q are exposed in this plot. Tie lines joint the compositional field that have been used for pressure and temperature estimates.

garnet-omphacite pairs of samples sv915q (basic dyke within the orthogneisses of the polycyclic basement and MB24 (metabasalts of the monometamorphic cover sequences). The results of the calibrations, calculated for pressure equal to 15 and 12 Kbars are listed on the right.

The results of these calibration are coherent with the values obtained by the previous authors who used the same geothermometers (see table on the right).

A minimum pressure for the analysed samples can be determined with the jadeitic content of the omphacite. Both the samples have clinopyroxenes characterised by more than 40 molecular % of jadeitic content. According to Holland (1980, 1983) the garnet-pyroxene pairs were equilibrate above 12 Kbars (lower stability of the omphacite with Jd_{28} molecular %). A reasonable tentative of pressure estimation would suggest 13-14 Kbars as the equilibrium barometric conditions of the analysed pairs. The garnet-omphacite mineral pairs were plotted in the Mg-Ca-(Fe+Mn) ternary plot of Coleman et al. (1965) (Fig. 4.13); tie lines connect the average points of contact between the pairs that have been used for the temperature estimations. Sample sv915q displays a marked zonation of both garnet and pyroxene, while MB24 is relatively homogeneous. Accepting that garnet and omphacite of sample sv915q had a common growing history permitting the cation exchange between the two phases, a temperature estimation of the core equilibrium can be tentatively given. The temperatures obtained in this case are slightly higher than those given by the compositions at the edge (~560 °C). At the same time, the decrease in jadeite molecule from the core to the rim of the pyroxene, is consistent with a pressure decrease during growth of the pyroxene (cfr. Par. 4.6.). The pyroxenes of sample sv915q would recorded the initial phase of the retrograde path, characterised by an isothermal (560-530 °C) and decompressive trend (from jadeite₆₀ to jadeite₄₀ in the omphacite). This interpretation is coherent with the initial retrograde paths proposed by Reinsch (1979) and Lardeaux et al. (1982), while it does not agree with the increasing temperature model proposed by Oberhänsli et al. (1985) for the central Sesia zone.

Sample	Site	$\left(\frac{X_{Fe^{2+}}}{X_{Mg}}\right)_{Grn}$	$\left(\frac{X_{Fe^{2+}}}{X_{Mg}}\right)_{Omp}$	X_{Grn}^{Ca}	Kd	P (Kbars)	T (°C) Ellis and Green	T (°C) Powell
MB24	1	4.888	4.731	0.295	23.10	15	542	520
MB24	1	4.888	4.731	0.295	23.10	12	535	514
MB24	2	4.758	4.69	0.296	22.49	15	546	525
MB24	2	4.758	4.69	0.296	22.49	12	531	510
sv915q	1	5.346	4.50	0.307	24.06	15	542	521
sv915q	1	5.346	4.50	0.307	24.06	12	536	515
sv915q	2	3.411	4.13	0.145	14.09	15	528	502
sv915q	2	3.411	4.13	0.145	14.09	12	521	496

Source of data	T (°C) (Ellis and Green)	T (°C) (Powell)	structural unit
This work	530-546 (12-15 Kb)	510-525 (12-15 Kb)	monometamorphic cover sequences
This work	521-542 (12-15 Kb)	496-521 (12-15 Kb)	polycyclic basement
Oberhänsli et al.	486-625 (13Kb)		polycyclic basement (M. Mucrone)
Pognante et al.	465-569 (14 Kb)		polycyclic basement (southern Sesia zone)

4.7.3. GARNET-AMPHIBOLE THERMOMETRY

The geothermometer proposed by Graham and Powell (1984) for the garnet-hornblende pair was used to test the equilibrium temperature of the Fe²⁺/Mg cation exchange between garnets and coexisting Na-rich amphiboles of the monometamorphic cover lithologies.

The geothermometer garnet-amphibole proposed by Graham and Powell (1984) were obtained comparing the $KD_{garnet/amphibole}$ with the temperature given by the geothermometer garnet-pyroxene of Ellis and Green (1979) in lithologies with coexisting pyroxene, garnet and hornblende. This geothermometer has been tested by Pognante (1989a) on the glaucophane-garnet pair present in the basic lithologies of the southern Sesia zone.

The equation used to determinate the equilibrium temperature of the garnet-amphibole is the given below:

$$T (K) = \frac{2880 + 3280X_{Grn}^{Ca}}{2.426 + \ln Kd}$$

where

T = temperature in Kelvin degrees,

P = pressure in Kbars

X_{Grn}^{Ca} = grossular component in the garnet

$$Kd = \frac{\left(\frac{X_{Fe^{2+}}^{Gt}}{X_{Mg}^{Gt}}\right) \cdot \left(\frac{X_{Mg}^{Hbl}}{X_{Fe^{2+}}^{Hbl}}\right)}{\left(\frac{X_{Fe^{2+}}^{Gt}}{X_{Mg}^{Gt}}\right) \cdot \left(\frac{X_{Mg}^{Hbl}}{X_{Fe^{2+}}^{Hbl}}\right)}$$

The geothermometer of Graham and Powell

(1984) was applied to garnet-glaucophane pairs of three samples collected in the monometamorphic cover sequences. The temperatures obtained with this method yield values around 440 ± 20 °C, which represent values consistent with the temperatures deduced by petrographic observations (e.g. coexistence of garnet, glaucophane and chloritoid for $T > 430$ °C at $P > 8$ Kbars (Kienast and Triboulet, 1972).

The results of the cation exchange calibrations are listed in the table on the right.

Another useful method to estimate the temperature reached by amphiboles was proposed by Colombi (1989). In this calibration a correlation between Ti content in the amphiboles and temperature is proposed. Two different equations are proposed, depending to the Ti content:

$$Ti < 0.08 \quad T (\text{°C}) = 2816 * Ti + 445$$

$$Ti > 0.08 \quad T (\text{°C}) = 980 * Ti + 600$$

The amount of Ti (expressed as formula proportion) of the investigated amphiboles of this work is generally lower or equal to 0.01, thus it begins negligible in the equation, and all the obtained temperatures yield 445 to 480 °C, which are slightly higher, but in general agreement, than those obtained the cation exchange calibrations, considering the uncertainties of both thermometers.

The determination of the pressure conditions of the exchange equilibrium between garnet and amphibole cannot be precisely determined, whereas it has to be higher than ~7-8Kbar (lower limit of the glaucophane stability at 450 °C) and probably lower 11 Kbars (jadeite in at 450°C). In MB24 the amphibole surrounds the porphyroblasts of omphacite, which are characterised by a jadeitic content comprised between 40 and 50 molecular %. Whereas no direct proves testify the successive destabilisation of the omphacite, we can reasonably suggest the lower stability of the Na-rich pyroxene as the upper pressure limit of the coexisting garnet-glaucophane equilibrium.

4.7.4. FORMATION CONDITIONS FOR THE PROGRADE ACTINOLITE

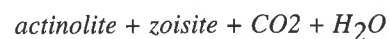
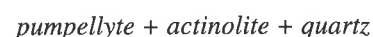
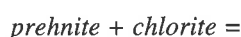
Several contributions are available for the geothermobarometric determinations of the amphiboles (Raase, 1974; Maruyama et al., 1986; Colombi, 1989, Spear, 1993). Most of these studies are based on both the chemical composition of the

Sample	Site	$\left(\frac{X_{Fe^{2+}}}{X_{Mg}}\right)_{Gm}$	$\left(\frac{X_{Fe^{2+}}}{X_{Mg}}\right)_{Gln}$	X_{Ca}^{Ca}	Kd	T (°C) Graham and Powell
MB24	1	7.574	3.81	0.291	18.61	443
MB24	2	4.758	3.98	0.296	18.93	443
sv919b	1	12.13	1.37	0.255	16.63	437
sv919b	2	11.44	1.36	0.262	15.55	450
sv919b	3	10.42	1.37	0.248	14.27	454
sv912i	1	3.756	5.04	0.21	18.91	432

amphiboles and their chemical zonation (Holland and Richardson, 1979; Ungaretti et al., 1983; Sperlich, 1988).

Unfortunately the majority of these studies yield doubtful results, because of the strong chemical variation, complex substitution possibilities and compositional gap of the amphiboles (Klein, 1968, 1969; Himmelberg and Papike, 1969; Ernst, 1979; Robinson et al., 1982; Ungaretti et al., 1983; Reinard and Ballevre, 1988). The application of some of these studies to the pressure and temperature characterisation of the prograde Ca-amphiboles provided preliminary results, which are carefully interpreted.

The upper temperature limit of the actinolite has been defined by Spear (1981; 1993); the transition actinolite-hornblende is situated at approximately 500°C; this represent an upper temperature limit for the prograde actinolite of the Sesia zone. The lower limit is given by the following reactions (Spear, 1993):



which is located between 200 and 300 °C, depending to the pressure.

A first estimation of the temperature can be obtained by the diagram Si-Al^{VI} of Raase (1974) (Fig. 4.14a). The author pointed out the dependence of the Si/Al ratio from the pressure. The data of prograde actinolite of the central Sesia zone yield pressures higher or equal to 5 Kbars; the same values have been obtained plotting the data in the Na_{M4}-Al^{VI} diagram of Brown (1977) (Fig. 4.14b). In this case actinolites give values comprised between 4 and 6 Kbars. The Na_{M4} content in the calcic amphibole is pressure dependent only in mineral assemblages where the amphibole is buffered by albite, chlorite

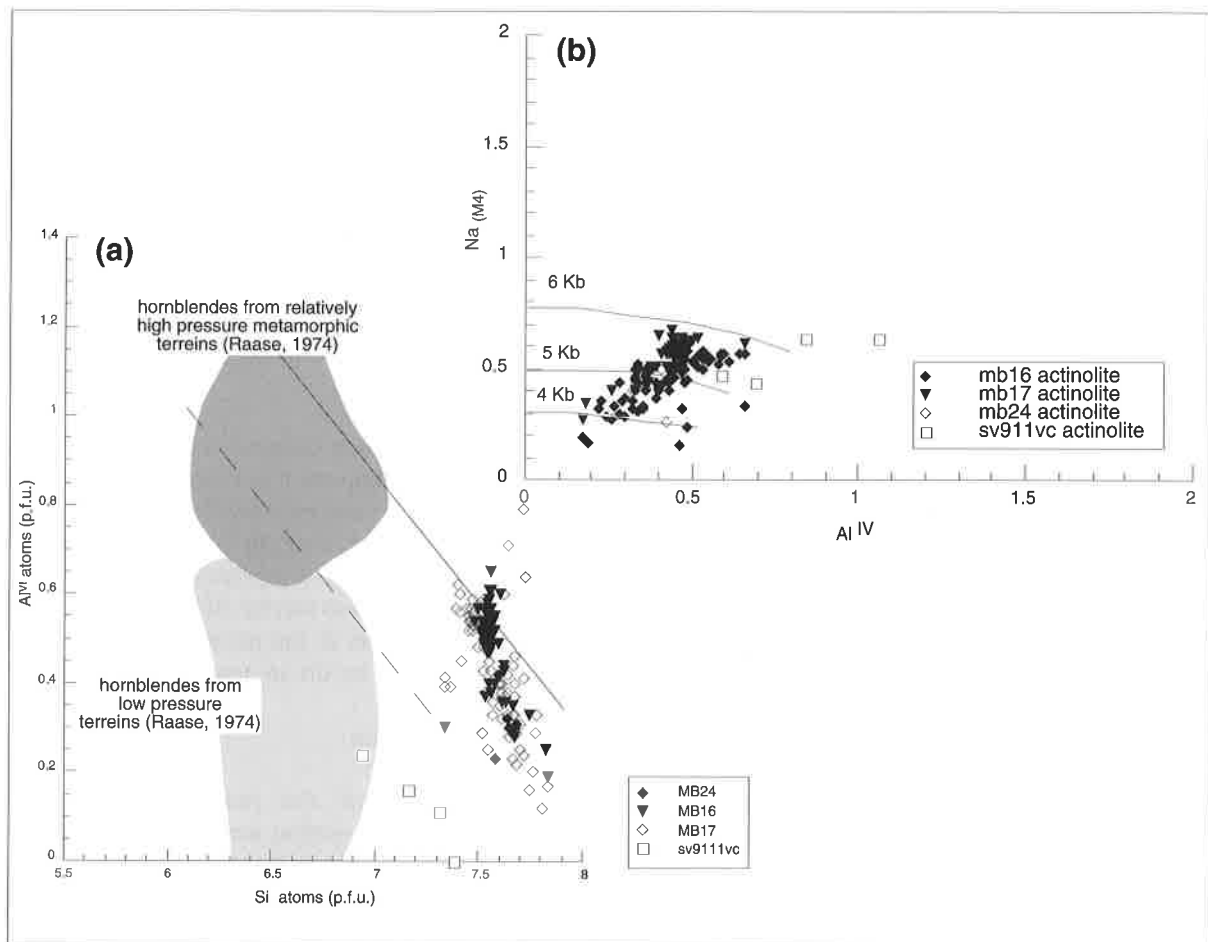


Fig. 4.14 - Diagrams of Raase (1974) (a) and Brown (1977) (b) permitting to estimate the pressure conditions of formation for the calcic amphiboles of the monometamorphic cover sequences. In both diagrams a range between 5 and 7 Kbars is indicated for the formation of calcic amphiboles.

and iron oxide. Although chlorite and oxides were observed in the prograde assemblages, the coexistence of albite in this paragenesis could not be ruled out, so that the previous pressure determinations have to be considered as possible but not reliable. In conclusion, we can reasonably postulate that the actinolite was formed in the greenschist facies at pressure certainly higher than 4 Kbars, according to Raase (1974) and Brown (1977) and probably between 4 and 7 Kbars. The temperature can be reasonably estimated to lie between 300 and 500°C (Spears, 1993).

4.8. Oxygen isotope geochemistry

Oxygen isotope investigations on samples of both the polycyclic basement and the monometamorphic cover sequences were carried out in this study.

The $\delta^{18}\text{O}/\delta^{16}\text{O}$ ratio of rock-forming silicates were determined in order to define the isotopic equilibrium temperatures between the different pair of

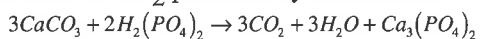
minerals. This method was previously applied with success in the Sesia zone by Desmons and O'Neil (1978) and Robert et al. (1985). Two samples of the polycyclic basement (sv923p and sv911f) and three lithologies of the monometamorphic cover sequences (sv914b, sv915m and sv913q) provided the mineral assemblages for the isotopic determinations. Two samples (sv914b - metagabbro, and sv923p - polymetamorphic marble) furnished all the eclogite facies-forming minerals (garnet-omphacite-rutile-quartz-epidote *s.l.* ± phengite, calcite, albite) while the other three lithologies provided the pairs phengite-calcite. The aim of these investigations was to:

- 1) define the oxygen isotope exchange equilibrium temperatures of the different mineral pairs;
- 2) determine the equilibrium temperatures for the pairs phengite-calcite in those samples that were successively used for dating the cooling history of the central Sesia zone.

The rock-forming minerals to analysed were mechanically separated (sv914b) or attacked with HCl 35% molar. Silicate minerals were handpicked and charged in a sample block and finally put in the extraction vacuum line.

4.8.1. INTRODUCTION OF TECHNIQUES

The silicate mineral were handled with the laser fluorination system of the Isotope Laboratory of the University of Lausanne (Sharp, 1992). The principle of the oxygen extraction method with laser is identical to that of the conventional fluorination (Clayton and Mayeda, 1963; O'Neil and Epstein, 1965). The sample is charged in vacuum line and heated with a laser⁴ beam in presence of a BrF₅ atmosphere. During heating the mineral is oxidised by the fluorine, liberating O₂. The oxygen is converted in CO₂ by a combustion with a hot graphite rod. The CO₂ is analysed by conventional mass spectrometry. The oxygen of calcite was extracted following the method of McCrea (1950). The powder of the sample to analyse is attached with phosphoric acid for twelve hours at 25°C. CO₂ produced by the reaction:



The gas trapped is successively analysed in a conventional mas spectrometer.

4.8.2. RESULTS

Equilibrium temperatures for five different mineral pairs have been obtained by using the calibration curves proposed by Blattner and Bird (1974), Bottinga and Javoy (1975) and Matthews et al (1983a, 1983b). The temperature estimation derives from an equation of the form:

$$1000 \ln \alpha = A \times 10^6 T^{-2}$$

which can be write as follow:

$$T(K) = \sqrt{\frac{A \times 10^6}{\Delta}}$$

where:

T = temperature in Kelvin degrees

$\Delta = 1000 \ln \alpha = \delta^{18}O$ relative difference of $\delta^{18}O$

sample	quartz	calcite	phengite	albite	zoisite	garnet	omphacite	rutile
sv923p	21.59	21.03	19.73		17.84 17.8	18.1	17.06	14.48
sv914b	9.79			8.72 8.68 8.59	7.24	5.31 5.38 5.21	4.73 4.96 4.97	
sv915m		25.05	23.4					
sv911f		20.72	19.38					
sv913q		22.4	21.07					

the values are given in $d^{18}O_{SMOW}\%$

between two phases

A = empirical constant depending from the mineral pair considerate.

$^{18}O/^{16}O$ ratio are reported in the δ notation as per mil (‰) deviation from SMOW standard (Craig, 1957; Clayton et al., 1975).

The isotopic values obtained for the different mineral separates of the polycyclic basement and monometamorphic cover sequences are listed in the table below:

The equilibrium isotopic fractionation temperatures for the mineral listed above, obtained with the fractionation curves proposed by Blattner and Bird (1974), Bottinga and Javoy (1975) and Matthews et al. (1983a, 1983b). These temperature estimations are based on the hypothesis that the different mineral pairs were in equilibrium at the moment of the isotopic fractionation. The results are represented in table 4.5

4.8.3 DISCUSSION

The results of the isotope fractionation temperatures fractionation are consistent with the existing petrographic and petrologic data for the central Sesia zone. The fractionation curves of Bottinga and Javoy (1975) for the different mineral pairs yield temperatures constantly higher than those given by the Matthews et al. (1983a, 1983b) calibrations. In both cases, the range of temperature is coherent with previous isotopic estimations (Desmons and O'Neil, 1978; Robert et al., 1985). In sample sv923p the isotopic fractionation equilibrium temperature obtained for the pyroxene-quartz pair seems using the calibration of Matthews et al. (1983a) provide values of 415 °C, which are not consistent with the general petrographic and petrologic observations.

Figure 4.14 show a plot of $\delta^{18}O_{SMOW}\%$ values of mineral separates of samples sv914b and sv923p versus the fractionation temperature coefficient a ; the fractionation coefficients are taken from Matthews et al. (1983a, 1983b, 1994). The relation between the two parameters of the plat must be linear if the phases are in equilibrium (Javoy et al., 1970). Rutile, quartz and garnet of sample

⁴The laser extraction system at the University of Lausanne uses a 20-W, air cooled CO₂ laser.

sample	qtz-grn		quartz-rutile		quartz-omphacite		phengite calcite	quartz-albite
	M T (°C)	B T (°C)	M T (°C)	B T (°C)	M T (°C)	B T (°C)	Bl T (°C)	M T (°C)
sv923p	573 539	605 585	563	630	414	480	508	
sv914b	549					445 470 472		400 398 372
sv915m							605	
sv911f							592	
sv913q							580	

M = Matthews et al. (1983a, 1983b)
 B = Bottinga and Javoy (1979)
 Bl = Blatner and Bird (1974)

Tab. 4.5 - Synoptic table of the the temperature estimations for different mineral pairs. separated from samples of the monometamorphic cover sequences.

sv923p lie on the same line, underlining the presence of an isotopic equilibrium between them. The same compartment is displayed by quartz-garnet and zoisite of sample sv914b. Omphacite falls instead out of the tie line in both sv914b and sv923p, while it lies on line joining quartz and albite. Consequently, the omphacite-garnet pair cannot be used in these sample for isotopic temperature estimations

The assemblage quartz-garnet-rutile displays equilibrium temperatures of 540-560 °C (Matthews et al., 1983a) or 580-630 °C (Bottinga and Javoy, 1975). The quartz-omphacite pair gives values comprised between 445 and 480 °C; this fact could be interpreted either with the absence of an isotopic equilibrium between these two phases, or as a result of retrograde reequilibration between quartz and pyroxene, or a calibration problem. The albite-quartz yields temperatures of 380±20°C, which agree with the

retrograde grows of the albite due to the stabilisation of the Na-rich pyroxene. Finally the phengite-calcite pair of the monometamorphic cover marbles provides temperatures of 590±20 °C, which represent the highest temperatures obtained with both the cation exchange geothermometers and the stable isotope fractionation methods.

In conclusion, the stable isotope equilibrium isotopic fractionation investigations carried out in this thesis provide temperatures coherent with those deduced with cation exchange geothermometers (see previous paragraphs) and with the petrographic analyses.

4.9. Hydrogen isotope geochemistry

Fourteen phengites from the different units of the polycyclic basement, the pre-Alpine high grade

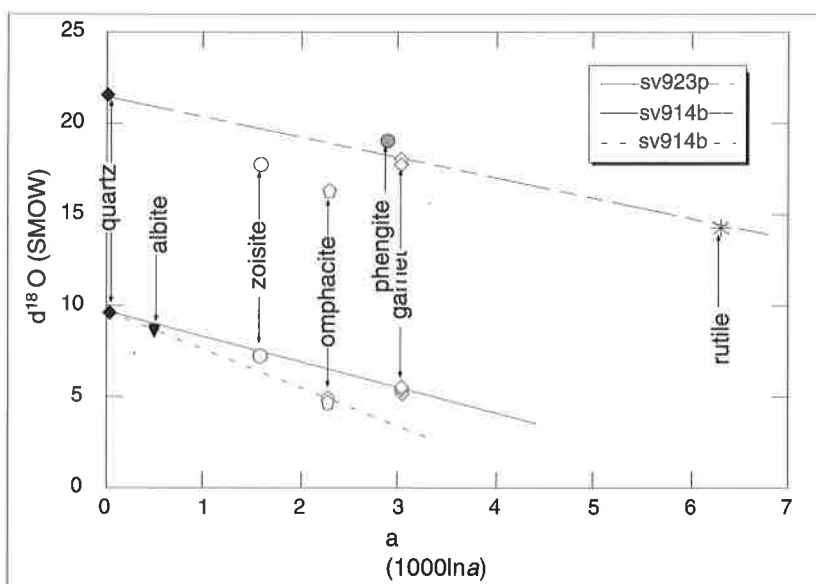


Fig. 4.15 - Measure $d^{18}O_{SMOW}$ of different mineral phase vs. the isotopic fractionation factor a . Fractionation constants are from Matthews et al. (1983a, 1983b). If the analysed minerals were in isotopic equilibrium, the point should fall a straight line. This is the case for the garnet-quartz-rutile parageneses, while, omphacite is not in isotopic equilibrium with these phases.

basement complex and the monometamorphic cover sequences were analysed for their deuterium content. The analyses were carried out to investigate the fluid interaction occurring between the different units of the Sesia zone. Previous works on deuterium composition of the high pressure lithologies in the western Alps were provided by Frey et al. (1976), Desmons and O'Neil (1978), Friedrichsen and Morteani, 1979; Sharp et al., 1993). In the western Alps, Frey et al. (1976) Desmons and O'Neil (1978) and Sharp et al. (1993) pointed out the presence of large scale hydrogen equilibrium in the eo-Alpine hydrated minerals (phengites and glaucophane). Desmons and O'Neil (1978), based on the measured $\delta^{18}\text{O}$ values, suggested that the fluids of the samples collected in the Sesia zone were dominantly inherited and buffered isotopically by isotopic composition of the existing rocks. Sharp et al. (1993) suggested the dehydration of a metamorphosed, hydrated oceanic crust during the eo-Alpine subduction as possible source of high deuterium values recorded by phengites of coesite-bearing whiteschists of the Dora Maria massif.

4.9.1 INTRODUCTION TO TECHNIQUES

Hydrogen isotope ratio was determined following procedures of Vennemann and O'Neil (1993). Hydrogen was separated from phengites placing 20-40 mg of purified mineral in a silica glass tube. After evacuation the samples were heated with a gas-oxygen flame until the mineral melted. All H_2O was transferred to a cold trap during melting. Minor H_2 produced was reacted with CuO at 550°C and converted to H_2O . The two water sources were cryogenically purified and frozen into Pyrex[®] tubes with excess zinc. The tubes were sealed and heated at 475°C for 30 minutes, quantitatively reducing H_2O to H_2 by reaction with zinc. The δD values were

determined with the mass spectrometer.

4.9.2. RESULTS.

Fourteen phengites have been chosen and isotopically analysed in order to investigate the differences in deuterium composition of the in the different Sesia zone-forming complexes.

Two calcschists (sv915m and sv925vc) have been collected from the monometamorphic cover sequences together with one mylonitic metagabbro (sv914b). KAW 473 and sv939lz are representative of the internal unit of the polycyclic basement, while sample sv921dz and KAW474 come from the intermediate unit. KAW 415 and KAW 475 provided phengites of the external unit; finally four samples have been collected in the pre-Alpine high grade basement complex; two of those (sv931dk and sv932dk) come from Punta Plaida (Gosso, 1977) high pressure slice, comprised into the pre-Alpine Vogna-Gressoney valley klippen (Dal Piaz et al., 1971). The other two samples are representative of slightly transformed pre-Alpine lithologies of the pre-Alpine high basement complex in the Fert Valley and Chiusella valley.

The measured deuterium values, reported in the δ notation as per mil (‰) deviation from SMOW, are listed below:

4.9.3. DISCUSSION

The δD of analysed samples ranges between -20 and -40 ‰ (Fig. 4.16, with most of the values comprised between -32 and -40 ‰). This interval of data agrees with the results presented by Desmons and O'Neil (1978) and confirms the existence of a

Unit	mineral	Lithology	sample	δD
polycyclic basement				
internal unit	phengite	micaceous gneiss	KAW 473	-38
internal unit	phengite	silicate-bearing marble	sv911f	-30
internal unit - southern Sesia zone	phengite	metakinzigite	sv939lz	-35
intermediate unit	phengite	metagranodiorite	sv921dz	-38
intermediate unit	phengite	metagranodiorite	KAW 474	-33
external unit	phengite	micaceous gneiss	KAW 415	-36
external unit	phengite	micaceous gneiss	KAW 475	-40
monometamorphic cover sequences				
Bonze region	phengite	metagabbro	sv914b	-35
Mombarone	phengite	calcschist	sv915m	-38
Chiusella valley	phengite	calcschist	sv925vc	-34
pre-Alpine high grade basement complex				
P.ta Plaida high pressure slice	phengite	micaschist	sv931dk	-32
P.ta Plaida high pressure slice	phengite	micaschist	sv932dk	-29
pre-Alpine Fert valley unit	phengite	acid granulite	sv932ft	-25
pre-Alpine Dondogna unit	phengite	kinzigite	sv937vc	-21

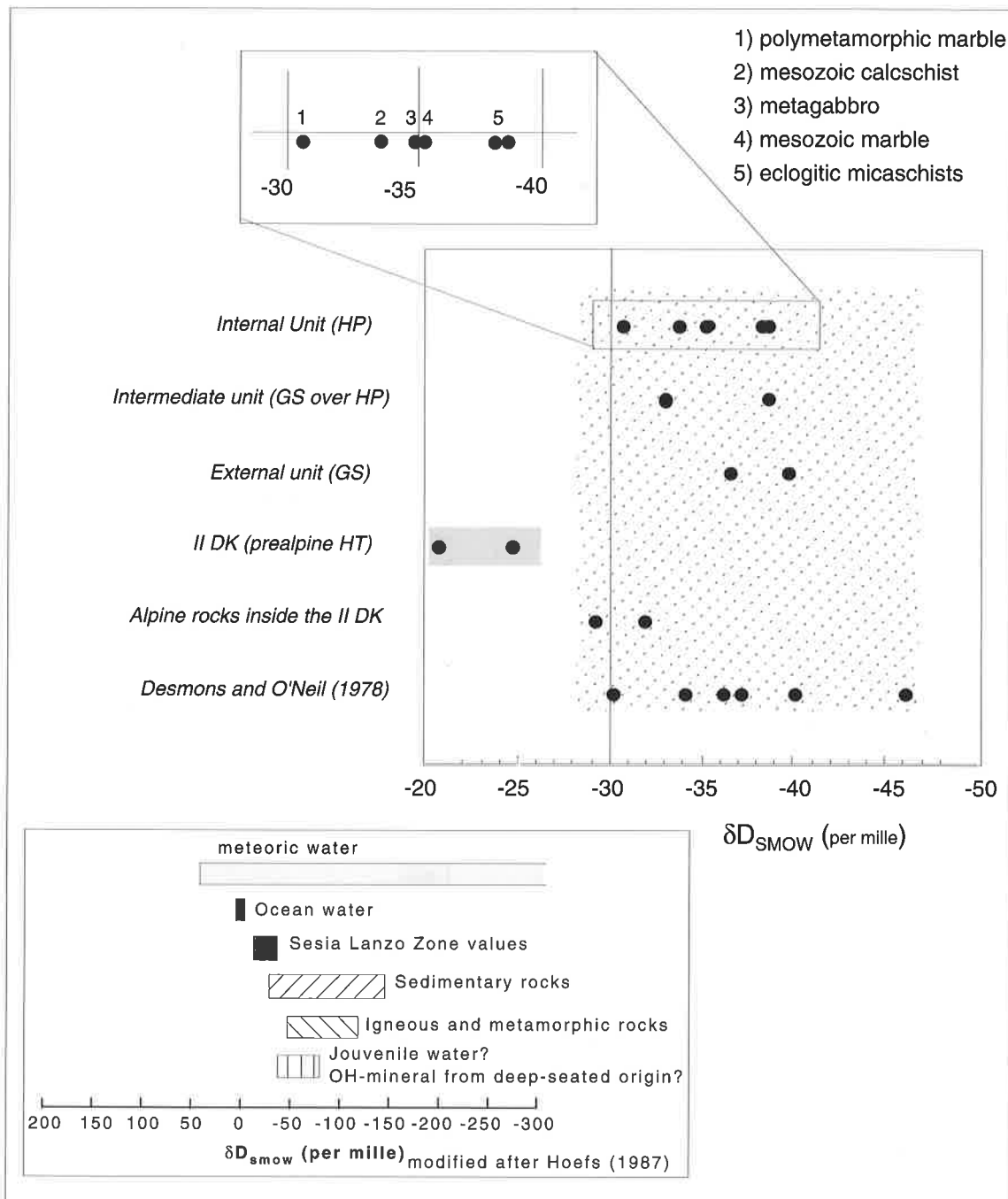


Fig. 4.16 - Hydrogen isotopic composition of phengites from the central Sesia zone. Samples collected in of the polycyclic basement and in the monometamorphic covers are comprised between -30 and -40‰ and indicate a pervasive isotopic equilibrium reached by the Sesia basement lithologies during the Alpine metamorphic cycle (Desmons and O'Neil, 1978). The pre-Alpine high grade basement samples display higher values, which suggest their partial isotopic disequilibrium with respect the other units. Values close to the zero indicate an oceanic crustal slab as origin fluid source.

widespread equilibrium with the deuterium-rich fluid system in the Sesia zone during the Alpine metamorphic cycle. According to Sharp et al. (1993), the heavy hydrogen affecting the hydrous mineral could be supplied by an dehydrating oceanic crust slab, undergone high pressure metamorphism together with the Sesia zone polycyclic basement and metamorphic

covers. If we compare the obtained data with the geological unit subdivisions, we can advance the following considerations:

- 1) there is no remarkable difference in deuterium content between the different units of the polycyclic basement complex. This is consistent with the fact

that the internal, intermediate units and central-southern sectors of external unit underwent the same metamorphic conditions during the eo-Alpine time.

2) The deuterium content of the phengites of the external unit, developed under Tertiary retrograde greenschist conditions (Hunziker, 1974; Spalla et al., 1991) is similar to that of the high pressure phengites of the internal unit. This entails three different solutions: a) the source of heavy fluids which interests the Sesia zone lithologies during the eo-Alpine metamorphism was already active during the Tertiary reequilibration; b) the greenschists phengites overgrow previous eo-Alpine white mica in a close system, which does not permit the reequilibration of the hydrogen values. This hypothesis is hardly defensible, because the K/Ar system of these samples was completely reset (Hunziker, 1974; geochronology chapter of this thesis) and we would expect the same behaviour for the hydrogen system; c) The deuterium reequilibration through the different geological unit of the Sesia took place after the closure system of both the Tertiary phengites and the eo-Alpine phengite. In this case we would admit the possibility of hydrogen diffusion an reequilibration below 450°C, which is the probable temperature reached by the lithologies of the internal unit during the Tertiary greenschist reequilibration of the external edge of the Sesia zone (Lattard, 1974) (crf. next chapter). The first hypothesis seems to be the more

reasonable and consistent with the accepted Tertiary evolutionary models for the western Alps.

3) the phengites of the monometamorphic cover samples yield values similar to those of the polycyclic basement samples, confirming that these minerals were formed in the same fluid metamorphic conditions of the polycyclic lithologies.

4) the deuterium contents of the preserved pre-Alpine high grade samples (-21 and -24‰) are heavier by 10 to 20 ‰ in comparison to the other measured values. This means that the Alpine phengites, which partially substitute the pre-Alpine assemblages, grown in presence of a fluid similar to an hypothetical «oceanic source» (=SMOW). The fact, if confirmed by further investigations, entails some considerations on the fluid activity of the pre-Alpine high grade basement complex: a) this slice of basement, partially reequilibrated under Alpine metamorphic conditions, had to be not far from the fluid source, because the relatively well preserved values of the original fluid (close to 0‰). b) its deuterium system was not in equilibrium with the other those of the polycyclic and cover units, according to the models that describe the pre-Alpine high grade basement complex as an independent unit of the Sesia zone (Carraro et al., 1971; Dal Piaz et al., 1972; Compagnoni et al., 1977a; Pognante, 1989).

- Chapter 5 -

$^{40}\text{Ar}/^{39}\text{Ar}$ Geochronological Investigations

5.1. Introduction

Several Rb/Sr, K/Ar, $^{40}\text{Ar}/^{39}\text{Ar}$ age determinations on whole rock samples and minerals (phe, bt, omp, grn, ab), zircon and apatite fission track data, and a few U/Pb age determinations on zircons and monazites have been published since 1974 for the Sesia zone (Hunziker, 1974; Hy, 1984; Oberhänsli et al., 1985; Stöckhert et al., 1986; Paquette et al., 1989; Hurford et al., 1991, Hunziker et al., 1992) (Tab. 5.1). In addition, many other age determinations on the Sesia zone have been presented in short or extended abstracts (Stöckhert, 1989; Venturini and Hunziker, 1992; Ruffet et al., 1993, 1994; Reddy et al., 1994; Inger and Cliff, 1994).

Hunziker (1974) dated the age of the eclogitic metamorphism of the Sesia zone, using both Rb/Sr and K/Ar techniques, defining a Lower Cretaceous (eo-Alpine) metamorphic episode overprinted by a later Tertiary event. Hy (1984) and Oberhänsli et al. (1985), confirmed these age determinations in the Monte Mucrone region, using Rb/Sr and $^{40}\text{Ar}/^{39}\text{Ar}$ techniques. Stöckhert et al. (1986) studied the age relations between the eclogitic phengites and the recrystallised white micas in the lower Aosta valley, showing that both generations yield K/Ar ages of approximately 80 Ma, while the fine grain phengites yield ages down to 70 Ma. Paquette et al. (1987) measured lower Permian U/Pb ages for zircons of the Monte Mucrone granite, Finally, Hurford and Hunziker (1991) published several fission track age determinations on zircons and apatites.

Plate 2a shows the distribution of ages determined in the Sesia zone. Of these studies, over eighteen concentrate on the Monte Mucrone area (Plate 2b), where all the available methods, with the exception of Sm/Nd, have been used to investigate the eclogitised granodiorites and paraschists (Hunziker, 1974; Hy, 1984; Oberhänsli et al., 1985; Paquette et al., 1989; Bussy et al., in progress). Several age determinations also exist for the lower Aosta and Gressoney valleys (Plate 2b; Fig. 5.1). Unfortunately, until now, only a few scattered age determinations have been available for the northern and southern Sesia zone.

Published Rb/Sr whole rock and mineral (phengite and biotite) ages are 120 ± 15 Ma (whole rock) and 66 ± 1 Ma (phengite) for the internal Sesia zone and 44 ± 12 (phe) and 36 ± 6 (bt) Ma for the external Sesia zone (Hunziker, 1974; Oberhänsli et al., 1985). K/Ar ages of phengites range between 108 and 52 Ma for the internal Sesia zone and 47 Ma for the external Sesia zone (Hunziker, 1974; Stöckhert et al., 1986). Available $^{40}\text{Ar}/^{39}\text{Ar}$ ages (Hy, 1984; Ruffet et al., 1993) agree with the K/Ar ages. Fission tracks ages on zircons vary between 40 and 27 Ma while apatite fission track ages fall between 29 and 24 Ma (Hurford et al., 1991) (Tab. 5.1, Plate 2b and Fig. 5.1).

U/Pb age determinations on zircons and monazites from the M. Mucrone granite vary between 286 ± 2 Ma (six discordant zircons, Paquette et al., 1989) and 293 ± 2 Ma (concordant zircons and monazites, Bussy et al., in progress) and are interpreted to reflect the emplacement ages of the granodioritic-granitic stock.

5.2. Analytical methods

5.2.1. Introduction of techniques

The $^{40}\text{Ar}/^{39}\text{Ar}$ dating technique was spawned by the works of Merrihue (1965) and Merrihue and Turner (1966). This dating method is based on the ^{40}K decay to ^{40}Ar , following the same principals as the K/Ar dating technique.

For the $^{40}\text{Ar}/^{39}\text{Ar}$ method the sample is first irradiated in a nuclear reactor to transform the ^{39}K atoms to ^{39}Ar by fast neutron interaction. Following irradiation, the sample is placed in an ultrahigh vacuum system and the Ar extracted from it by progressive heating to fusion in one or more steps. The argon is then concentrated and analysed isotopically in a mass spectrometer. The mass abundance of ^{40}Ar , ^{39}Ar , ^{38}Ar , ^{37}Ar and ^{36}Ar are measured.

The $^{40}\text{Ar}^*/^{39}\text{Ar}_k$ is determined, where $^{40}\text{Ar}^*$ is the radiogenic argon, and $^{39}\text{Ar}_k$ is the ^{39}Ar produced from ^{39}K during the irradiation.

The $^{40}\text{Ar}^*/^{39}\text{Ar}_k$ is corrected by subtraction of the atmospheric ^{40}Ar and other isotopic interferences

caused during irradiation. The atmospheric ^{40}Ar is calculated by the equation

$$^{40}\text{Ar}_{\text{atm}} = 295.5 * ^{36}\text{Ar}$$

The age of the sample is obtained by the equation:

$$t = 1/\lambda \ln[(J)(F)+1]$$

where:

$$1/\lambda = 1804 * 10^6 \text{ yrs}$$

$$F = ^{40}\text{Ar}^*/^{39}\text{Ar}_k$$

and J = the neutron flux value which affects the samples during the irradiation.

The great advantage of the $^{40}\text{Ar}/^{39}\text{Ar}$ method is that

- 1) the daughter ($^{40}\text{Ar}^*$ parent (^{40}K) ratio is measured in a single isotopic analysis
- 2) the samples does not need to be immediately fused to release argon, but can be heated in steps.
- 3) The argon extracted for each step can be analysed isotopically and provide an apparent age.

This method, introduced by Merrihue and Turner (1966), is known as the step heating incremental heating technique and offers the possibility to obtain information on the thermal and geological history of the analysed sample.

Samples incrementally heated to fusion with the number of steps determined by the amount of information desired. For the phengites, the low temperature (<750°C) steps largely contain atmospheric argon, and the majority of the $^{40}\text{Ar}^*$ is released at higher temperatures.

There are two conventional means of displaying $^{40}\text{Ar}/^{39}\text{Ar}$ data. The first is an age spectrum, which plots the apparent ages vs. the % $^{39}\text{Ar}_k$ released. In theory, if argon is homogeneously distributed in all the crystallographic sites of the mineral, the first steps release argon trapped in the rim of the crystal, while, with increasing temperature, the core of the mineral provides the most of the gas. Recent work has challenged the validity of this assumption. A flat age spectrum, or plateau, indicates that the $^{40}\text{Ar}^*/^{39}\text{Ar}_k$ ratio was homogeneous in all the crystallographic sites. Because of this, age plateau spectra are generally interpreted as undisturbed cooling ages, while step-like

spectra indicate a more complex distribution of the argon in the sample. This distribution could depend from a loss/excess of argon from certain crystallographic sites during a partial reequilibration of the sample (McDougall and Harrison, 1988).

Another method of displaying $^{40}\text{Ar}/^{39}\text{Ar}$ data is isochron analysis, where $^{40}\text{Ar}/^{39}\text{Ar}$ ratio is plotted against $^{36}\text{Ar}/^{40}\text{Ar}$ ratio. The isochron analysis can permit the detection of possible excess or loss of argon.

In an ideal case, if a sample was not affected by any excess/loss of argon, the different points corresponding to each heating step, fall on a line with a $^{40}\text{Ar}/^{36}\text{Ar}$ ratio equal to 295.5 (atmospheric $^{40}\text{Ar}/^{36}\text{Ar}$ ratio).

If the points are well distributed on the line, but the $^{40}\text{Ar}/^{36}\text{Ar}$ intercept is different from the expected value of 295.5, this means that the sample was partially affected by excess argon or argon loss. If the data point on the diagram are too clustered, the isochron cannot be reliably constructed, but this does not mean that the age of the sample is geologically meaningless.

5.2.2. Sample preparation

Phengites and biotites from the basic lithologies and micaschists have been separated starting from representative samples. Basic lithologies, gneisses and micaschists have been crushed and successively sieved. Marbles and calcschists have been crushed and dissolved with HCl (35% concentrate). Phengites and biotites have been separated with a dry shaking table and finally purified with the magnetic separator and cleaned with an agate mortar. For each sample, 40 mg of material have been hand picked and loaded in tin foil. The samples have been introduced in a quartz tube, together with salts and standards, and evacuated. The tubes have been sent to the U.S.G.S. research nuclear reactor in Denver (USA) for the irradiation. Once irradiated, they have been loaded in the ultrahigh vacuum line to be analysed.

5.2.3. Experimental procedure

Irradiated samples have been heated to increasing steps from 600°C to fusion. Twelve heating steps have been done for both phengites and biotites. A first heating for 15 min at 550°C with the outlet valve open permits eliminating part of the atmospheric argon contamination of the sample. About 80% of radiogenic argon is generally released between 750 and 1050 °C.

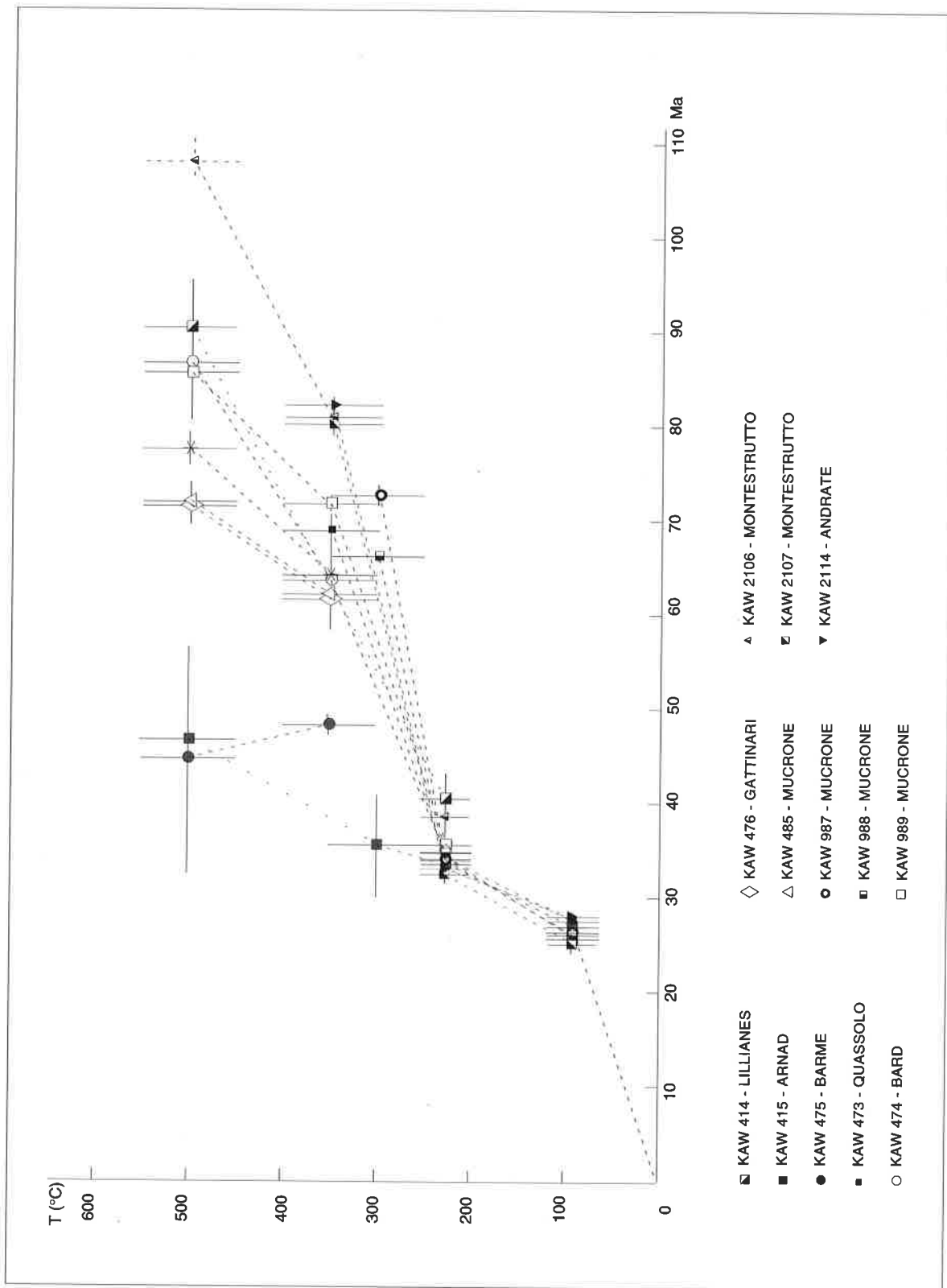


Fig. 5.1 - Reconstruction of the cooling curves for the Sesia zone on the basis of the available data. Every curve is reconstructed using the data obtained with different dating methods on the same sample. Source of data from Hunziker (1974), Oberhänsli et al., (1985), Stöckhert et al. (1986), Hurford et al. (1991).

sample (KAW)	Loc	Rb/Sr (Ma)		K/Ar (Ma)		ZFT (Ma)		AFT (Ma)	
414	Phe lillianes			90 ± 5	1	40 ± 3	5	25 ± 2,8	5
415	Phe arnad	46,8 ± 4,1	1			33 ± 2	5	28,6 ± 4,6	5
473	Phe quassolo	167 ± 288	1	67,7 ± 3,9	1	33 ± 2	5	27 ± 2,5	5
474	Phe bard	86 ± 6	2	63,4 ± 3,4	1	33 ± 2	5		
475	Phe barme	44,1 ± 12	1	47,3 ± 2,7	1				
476	Phe gattinari	70,7 ± 38	1	61,3 ± 4,4	1				
485	Phe mucrone	70,8 ± 13,7	1	61,7 ± 3,2	1				
		71 ± 2	2	62,4 ± 3,3	1				
987	Bio mucrone	72 ± 2	2			34 ± 2	5	26 ± 1,6	5
988	Bio mucrone	66 ± 1	2			35 ± 2	5	26 ± 1	5
989	Phe mucrone	85 ± 1	2	71,2 ± 3,2	1	35 ± 2	5		
2106	Phe Montestrutto	105-110	3	81 ± 1	4	37±2	5	24±1	5
2107	Phe Montestrutto			80 ± 1	4	32±2	5	24±1	5
2110	Phe Andrate			79 ± 1	4			27±2	5
2113	Phe Andrate			74 ± 1	4			25±1	5
2114	Phe Andrate			82 ± 1	4	33±2	5	27±2	5

1 Hunziker, 1974
2 Oberhansli et al., 1985
3 Hurford et al. in Stockhert et al., 1986
4 Stockhert et al., 1986
5 Hurford et al., 1991

Tab. 5.1 - Synoptic table of the available geochronological data obtained on the same sample by using different dating methods. $^{40}\text{Ar}/^{39}\text{Ar}$, K/Ar and Rb/Sr age determinations have been done on the same mineral fraction.

A mass spectrometer MAP 215-50 provided the spectroscopic analyses. For each analysis, five to seven acquisitions cycles have been done per step. Some samples have been analysed with the Faraday detector other with the Multiplier. Blanks were measured of varies temperatures and these values were corrected from the unknowns.

5.2.4. Presentation of the results.

In the next paragraphs, the geochronological results of the Ar/Ar incremental heating experiments for the phengites and biotites of the central Sesia zone will be given.

In most of the cases, the obtained age spectra are flat and often provide plateau ages. The majority of the isochrons are instead characterised by points clustering near the abscissa, so that no isochron age can be calculated in these cases; as explained above, this fact does not mean that the samples were affected by excess argon phenomena. Most of the $^{40}\text{Ar}/^{36}\text{Ar}$ intercepts gives reasonable values close to 295.5; this is often due to the influence of the lower heating steps, which are enriched in atmospheric argon. Thus, in the majority of the cases a good intercept does not permit affirmation that the obtained age is reliable.

5.3. ^{40}Ar - ^{39}Ar Data of Phengites

5.3.1. Choice of the Sample

This study presents over thirty $^{40}\text{Ar}/^{39}\text{Ar}$ step heating analyses in order to:

- 1) confirm the K/Ar age determinations of Hunziker (1974) by the $^{40}\text{Ar}/^{39}\text{Ar}$ method;
- 2) investigate the age of metamorphism of monometamorphic cover sequences in the lower Aosta and Chiusella valleys;
- 3) contribute to the broad body of geochronological work in the Sesia zone;
- 4) suggest a P-T-t path for the monometamorphic cover sequences of the central Sesia zone.

Tab. 5.2 summarises macroscopic and microscopic characteristics of the analysed samples. The twelve samples labelled KAW were collected by Hunziker and partially analysed with the Rb/Sr and K/Ar methods. $^{40}\text{Ar}/^{39}\text{Ar}$ investigations of these samples used the same separates as the earlier studies of Hunziker, with exception of KAW 476. The aim of the (re)measurement of the KAW samples was to detect possible excess argon or ^{40}Ar loss phenomena, which cannot be rescued with the K/Ar method, and to complete the cooling history for those samples that where analysed only with the Rb/Sr method. Five of the KAW samples had not been previously analysed.

Additional samples were chosen following specific criteria:

- 1) phengites define the main foliation and are in equilibrium with the eclogitic paragenesis (garnet-omphacite-glaucophane±jadeite-albite); biotites define the HG pre-Alpine foliation together with garnet-sillimanite-K-feldspar-plagioclase.

<i>lithology - sample - locality</i>	<i>Sesia unit</i>	<i>macroscopic aspect</i>	<i>main assemblage</i>
basement samples			
<i>KAW samples</i>			
415 - Arnad *	central external unit	phengitic alkalifeldspar gneiss with dark levels rich in bt and chl	ab-phe-qtz±bt-ep-ru-omp-gln
475 - Barne *	central external unit	fine grained spotted phengite-albite gneiss	ab-qtz-phe-cc-gln-omp±bt-grn-ep
700 - isoello *	northern external unit	fine-grained biotite-phengite-bearing alkalifeldspar gneiss	pl-qtz-Kf±bt-phe-chl -czo/ep-omp
1521 - S. Maria *	northern external unit	biotite-phengite-bearing alkalifeldspar gneiss	pl-qtz-Kf±bt-phe-chl -czo/ep
476 - Gattinari *	intermediate unit	greenish banded phengite alkalifeldspar augengneiss	ab-qtz-phe±czo/ep-chl
702 - Ingria *	intermediate unit	fine grained spotted phengite-albite micaschist	ab-qtz-czo-phe-±ru -gln-grn
992 - Corio *	southern internal unit	albitic gneiss with stretched qtz levels	ab-qtz-mc-phe-chl -bt±czo-opaques
473 - Quassolo *	central internal unit	greenish omphacite-phengite heterogeneous gneiss with lens of eclogites	ab-omph-phe-qtz-grn-gln±zo-opaques
698 - Favaro *	central internal unit	grn-micaschist (inclusion in trachyandesite)	phe-qtz-pl-grn-chl -cc±ru-omp-gln
988 - Mucrone	central internal unit	biotite-granite with both texture and mineral preservation	qtz-pl (jd-qtz)-mc-bt-grn±ru-zr
1424 - Fontainemore	central internal unit	banded phengitic metagranodiorite	ab-qtz-czo-phe-±gln -grn-ru-omp
1425 - Ivery	central internal unit	banded phengitic orthogneiss	ab-qtz-czo-phe-±gln -grn-ru-omp
1432 - Fondo	central internal unit	banded phengitic ortholeucogniss	ab-qtz-czo-phe-±grn -ru
<i>SV samples</i>			
92 1dz - Donnaz	central intermediate unit	Strongly deformed greenish orthogneiss with scattered relics of the magmatic texture	phe-qtz-gln/bar-czo(ep)-ab-aegr-grn±chl
92 2t - Tavagnasco	central internal unit	leucocratic metagranite with big flakes of green phe and jd	jd(ab)-qtz-phe-zo/czo-aegr±grn-mc-chl
91 1f - Fontainemore	central internal unit	greenish banded polymetamorphic marbles	cc-phe-sph-czo±dio -amph
92 3p - Perlioz	central internal unit	impure polymetamorphic marbles closely related to omp-micaschists.	cc-omp-grn-czo -sph±dio-gln-ru
92 1d - Dolca	central internal unit	chlorite-rich micaschist surrounding decimetric to metric boudins of glaucophanites	phe-ru-chl -czo/ep±gln-opaques
1k/91 - Savenca	central internal unit	preserved pre-Alpine HG mesocratic gneiss crosscut by thin leucocratic dikes	bt-grn-sill-kf-qtz±ilm-wm-zo
126/91 - Savenca	central internal unit	preserved pre-Alpine HG mesocratic gneiss crosscut by thin leucocratic dikes	bt-grn-sill-kf-qtz±ilm-wm-zo
Monometamorphic cover samples			
<i>SV samples</i>			
92 11c - Cavalcurt	central internal unit	qtz-rich impure marbles/calcschist	cc-qtz-phe±do-sph -grf-opaques
91 3q - Quincinetto	central internal unit	qtz-rich impure marbles/calcschist	cc-qtz-phe±do-sph -grf-opaques
92 3q - Quincinetto	central internal unit	qtz-rich impure marbles/calcschist	cc-qtz-phe-zo±do-sph -grf-opaques
92 5m - Mombarone	central internal unit	qtz-rich impure marbles/calcschist	cc-qtz-phe±do-sph -grf-opaques
92 5vc - Tallorno	central internal unit	qtz-rich impure marbles/calcschist	cc-qtz-phe±do-sph -grf-opaques
92 4b - Bonze	central internal unit	metagabbro with main foliation underlined by alternances of zo/czo and gln-grn layers	gln-czo-Mg chl-wm -grn±omp-ru-spe-qtz

Tab. 5.2 - Location and main macroscopic and microscopic characteristics of the samples which have been collected for the $^{40}\text{Ar}/^{39}\text{Ar}$ age determinations.

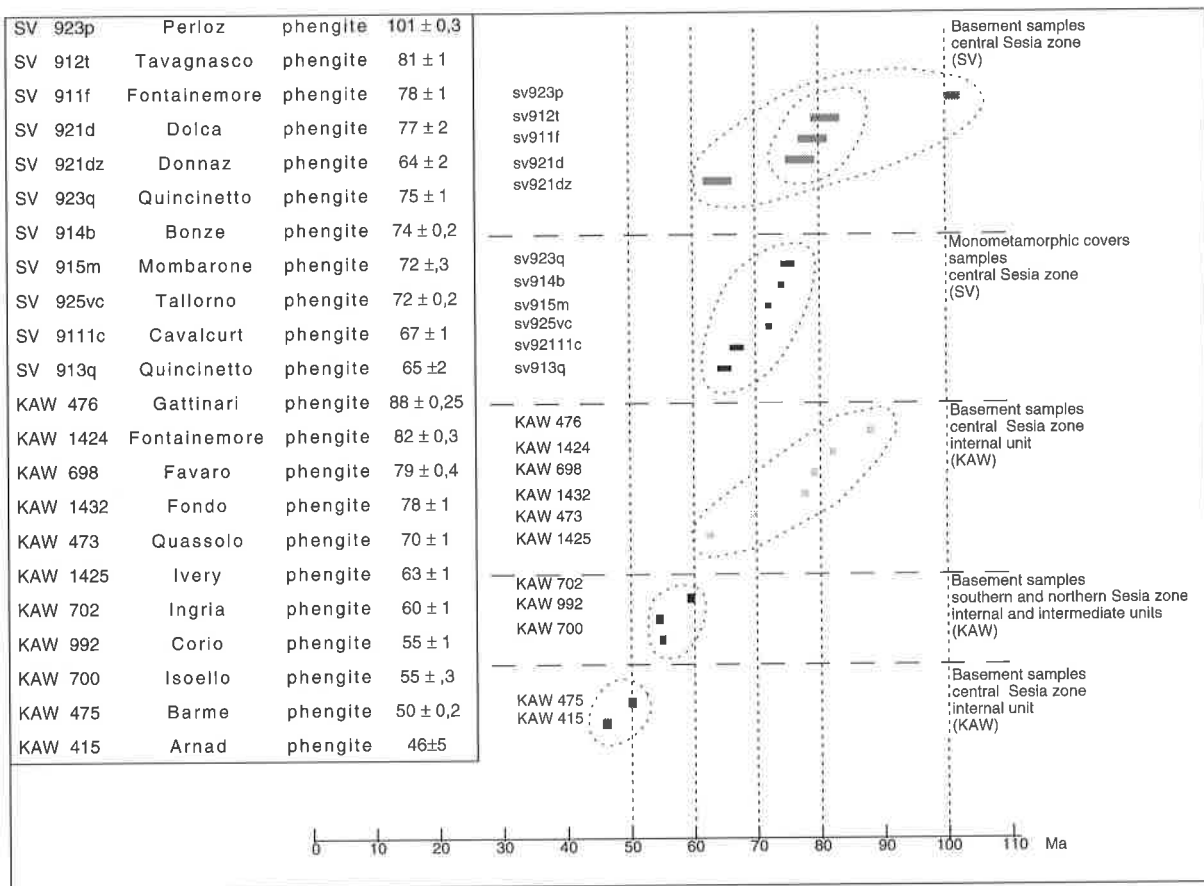


Fig. 5.2 - Summazing table of the ages obtained with the $^{40}\text{Ar}/^{39}\text{Ar}$ dating method on phengites. The $^{40}\text{Ar}/^{39}\text{Ar}$ age data were grouped in function of the unit- appartenance and of range of ages. The monometamorphic cover sequences yield ages comprised between 64 and 75 Ma. The polycyclic basement ages are comprised between 45 Ma (external unit) and 101 Ma.

- 2) samples display the least possible folding and kinking at the macroscopic scale.
- 3) phengites are generally coarse-grained and not deformed.
- 4) the micas are not retrogressed to chlorite (the chemistry of the analysed micas was checked in thin section with a microprobe⁵).
- 5) the samples of the monometamorphic cover sequences represent a well-defined lithologic horizon (quartz-rich impure marbles/calcschists), which can be easily followed in the field. One exception, sample sv91 4b, is a mylonitic metagabbro; in this case we studied the prograde foliation displayed by this rock.

Three to five kilograms of material for each sample were collected. Micas were separated either mechanically (gneisses and micaschists) or by dissolution in HCl. The minerals were then further separated in the magnetic separator and the agate mills. Between twenty and thirty milligrams of micas from each sample were then hand-picked and re-analysed with a microprobe to ensure of the quality and purity of the mineral separates. All separates represent size

fractions greater than 100μ in order to avoid the later sericitic recrystallisation described by Stöckhert et al. (1986). KAW samples were collected from different units of the polycyclic basement (Tab.5.2). Their $^{40}\text{Ar}/^{39}\text{Ar}$ ages range from 87 to 46 Ma, for the central and southern Sesia zone, and 23 Ma for the north-eastern Sesia zone. In the central sector five $^{40}\text{Ar}/^{39}\text{Ar}$ age determinations range between 87 and 67 Ma, three between 60 and 50 Ma, and two between 46 and 50 Ma. Finally, a biotite from the late Paleozoic granite of Monte Mucrone gives an $^{40}\text{Ar}/^{39}\text{Ar}$ age of 200 Ma. The other samples represent either the basement or the monometamorphic cover sequences. Phengite $^{40}\text{Ar}/^{39}\text{Ar}$ ages range between 103 and 65 Ma, clustering between 82 and 70 Ma.

Plate 3a reports all the phengite $^{40}\text{Ar}/^{39}\text{Ar}$ ages presented in this study for the central and southern Sesia zone. For the analytical discussion, the $^{40}\text{Ar}/^{39}\text{Ar}$ ages of phengites have been grouped in five main sets: 1) younger than 50 Ma, 2) between 50 and 60 Ma, 3) between 61 and 70 Ma, 4) between 71 and

⁵ microprobe CAMECA SX50 of the University of Lausanne

80 Ma and 5) 81 and 110 Ma (Fig. 5.2).

AGES YOUNGER THAN 50 MA

Samples KAW 415 and 475 samples, collected at the western edge of the external unit, yield ages between 45 and 50 Ma. The spectra and isochrons of these two samples are given in Fig. 5.5. Sample KAW 475 gives a reasonable $^{39}\text{Ar}/^{40}\text{Ar}$ isochron with an $^{40}\text{Ar}/^{36}\text{Ar}$ intercept higher than the expected value (295.5). This phenomena could indicate a loss of argon successive to the closure of the system (Lanphere and Dalrymple, 1976), decreasing the apparent age. No differences in age are displayed by the isochron calculated with all the steps respect to those calculated using only the central steps. As a result, we consider 50 Ma to be the minimum age of sample KAW 475. Sample KAW 415 shows a preferred age of 46 ± 0.5 Ma, which unfortunately cannot be confirmed by the isochron plots, as the data are too clustered.

50-60 MA AGES

Three phengite separates from KAW yield ages between 55 and 60 Ma. Sample KAW 700 (55 ± 0.5 Ma) was collected in the northern sector of the Sesia zone. Samples KAW 702 (59 ± 1 Ma) and 992 (55 ± 1 Ma) come from the southern internal unit. All spectra from these samples yield age plateaux. The $^{39}\text{Ar}/^{40}\text{Ar}$ isochron plots, however, are difficult to interpret because the points cluster near the abscissa, and no reasonable isochron can be drawn. As explained in paragraph 5.2.4., the presence of data clustering to the isochron does not imply that the samples were affected by excess argon or argon loss, but exclude additional information about the reliability of the age determination.

60-70 MA AGES

This interval comprises four samples (phengite separates) from both the polycyclic basement (KAW 1425 and sv921dz) and the monometamorphic cover sequences (sv9111c and 913q; Fig. 5.6). The step heating spectrum of KAW 1425 (TF age (Total fusion age) = 67 ± 0.2 Ma) increases gradually from lower to higher steps, while sv911c (TF age = 67 ± 0.2) is characterised by a central minimum in the heating spectrum. The other three samples exhibit plateaux that are flat and undisturbed. Sample sv921dz shows an ideal $^{39}\text{Ar}/^{40}\text{Ar}$ isochron correlation, and the isochron age agrees perfectly with the plateau age (64 ± 0.2 Ma). The data of this sample are aligned and reasonably distributed, although data representing 80% of the gas are cluster. It has been possible to calculate reasonable

isochron for this sample, even when only data clustered near the abscissa are considered. Sample sv913q displays a reasonable isochron correlation (MDWS=7.2) with a $^{40}\text{Ar}/^{36}\text{Ar}$ intercept of 293 ± 5 , although the points cluster around the abscissa. The isochron plots for the other two samples show too little dispersion of their points and are difficult to evaluate.

70-80 MA AGES (MONOMETAMORPHIC COVER SEQUENCES)

Four phengite separates from the monometamorphic cover and five from the polycyclic basement samples yield ages between 70 and 80 Ma. All the spectra are plateaux and correlate well with the isochron plots.

The monometamorphic cover samples yield ages between 72 and 75 Ma (Fig. 5.7). Their spectra show central flat plateau with preferred ages of 74 Ma. Samples sv914b and 923q are characterised by a decreasing steplike spectra. The $^{39}\text{Ar}/^{40}\text{Ar}$ isochrons display reasonable correlations, for sample sv914b and sv923q, while they cannot be calculated for the other samples, because all point cluster near the abscissa. All ages calculated with the isochron method show a bigger uncertainty than those deduced by the plateau spectra.

70-80 MA AGES (MPOLYCYCLIC BASEMENT ROCKS)

The polycyclic lithologies yield TF ages of 78 Ma except for KAW 473 which is 71 Ma (Plate 3b). Plateau spectra for these samples display flat profiles. $^{36}\text{Ar}/^{40}\text{Ar}$ - $^{39}\text{Ar}/^{40}\text{Ar}$ isochron of KAW 1432 and KAW 473 display ideal correlations with $^{40}\text{Ar}/^{36}\text{Ar}$ intercepts equal to the expected value and with a very low MSWD value. The other samples show reasonable isochrons with the exception of sv911f for which it is not possible to determinate any reasonable isochron.

80-110 MA AGES

Three samples yield ages between 80-90 Ma, and one sample give an age 105 Ma. KAW 1424 (TFage = 83 Ma) and sv912t (Preferred age = 83 Ma) show flat plateau spectra, while sv923p is partially characterised by a steplike spectrum. None of the isochron correlations for these sample offer unequivocal results, because data releasing more than 80% of radiogenic gas cluster near the abscissa. The consistent $^{40}\text{Ar}/^{36}\text{Ar}$ intercepts are mostly due to the influence of the lower heating steps representing the system blank. Any further

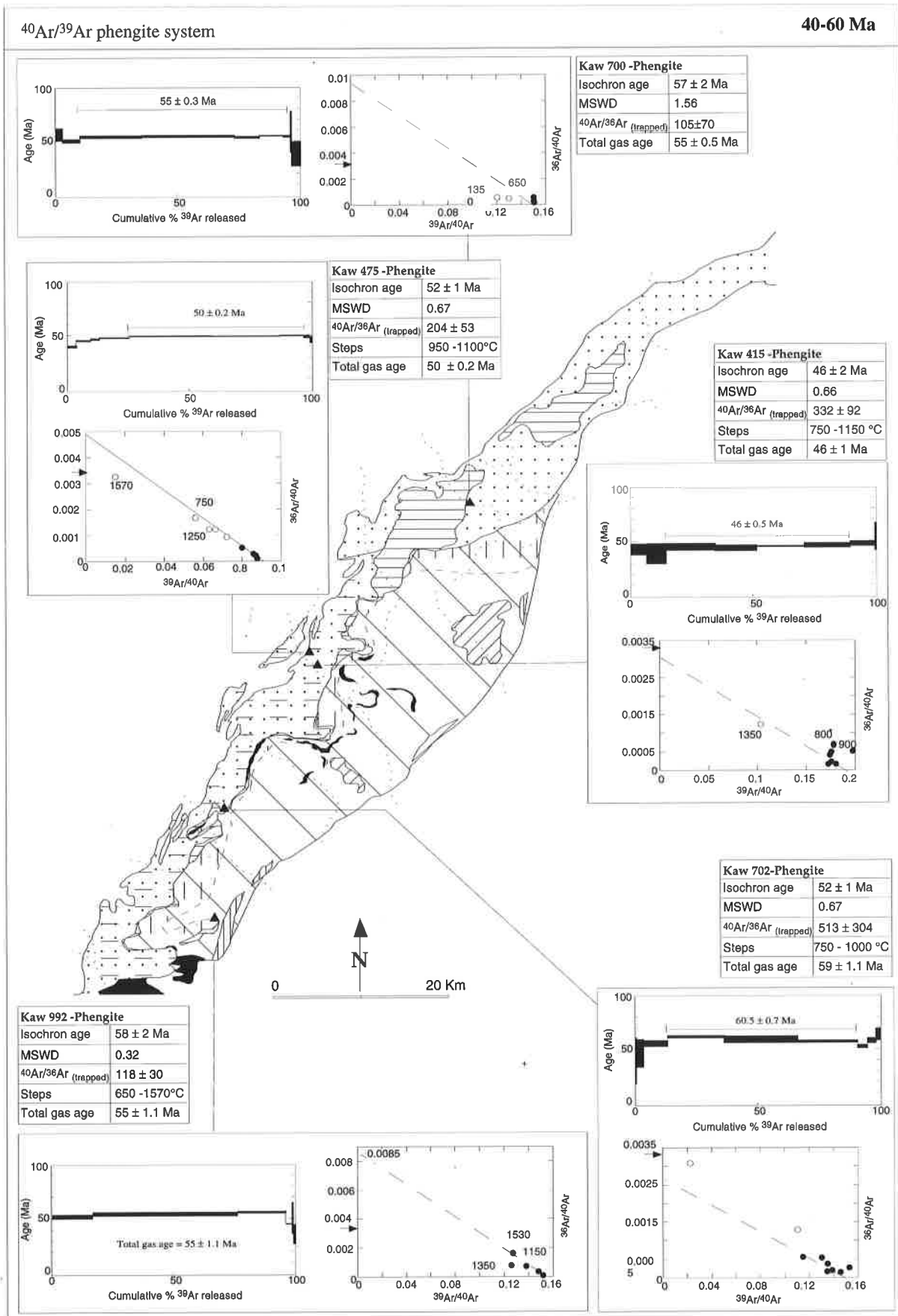


Fig. 5.3 - 40-60 Ma age interval for $^{40}\text{Ar}/^{39}\text{Ar}$ dating on phengite system

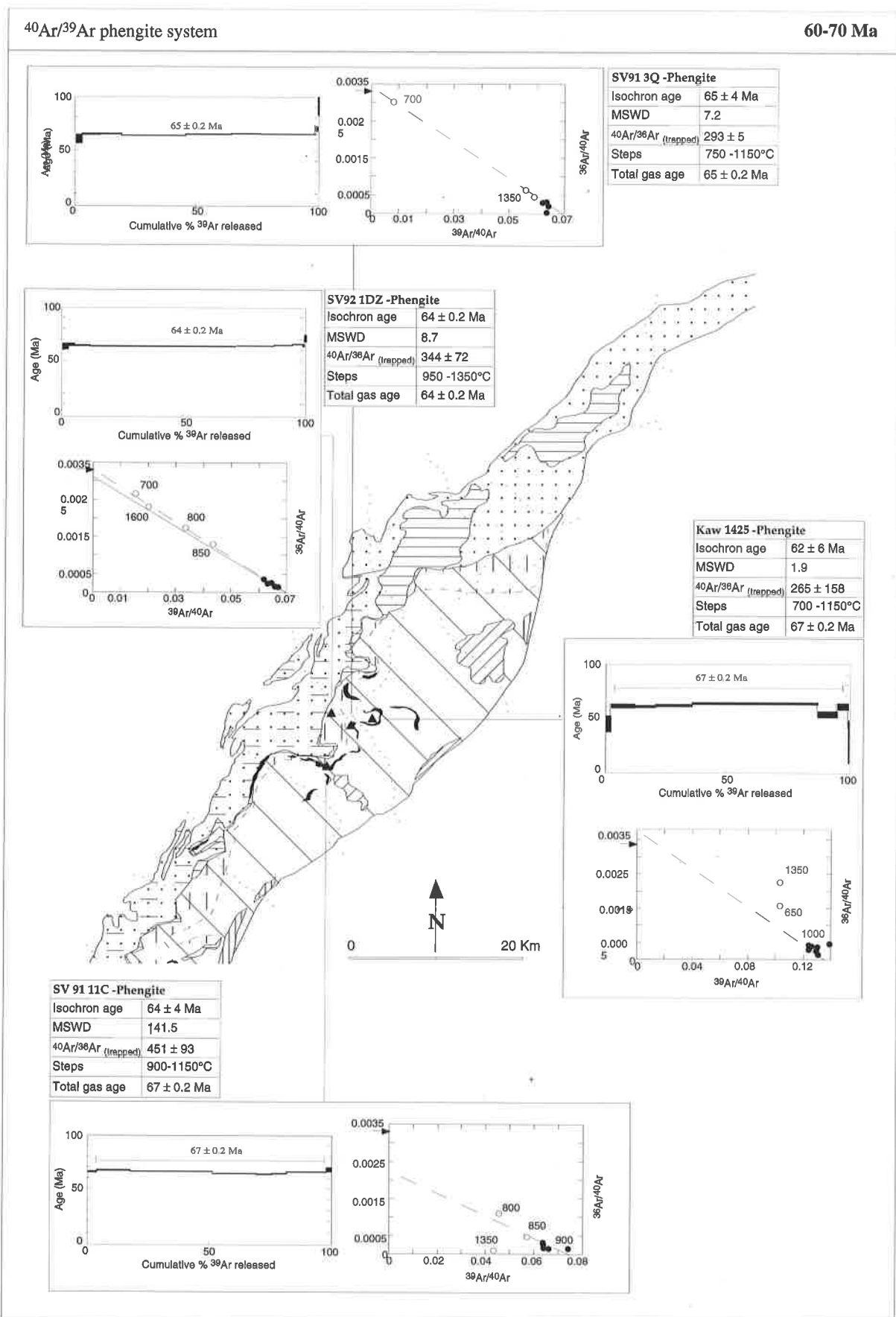


Fig. 5.4 - 60-70 Ma age interval for $^{40}\text{Ar}/^{39}\text{Ar}$ dating on phengite system

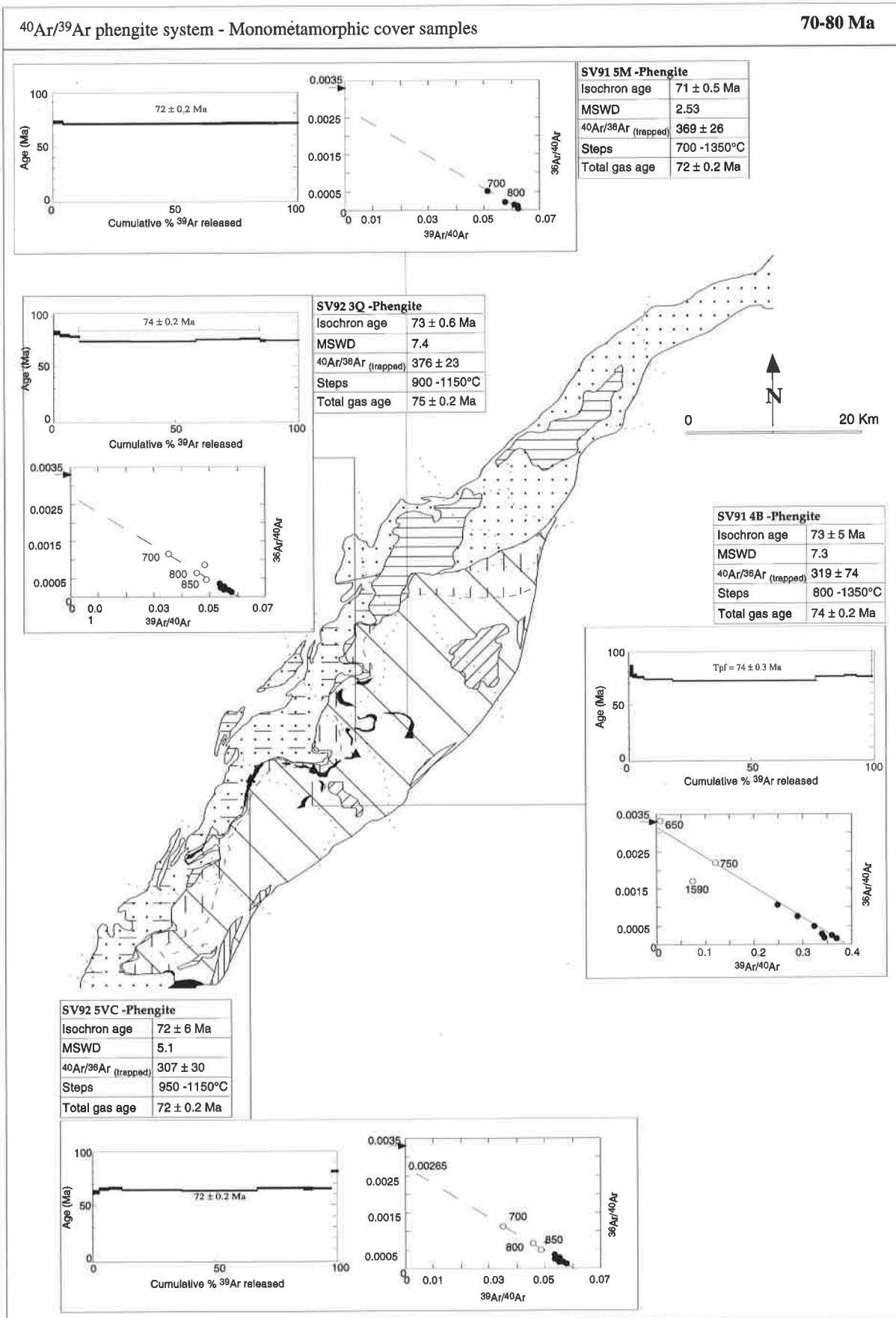


Fig. 5.5 - 70-80 Ma age interval for $^{40}\text{Ar}/^{39}\text{Ar}$ dating on phengites of samples collected in the monometamorphic covers

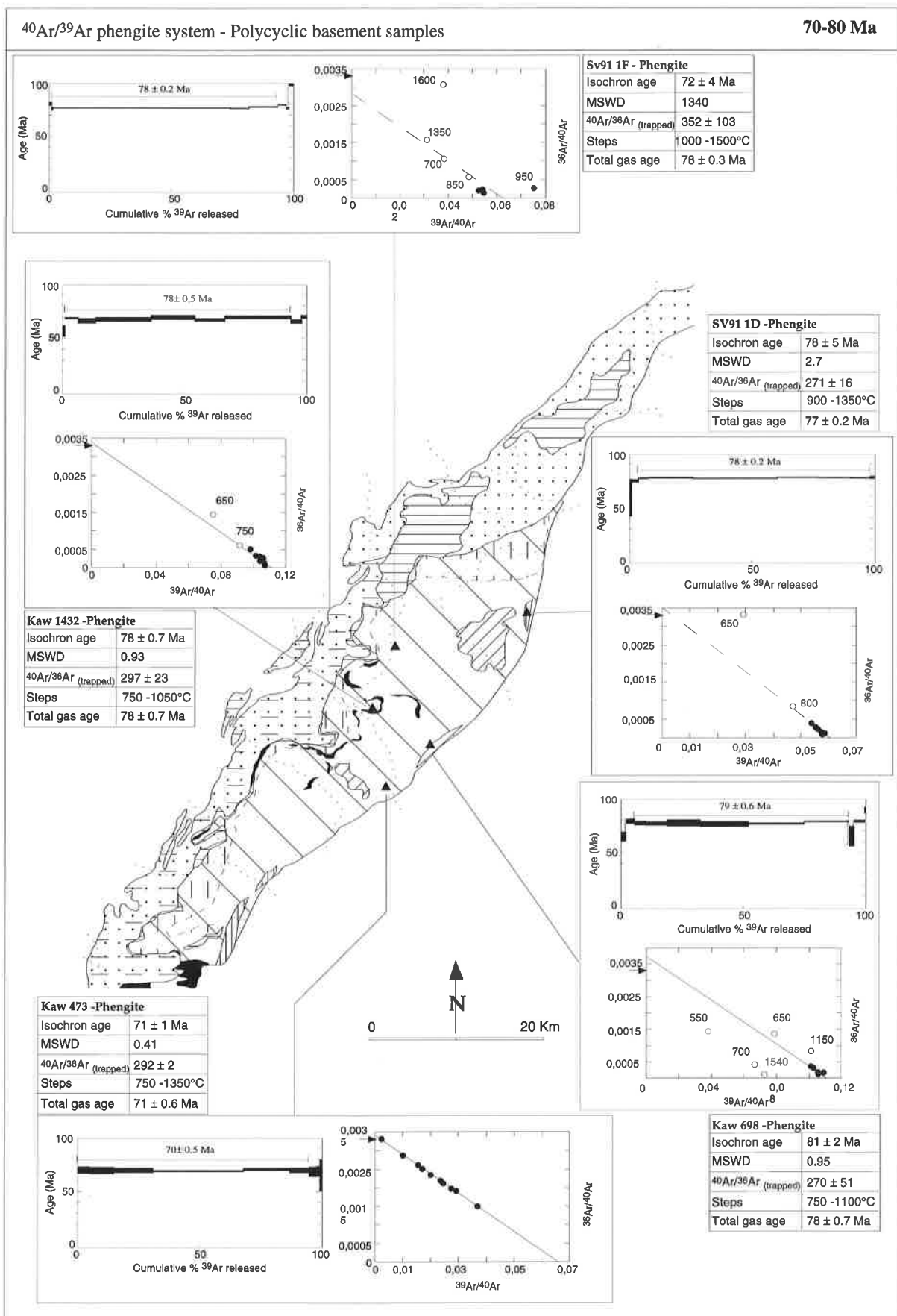


Fig. 5.6 - 70-80 Ma age interval for $^{40}\text{Ar}/^{39}\text{Ar}$ dating on phengites of samples collected in the polycyclic basement

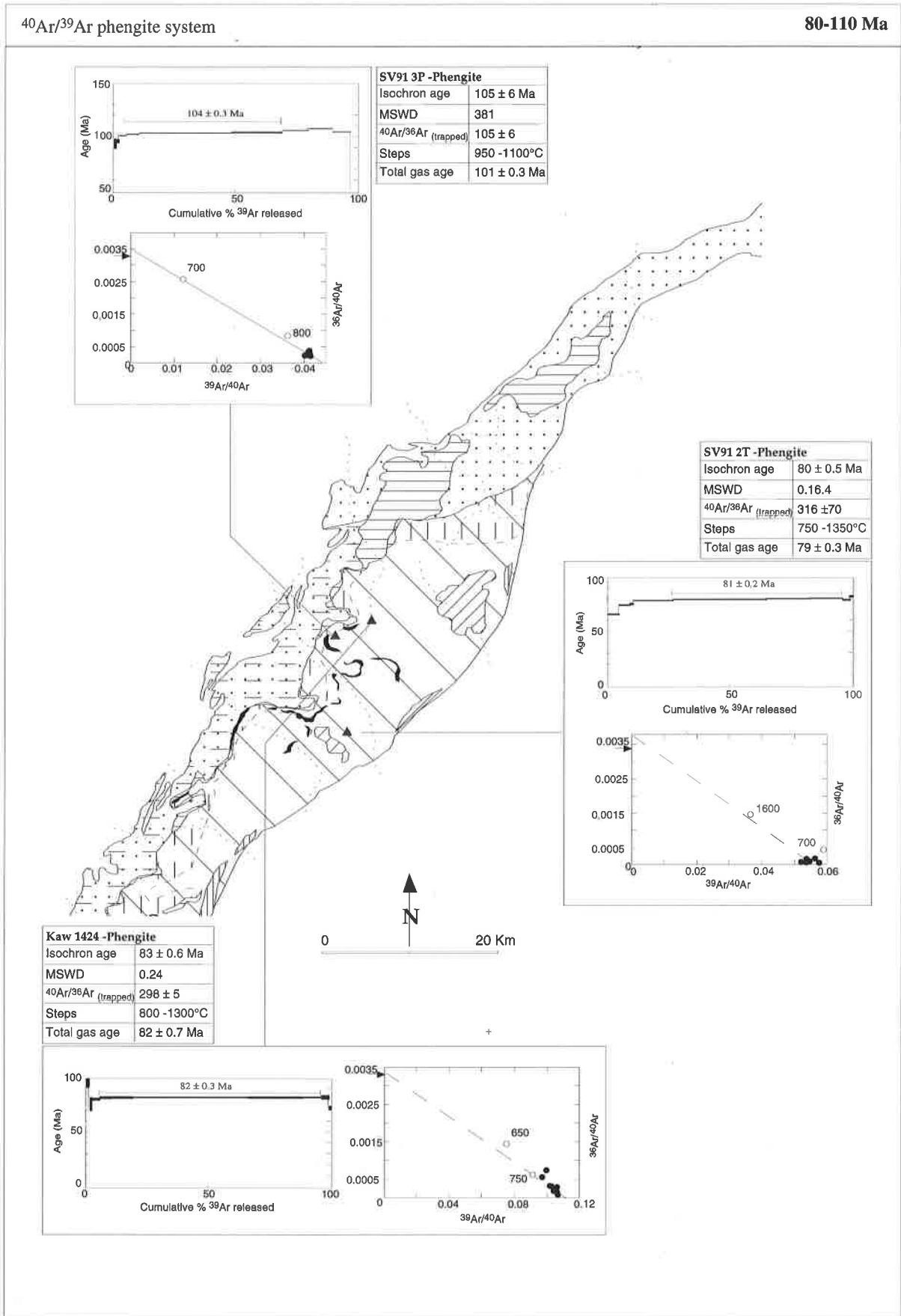


Fig. 5.7 - 80-110 Ma age interval for $^{40}\text{Ar}/^{39}\text{Ar}$ dating on phengites of samples collected in the polycyclic basement

consideration on the reliability of these age determinations will require application of other dating techniques, like the Rb/Sr method.

5.3.2. Discussion

The analysis of the age sets provides some useful information for the interpretation of the geochronological data. The first group of ages, between 46 and 50 Ma, is composed of two age determinations, the older of those (KAW 475) can be considered a minimum age. This range of data agrees with the previous Rb/Sr determinations of Hunziker (1974), with Rb/Sr ages between 47 ± 4 Ma (KAW 415) and 44 ± 12 Ma (KAW 475) (Fig. 5.1 and Plate 3b).

The samples yielding ages between 50 and 60 Ma (second set) have been collected in the intermediate or northern external unit of the polycyclic basement and display greenschist assemblages, with relics of high pressure assemblages in samples KAW 702 and 992 (Tab. 5.2). This set of ages does not allow an unequivocal interpretation because of the impossibility to define reasonable isochron

correlations. Two different interpretations can be advanced for these ages:

1) they represent late eo-Alpine cooling ages not disturbed by the successive Tertiary metamorphic event; in this case the Rb/Sr method on the same samples should provide coherent answers.

2) they are mixed ages, due to the superposition of the Tertiary greenschist reequilibration on the eo-Alpine metamorphism. This hypothesis can be solved only with further investigation.

The ages between 60 and 70 Ma years show flat plateaux and reliable isochron correlation, with the exclusion of SV 911c, which is a disturbed age determination. These can be interpreted as cooling ages, e.g. ages recording an «unperturbed» cooling path followed by the samples during its uplifting history; samples between 70 and 80 Ma can be interpreted in the same way.

KAW 1424 (83 Ma) and SV 923p (104 Ma), provide the oldest age determinations. KAW 1424 is characterised by a reasonable $^{36}\text{Ar}/^{40}\text{Ar} - ^{39}\text{Ar}/^{40}\text{Ar}$ isochron correlation with a very low MDWS value.

Range of ages (Ma)	Sample	spectrum type	spectrum age (Ma)	Isochron type (Ma)	isochron age (Ma)	comment	age Ma
40-50	KAW 415	plateau	46 ± 0.5	not reliable	(46 ± 2)	reasonable*	46
	KAW 475	plateau	50 ± 0.2	reasonable	52 ± 1	minimum age	• 51
50-60	KAW 700	plateau	55 ± 0.3	not reliable	(57 ± 2)	possible	
	KAW 702	plateau	59 ± 3	not reliable	(59 ± 3)	possible	
	KAW 992	plateau	55 ± 1	not reliable	(58 ± 2)	possible	
60-70	sv921dz	plateau	64 ± 2	ideal	64 ± 0.4	reliable	• 64
	sv913q	plateau	65 ± 2	reasonable	65 ± 4	reasonable	65
	sv911c	steplike	67 ± 0.2	not reliable	(61 ± 4)	reasonable*	67
	KAW 1425	plateau	67 ± 0.2	not reliable	(62 ± 6)	possible	
70-80	KAW 473	plateau	70 ± 0.5	ideal	71 ± 1	reliable	• 71
	sv915m	plateau	72 ± 0.2	reasonable	71 ± 0.5	reasonable	72
	sv925vc	plateau	72 ± 0.2	reasonable	72 ± 6	reasonable	72
	sv923q	plateau	74 ± 0.2	good	73 ± 0.6	good	• 73
	sv914b	plateau	74 ± 0.3	good	73 ± 5	good	• 73
	sv921d	plateau	78 ± 0.2	good	78 ± 5	good	• 78
	KAW 698	plateau	79 ± 0.6	reasonable	(81 ± 2)	reasonable	80
	KAW 1432	plateau	78 ± 0.5	good	78 ± 2	good	• 78
	sv911f	plateau	78 ± 0.2	not reliable	(72 ± 4)	possible	
80-110	sv912t	plateau	81 ± 0.2	not reliable	(80 ± 0.5)	possible	
	KAW 1424	plateau	82 ± 0.3	good	(83 ± 0.6)	reasonable	83
	sv913p	steplike	104 ± 0.3	not reliable	(105 ± 6)	possible	

* coherent with Rb/Sr data of Hunziker (1974)

sv923p is otherwise characterised by a steplike plateau and no reliable isochron. These age determinations, which otherwise give reasonable results, cannot be unambiguously interpreted as a cooling age. Only further application of the Rb/Sr method can confirm or deny the oldest ages. A summary of the reliability of the different age determination on the phengites is listed below:

None of the age plateaux and isochrons has shown evident excess argon phenomena. Ages which could not be confirmed by both spectra and isochrons have been classified as «possibles»; ages for which the isochron correlation was consistent, have been considered as reasonable: Ages displaying good plateaux and coherent isochron have been accepted as reliable.

The samples of the monometamorphic cover sequence yield ages between 72 and 74 Ma, which are coherent with those obtained from the polycyclic basement samples.

Inger and Cliff, (1994) analysed a sphene of a sample of the monometamorphic cover sequence. The U/Pb age yield 66 Ma, which was assumed by the authors as the age of the «eclogitic» event. The petrographic data from the internal Sesia zone (e.g. Dal Piaz et al, 1972; Compagnoni, 1977; Compagnoni et al., 1977a; Gosso, 1977; Pognante et al., 1980; Venturini et al., 1991) show that sphene is not a phase related to the high pressure climax, but to the retrograde blueschist-greenschist assemblages. The age of 66 Ma agrees with the other available data referred to the cooling history of the internal Sesia zone.

Recently, several studies address the effect of argon diffusion in the coarse and fine-grained phengites of the Sesia zone (Ruffet et al., 1993, 1994, Reddy et al., 1994). One hypothesis advanced by the authors is that the Cretaceous K/Ar and $^{40}\text{Ar}/^{39}\text{Ar}$ ages of the Sesia zone could be due to excess argon. The results of these investigations, however, should be compared with well-known age determinations, whose Rb/Sr, $^{40}\text{Ar}/^{39}\text{Ar}$ and K/Ar age determinations yield concordant results (Plate 3b).

5.3.3. Cooling History of the central Sesia Zone

In the previous paragraph we have shown reliable $^{40}\text{Ar}/^{39}\text{Ar}$ age determinations on phengites ranging from 46 to 78 Ma. Ages comprised between 46 and 51 Ma are found *only* in the external unit, while ages ranging from 64 to 82 Ma correspond to lithologies of the intermediate and internal unit respectively. The

older reliable age determinations are located in the internal unit, in the Gressoney valley and in the lower Aosta valley, while the younger ages correspond to the eastern edge (Quassolo) and to the intermediate unit (Donnaz)(Plate 2b; Plate 3b and Fig. 5.2).

Samples KAW 702 and 992, located in the southern internal and intermediate Sesia zone, yield possible ages between 55 and 59 Ma. Although different interpretations of these age determinations have been given above (Par. 5.3.2), they could also be explained as the result of a tilting of the internal unit which provided the exhumation of the central Sesia zone later followed by the southern sector.

In Plate 3b, the $^{40}\text{Ar}/^{39}\text{Ar}$ age determinations of phengites discussed above, are superposed with the available geochronological data reported in temperature-time graphic of Fig. 5.1. Red dots indicate reliable ages, while yellow and green dots represent reasonable and possible ages respectively.

The data of this work are coherent with previous geological data. Plate 3b confirms the presence of two separated sets of ages, according to Hunziker (1974), and suggests two different cooling paths (Venturini and Hunziker, 1992). The first cooling path involves lithologies of the internal unit and starts in the middle Cretaceous, while the second cooling path is followed by the external edge of the Sesia zone and begins in the Early Eocene. The first cooling trend corresponds to the uplift of a shallower level of unit subducted during the early Cretaceous and not reequilibrated under greenschist conditions, while the second trend is probably due to the Tertiary greenschist overprint which affected mainly the external edge of the Sesia zone during the continental collision.

Fig. 5.8 shows a P-T-t path for the central Sesia zone reconstructed following the pressure-temperature diagram of Fig. 4.12, in which closure temperature intervals for Rb/Sr ($500\pm 50^\circ\text{C}$) and K/Ar ($350\pm 50^\circ\text{C}$) systems in phengites have been inserted. Phengites age data of Hunziker (1974) and Oberhänsli et al. (1985) give values between 86 and 71 Ma for $T=500\pm 50^\circ\text{C}$ and $P=10\pm 2$ Kbars for Rb/Sr and values between 71 and 62 Ma for $T=350\pm 50^\circ\text{C}$ a $P=3\pm 1$ Kbars for K/Ar on the same mineral from the same samples. These data indicate an unroofing rate of approximately $2.8\text{ Km}/\text{Ma}$ during the upper Cretaceous for the internal Sesia zone.

The greenschist pressure-temperature conditions of the external unit were determined by Lattard (1974) as $400\text{--}450^\circ\text{C}$ and 5 Kbars. This means that phengites related to the greenschist assemblage never exceeded

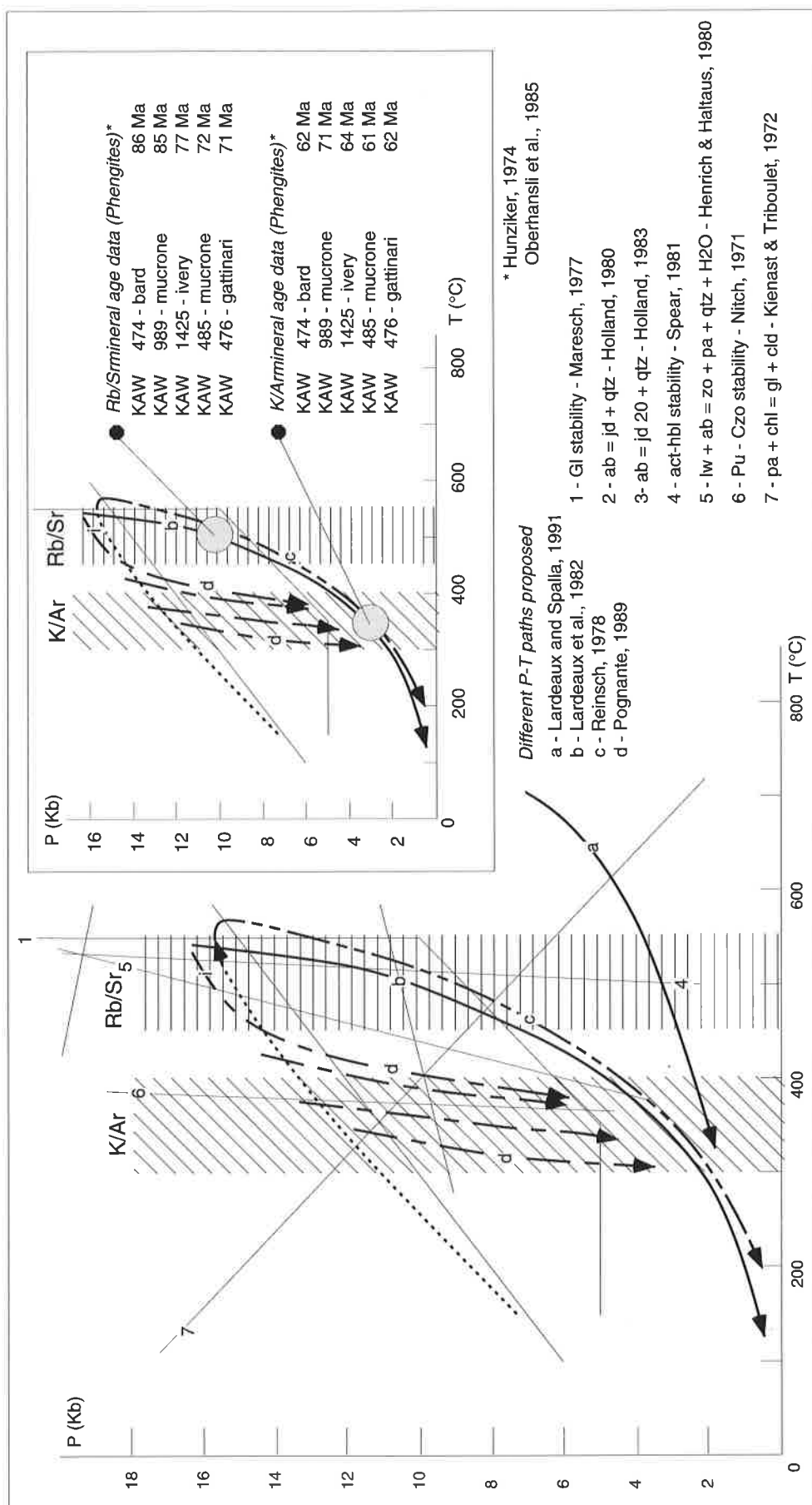


Fig. 5.8 - Compilation pressure-temperature diagram for the central Sesia zone based on the pressure-temperature paths of Fig. 4.12 and geochronological data of Hunziker (1974) and Oberhänsli et al. (1985). The age data are related to the sector which recorded a first decompression path followed by a cooling path. Rb/Sr and K/Ar mineral ages on phengites are consistent and show a gap of approximately 10 Ma. The calculated cooling rate is 10-14 °C/Ma and an uplifting of 2.8 Km/Ma.

500 °C, which explains the small age difference existing between the Rb/Sr and the K/Ar and $^{40}\text{Ar}/^{39}\text{Ar}$ age determinations for the samples of the external unit.

The two cooling trends converge to the same trajectories from the early Oligocene, as evidenced by the zircon and apatite fission tracks (Hurford et al., 1991). The path followed by the internal and external unit during the Oligocene shows rapid cooling (~1mm/year), probably due to the post-collision extension phase (Hurford et al., 1991).

5.4. $^{40}\text{Ar}/^{39}\text{Ar}$ Data of Biotites and Glaucophane

5.4.1. Introduction

Three $^{40}\text{Ar}/^{39}\text{Ar}$ age determinations of pre-Alpine biotites of the polycyclic basement were carried out during this study in order to provide new information on the early evolution of the Sesia zone.

Biotite represents one of the most widespread phases related to both the Paleozoic high grade metamorphism in the polycyclic basement and the late-Paleozoic granodiorites and granites. These minerals were previously dated in the Sesia zone using the Rb/Sr, K/Ar and $^{40}\text{Ar}/^{39}\text{Ar}$ techniques (Hunziker, 1974; Hy, 1984; Oberhänsli et al., 1985). $^{40}\text{Ar}/^{39}\text{Ar}$ age determinations on the kinzigite biotites yield 203 Ma in the Monte Mucrone region (Hy, 1984); in the same area Rb/Sr age determinations on biotites of a metagranodioritic stock provided eo-Alpine ages of 72 and 66 Ma (Oberhänsli et al., 1985). In the external unit (Arnad) of the polycyclic basement, a Rb/Sr age determination on biotite yielded 36 Ma (Hunziker, 1974), related to the Tertiary greenschist metamorphism. In the northern sector of the polycyclic basement (Ossola valley) the same generation of biotite provided a K/Ar age of 28 Ma. Recently Reddy et al. (1994) analysed biotites from the pre-Alpine high grade basement complex (II DK) with both the Rb/Sr and the $^{40}\text{Ar}/^{39}\text{Ar}$ laser spot analysis method. The Rb/Sr ages are pre-Alpine, while the $^{40}\text{Ar}/^{39}\text{Ar}$ ages range between the Upper Permian and the Lower Cretaceous. Similar ages were recorded by the biotites in the Ivrea Zone (Zingg et al., 1990 and ref. therein), outside the Alpine imprint and in the Valpelline Serie (Hunziker, 1974; Cosca et al., in prep.).

The previous summary of the available data on biotite ages in the Sesia zone shows a remarkably widespread distribution of ages. Several articles pointed out that metamorphic biotites are particularly

susceptible to the problems of excess Argon and Argon loss (Richards and Pidgeon, 1963; Pankhurst et al., 1973; Roddick et al., 1980; Dallmeyer and River, 1983; Foland, 1983). Hence, $^{40}\text{Ar}/^{39}\text{Ar}$ age spectra obtained from metamorphic biotites have to be cautiously interpreted.

Age determinations on the Na-rich amphiboles, as with biotite, are extremely difficult to interpret (Coleman and Lanphere, 1971; Suppe and Armstrong, 1972; Mc Dowell et al., 1984, Sisson and Onstott, 1986). Because of its crystallographic structure, glaucophane is particularly susceptible to the problems of excess Argon and Argon loss; in blueschist terrains, glaucophane generally yields ages younger than coexisting white micas (Mc Dougall and Harrison, 1988). In the Sesia zone, $^{40}\text{Ar}/^{39}\text{Ar}$ age determinations of glaucophane were completely lacking. Two K/Ar age determinations yielded 369 and 339 Ma (Hunziker, 1974). In the Pennine region, Alpine K/Ar ages on glaucophane have been reported (Hunziker, 1974)

5.4.2. Choice of Samples

Two biotites from perfectly preserved relics of pre-Alpine high grade amphibolites (mb1k/91 and 126/91) were collected in the internal unit of the polycyclic basement of the Sesia zone (Savenca valley, see Venturini et al., 1994a, Fig. 1b for the location of the outcrop). The biotites constitute the primary pre-Alpine assemblage together with plagioclase, sillimanite, pink garnet, ilmenite and quartz. Another sample containing biotite was collected by J.C. Hunziker in the metagranodiorite of the Monte Mucrone (polycyclic basement, internal unit). The sample containing glaucophane comes from the Dolca valley, close to the Insubric line (sv921d). This blue amphibole outlines a mylonitic foliation together with clinozoisite, rutile and garnet. This foliation is crosscut by a late paragenesis outlined by phengite which gives a reliable $^{40}\text{Ar}/^{39}\text{Ar}$ age of 78 Ma (§ 5.2.1).

5.4.3. Presentation of the results and discussion

Figure 5.13 reports $^{40}\text{Ar}/^{39}\text{Ar}$ age spectra and isochrons of the three biotites and of the analysed glaucophane. The two pre-Alpine biotites collected from the polycyclic basement of the internal zone are characterised by steplike spectra and ages of 160 Ma (126/91) and 202 Ma (mb1k/91). Their isochrons are meaningless because all points cluster near the abscissa. The biotites of sample KAW 988, a metamorphosed granodiorite of the Monte Mucrone stock, has a preferred age of 198 Ma, similar to that of sample mb1k/91. The isochron diagram is also uninformative.

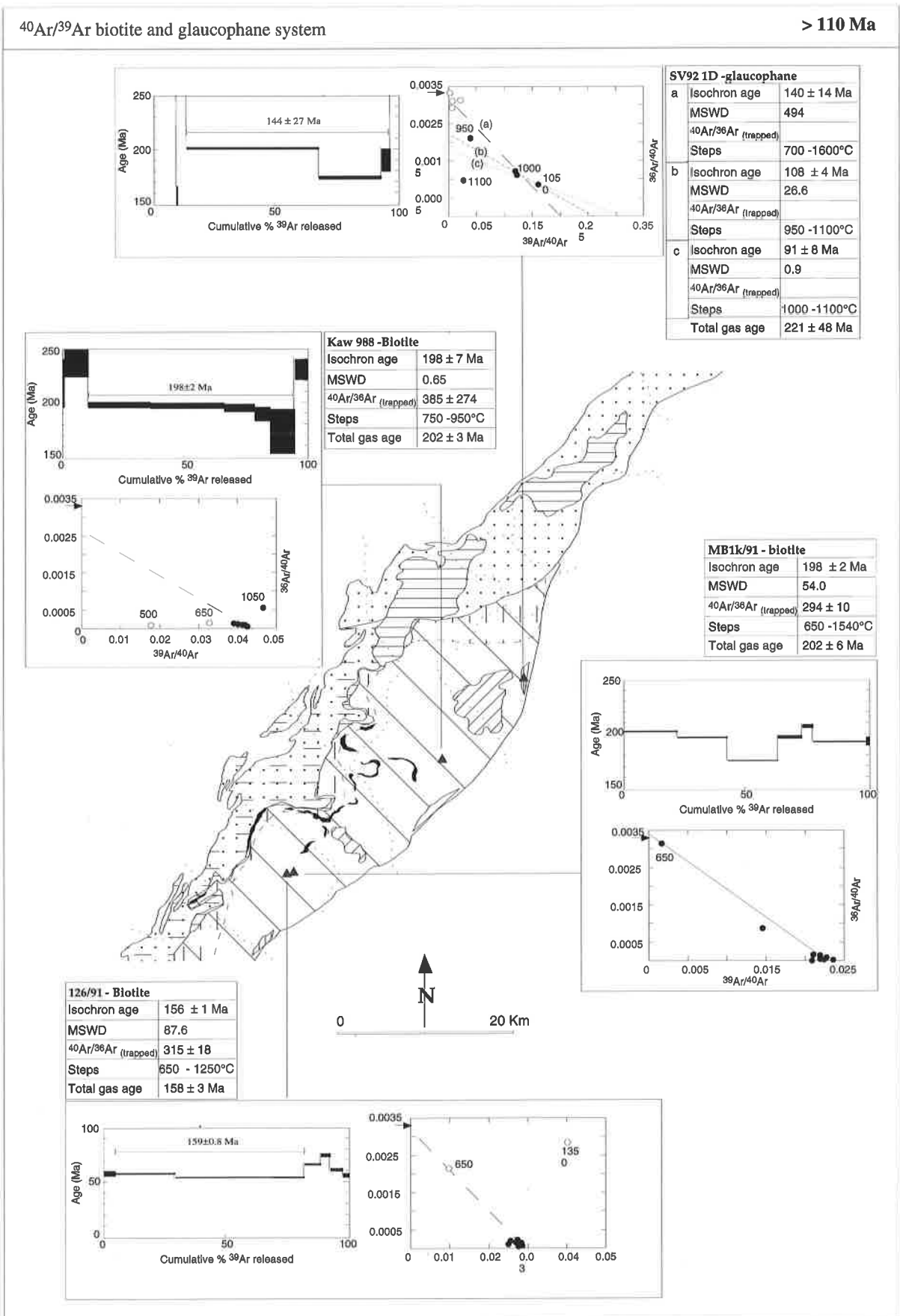


Fig. 5.9 - Ages older than 110 Ma for $^{40}\text{Ar}/^{39}\text{Ar}$ dating on biotite and glaucophane systems.

The glaucophane (sv921d) displays a strongly disturbed age spectrum, with most of the gas released during the two central heating steps. The preferred age, based on the steps between 950 and 1100 °C, is 144 Ma. This age is incongruous with other eo-Alpine metamorphic ages reported in the literature (Hunziker et al., 1992 and ref. therein). The isochron diagram of the glaucophane shows two distinct populations of points, the lowest and highest heating steps, characterised by a very low amount of radiogenic gas, plot close to the $^{36}\text{Ar}/^{40}\text{Ar}$ axis. An isochron constructed taking in account only the central steps (line b) has an age of 96 Ma. This age is consistent with those obtained with the $^{40}\text{Ar}/^{39}\text{Ar}$ method on the phengites of the same samples (78 Ma), although the $^{36}\text{Ar}/^{40}\text{Ar}$ intercept is anomalously low.

Any geological interpretation of the biotite ages of the polycyclic basement of the Sesia zone must take in account not only the analytical data presented in this work but also the available analogous values. Although there are no analytical reasons to eliminate some of the analysed biotite samples presented here,

we believe that ages near 200 Ma are the most geologically meaningful. These ages (samples KAW 988 and mb1k/91) are consistent with Hy (1984), Zingg et al. (1990), Hunziker (1974), and Cosca et al. (in prep.). The presence of ages at around 200 Ma, recorded by the K/Ar system of biotites, in both the parashists and the metagranodiorites intruded within them, suggests a complex cooling history. The granodioritic stock of the Monte Mucrone was intruded at relative shallow levels (Oberhänsli et al., 1985) during the lower Permian (Paquette et al., 1989; Bussy et al., in prep). This observation suggests that the country rocks reached the upper part of the continental crust, and, consequentially, the closure temperatures for the K/Ar system in biotites ($300\pm 50^\circ\text{C}$) between the lower Permian and the Triassic. At the same time, the biotites of the granodioritic intrusion certainly cooled below 300°C before 200 Ma. Thus, the age of 200 Ma could reflect a partial resetting of the Ar system in the biotite due to the uplifting of the mantle asthenosphere and to the consequential heating of the thinned continental crust.

- Chapter 6 -

Conclusions

In the previous chapters different constraints on the geological, geochemical, petrologic, and geochronological setting of the central Sesia zone have been presented.

In this chapter, the conclusions of each chapter will be discussed and incorporated into a geodynamic model for the Permo-Mesozoic evolution of this sector of the western Alps.

6.1 The Monometamorphic Cover Sequences

Monometamorphic cover sequences were recognised in the central sector of the Sesia zone. They are laterally continuous from the northern side of the Soana valley to the lower Gressoney valley. Reinterpretation of published data and maps, together with some field controls, permit us to postulate the presence of the monometamorphic cover sequences also in the southern sector of the Sesia zone (Chiaves, Malone valley, Vasario) as well as in the northern region (Carcoforo; Chabloz, 1990; Colle d'Egua; Simic, 1992).

6.1.1. The monometamorphic cover sequences

These sequences are interpreted as post-Variscan monometamorphic covers of the Sesia zone for the following reasons:

- 1) they do not contain trace of previous metamorphic cycles (especially in regard to the Paleozoic high grade metamorphic cycle);
- 2) they display clear and identifiable contacts with the polymetamorphic basement;
- 3) they are composed of lithologies characterised by textural and compositional features which permit them to be distinguished from the polycyclic basement rocks;
- 4) the cover-forming lithologies display sequential and coherent field relationships;
- 5) the cover lithologies are similar, and in some case identical, to other Mesozoic covers of the western Alps, which are indisputably recognised as monometamorphic sequences.

6.1.2. The provenience of the monometamorphic cover sequences

The monometamorphic sequences are the detached covers of the Sesia zone for the following reasons:

- 1) blocks of polycyclic basement are found within detritic calcschists, as well as in metaconglomeratic horizons of the Permo-Triassic volcanic sequence.
- 2) presumed stratigraphic contacts have been found between the polycyclic basement and the monometamorphic cover sequences at several localities (e.g. Alpe Dondogna, Col Fênêtre, Mombarone, Colle Valdobbia);
- 3) the monometamorphic cover sequences are laterally continuous throughout the central Sesia zone and, probably, also in its northern and southern portions;
- 4) the absence of serpentinites are consistent with a cover sequence having been deposited on a continental crust. The best candidate is the Sesia zone, not slice of another continental domain.

The arguments proposed above, although admittedly quite weak, are similar to those generally used for the other paleogeographic reconstructions in the highly deformed and metamorphosed units of the Alps.

6.1.3. The lithostratigraphic reconstruction of the cover sequences

The monometamorphic cover of the central Sesia zone is composed of a succession of rock-types of sedimentary and volcanic origin. Its stratigraphic age cannot be inferred from the classical paleontological methods, because of the widespread metamorphic recrystallization and structural reworking which during the Alpine subduction and unroofing. In spite of this, reasonable stratigraphic and age attributions can be tentatively suggested by using the «facies analogy method», and taking into account the limits provided by the available geochronological constraints.

On the basis of field and petrographic results, the most reliable *lithostratigraphic* sequence of the monometamorphic cover rocks in the central Sesia

zone is the following (going from older to younger lithologies) (Fig. 6.1).

1) Decimetric to metric alternance of mesocratic paragneisses, containing thin levels and/or boudins of basic lithologies (gneiss pipernoïdes). The mafic rocks display a tholeiitic composition and a WPB affinity. The paragneisses locally contain decimetric layers of dolomite-ankerite bearing marbles and decimetric blocks of leucocratic orthogneisses. The geochemical investigations on the gneiss pipernoïdes, previously discussed in § 3.5., do not provide additional constraints on the interpretation of this enigmatic sequence.

There are at least two possible origins of the gneiss pipernoïdes:

- a) they are the result of a strong and pervasive mylonitization of the polycyclic lithologies;
- b) they are a deformed volcano-sedimentary sequence of Permo-Triassic affinity.

In the first interpretation, the mesocratic paragneisses would be strongly transformed metakinzigites, while the basic and leucocratic inclusions would be interpreted as transformed pre-Alpine amphibolites boudins and relics of aplitic/pegmatitic dykes respectively. The carbonate horizons would be stretched pre-Alpine marbles.

Although the geochemical results are not incisive, the field observations are consistent with the second hypothesis. In fact, the lithological alternance of this basal sequence and its contacts with the surrounding rocks (marbles, quartzites, calcschists) show a geometry and a repetition which seem to agree better with a sedimentary context than a mylonitic horizon. In the upper Scalero valley, the gneiss pipernoïdes and the polycyclic basement are juxtaposed. Although both the gneiss pipernoïdes and the polycyclic basement are strongly reworked and deformed, a recognisable difference already exists between them, and this difference excludes the possibility that the former are the product of a strong mylonitization of the latter.

The Permo-Triassic age of this volcano-sedimentary sequence, or a shorter interval of this time span, can be tentatively inferred from the facies analogy with other similar detritic sequences described in the western and Southern Alps. The tholeiitic geochemical feature of the basaltic layer would be consistent with a thin continental crust and the existence of an upwelling asthenospheric source.

2) Decimetric to metric levels of pure and impure

quartzites, locally alternating with brown pelitic gneisses. They would represent the top of the Upper Permian-Lower Triassic volcano-detritic sequence. These lithologies were never observed within the polycyclic basement of the central Sesia zone and represent a key-level for the monometamorphic sequences.

3) Yellow dolomitic marbles, quartz-rich marbles, calcschists and detritic calcschists with centimetric to decametric blocks of dolomitic marbles, mafic rocks, quartzites and basement lithologies. The dolomitic marbles, presumably Middle to Upper Triassic from facies analogy, locally crop out as coherent extensions of original carbonate platforms and/or structural highs (Mombarone region). Metric levels of dolomitic marbles have also been observed as interbedding within metabasalts, or as centimetric to metric blocks within the calcschists. The quartz-rich marbles represent the gradual passage from the impure quartzites of the top of the Permo-Triassic sequence to the calcschists.

The calcschists are probably Upper Triassic or Early Jurassic in age for the following reasons:

- a) they contain breccia levels made of clasts of Triassic dolomitic marbles; locally they embody metric to decametric olistoliths of dolomitic marbles and metabasalts. This is consistent with basinal calcschists deposited near the carbonatic platforms and the basaltic extrusions, in deeper position;
 - b) calcschists commonly contain levels enriched in manganese, which denote the presence hydrothermal activity of oceanic origin at the same time of the deposition of the detritic carbonates. The Mn-rich fluids reasonably reached the detritic carbonates using fractures through the neo-formed oceanic crust. This entails that sedimentation of the detritic carbonates appended not far neither in space nor in time from the oceanic ridge.
- 4) The metabasalts and their related metasediments (quartz-rich levels, Al-rich horizons, pillow and/or pillow breccias) constitute metric to decametric massive layers, locally interbedded with the dolomitic marbles. The whole rock geochemistry indicates a MORB affinity for the tholeiitic effusive rocks.

The basaltic breccias associated with the basalt flows seem to display a spilitic affinity; however, this interpretation can not be definitively proved due

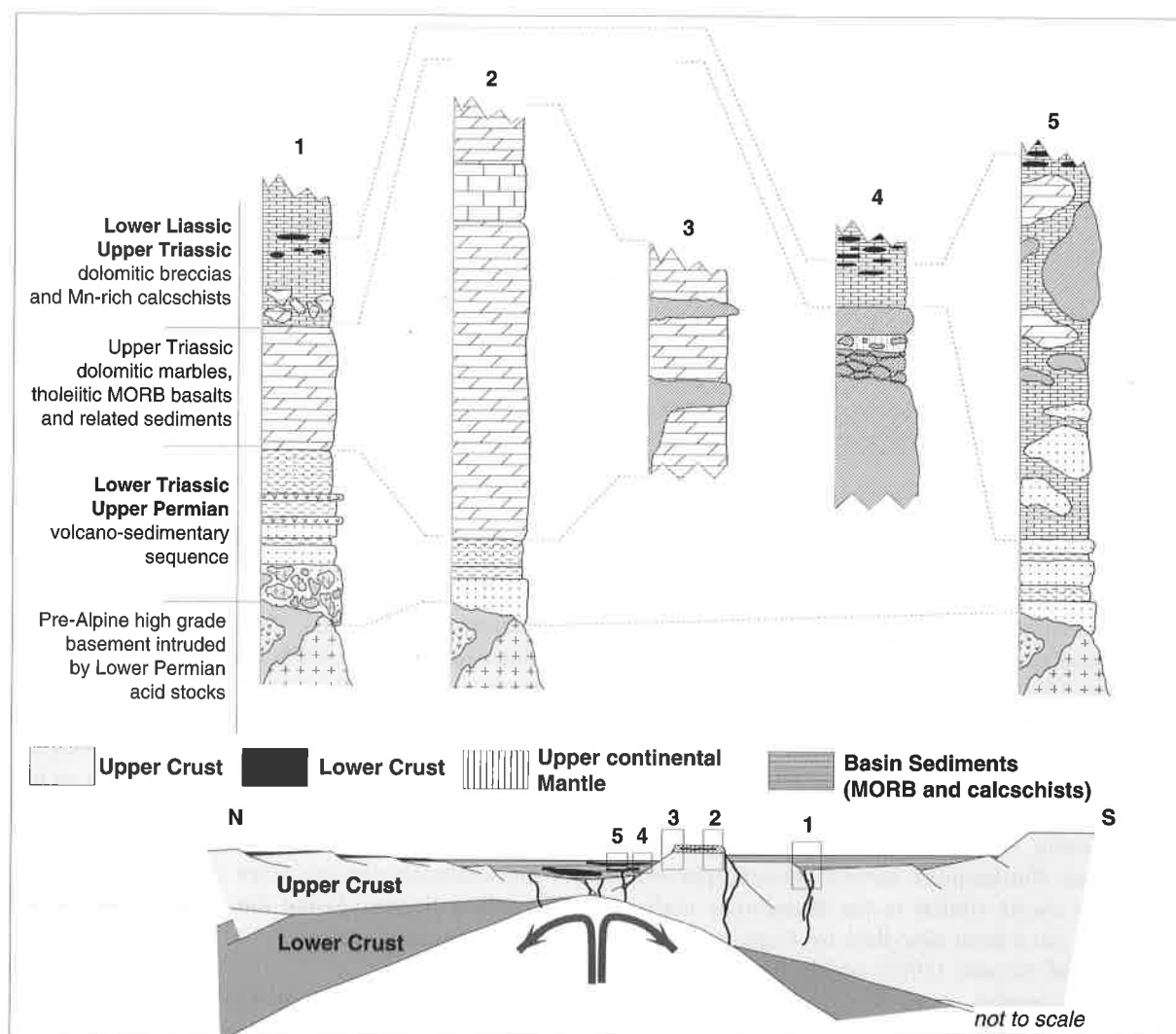


Fig. 6.1 - Lithostratigraphic reconstruction of the monometamorphic cover sequences of the Sesia zone.

to the low number of analysed samples and the especially pervasive mobility of the elements during the Alpine metamorphic cycle.

The supposed age of the metabasalts and related sediments has already been discussed. It is assumed that the extrusive mafic rocks are contemporary to the yellow dolomitic marbles (Upper Triassic-Early Lias). If this is true, the metabasalts of the monometamorphic cover sequences might represent the precursors of the ophiolitic sequences of the Zermatt-Saas-type zone, as well as the western equivalents or exotics of the mafic sequences of the Triassic Meliata-Vardar ocean (Stampfli and Marchant, in press).

Therefore, the monometamorphic volcano-detritic sequence cropping out in the central Sesia zone probably yield a Permo-Triassic age. It was originally composed of Permian pelitic arkoses and

greywakes, conglomerates with clasts of polycyclic basement, locally interbedded with Triassic Fe- and Mg-rich carbonate levels, and with mafic volcanic horizons. The tholeiitic affinity of the basic levels suggests that the continental crust, onto which the volcano-detritic sequence was deposited, was already thinned and the asthenosphere was partially uplifted.

During the Upper Triassic, the carbonate platforms and/or structural highs were not far from the crustal fractures, which permitted the emplacement of lava flows and dolerites of tholeiitic composition. The continental lithosphere was progressively thinned, as testified by the geotectonic signature of the MORB basalts, which do not seem to record crustal contamination.

At the same time or shortly later (Upper Triassic-Early Jurassic), deeper water detritic carbonates were

deposited. The mafic extrusive activity permitted a generalised circulation of Mn-rich fluids. No other sedimentary horizons have been found above the calcschists.

6.2. The mylonitic metagabbros

The mylonitic metagabbros, were initially assumed to be an ophiolitic-type sequence by Venturini et al. (1991). The can reinterpreted here as intrusive bodies with a distinct evolution respect to the monometamorphic covers before the eo-Alpine subduction. This distinction is supported by new field, geochemical and geochronological investigations.

- 1) The structural position of the mylonitic metagabbros relative to other lithologies varies along the monometamorphic cover complex. In the Bonze region, they are associated with metabasalts and related metasediments, while in other sectors they are in contact with calcschists and marbles (Alpe Pianezza, Bec Renon, Alpe Prà). In all localities, they show tectonic contacts with metabasalts, marbles and calcschists (Venturini et al., 1991, 1994). An hectometric outcrop of metagabbro, located above Ivery in the lower Aosta valley, is tectonically emplaced within the polycyclic basement. Furthermore several metamorphosed gabbroic stocks similar to the Bonze-type mafic intrusion have been described by Pognante et al. (1987) and Accotto (1992) within the polycyclic basement complex.
- 2) The geochemical analyses of the Bonze-type metagabbros have shown the similarities between these rocks and the under-plate cumulate Mg-gabbros bodies of the Sesia zone and the western Austroalpine system, especially in regard to the Matterhorn-Collon gabbros (Dal Piaz et al., 1977), the M. Nery gabbro (Stünitz, 1989), and the Anzasca valley differentiate stock (this work). The chemical similarities of the Bonze gabbro with the other mafic intrusions suggest a strong similarity in the evolutionary history of these gabbros.
- 3) The original hypothesis of the mylonitic metagabbros as part of an ophiolitic-type sequences has been re-interpreted due to the absence of a true oceanic crust within the monometamorphic cover sequences in the central Sesia zone. The few outcrops of ultramafic rocks known in the Sesia zone in the Ivozio region, (Compagnoni et al. (1977a), Pognante et al. (1980)), in the internal edge of the Sesia zone (Pognante, 1989) and in the Vogna valley (Artini and Melzi, 1900) do not seem to be related to the monometamorphic cover sequences described in this thesis.
- 4) The monometamorphic cover calcschists contain blocks of all the other cover-forming lithologies, except the Mg-gabbros. Although it is not necessary to exclude a partial reworking of the Mg-gabbros during the deposition of the detritic carbonates, this would be expected if the gabbros should be exposed at the surface together with the tholeiitic basalts.
- 5) New U/Pb age determinations on four fraction of zircons of Anzasca valley gabbroic stock yield an age at around 295 Ma (sv913az) (F. Bussy et al., in prep.), consistent with the Lower Permian age of the gabbro intrusion of the Matterhorn (Dal Piaz et al., 1977) as well as the granitic body of Monte Mucrone (Paquette et al., 1989; Bussy et al., in prep.). A sample of mylonitic metagabbro, collected in the Chiusella valley and in tectonic contact with the calcschists of the monometamorphic covers, yields an older age of 360 Ma (sv9215vc) (Bussy and Venturini, in progress). This preliminary age data, obtained using the U/Pb method on two poorly-preserved zircon fractions, can be interpreted in different ways: a) it represents the age of an Early Carboniferous basic intrusion within the pre-Alpine lower crust; this gabbro would later escape an high grade re-equilibration, as testified by the lack of both high grade textures and mineralogical relic; b) the analysed zircons were inherited from the continental crust during the emplacement of the mafic magma.

On the basis of these preliminary U/Pb data, the Anzasca Mg-gabbro that in this study has been related to the mylonitic metagabbros intimately associated to the monometamorphic cover sequences, can reliably be related to the Permian magmatic underplating envisaged for the Austroalpine and South-Alpine gabbros (Dal Piaz et al., 1977, Dal Piaz, 1992b, 1993). On the other hand, the mylonitic metagabbros cropping out in the lower Aosta valley and in the Chiusella Valley should be older (Early Carboniferous) or younger in age. Although we have no reasons to exclude the Mesozoic age of these gabbros, we prefer to relate them to the other mafic cumulate intrusions on the basis of the considerations listed above.

6.3. Geochronological considerations derived from radiometric data.

Petrographic, petrologic, and stable isotope investigations carried out in this study show that the monometamorphic cover sequences experienced the same pressure-temperature-time trajectories of the polycyclic basement of the central Sesia zone during the Alpine orogeny. The geochronological data

available for the internal and the intermediate units of the polycyclic basement provide temporal constraints on the depositional age of the monometamorphic covers. The upper limit is the end of the Paleozoic orogenic cycle, while the lower limit is the beginning of the Alpine orogenic cycle.

The upper limits of the age of the monometamorphic cover sequences is furnished by the late Paleozoic intrusions of the Monte Mucrone (Paquette et al., 1989; Bussy et al., in prep.) and by the age of the basic intrusions of the Anzasca valley (this work, Bussy et al., in prep.). The Monte Mucrone granitic stocks was interpreted by Oberhänsli et al. (1985) as a type I shallow intrusion. This interpretation is consistent with the field observation of the Anzasca valley basic intrusion, which seem to constitute part of a differentiated calc-alkaline pluton intruded in a low-grade metamorphic sequence (Martinotti, pers. comm; Bussy et al., in prep.). This magmatic activity has been recently interpreted by Dal Piaz (1993) as the result of the late Paleozoic migmatization and partial fusion of the lower crust., probably due to the beginning of the Alpine thinning and distension. If we accept that the monometamorphic cover sequences represent the detached covers of this continental crust (e.g. Sesia zone pre-Alpine basement), sedimentation began after the Lower Permian.

The lower limit is determined by the beginning of the Alpine orogenic cycle. The geochronological investigations of this the study confirm the results of Hunziker (1974) Oberhänsli et al. (1985) and Stöckhert et al. (1986). The $^{40}\text{Ar}/^{39}\text{Ar}$ method constrains a reasonable cooling age between 71 and 78 Ma for the K/Ar system of phengites from the internal Sesia zone. This requires that the high pressure metamorphic belt cooled below 350°C in the upper Cretaceous. The evaluated pressure conditions for the closure temperatures of 350 ± 50 °C are of 2-5 Kbars (§5.3.3) - (Fig. 5.11). These relatively low pressure conditions indicate that the Sesia zone reached shallower crustal levels in the Upper Cretaceous (Hunziker, 1974; Hurford et al., 1991; Hunziker et al., 1992, and ref. therein). Glaucofane-bearing clasts, present in the Upper Cretaceous flysch of the southern Alps could support this interpretation although no proves exist to demonstrate that the blueschist clast are originated from the erosion of the Sesia zone.

The application of two different geochronological method on the same mineral allows us to not only confirm the reliability of the age determinations, but also to deduce the unroofing rate of approximately 2.8 Km/Ma affecting the lithologies of the Sesia zone

between the Middle and the Upper Cretaceous. This uplift rate, calculated for a range in pressure of 11 and 4 Kbars, and temperature between 500 and 350 °C, could be extrapolated to the initial part of the retrograde trajectory, starting from 550 ± 50 °C and 16 Kbars. Based on this rate determination, we suggest that the age of high pressure metamorphism is the upper limit of the Lower Cretaceous. This range in ages is consisting with, although slightly younger than, the Rb/Sr age of 114 ± 1 determined by Oberhänsli et al. (1985) for the Monte Mucrone (obtained with a garnet-omphacite-albite-phengite mineral isochron). No geochronological determinations are available for the reconstruction of the prograde subduction path followed by the Sesia zone. In spite of this, it is our opinion that a reasonable range of time, permitting the subduction of the continental basement and its covers to the deeper crustal levels (~50 km) and the beginning of the unroofing path, would have been on the order of 10 to 15 Ma. This requires that the beginning of the subduction of the central Sesia zone was during the Upper Jurassic. The lower age limit of the monometamorphic cover sequences has to be the Upper Jurassic. These limit determinations, are consistent with the ages which have been given to the monometamorphic cover sequences using the facies analogy method.

6.4. Paleogeographic evolution of the central Sesia zone

The Sesia zone has always played an important role in all the paleogeographic reconstruction of the western Alps. Dal Piaz et al. (1972) proposed the first modern geodynamic model for the Sesia zone. They suggested the existence of an Early Cretaceous southeast-plunging subduction sheet, which resulted in the eclogite and/or greenschist facies metamorphism of the Austroalpine polymetamorphic belt and of all the other western Alpine domains. Subsequently, several other models have been proposed to explain the paleogeographic and metamorphic conditions of the Sesia zone and the western Alpine chain. In most models, the Sesia zone was located in the southern margin of the Alpine tethys, with the exception of the model by Auboin et al. (1976) considering the Sesia zone to be located along the European passive margin of the Alpine tethys.

Clear and helpful reviews of the different paleogeographic and metamorphic interpretations of the Sesia zone can be found in Dal Piaz et al. (1972), Compagnoni et al. (1977a), Martinotti and Hunziker (1984), Hunziker and Martinotti (1984), Oberhänsli et

al. (1985), Dal Piaz and Gosso (1985), Desmons et al. (1989) Mattauer et al. (1987), Polino et al. (1990), Avigar et al. (1993) and Dal Piaz, (1993, 1994). We will briefly try to analyse which models are most consistent with the present knowledge of the polycyclic basement of the Sesia zone and of its monometamorphic cover sequences.

The first approach in the analysis of the different paleogeographic and evolutionary sketches, is to start from actual models. If we accept the reliability of the lithostratigraphic reconstruction of the monometamorphic covers proposed in the previous paragraphs, a geotectonic model must be able to explain the presence of MORB tholeiitic basalts during the upper Triassic. Thus some of the geodynamic models have assumed an early rifting phase (Voggenreiter et al., 1988; Stampfli et al., 1991; Stampfli and Marchant, in press). Following Stampfli and Marchant, (in press), six different stages in the evolution of a rift have been proposed, starting from the moment t_0 (beginning of the simple shear distension) to t_{0+40} Ma (formation of oceanic floor). If we apply this model to the palaeographic setting of the western Alps, the stage t_{0+40} Ma can be tentatively located in the Upper Jurassic (Stampfli et al., 1991 and ref. therein). This mean that the initial stage t_{0+10} Ma (single shear stage), corresponding to the initial formation of the upper and lower plates would be situated at least in the Early Jurassic. This reconstruction does not agree with the recent models proposed by Lardeaux and Spalla (1991) and by Dal Piaz (1992a), in which a initial expansive phase in the lower Permian is proposed.

The rift model of Stampfli and Marchant (in press.) do not agree also with the lithostratigraphic reconstruction proposed for the monometamorphic covers of the Sesia zone, because it cannot explain the presence of MORB tholeiitic basalts before the Early Jurassic. This entails three possible explanations:

- a) the lithostratigraphic reconstruction of the monometamorphic covers of the Sesia zone is wrong and the dolomitic marbles have to be considered younger than the expected age as well as the related metabasalts;
- b) the proposed model cannot be applied to the paleogeographic reconstruction of the Alpine tethys;
- c) either the first thinning precursors pointed out by Lardeaux and Spalla (1991) and Dal Piaz (1992a) (*i.e.* retrograde path from granulite to amphibolite facies of the pre-Alpine paraschists of the Sesia

zone; emplacement of under plating gabbroic stocks in the Ivrea, Sesia and Dent Blanche nappe) or the deposition of monometamorphic cover sequences described in this study cannot be related to the same rifting episode which formed the Alpine tethys. In this case they would represent a witness of an early rifting phase comprised between the Permo-Triassic and Upper Jurassic.

Point a), whereas founded on not indubitable arguments, is the result of several detailed field and laboratory investigations, which support the adopted conclusions. The discussion of point b) requires a larger and more detailed discussion than is contained in this thesis. The third hypothesis c) could be supported by observations on the physical properties of the lithosphere (e.g. Cloetingh and Banda, 1992), which indicate that aborted rifting zones should be extremely rigid and reactivate only with great difficulty. This hypothesis would permit us to postulate the presence of a first rifting zone active from the Middle Permian to the Upper Triassic within the Austroalpine continental crust. This rifting sector became inactive in the Upper Triassic-Early Jurassic. The mantle asthenosphere present under the Austroalpine domain became too rigid to be newly crashed by the middle Jurassic rifting related to the opening of the Alpine tethys, which developed probably hundreds of kilometers the side.

Another possibility, postulated by Stampfli and Marchant (in press) is that the monometamorphic covers of the Sesia zone are an «exotic terrain» that was misfit from its original paleogeographic position (the Meliata ocean) and juxtaposed into its actual position by Early Cretaceous transpressive movements. Although this sketch cannot be excluded «a priori», we think that it is too complicated and does not take in account the relationships and the correspondence of the Sesia zone with other units. In addition, the Upper Triassic mafic vulcanism is present not only in the Sesia zone, but also in the Pelvoux massif (Aumaître and Buffet, 1973), in the Helvetic domain (Mamin, 1992), in the Furgg zone (Jaboyedoff, 1986). This wide diffusion of Upper Triassic extrusive mafic rocks suggests the presence of a unique geodynamic phenomenon intersecting different paleogeographic domains, and not only in the Austroalpine system.

Conversely, the Upper Triassic and Early Jurassic intervals of the monometamorphic cover sequences of the Sesia zone may have been deposited at the foot of the margin of the Alpine Tethys. In this model, neither the under-plate gabbros of the Austroalpine domain nor the Permo-Triassic volcano-sedimentary

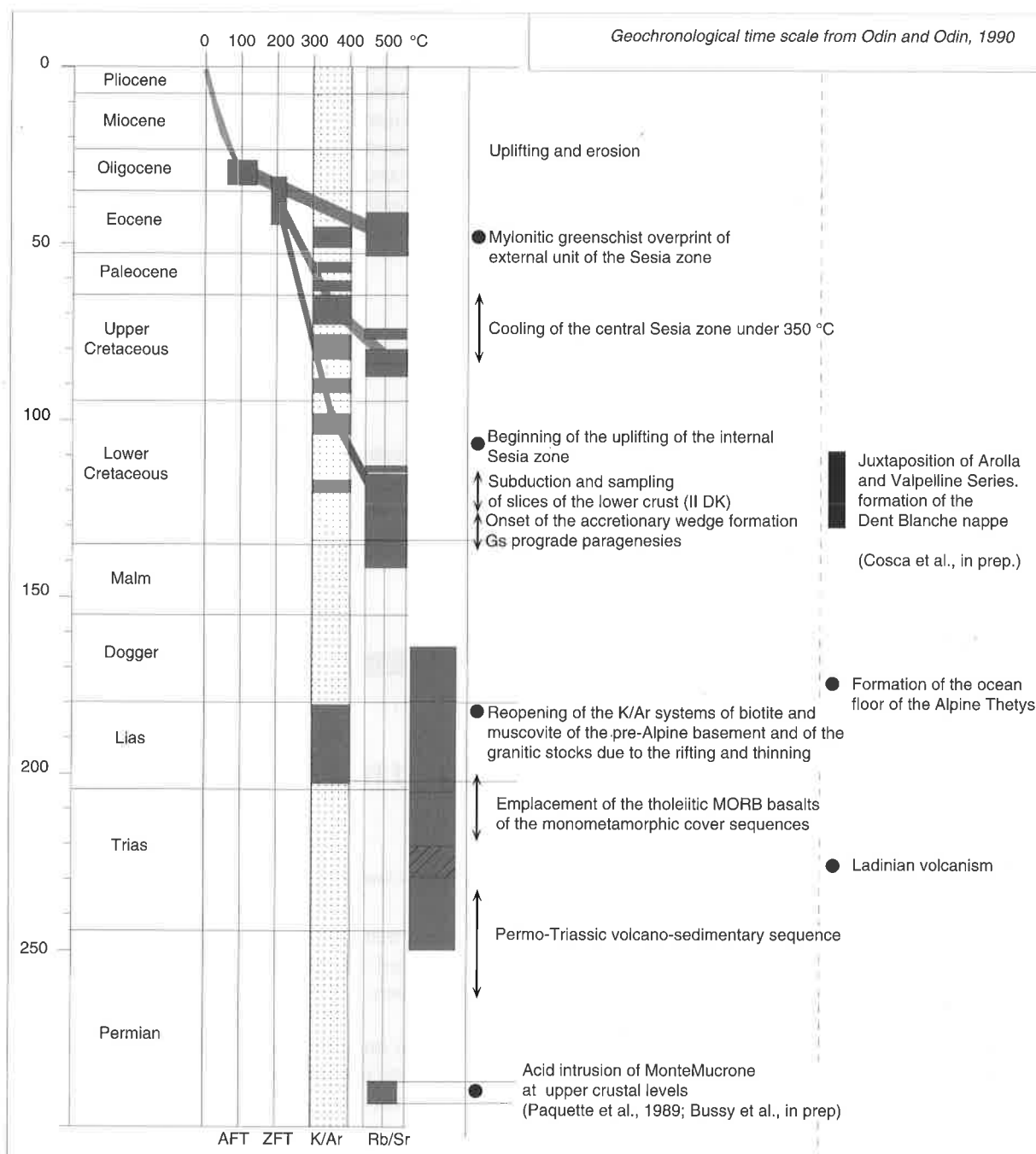


Fig 6.2- Chronology of the evolution of the Sesia zone from the Lower Permian to the present

sequences of tholeiitic affinity are related to this rifting stage. This model also requires the presence, during this time, of a thinned continental crust or a crust defined by faulted and detached blocks of basement. As geodynamic conditions changed, this part of the margin, composed of relatively thin blocks of basement and interposed Mesozoic covers, was firstly accreted and successively subducted.

Figure 6.2 summarises the evolution of the Sesia zone and the western Austroalpine system from the

lower Permian to the present according to the model presented above.

1) In the lower Permian, the Austroalpine basement was intruded by calco-alkaline granitoid bodies (Paquette et al., 1989; Bussy et al., in prep, this work) and by mafic stocks of mantle origin (Dal Piaz et al., 1977; Dal Piaz and Ernst, 1978; Dal Piaz, 1992a). There are two explanations for this bimodal magmatism. Dal Piaz (1992a) suggests that the lower portion of the continental crust melted and

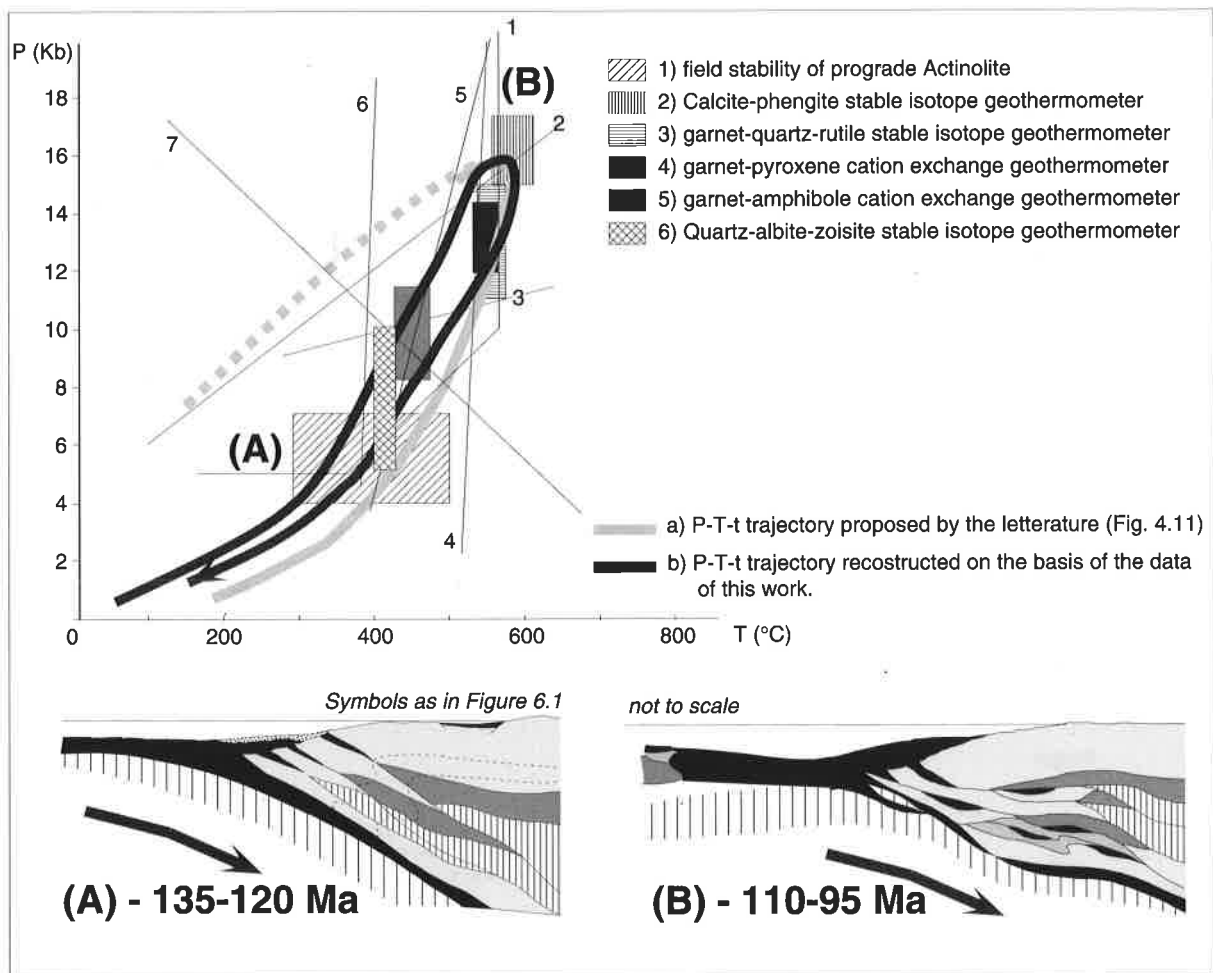


Fig. 6.3 - P-T-t trajectory of the Central Sesia zone.

rose due to underplating hot gabbroic intrusions. Stampfli and Marchant (in press) interpret the calc-alkaline magmatism as proof of a magmatic arc.

- 2) In the Middle Permian, the continental crust intruded by the intermediate to acid bodies reached the surface. Deposition of a volcano-detritic sequence began.
- 3) During the Permo-Triassic, the progressive thinning of the continental crust permitted the emplacement of mafic sills and extrusions of tholeiitic affinity into detritic sediments composed of basement components (gneiss piperoides).
- 4) During the Upper Triassic, the paleomorphology of the Austroalpine basement was constituted of detached and tilted blocks of basement on the top of which carbonatic platforms and/or structural highs were forming. The continental crust was further thinned and crosscut by fractures, permitting the emplacement of MORB tholeiitic metabasalts.
- 5) At the same time or a bit later, calcschists were deposited in the deeper portions of the basin, not far from the neo-formed ridge. These detritic carbonatic sequences received material from both the Mesozoic covers and the basement crust. During their deposition the ridge was already active, as testified by high-manganese contents.
- 6) In the Upper Liassic, the Austroalpine basement was affected by a partial and static heating at around 300-350°C due to rising asthenospheric bodies.
- 7) During the Middle Jurassic, sedimentation was less important than before, although other sectors of the Austroalpine system were continued to receive clastic material supply (dolomitic and polygenic breccias of Mont Dolin and Roisan zone; Dal Piaz, 1976; Ayrton et al., 1982).

These metabasalts were either extruded over or emplaced as doleritic sills within the carbonatic sequences.

- 8) During the Upper Jurassic, the detached blocks of the Austroalpine basements and their sedimentary covers were embricated and involved in the formation of a first accretionary prism. The juxtaposition of upper continental crust slices (i.e. Arolla Serie) with lower crust slice (Valpelline Serie), which seems to be Upper Jurassic-Lower Cretaceous in age (Cosca et al., in prep.), could reflect this first compressive phase. The prograde foliation recorded by the monometamorphic cover sequences of the Sesia zone (Par. 4.7.4) may also be related to this first phase. Actinolites formed during the prograde metamorphism record pressures and temperatures of 4 and 7 Kbars and 300 and 500°C. Such metamorphic conditions could have been reached by superposition of different slices of continental crust and Mesozoic covers in the accretionary wedge.
- 9) The monometamorphic cover sequences and the polycyclic basement complex underwent high pressure metamorphism during the Early Cretaceous and part of the Upper Cretaceous. The eclogitic climax was reached during the upper part of the Lower Cretaceous (Hunziker et al., 1992 and ref. therein). The subducted slices of continental crust and monometamorphic covers were rapidly unroofed from the Albian onward. According to Dal Piaz et al. (1972), Compagnoni et al. (1977a), Rubie (1984) Oberhänsli et al., (1985), they were rapidly decompressed. Garnet-clinopyroxene and garnet-amphibole geothermometers and isotopic fractionation geothermometers indicate the decompression from 16 to 8 Kbars was associated with a weak cooling, which began more accentuate from 7 Kbars to 3 Kbars, both the polycyclic basement and the monometamorphic covers underwent the same cooling path (Fig. 6.1c).
- 10) The basement crust and the Mesozoic covers were subducted together with a slab of oceanic crust, which played an important role as source of fluids during the entire Alpine metamorphic cycle. These fluids were probably the result of the dehydration of oceanic serpentinites.
- 11) The different units of the inner Central Sesia zone reached temperatures of approximately 350°C during the middle part of the Upper Cretaceous. Based on all the available data and according to Stöckhert et al. (1986), we suggest a composite uplifting of the inner Sesia zone. The portion of the belt close to the Canavese line, reached temperatures below 350°C at around 80 Ma, while the other sectors of the inner Sesia zone were cooled below 350°C between 80 and 65 Ma. This partitioning in cooling ages reflects the structural features of the examined lithologies. Rocks with cooling ages around 80 Ma are weakly affected by the F3 fold phase, which developed in association with partial retrogression to the greenschist facies. On the other hand, the lithologies with ages of 65 Ma (intermediate zone) show a pervasive axial plane foliation related to the F3 fold. No Cretaceous ages are found in the external unit, although we cannot exclude that this part of the Sesia zone experienced the same pressure-temperature-time history of the inner sector (Spalla et al., 1991). The external unit records a strong Early Eocene greenschist reequilibration, which is probably due to the beginning of the continental collision. From the middle Eocene, the entire Sesia zone followed a common unroofing trajectory, as testified by the fission track data of Hurford et al. (1991). A rapid uplifting caused the exposure at the surface of the central Sesia zone in the Early Oligocene, as testified by the autochthonous covers cropping out in the innermost Sesia zone.

Acknowledgements

This work is dedicated to the memory of Ugo Pognante

The Swiss National Science Foundation provided support for this work.

I am deeply obliged to Johannes Hunziker, without whom this work would not have been possible. He familiarised me with geochronology and has guided me through my research over the past three years. His kindness and generosity in the office and at the dinner table are particularly appreciated. This work involved a collaboration between l'Université de Lausanne, the University of Torino and the Department of Earth Sciences of Cerati (Cn). I would like to thank Giorgio Martinotti for sharing with me both geology and life. Mike Cosca patiently taught me the ins and outs of lab work. I would like to thank Giorgio Vittorio Dal Piaz for his detailed and careful review of the manuscript. Jean Hernandez had the patience to listen to me during my crises. François Bussy assisted me day and night with my microprobe analyses. Henri Masson taught me how to understand and discuss sedimentary rocks and spent valuable and illuminating time in the field with me. I am obliged to Hans Rudi Pfeiffer for his incisive observations. I would also like to thank David Kirschner for seeing his way to the end of the trial of this thesis and for his instructive comments on my work. Zachary Sharp quickly and dynamically taught me stable isotopes and made helpful comments on my work. Albrecht Steck accompanied me in the field and provided useful suggestions on my research. I would also like to thank Gérard Stampfli for teaching me to interpret geodynamics, geopoetry, and poetry. I appreciate Robin Marchant for having taught me what his advisor had not already taught me. Jim O'Neil and Giorgio Vittorio Dal Piaz shared their wealths of scientific knowledge with me. Jean Claude Lavanchy assisted me with many time-consuming analyses. Anne Marie Magnenat and Michele Brousse helped me survive day and night in the geology department.

Without Paola, I would not have arrived at the end of this path in one piece. Giovanni, Mizzi, Michelle, Andrea, Annachiara, Filomena, Elena, Antonio, and Francesca followed me in my Swiss adventure and formed a warm and entertaining community here in Lausanne. Mizzi and Giovanni assisted me in the field, as did Roberto Danieli. Without Annachiara and Filomena, the cuisine would certainly have been less appetising. Andrea is particularly thanked for giving me the energy to continue in these last few months. Alain, Pascale, Benoit, Romano, Lucas, Popoff, Jean Luc, Spela, Luis, Alice, Glynn, Yvan, Gianni, Jean Claude, Laurent, the two Phillippes, John, Bubker, Halter, Darko, François, Markus, Lucia, Raffaella, Paola, Miriam, Dan, Hugo, and Vincent helped make the past three years particularly agreeable. Lillian, Raymond, and Laurent helped me do the actual work involved in this research and provided me with beautiful thin sections. Adriana and Antonella are particularly thanked for their willingness to help. My friends at Quincinetto and Traversella housed me and made me appreciate my sojourns in the field.

My thoughts have been with the one who could not be with me during these past years. Last and not least I would like to thank all my family for all kind of supports.

The author is indebted to the following Foundations, which provided financial support for this publication: Faculté de Sciences de l'Université de Lausanne, Société Académique Vaudoise, Fondation De Giacomi of the Société Helvétique de Sciences Naturelles and Institut de Géologie et Paléontologie of Lausanne University.

References

- Accotto, A. (1992) Studio geologico petrografico dell'alta e media Valle di Champorcher (Settore Orientale). University of Torino, Unpublished diploma Thesis.
- Amstutz, A. (1962). Notice pour une carte géologique de la vallée de Cogne et de quelques autres espaces au sud d'Aoste. Arch. Sci. (Genève), 15, 1-114.
- Andreoli, M., Compagnoni, R. & Lombardo, B. (1976). Jadeite megablasts from Valchiusella (Sesia-Lanzo Zone, Western Alps). Rend. Soc. Geol. It., 32, 681-698.
- Argand, E. (1908). Carte géologique du Massif de la Dent Blanche (moitié septentrionale), 1:50.000. Mat. Carte géol. Suisse N.S., 23, carte spéciale n°32.
- Argand, E. (1911). Les nappes de recouvrement des Alpes Pennines et leurs prolongements structuraux. Mat. Carte géol. Suisse N.S., 31, 26.
- Argand, E. (1934). La zone Pennique. Guide Géologique Suisse, 3, (s), 149-189.
- Armando, G. (1992) Studio geologico dell'alta valle dell'Elvo (Zona Sesia Lanzo, Alpi Occidentali). University of Torino, unpublished diploma Thesis.
- Artini, E. & Melzi, G. (1900). Ricerche geologiche e petrografiche sulla Valsesia. Mem. R. Ist. Lomb. Sci. Lett. Art., 48, (1), 113-122.
- Auboin, J., Blanchet, R., Labesse, B. & Wozniak, J. (1977). Alpes occidentales et Alpes orientales: la zone du Canavese existe-t-elle? C.R. somm. Soc. géol. Fr., 3, 155-158.
- Aumaître, R. & Buffet, G. (1973) Minéralogie, Pétrographie et Géochimie des laves spilitiques et des filons basiques associés du massif des Ecrain-Pelvoux. University of Grenoble, Ph.D Thesis.
- Avigar, D., Chopin, C., Goffé, B. & Michard, A. (1993). Tectonic model for the evolution of the Western Alps. Geology, 21, 659-662.
- Bates, R.L. and Jackson J.A., Eds. (1987). Glossary of Geology. American Geological Institut, Alexandria (Virginia), 1-788, Third Edition.
- Ballèvre, M., Kienast, J.-R. & Vuichard, J.-P. (1986). La «nappe de la Dent-Blanche» (Alpes occidentales): deux unités austroalpines indépendantes. Eclogae geol. Helv., 79 (1), 57-74.
- Banno, S., Chihiro, S. & Higashino, T. (1986). Pressure-temperature trajectory of the Sanbagawa metamorphism deduced from garnet zoning. Lithos, 19, 51-63.
- Barbero, M. (1992) Geologia dell'alto vallone del Savenca (Zona Sesia Lanzo, Alpi Occidentali). University of Torino, unpublished diploma Thesis.
- Battiston, P., Benciolini, L., Dal Piaz, G.V., De Vecchi, G., Marchi, G., Martin, S., Polino, R. & Tartarotti, P. (1987). Geologia della traversa dal Gran Paradiso alla Zona sesia lanzo in alta Val Soana, Piemonte. Mem. Soc. Geol. It., 29, 209-232.
- Beareth, P., Dal Piaz, G.V., Elter, G., Gosso, G., Martinotti, G. & Nervo, R. (1980). Il Lembo di ricoprimento del Monte Emilius, Dent Blanche s.l. Osservazioni Preliminari. Atti della Acc. Sci. di Torino, 144, 227-241.
- Beccaluva, L., Macciotta, G., Piccardo, G.B. & Zeda, O. (1984). Petrology of lherzolitic rocks from the Northern Apennine ophiolites. Lithos, 17, 299-316.
- Benciolini, L. (1989) Evoluzione tettonico metamorfica del corpo ultrabassico di Arpisson. University of Padova, Ph.D Thesis.
- Bianchi, A. & Dal Piaz, G.B. (1963). Gli inclusi di «Micascisti eglogitici» della zona Sesia nella formazione porfiriteica permiana della zona del Canavese fra Biella e Oropa. Giornale di Geologia, 31, (2), 39-76.
- Bianchi, A., Dal Piaz, G.B. & Viterbo, C. (1964). Le masse di anfiboliti gabbriche a gastaldite di Corio e Monastero e di altre località della zona Sesia-Lanzo. Mem Acc. Sci. Torino, Cl. Sci. M.F.N., (Sez. 4), 1-37.
- Biino, G. & Compagnoni, R. (1988). La scaglia di grun in Val d'Aosta: un lembo austroalpino composito, incluso nelle meta-ofioliti della zona piemontese. Boll. Soc. Geol. It., 107, 101-107.
- Blattner, P. & Bird, G.W. (1974). Oxygen isotope fractionation between quartz and K-feldspar at 600°C. Earth Plan. Sci. Letters, 23, (1), 21-27.
- Bottinga, Y. & Javoy, M. (1973). Comments on oxygen isotope geothermometry. Earth Plan. Sci. Letters, 20, 250-265.
- Bottinga, Y. & Javoy, M. (1975). Oxygen isotope partitioning among the minerals in igneous and metamorphic rocks. Reviews of Geophysics and Space Physics, 13, 401-418.

- Brown, E.H. (1977). The crossite content of Ca-amphibole as a guide to pressure of metamorphism. *J. Petrol.*, 18, 53-72.
- Bussy, F., Venturini, G., Hunziker, J.C. & Martinotti, G. (in prep). High resolution U/Pb age determinations of the magmatism in the Western Austroalpine system.
- Callegari, E. & Viterbo, C. (1966). I granati delle eglogiti comprese nella «formazione dei Micascisti Eglogitici» della zona Sesia-Lanzo. *Rend. Soc. It. Mineral. Petrogr.*, 1-25.
- Callegari, E., Compagnoni, R., Dal Piaz, G.V., Frisatto, W., Gosso, G. & Lombardo, B. (1976). Nuovi affioramenti di Metagranitoidi nella Zona Sesia-Lanzo (Alpi Occidentali). *Rend. Soc. It. Mineral. Petrogr.*, 32, 97-111.
- Canepa, M., Castelletto, M., Cesare, B., Martin, S. & Zaggia, L. (1990). The Austroalpine Mont Mary nappe (Italian Western Alps). *Mem. Sci. Geol.*, 42, 1-17.
- Carlswell, D.A. & Harley, S.L. (1990). Mineral barometry and thermometry. In «Eclogite facies rocks». Blackie (London) pp. 396.
- Carraro, F., Dal Piaz, G.V. & Sacchi, R. (1970). Serie di Valpelline e II Zona diorito-kinzigitica sono i relitti di un ricoprimento proveniente dalla zona Ivrea-Verbanò. *Mem. Soc. Geol. It.*, 9, 197-224.
- Carraro, F. & Charrier, G. (1972). Paleontological evidence for the late-carboniferous age of the volcano-detrital cover of the «Micascisti Eglogitici» (Sesia Lanzo Zone, Western Alps). *Boll. Soc. Geol. It.*, 91, 185-194.
- Castellarin, A., Lucchini, F., Rossi, P.L., Simboli, G., Bosellini, A. & Sommariva, E. (1980). Middle Triassic magmatism in southern Alps II: a geodynamic model. *Riv. It. Paleont.*, 85, (3-4), 1111-1124.
- Castellarin, A., Lucchini, F., Rossi, P.L., Selli, L. & Bosellini, A. (1988). The Middle Triassic magmatic-tectonic development in the southern Alps. *Riv. It. Paleont.*, 146, 79-89.
- Castelli, D. (1991). "Eclogitic metamorphism in carbonate rocks: the example of impure marbles from the Sesia-Lanzo Zone, Italian Western Alps." *J. Metamorphic Geol.*, 9,
- Cesare, B., Martin, S. & Zaggia, L. (1989). Mantle Peridotites from Austroalpine Mt. Mary nappe (Western Alps). *Schweiz. Mineral. Petrogr. Mitt.*, 69, 91-97.
- Chaboz, O. (1990) Etude géologique et pétrographique de la région de Carcoforo, haute Val Sesia, Italie du nord. Lausanne, Diplôme inédit.
- Clayton, R.N. & Mayeda, T.K. (1963). The use of bromine pentafluoride in the extraction of oxygen from oxides and silicates for isotopic analysis. *Geoch. and Cosmoch. Acta*, 27, 43-52.
- Clayton, R.N., Goldsmith, J.R., Karel, K.J. & Mayeda, T.K. (1975). Limits of the effect of pressure on isotopic fractionation. *Geoch. and Cosmoch. Acta*, 39, 1197-1201.
- Cloetingh, S. & Banda, E. (1992). Europe's lithosphere - mechanical structure. In: «A continent revealed - the European Geotraverse». University Press, Cambridge, p. 80-90.
- Coleman, R.G., Lee, D.E., Beatty, L.B. & Brannock, W.W. (1965). Eclogites and eclogites: their differences and similarities. *Geol. Soc. Am. Bull.*, 76, 483-508.
- Coleman, R.G. & Lanphere, M.A. (1971). Distribution and age of high grade blueschist, associated eclogites, and amphibolites from Oregon and California. *Geol. Soc. Am. Bull.*, 82, 2397-2412.
- Colombi, A. (1989). Métamorphisme et Géochimie des roches mafiques des Alpes Ouest-centrales. *Mémoires de Géologie (Lausanne)*, 4,
- Colombi, A. & Pfeifer, H.-R. (1989). Ferrogabbroic and basaltic meta-eclogites from the Antrona mafic-ultramafic complex and the Centovalli-Locarno region (Italy and Southern Switzerland)-First results. *Schweiz. Mineral. Petrogr. Mitt.*, 66, 99-110.
- Compagnoni, R. (1977). The Sesia-Lanzo Zone: high pressure-low temperature metamorphism in the austroalpine continental margin. *Rend. Soc. It. Mineral. Petrogr.*, 33, (1), 335-374.
- Compagnoni, R. & Maffeo, B. (1973). Jadeite-Bearing Metagranites l.s. and Related Rocks in the Mount Mucrone Area (Sesia-Lanzo Zone, Western Italian Alps). *Schweiz. Mineral. Petrogr. Mitt.*, 53, (3), 355-378.
- Compagnoni, R., Dal Piaz, G.V., Hunziker, J.C., Lombardo, B. & Williams, P.F. (1977a). The Sesia-Lanzo Zone, a slice of continental crust with alpine high pressure-low temperature assemblages in the Western Italian Alps. *Rend. Soc. It. Mineral. Petrogr.*, 33, (1), 281-234.
- Compagnoni, R., Dal Piaz, G.V., Fiora, L., Gosso, G., Lombardo, B., Maffeo, B. & Williams, P.F. (1977b). Excursion to the Sesia-Lanzo Zone and Valtournanche metamorphic Ophiolites. *Rend. Soc. It. Mineral. Petrogr.*, 33, (1), 473-491.
- Cosca, M., Sharp, Z., Hunziker, J.C. & Venturini, G. (1994). Polyphase deformation and metamorphism in the Dent Blanche Nappe (Western Alps). in prep.
- Craig, H. (1957). Isotopic standards for carbon and hydrogen and correction factors for mass-spectrometric analysis of carbon dioxide. *Geoch. et Cosmoch. Acta*, 12, 133-149.
- Dahl, P. (1980). The thermal-compositional dependence of Fe²⁺-Mg distribution between coexisting garnet and

- pyroxene. applications to geothermometry. *Am. Mineralogist*, 65, 852-866.
- Dal Piaz, G. (1976). Il lembo di ricoprimento del Pillonet. *Mem. Ist. Geol. Min. Univ. Padova*, 31, 1-60.
- Dal Piaz, G.V. (1992a). Le alpi dal Monte Binco al Lago Maggiore, primo volume. BE-Ma editrice, Milano.
- Dal Piaz, G.V. (1992b). Le alpi dal Monte Binco al Lago Maggiore, secondo volume. BE-Ma editrice, Milano.
- Dal Piaz, G.V. (1993). Evolution of Austroalpine and upper Penninic basement in the north-Western alps from Variscan convergence to post-Variscan extension. In: *Pre-Mesozoic Geology in the Alps*. von Raumer and Neubauer Ed., Springer Verlag, Amsterdam, 327-344.
- Dal Piaz, G.V. & Sacchi, R. (1969). Osservazioni geologiche sul lembo di ricoprimento del Pillonet (Dent Blanche s.l.). *Mem. Soc. Geol. It.*, 8, 835-846.
- Dal Piaz, G.V. & Nervo, R. (1971). Il lembo di ricoprimento del Glacier-Rafray (Dent Blanche l.s.). *Boll. Soc. Geol. It.*, 90, 401-414.
- Dal Piaz, G.V., Gosso, G. & Martinotti, G. (1971). La II Zona Diorito-kinzigitica tra la Valsesia e la Valle d' Ayas (Alpi Occidentali). *Mam. Soc. Geol. It.*, 10, 257-276.
- Dal Piaz, G.V., Hunziker, J.C. & Martinotti, G. (1972). La zona Sesia-Lanzo e l'evoluzione tettonico-metamorfica delle Alpi nordoccidentali interne. *Mem. Soc. Geol. It.* 11, 433-460,
- Dal Piaz, G.V., Hunziker, J.C. & Martinotti, G. (1973). Excursion to the Sesia Zone. *Schweiz. Mineral. Petrogr. Mitt*, 53, 477-490.
- Dal Piaz, G., De Vecchi, G. & Hunziker, J. (1977). The Austroalpine layered gabbros of the Matterhorn and Mt. Collon-Dents de Bertol. *Schweiz. Mineral. Petrogr. Mitt*, 57, 59-88.
- Dal Piaz, G.V. and Ernst, W.G. (1978). Areal geology and petrology of eclogites and associated metabasites of the Piemonte ophiolite nappe, Breuil-St. Jacques area, Italian Western Alps. *Tectonophysics* 51., 99-126.
- Dal Piaz, G.V., Venturelli, G., Spadea, P., Di Battistini, G. (1981). Geochemical features of metabasalts and metagabbros from Piemonte ophiolite nappe, Italian Western Alps. *Neues Jahrb. Mineral. Abh.* 142: 248-269.
- Dal Piaz, G.V. & Gosso, G. (1985). Le moderne interpretazioni delle Alpi. Cento anni di geologia italiana., Società Geologica Italiana, Bologna, 95-112.
- Dal Piaz, G.V., Nervo, R. & Polino, R. (1979). Carta geologica del lembo del Glacier-Rafray (Dent Blanche l.s.) alla scala 1:25.000. CNR - Centro Studio Problemi Orogeno Alpi Occidentali. Silca, Firenze.
- Dal Piaz, G.V., Lombardo, B. & Gosso, G. (1983). Metamorphic evolution of the Mont Emilius klippe, Dent Blanche nappe, Western Alps. *Am. J. Sciences*, 283, 438-458.
- Dal Piaz, G. V. and S. Martin (1986). Dati Microchimici sul metamorfismo alpino nei lembi Austroalpini del Pillonet E di Chatillon (Valle d'Aosta). *Rend. Soc. Geol. It.* 9: 15-16.
- Dal Piaz, G. V., G. Venturelli, et al. (1979). Calcalkaline to ultrapotassic postcollisional volcanic activity in the internal NW Alps. *Mem. Ist. Geol. Mineral. Univ. Padova* 32.
- Dal Piaz, G.V., Gosso, G., Pennacchioni, G., Spalla, M.I. (1993). "Geology of eclogites and related rocks in the Alps." 4th Intern Eclogite Confer, Acc Naz Sci XL, Roma, scritti doc 13 17-58.
- Dallmeyer, R.D. & Sutter, J.F. (1976). $^{40}\text{Ar}/^{39}\text{Ar}$ incremental release ages of biotite and hornblende from variably retrograded basement gneisses of the northeasternmost Reading Prong, New York. Their bearing on early Paleozoic metamorphic history. *Am. J. Sciences*, 276, 731-747.
- La Roche, de, H.D. (1972). Revue dommaire de quelques diagrammes chimico-minéralogiques pour l'étude des associations ignées ou sédimentaires et de leur dérivés métamorphiques. *Sciences de la Terre*, 17, (31-46), 31-46.
- De Zanche, V. (1990). A review of Triassic stratigraphy and paleogeography in the Eastern Southern Alps. *Boll. Soc. Geol. It.*, 109/1, 59-71.
- De Zanche, V. & Sedeà, R. (1972). Nuovi aspetti del Vulcanesimo triassico nei dintorni di Recoaro (Vicenza). *Boll. Soc. Geol. It.*, 91, 523-532.
- Desmons, J. & Ghent, E.D. (1977). Chemistry, Zonation and distribution coefficients of elements in eclogitic minerals from the eastern Sesia Unit, Italian Western Alps. *Schweiz. Mineral. Petrogr. Mitt*, 57, 397-411.
- Desmons, J. & O'Neil, J.R. (1978). Oxygen and Hydrogen isotope composition of eclogites and associated rocks from the Eastern Sesia Zone (Western Alps, Italy). *Contrib. Mineral. Petrol.*, 67, 79-85.
- Diehl, E.A., Masson, R. & Stutz, A.H. (1952). Contributi alla conoscenza del Ricoprimento Dent Blanche. *Mem. Ist. Geol. Min. Univ. Padova*, 17, 1-53.
- Droop, G.T.R., Lombardo, B., Pognante, U. (1990). Formation and distribution of eclogite facies rocks in the Alps. In:

- Carswell D.A.(Ed): Eclogite facies rocks. Blakie, 225-259.
- Ellis, D.J. & Green, D.H. (1979). An experimental study of the effect of Ca upon garnet-clinopyroxene Fe-Mg exchange equilibria. *Contrib. Mineral. Petrol.*, 71, 13-22.
- Ernst, W.G. (1979). Coexisting sodic and calcic amphiboles from high-pressure metamorphic belts and the stability of barroisitic amphibole. *Mineral. Mag.*, 43, 269-278.
- Essene, E.J. & Fyfe, W.S. (1967). Omphacite in californian metamorphic rocks. *Contrib. Mineral. Petrol.*, 15, 1-23.
- Essene, E.J. (1989). The current status of Thermobarometry in metamorphic rocks. Evolution of metamorphic belts. *Geol. Soc. Spec. Publ.*, 43, 1-44.
- Floyd, P.A. & Winchester, J.A. (1975). Magma type and tectonic setting discrimination using immobile elements, *Earth Planet. Sci. Lett.*, 211-218
- Fiorentini Potenza, M. & Morelli, G.L. (1968). Le paragenesi delle metamorfite a fengite 3T e muscovite 2M1, in Valchiusella, Zona Sesia Lanzo. *Atti Soc. It. Sc. Nat.*, 107, (1), 55-86.
- Foland, K.R. (1983). 40Ar-39Ar incremental heating plateaus for biotites with excess Argon. *Isot. Geosc.*, 1, 3-21.
- Fontéilles, M. (1976) Essai d'interprétation des compositions chimiques des roches d'origine métamorphique et magmatique du massif hercynien del'Agly (Pyrénées orientales). Université de Paris VI, Ph.D. thesis, pp. 1-685.
- Franchi, V. (1902). Contribuzione allo studio delle rocce a glaucofane e del metamorfismo onde ebbero origine nella regione ligure alpina occidentale. *Boll. R. Uff. Geol. It.*, 33, 255-318.
- Franchi, S. (1905). Appunti sulla zona kinzigitica Ivrea-Verbano e sulle formazioni adiacenti. *Boll. R. Uff. Geol. It.*, 36, 270-298.
- Frey, M., Hunziker, J.C., O'Neil, J.B. & Schwander, H.W. (1976). Equilibrium-disequilibrium relations in the Monte Rosa granite, Western Alps: petrological, Rb-Sr and stable isotope data. *Contrib. Mineral. Petrol.* 55, 147-179.
- Friedrichsen, H. & Morteani, G. (1979). Oxygen and hydrogen isotope studied on minerals from Alpine fissure and their gneissic host rocks, Western Tauern Window (Austria). *Contrib. Mineral. Petrol.*, 70, 149-152.
- Fröhlisch, F. (1960). Ein Beitrag zur Geochemie der Chrons. *Geochimica et Cosmochimica Acta*, 20.
- Ganguly, J. (1979). Garnet and clinopyroxene solid solution, and geo-thermometry based on Fe-Mg distribution coefficient. *Geoch. and Cosm. Acta*, 43, 1021-1029.
- Gastaldi, B. (1871). Studi geologici sulle Alpi Occidentali, parte I. *Mem. R. Com. Geol. It.*, 1, 1-47.
- Gastaldi, B. (1874). Studi geologici sulle Alpi Occidentali, parte II. *Mem. R. Com. Geol. It.*, 2, 1-64.
- Gerlach, H. (1869). Die Penninischen Alpen. *N. Denschrift All. Schweiz. Naturf. Ges.*, 23, 1-132.
- Gosso, G. (1977). Metamorphic evolution and fold history in the Eclogitic micaschist of upper Gressoney Valley (Sesia-Lanzo Zone, Western Alps). *Rend. Soc. It. Mineral. Petrogr.*, 33, (1), 389-407.
- Gosso, G., Dal Piaz, G.V., Piovano, V. & Polino, R. (1979). High pressure emplacement of Early-Alpine nappes postnappe deformation and structural levels (Internal northWestern Alps). *Mem. Ist. Geol. Mineral. Univ. Padova*, 32, 5-15.
- Gosso, G., Messiga, B., Spalla, M.I., Tribuzio, R. & Bottazzi, P. (1994). La transizione anfibolite-eclogite nelle rocce femiche della zona Sesia-Lanzo: le trasformazioni tessiturali, mineralogiche e chimiche. *Rapporti Alpi Appennini*, Cuneo.
- Graham, C.M. & Powell, R. (1984). A garnet-hornblende geothermometer: calibration, testing, and application to the Pelona Schist, Southern California. *J. Metam. Geol.*, 2, 13-21.
- Guidotti, C.V., Ed. (1984). Micas in metamorphic rocks. Micas. In: « Micas». S.W. Beiley Ed., *Reviews in Mineralogy*, 13, 1-372.
- Hagen, T. (1948). Geologie des MontDolin und des Nordranden der Dent Blanche Dcke zwischen Mont Blanc des Cheillon und Ferpècle (Wallis). *Matériel pour la Carte géologique Suisse N.S.*, 90.
- Halter, W. (1992) Etude géologique et minéralogique au Nord-Est d'Alagna Valsesia (Italie). Lausanne, dipl. Inédit.
- Henrich, H. & Althaus, S. (1980). die obere stabilitätsgrenze von Lawsonit plus Albit bzw Jadeit. *Fortschr. Miner.*, 58, (1), 635-649.
- Himmelberg, G.R. & Papike, J.J. (1969). Coexisting amphiboles from blueschist facies metamorphic rocks. *J. Petrol.*, (10),
- Holland, T.J.B. & Richardson, S.W. (1979). Amphibole zonation in metabasites as a guide to evolution of metamorphic conditions. *Contrib. Mineral. Petrol.*, 70, 143-148.
- Holland, T.J.B. (1980). The reaction albite = jadeite + quartz determined experimentally in the range 600° - 1200°C. *Am. Mineralogist*, 64, 129-134.

- Holland, T.J.B. (1983). The experimental determination of activities in disordered and short-range ordered jadeitic pyroxenes. *Contrib. Mineral. Petrol.*, 82, 214-220.
- Howthorne, F.C. (1983). The crystal chemistry of the amphiboles. *Canadian Mineralogist*, 21, 173-480.
- Hunziker, J.C. (1974). Rb-Sr and K-Ar age determination and the alpine tectonic history of the Western Alps. *Mem. Ist. Geol. Mineral. Univ. Padova*, 31, 1-55.
- Hunziker, J.C. & Zingg, A. (1980). Lower Palaeozoic amphibolite to granulite facies metamorphism in the Ivrea zone (Southern Alps, northern Italy). *Schweiz. mineral. petrogr. Mitt.* 60, 181-213.,
- Hunziker, J.C. & Martinotti, G. (1984). Geochronology and Evolution of the Western Alps, a review. *Mem. Soc. Geol. It.*, 29, 43-56.
- Hunziker, J.C., Desmons, J. & Hurford, A.J. (1992). Thirty-two years of geochronological work in the Central and Western Alps: a review on seven maps. *Mémoires de Géologie (Lausanne)*, 13, 1-52.
- Hurford, A.J., Stöckhert, B. & Hunziker, J.C. (1991). Constraints on the late thermotectonic evolution of the Western Alps: evidence for episodic rapid uplift. *Tectonics* 10, 758-769.
- Hy, C. (1984). Métamorphisme polyphasé et évolution tectonique dans la croûte continentale éclogitisée: les séries granitiques et pélitiques du Monte-Mucrone (zone Sesia-Lanzo, Alpes italiennes). Thèse Univ. Paris VI, 1-199.
- Inger, S. & Cliff, B. (1994). Dating high pressure metamorphism in the Western Alps; refining isotopic and tectonic interpretations. *U.S. Geological Survey circular*, 1107, (ICOG 8), 149.
- Jaboyedoff, M. (1986) Un vision de la Zone du Furgg. University of Lausanne, unpublished These du Diplôme.
- Kienast, J.-R. & Triboulet, C. (1972). Le chloritoïde dans le paragenèses à glaucophane, albite ou paragonite. *Bull. Soc. Fr. Mineral. Petrogr.*, 95, 565-573.
- Kienast, J.R. (1983) Le métamorphisme de haute pression et basse température (éclogites et schistes bleus): données nouvelles sur la pétrologie des roches de la crôte océanique subductée et des sédiments associés. Paris VI, Thèse doctorat d'Etat.
- Klein, C.J. (1968). Coexisting amphiboles. *J. Miner. Petrol.*, 9, 281-330.
- Klein, C.J. (1969). Two-amphibole assemblages in the sistem actinolite-hornblende-glaucophane. *Am. Mineralogist*, 54, 212-237.
- Koons, P.O. (1984). Implications to garnet-clinopyroxene geothermometry of non ideal solid solutions in jadeitic pyroxenes. *Contrib. Mineral. Petrol.*, 88, 340-347.
- Krogh, E.J. (1988). The garnet-clinopyroxene Mg-Fe geothermometer. A reinterpretation of the existing experimental data. *Contrib. Mineral. Petrol.*, 99, 44-48
- Lardeaux, J.M. (1981). Evolution tectono-metamorphique de la Zone Nord du Massif Sesia-Lanzo (Alpes Occidentales): un exemple d'éclogitisation de La Croûte Continentale. Paris IV, Thèse du 3.eme cycle, 1-226.
- Lardeaux, J.-M., Gosso, G., Kienast, J.-R. & Lombardo, B. (1982). Relations entre le métamorphisme et la déformation dans la zone de Sésia-Lanzo (Alpes occidentales) et le problème de l'éclogitisation de la croûte continentale. *Bull. Soc. géol. Fr.*, 24, (4), 793-800.
- Lardeaux, J.M. & Spalla, M. (1991). From granulites to eclogites in the Sesia zone (Italian Western Alps): a record of the opening and closure of the Piedmont ocean. *J. Metam. Geol.*, 9, 35-59.
- Lattard, D. (1974) Le rochés de la faciès schiste vert dans la zone Sesia Lanzo (Alpes Italiennes). Paris VI, Thèse du 3.eme cycle, 1-76.
- Leake, B.E. (1978). Nomenclature of amphiboles. *Am. Mineralogist*, 63, 1023-1052.
- Liebeaux, C. (1975) Caractères généraux des roches du faciès éclogitique de la zone Sesia Lanzo (Alpes Italiennes). Paris IV, Thèse du 3.eme cycle, 1-76.
- Lombardo, B., Compagnoni, R., Fiora, L. & Facchinelli, A. (1977). Composition of some Na-pyroxenes from the eclogitic micascists of lower Val d'Aosta (Sesia-Lanzo Zone, Western Alps). *Rendiconti della Societa Geologica Italiana*, 33, 375-388.
- Mamin, M. (1992) Geologie du Haut Val Ferret Italien. University of Lausanne, Diplôme inedit..
- Martinotti, G. (1970). Studio petrografico delle eclogiti della zona del Monte Mucrone e dei loro rapporti con i «micascisti eclogitici» incassanti. Univ. Torino, unpublished Thesis.
- Martinotti, G. & Hunziker, J.C. (1984). The Austroalpine System in Western Alps: a review. *Mem. Soc. Geol. It.*, 29, 233-250.
- Maruyama, M.S., cho, M. & Liou, J.G. (1986). Experimental investigations of blueschist- greenschist transition equilibria: pressur dependence of Al₂O₃ contents in sodic amphiboles. A new geobarometer. *Mem. Geol. Soc. Am.*, 164, 1-16.
- Mattauer, M., Malavieille, J. & Monié, P. (1987). Lithospheric sections of the Western Alps assuming that Sesia is not of South Alpine origin. *Comptes rendus de*

- l' Académie des Sciences, Paris, 304, 43-48.
- Matthews, A., Goldsmith, J.R. & Clayton, N. (1983a). Oxygen isotope fractionations involving pyroxenes: the calibration of mineral pair geothermometers. *Geochimica et Cosmochimica Acta*, 47, 631-644.
- Matthews, A., Goldsmith, J.R. & Clayton, N. (1983b). Oxygen isotope fractionation between zoisite and water. *Geochimica et Cosmochimica Acta*, 47, 645-654.
- Matthews, A. (1994, in press). Oxygen isotope geothermometers for metamorphic rocks. *J. Metam. Geol.*, 12.
- Mc Dougall, I. & Harrison, M. (1988). *Geochronology by the $^{40}\text{Ar}/^{39}\text{Ar}$ method*. Oxford University Press, New York.
- McCrea, J.M. (1950). On the isotope chemistry of carbonates and paleotemperature scale. *J. Chem. Phys.*, 18, 849-857.
- McDowell, F.W., Lehman, D.H., Gucwa, P.R., Fritz, D. & Maxwell, J.C. (1984). Glaucophane schist and ophiolites of the northern California Coast Ranges. Isotopic ages and their tectonic implications. *Geol. Soc. Am. Bulletin*, 95, 1373-1382.
- Merrihue, C. (1965). Trace-elements determinations and potassium-argon dating by mass spectroscopy of neutron-irradiated samples. *Trans. Am. Geophys.*, 46, 125 (Abstract).
- Merrihue, C. & Turner, G. (1966). Potassium-argon dating by activation with fast neutrons. *J. Geophys. Res.*, 71, 2852-2857.
- Minnigh, L.D. (1978) Petrological and structural investigations of the Sparone area in the Orco valley (southern Sesia-Lanzo border zone, Western Alps, Italy). Leiden, Ph.D thesis.
- Moine, B. (1969). Orthoamphibolites et formations métasédimentaires calco-magnésienne de la région d'Ambatofinandrahana (Madagascar). *Science de la Terre*, 14, (2), 107-138.
- Morse, S.A. (1988). Motion of crystals, solute and heat in layered intrusions. *Canadian Mineral.*, 26, 209-224.
- Nitsch, K.H. (1974). Neue Erkenntnisse zur Stabilität von Lawsonit. *Fortschr. Miner.*, 51, 34-35.
- Nervo, R. and R. Polino (1976). Un lembo di cristallino Dent Blanche alla Torre Ponton (Valle d'Aosta). *Bollettino della Società Geologica Italiana* 95: 647-657.
- Novarese, V. (1931). La formazione diorito-kinzigitica in Italia. *Bol. R. Uff. Geol. It.*, 56, (7), 1-62.
- O'Neil, J.R. & Epstein, S. (1966). A method for oxygen isotope analysis of milligram quantities of water and some of its applications. *J. Geophys. Res.*, 71, 4955-4961.
- Oberhänsli, R., Hunziker, J.C., Martinotti, G. & Stern, W.B. (1985). Geochemistry, geochronology and petrology of Monte Mucrone: an example of Eo-Alpine eclogitization of Permian granitoids in the Sesia-Lanzo Zone; Western Alps; Italy. *Chemical Geol.*, 52, 165-184.
- Odin, G.S. & Odin, C. (1990). Echelle numérique des temps géologiques. *Geochronique (Soc. Geol. Fr.)*, 35, 12-22.
- Pankhurst, R.J., Moorbath, S., Rex, D.C. & Turner, G. (1973). Mineral age patterns in ca. 3700 my old rocks from West Greenland. *Earth Planet. Sci. Letters*, 20, 157-170.
- Paquette, J.L., Chopin, C. & Peucat, J.J. (1989). U-Pb zircon, Rb-Sr and Sm-Nd geochronology of high- to very-high-pressure meta-acidic rocks from the Western Alps. *Contrib. Mineral. Petrol.* 101, 280-289.
- Passchier, C.W., Urai, J.L., Van Loon, J. & Williams, P.F. (1981). Structural Geology of central Sesia Lanzo Zone. *Geologie en Mijnbouw*, 60, 497-507.
- Pattison, D.R.M. & Newton, R.C. (1989). Reverse experimental calibration of the garnet-clinopyroxene Fe-Mg exchange thermometer. *Contrib. Mineral. Petrol.*, 101, (87-103),
- Pearce, J.A. & Cann, J.R. (1973). Tectonic setting of basic volcanic rocks determined using trace elements analyses. *Earth Planet. Sci. Letters*, 19, 290-300.
- Pearce, J.A. (1982). Trace element characteristic of lavas from destructive plate boundaries. In: *Andesites* (R.S. Thorpe, Ed.), 525-547.
- Pearce, J.A. (1984). A «users guide» to basalt discrimination diagrams. unpublished user guide, 1-37.
- Pearce, J.A., Harris, N.B.W. & Tindle, A.G. (1984). Trace element distribution diagrams for tectonic interpretation of granitic rocks. *Journal of Petrology*, 25, 956-983.
- Pennacchioni, G. (1989) *Struttura ed evoluzione metamorfica alpina del M. Emilius*. University of Padova, Ph.D Thesis.
- Pennacchioni, G. & Guermani, A. (1993). The mylonites of the Austroalpine Dent Blanche nappe along the northwestern side of the Valpelline Valley (Italian Western Alps). *Mem. Sci. Geol.*, 45, 37-55.
- Pennacchioni, G. (1991). Evoluzione strutturale del M. Emilius (Austroalpino, Alpi Occidentali). *Rend. Soc. Geol. It.*, 14.
- Pettijohn, F.J., Potter, P.E. & Siever, R. (1972). *Sand and sandstones*. Springer-Verlag, Amsterdam.

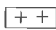



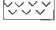


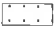

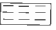


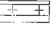

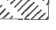
- Pfeifer, H.R., Arreaza, A. & Lavanchy, J.-C. (1989). Manuel du Centre d'Analyse Minérale (CAM). Sciences de la Terre, Université de Lausanne, 2nd edition, unpublished.
- Pfeifer, H.R., Lavanchy, J.-C. & Serneels, V. (1991). Bulk chemical analyses of geological and industrial materials by X-ray fluorescence, recent developments and application to materials rich in iron oxide. *J. Trace Microprobe Tech.*, 9, 127-147.
- Pfeifer, H.R., Colombi, A. & Ganguin, J. (1991). Zermatt-Saas and Antrona zone: A petrographic and geochemical comparison of polyphase metamorphic ophiolites of the West-Central Alps. *Schweiz. Mineral. Petrogr. Mitt.*, 69, 217-236.
- Piccardo, G.B. (1983). Genesi delle Ofioliti dell'Appennino settentrionale. *Mem. Soc. Geol. It.*, 25, 75-89.
- Pognante, U. (1979). Studio geologico petrografico del Complesso dei «Micasisti Eclogitici» lungo la valle d'Aosta tra Quincinetto, Ivosio e la Colma di Mombarone. University of Torino, Unpublished Diploma Thesis.
- Pognante, U., Compagnoni, R. & Gosso, G. (1980). Micro-structural relationships in the continental eclogitic rocks of the Sesia-Lanzo Zone: a record of a subduction cycle. *Ren. Soc. It. Miner. Petrogr.*, 36, 169-186.
- Pognante, U., Talarico, F., Rastelli, N. & Ferrati, N. (1987). High pressure metamorphism in the nappes of the Valle dell'Orco traverse (Western Alps collisional belt). *J. Metam. Geol.*, 5, 397-414.
- Pognante, U. (1989). Lawsonite, blueschist and eclogite formation in the southern Sesia zone (Western Alps, Italy). *Eur. J. Mineral.*, 1, 89-104.
- Polino, R., Dal Piaz, G.V. & Gosso, G. (1990). Tectonic erosion at the Adria margin and accretionary processes for the Cretaceous orogeny in the Alps. In «Deep structure of the Alps». F. Roure et al. Ed. *Mem. Soc. Geol. Fr.* 156; *Mém. Soc. Géol. Suisse* 1; *Soc. Geol. It.*, Vol. spec 1: 345-367.
- Postlethwaite, E. (1992). The Sesia zone: structural and metamorphic constraints on tectonic exhumation. In: *Geotelier Alpin*, Geologie Alpine, Univ. Grenoble, p. 79
- Powell, R. (1985). Regression diagnostics and robust regression in geothermometer / geobarometer calibration: the garnet-clinopyroxene geothermometer revisited. *J. Metam. Geol.*, 3, 231-243.
- Raase, P. (1974). Al and Ti contents of hornblende, indicators of pressure and temperature of regional metamorphism. *Contrib. Mineral. Petrol.*, 45, 231-236.
- Råheim, A. & Green, D.H. (1974). Experimental determination of the temperature and pressure dependence of the Fe-Mg partitioning coefficient for coexisting garnet and clinopyroxene. *Contrib. Mineral. Petrol.*, 48, 179-203.
- Reddy, S.M., Wheeler, J. & Kelley, S.P. (1994). The use of heterogeneous excess Argon and Argon loss to constrain thermal histories: laser $^{40}\text{Ar}/^{39}\text{Ar}$ dating of deformed micas from the Sesia zone, Italian Alps. *U.S. Geological Survey Circular*, 1107, 261.
- Reinard, B. & Balleve, M. (1988). Coexisting amphiboles in an eclogite from the Western Alps: new constraint on the miscibility gap between sodic and calcic amphiboles. *J. metam. Geol.*, 6, 330-350.
- Reinsch, D. (1979). Glaucophanites and Eclogites From Val Chiusella, Sesia-Lanzo Zone (Italian Alps). *Contrib. Mineral. Petrol.*, 70, 257-266.
- Richards, J.R. & Pidgeon, R.T. (1963). Some age measurement on micas from Broken Hill, Australia. *Geol. Soc. Aust.*, 10, 243-260.
- Ridley, J. (1989). Structural and metamorphic history of a segment of the Sesia-Lanzo zone, and its bearing on the kinematics of Alpine deformation in the Western Alps. In: «Alpine Tectonics», Coward et al. Ed. *Geol. Soc. Spec. Publ.*, 45, 189-201.
- Robert, C., Javoy, M. & Kienast, J.-R. (1985). Coefficients de distribution et mesures isotopiques $^{18}\text{O}/^{16}\text{O}$ comparaisons thermométriques et barométriques sur quelques éclogites et micaschistes de la zone Sesia-Lanzo (Alpes Italiennes). *Bull. Mineral.*, 108, 699-711.
- Roddick, J.C. (1978). The application of isochron diagrams in $^{40}\text{Ar}-^{39}\text{Ar}$ dating. A discussion. *Earth Planet. Sci. Letters*, 41, 233-244.
- Rossi, P.L., Morten, L. & Petersen, J.S. (1980). The Middle Triassic volcanic rocks from Non valley, north Italy. *Riv. It. Paleont.*, 85, (3-4), 1081-1092.
- Rubie, D.C. (1984). "A thermal-tectonic model for high-pressure metamorphism and deformation in the Sesia Zone, Western Alps." *J. Geol.* 92, 21-36.
- Ruffet, G., Féraud, G. & Ballèvre, M. (1993). Incorporation and loss of Ar in phengites: a $^{39}\text{Ar}/^{40}\text{Ar}$ laser probe study of effect of the Biella intrusion in the Eclogitic Micaschist unit of the Sesia zone (Western Alps). *Terra Abstract*.
- Ruffet, G. & Féraud, G. (1994). Incorporation and loss of Argon in Phengites: a $^{40}\text{Ar}/^{39}\text{Ar}$ laser probe study of the effect of the Biella intrusion in the Eclogitic Micaschists Unit of the Sesia Zone (Western Alps). *U.S. Geological Survey Circular*, 1107, 273.
- Saxena, S.K. (1979). Garnet-clinopyroxene geothermometer. *Contrib. Mineral. Petrol.*, 70, 229-235.

- Sharp, Z.D. (1992). In situ laser microprobe techniques for stable isotope analysis. *Chem. Geology*, 101, 3-19.
- Sharp, Z. D., Essene, E.J. and Hunziker, J. C. (1993). Stable isotope geochemistry and phase equilibria of coesite-bearing whiteschists, Dora Maira Massif, Western Alps. *Contrib. Miner. Petrol.* 114, 1-12.
- Shervais, J.W. (1982). Ti-V plots and the petrogenesis of modern and ophiolitic lavas. *Earth Planet. Sci. Letters*, 59, 101-118.
- Simic, D. (1992) Etude géologique et minéralogique du Hout Val Mastalone (Italie du nord). Lausanne, dipl. inédit.
- Sisson, V.B. & Onstott, T.C. (1986). Dating blueschists metamorphism: a combined $^{40}\text{Ar}/^{39}\text{Ar}$ and electron microprobe approach. *Geochimica et Cosmochimica Acta*, 50, 2111-2117.
- Spalla, M.I., De Maria, L., Gosso, G., Miletto, M. & Pognante, U. (1983). Deformazione e metamorfismo della Zona Sesia-Lanzo meridionale al contatto con la Falda Piemontese e con il Massiccio di Lanzo, Alpi Occidentali. *Mem. Soc. Geol. It.*, 26, 499-514.
- Spalla, M.J., Lardeaux, J.M., Dal Piaz, G.V. & Gosso, G. (1991). Métamorphisme et tectonique à la marge externe de la Zone Sesia-Lanzo. *Mem. Sci. Geol.*, 43, 361-369.
- Spear, F.S. (1981). An experimental study of hornblende stability and compositional variability in amphibolite. *Am. J. Science*, 281, 697-734.
- Spear, F.S. & Selverstone, J. (1983). Quantitative P-T paths from zoned minerals: theory and tectonic applications. *Contrib. Mineral. Petrol.*, 92, 348-357.
- Spear, F.S. (1989). Relative thermobarometry and metamorphic P-T paths. Evolution of Metamorphic Belts. *Geol.Soc., London* . 63-81.
- Spear, F.S. (1993). Metamorphic Phase Equilibria and Pressure-Temperature-Time Paths. *Miner. Soc. Am., Washington, D.C.*
- Sperlich, R. (1988). The transition from crossite to actinolite in metabasites of the Combin unit in Vallée St. Barthélemy (Aosta, Italy). *Schweiz. Mineral. Petrogr. Mitt.* 68, 215-224.
- Stampfli, G.M., Pilleveit, A., Marcoux, J. & Baud, A. (1991). Tethys margins in space and time. European Union of Geosciences EUG VI, Strasbourg, avril 1991.
- Stampfli, G.M. (1993): Le Briançonnais: terrain exotique dans les Alpes. - *Eclogae geol. Helv.*, 86/1, 146-159.
- Stampfli, G.M. & Marthaler, M. (1990). Divergent and convergent margins in North- Western Alps confrontation to actualistic models. *Geodynamica Acta*, 4/3, 159-184.
- Stampfli, G. & Marchant, R. (in press). Geodynamic evolution of the Tethyan margins of the Western Alps. Deep structure of Switzerland - Results from PNR 20. Birkhäuser AG Basel, .
- Stella, A. (1894). Relazione sul rilevamento geologico eseguito nell'anno 1893 nelle Alpi Occidentali (Valli dell'Orco e della Soana). *Boll. R. Uff. Geol. It.*, 25, 343-371.
- Stöckhert, B. (1985). Compositional control on the polymorphism (2M1-3T) of phengitic white mica from high pressure mineral assemblages of the Sesia Zone (lower Aosta Valley, Western Alps; Italy). *Contrib. Mineral. Petrol.*, 89, 52-58.
- Stöckhert, B., Jäger, E. & Voll, G. (1986). K-Ar age determinations on phengites from the internal part of the Sesia Zone, Western Alps, Italy. *Contrib. Mineral. Petrol.*, 92, 456-470.
- Stöckhert, B. (1989). Depth and timing of detachment in the 'Seconda Zona Diorito Kinzigitica', Western Alps. *Terra Abstracts* 1, 373.,
- Stünitz, H. (1989). Partitioning of metamorphism and deformation in the boundary region of the " II Zona diorito Kinzigitica", Sesia zone, Western Alps, PhD. Thesis, ETH, Zürich.
- Taylor, S.R. & McLemman, S.M. (1985). The continental crust: its composition and evolution. Blackwell Scientific Publication., London, Great Britain.
- Thélin, P. (1983) Les gneiss ocellé de la nappe du Grand Saint Bernard; essai d'évaluation des critères susceptibles d'en préciser l'héritage pré-métamorphique (alpes valaisannes, Suisse). Université de Lausanne, Ph.D. thesis, 1-485.
- Ungaretti, L., Lombardo, B., Domeneghetti, c. & Rossi, G. (1983). Crystalchemical evolution of amphiboles from eclogitized rocks of the Sesia-Lanzo Zone, Italian Western Alps. *Bull. Minéral.*, 106, 645-672.
- Velde, B. (1967). Si+4 content of natural phengites. *Contrib. Mineral. Petrol.*, 14, 250-258.
- Venneman, T.W. & O'Neil, J.R. (1993). A simple and inexpensive method of hydrogen isotope analysis of mineral and rocks based on zinc reagent. *Chem. Geology*, 103, 227-234.
- Venturini, G. (1991). I protoliti dei «Micascisti Eclogitici» sul versante destro della bassa Valle d'Aosta (Zona Sesia-Lanzo, Alpi Occidentali). Univ. Torino, unpublished Master Thesis, 1-224.
- Venturini, G. (1994). The II DK between the Aosta valley and the Chiusella Valley (Sesia zone, Western Italian Alps). 11.th Annual Meeting of Swiss Tectonic Studies Group, Neuchâtel.

- Venturini, G., Martinotti, G. & Hunziker, J.C. (1991). The Protoliths of the «Eclogitic Micaschists» in the lower Aosta Valley (Sesia-Lanzo Zone, Western Alps). *Mem. Sci. Geol.*, 43, 347-359.
- Venturini, G. & Hunziker, J.C. (1992). Geology and geochronology of the central part of the Sesia Lanzo Zone: the state of the art. *Géologie Alpine, Série Spec. Résumés et colloques*, Univ. Grenoble, 1, 102-103.
- Venturini, G., Cosca, M.A., Sharp, Z.D. & Hunziker, J.C. (1994b). Stable isotope and $^{40}\text{Ar}/^{39}\text{Ar}$ constraints on prealpine reconstructions and P-T-t paths within the central Sesia-Lanzo zone, Western Alps, northern Italy. U.G. Geological Survey circular, 1107, (ICOG 8), 339.
- Venturini, G., Martinotti, G., Armando, G., Barbero, M. & Hunziker, J.C. (1994a). The Central Sesia Lanzo Zone (Western Italian Alps): new field observations and lithostratigraphic subdivisions. *Schweiz. Mineral. Petrogr. Mitt.*, 74, 111-121.
- Venturini, G., Cosca, M.A., Sharp, Z.D. & Hunziker, J.C. (1994b). Stable isotope and $^{40}\text{Ar}/^{39}\text{Ar}$ constraints on prealpine reconstructions and P-T-t paths within the central Sesia-Lanzo zone, Western Alps, northern Italy. U.G. Geological Survey circular, 1107, (ICOG 8), 339.
- Voggenreiter, W., Hötzl, H. & Mechie, J. (1988). Low-angle detachment origin for the Red Sea Rift System ? *Tectonophysics*, 150, 51-75.
- Vuichard, J.P. (1987) La marge Austroalpine durant la collision Alpine: Evolution tectonometamorphique de la zone Sesia Lanzo. Rennes, 3eme cycle.
- Vuichard, J.P. & Ballèvre, M. (1988). Garnet-Chloritoid equilibria in eclogitic pelitic rocks from the Sesia zone (Western Alps): their bearing on phase relation in high pressure metapelites. *J. Metam. Geol.*, 6, 135-157.
- Weidmann, M. and L. Zaninetti (1974). Quelques données nouvelles sur la série du Mont-Dolin. Description des Foraminifères Triasiques. *Eclogae Geol. Helv.* 67(3): 597-603.
- Williams, P. & Compagnoni, R. (1983). Deformation and metamorphism in the Bard area of Sesia-Lanzo Zone, Western Alps, during subduction and uplift. *J. Metam. Geology*, 1, 117-140.
- Wimmenauer, W. (1984). Das prävarisken Kristallin in Schwarzwald. *Fortschr. Miner. Beih.*, 62, (2), 69-86.
- Zingg, A., Handy, M.R., Hunziker, J.C. & Schmid, S.M. (1990). Tectonometamorphic history of the Ivrea Zone and relationship to the crustal evolution of the Southern Alps. *Tectonophysics*, 182, 169-192.

Annex 1

Legend of lithologic columns and text abbreviations

Legend of lithologic columns (chapter 2)	
	Mylonitic metagabbros
	Mn-bearing calcschists
	Impure limestones and calcschists
	Grey pure limestones
	Metabasalts, pillow lavas and breccias
	Mn-bearing metasediments, quartzites, metapelites, with basic blocks and lenses
	Yellow dolomitic marbles
	Pure quartzites
	Impure quartzites
	Metapelites
	Graphitic metapelites
	Decimetric to metric levels and blocks of basic rocks
	Leucocratic gneisses with centimetric to decimetric blocks of basic rocks
	Metaconglomerates
	Polycyclic basement rocks

Mineral abbreviations

qtz	- quartz
wm	- white mica
phe	- phengite
mu	- muscovite
pa	- paragonite
bio	- biotite
gln	- glaucophane
hbl	- hornblende
act	- actinolite
tr	- tremolite
barr	- borroisite
cross	- crossite
omp	- omphacite
jd	- jadeite
aegr	- aegirine
grn	- garnet
clt	- chloritoid
zo	- zoisite
czo	- clinozoisite
ep	- epidote
sph	- sphene (titanite)
ru	- rutile
chl	- chlorite
ab	- albite
kf	- K-feldspar
mc	- microcline

Metamorphic abbreviations

HP	= high pressure
GS	= greenschists
BS	= blueschists
HG	= high grade (high temperature)

Geological abbreviations

EM	- eclogitic micaschists
GS	- Gneiss Minuti
IIDK	- II diorito-kinzigite zone

Annex 2

Whole rock geochemical analyses

(Analyst: J.-C. Lavanchy)

Annex 2.1

Whole rock geochemical analyses of acid rocks

(SV)	metakinzigites			metagranodiorites, metagranites and orthogneisses						
	1k	2k	7lz	5a	1dz	3e	4e	1mt	2ta	2tw
SiO ₂	66.44	59.69	67.33	61.85	63.17	64.89	77.05	75.16	77.24	76.33
TiO ₂	0.51	1.08	0.37	0.63	0.59	0.58	0.1	0.1	0.1	0.1
Al ₂ O ₃	15.2	18.54	14.71	16.09	15.06	16.31	12.57	13.03	12.74	13.03
Fe ₂ O ₃	0.87	0.95	1.95	2.14	0.67	1.23	0.46	0.6	0.57	0.59
FeO	3.86	6.93	1.37	2.96	3.84	3.94	0.67	0.72	0.79	0.89
MnO	0.08	0.11	0.04	0.08	0.08	0.08	0.03	0.02	0.03	0.03
MgO	1.24	3.35	1.14	1.8	1.89	1.19	0.1	0.13	0.08	0.1
CaO	3.51	2.18	1.22	4.72	3.66	3.43	1.11	0.39	0.47	0.48
Na ₂ O	3.65	1.15	4.23	3.55	5.14	3.76	1.94	3.12	2.46	2.42
K ₂ O	2.74	3.43	3.02	3.17	2.99	2.9	5.59	5.03	4.58	4.84
P ₂ O ₅	0.13	0.11	0.1	0.16	0.14	0.17	0.01	0.15	0.2	0.19
H ₂ O	1.44	1.54	2.66	1.67	1.63	0.85	0.54	0.63	0.76	0.82
CO ₂	0.08	0.16	0.48	0.6	0.9	0.08	0.05	0.2	0.08	0.09
Cr ₂ O ₃	0	0.02	0	0	0	0	0	0	0	0.01
NiO	0	0.01	0	0	0	0	0	0	0	0
Tot	99.75	99.25	98.62	99.42	99.76	99.41	100.22	99.28	100.10	99.92
-										
Nb	15	18	0	1	0	19	1	0	8	5
Zr	194	206	178	162	91	179	93	47	72	71
Y	33	40	17	31	0	23	13	20	25	23
Sr	136	76	129	216	276	143	84	22	26	25
U	0	0	0	0	0	0	0	0	4	4
Rb	134	145	84	96	0	140	137	270	274	287
Th	9	15	4	0	0	18	9	0	6	3
Pb	0	0	0	1	0	24	36	9	11	12
Ga	16	23	14	18	3	18	10	15	16	16
Zn	84	72	47	74	89	87	12	33	35	41
Cu	0	9	0	0	0	0	0	0	0	0
Ni	0	44	0	3	143	0	0	2	0	0
Co	9	25	22	31	120	11	0	35	0	0
Cr	1	122	5	13	491	5	0	0	0	88
V	51	163	38	77	383	66	0	4	0	0
Ce	65	73	73	45	73	97	33	19	22	17
Nd	28	39	21	8	36	42	13	1	8	5
Ba	353	676	667	765	0	411	275	0	45	0
La	28	39	36	13	33	51	15	5	6	6
S	181	231	54	179	103	49	43	0	39	37
Hf	0	0	3	1255	1190	1090	1110	1315	1265	1100

Annex 2.3

Whole rock geochemical analyses of basic rocks

(SV)	Bonze unit metagabbros						gln-eclogites-metabasalts				basic breccias		basic layers and blocks			
	sv912az	sv913az	sv914b	sv919b	9215vc	sv922i	sv915b	sv916b	v9112b	sv911q	sv918b	v9120c	sv9112c	v9116c	v9126c	v9127c
SiO ₂	49.93	47.89	49.75	43.91	50.22	46.63	48.6	46.19	43.68	47.44	52.11	49.98	45.72	51.25	52.04	49.72
TiO ₂	0.62	0.38	0.81	0.7	0.91	0.36	1.91	1.6	1.92	1.48	1.78	1.57	1.99	1.4	1.23	2.03
Al ₂ O ₃	18.97	15.32	15.8	12.98	13.03	18.23	15.79	17.16	13.08	14.4	18.34	18.06	13.54	16.65	17.29	15.45
Fe ₂ O ₃	1.18	0.69	1.1	4.7	2.43	7.58	0.44	2.73	0.89	0.26	6.09	3.19	2.43	2.4	2.46	1.29
FeO	5.52	8.57	5.67	7.87	3.88	0.8	9.04	6.75	10.22	10.91	4.68	6.58	8.86	5.86	5.59	9.12
MnO	0.12	0.17	0.13	0.18	0.09	0.12	0.2	0.19	0.24	0.17	0.13	0.2	0.24	0.16	0.11	0.19
MgO	8.3	12.65	8.76	15.75	9.53	9.28	7.23	8.39	6.25	8.35	2.63	4.02	5.93	6.45	4.09	5.9
CaO	9.95	9.28	11.31	7.34	12.84	11.33	10.69	10.86	10.97	9.43	3.63	5.75	9.69	5.14	6.69	8.28
Na ₂ O	2.73	2.32	3.18	1.15	3.03	2.59	3.24	2.53	3.1	3.57	5.14	3.13	3.23	4.81	3.15	2.57
K ₂ O	0.41	0.27	0.25	0.17	0.24	0.73	0.05	0.33	0.47	0.21	2.7	3.35	0.8	1.17	2.65	1.52
P ₂ O ₅	0.1	0.04	0.06	0.05	0.05	0.01	0.21	0.06	0.19	0.11	0.06	0.06	0.19	0.25	0.16	0.37
H ₂ O	0.85	1.6	2.21	4.47	1.79	1.49	1.69	2.53	2.46	2.27	1.56	2.36	2.46	2.74	2.95	2.38
CO ₂	0.77	0.99	0.13	0.05	0.3	0.2	0.18	0.05	5.61	0.88	0.16	0.88	4.47	0.96	1.29	0.28
Cr ₂ O ₃	0.03	0.03	0.05	0.12	0.06	0.05	0.03	0.04	0.02	0.03	0.01	0.03	0.02	0.02	0.01	0.04
NiO	0.01	0.03	0.02	0.03	0	0	0.01	0.01	0.01	0.01	0	0	0.01	0	0	0.01
Tot	99.49	100.23	99.23	99.47	98.4	99.4	99.31	99.42	99.11	99.52	99.02	99.16	99.58	99.26	99.71	99.15
Nb	0	2	2	0	0	0	5	1	14	6	11	15	16	5	7	64
Zr	65	51	67	44	47	0	161	61	131	89	387	284	133	165	107	204
Y	9	5	16	7	13	4	37	16	28	31	58	61	28	27	18	34
Sr	428	330	343	57	200	247	240	459	234	162	101	161	212	301	654	250
U	0	0	0	0	0	0	0	0	0	0	1	0	0	0	1	0
Rb	11	9	13	6	7	19	4	11	24	11	84	121	34	56	109	70
Th	0	0	0	0	0	0	0	0	0	0	6	5	0	0	2	5
Pb	0	0	0	0	0	0	0	0	0	0	0	0	0	0	17	0
Ga	12	7	9	5	8	15	13	13	14	14	29	23	15	14	13	14
Zn	70	91	47	70	29	61	79	50	137	133	123	157	138	78	100	168
Cu	25	8	0	34	0	25	13	0	92	112	0	0	90	13	0	9
Ni	85	192	109	252	78	127	65	54	42	92	0	10	45	36	0	76
Co	32	53	37	75	44	52	42	43	49	45	26	21	47	32	18	36
Cr	207	203	308	777	428	443	191	243	110	177	27	186	147	163	72	249
V	89	90	168	137	197	142	280	282	320	333	249	181	300	205	211	178
Ce	21	0	0	0	0	0	15	0	28	0	64	40	23	24	22	52
Nd	11	10	8	12	3	0	26	10	21	16	47	22	19	15	12	30
Ba	67	81	61	0	0	79	1	8	39	34	483	830	141	186	871	347
La	11	0	2	0	0	0	0	0	7	6	28	13	14	7	3	29
S	213	267	64	59	65	101	61	52	253	781	40	288	177	45	654	286
Hf	0	0	0	0	0	0	2	0	1	0	4	0	0	0	0	0

(SV)	hbl-amphibolites					phl-eclogites		Corio mafic rocks		indistinct mafic rocks			
	sv911v	sv932v	sv932v	sv933v	sv934v	sv914q	sv915q	sv9311tz	v9312tz	sv9311ft	v9313ft	sv913a	sv923i
SiO ₂	45.77	44.01	47.49	44.41	47.29	48.31	48.6	45.05	45.11	46.67	47.32	48.41	43.0
TiO ₂	2.26	3.39	1.68	2.4	2.2	1.94	1.44	2.61	2.42	1.5	1.28	3.31	2.9
Al ₂ O ₃	16.5	12.39	14.67	10.56	10.9	15.86	15.82	18	17.97	16.3	20.71	14.08	10.8
Fe ₂ O ₃	2.84	2.98	4.01	3.82	3.03	6.3	2.99	6.22	6.32	3.89	3.82	7.41	3.9
FeO	8.63	10.98	7.62	8.25	9.26	3.26	6.08	4.89	5.14	6.05	4.21	5.38	9.8
MnO	0.2	0.17	0.17	0.15	0.16	0.18	0.14	0.09	0.11	0.17	0.09	0.24	0.2
MgO	5.97	9.07	6.67	12.29	11.99	7.21	7.03	5.28	5.37	9.66	3.58	5.65	12.0
CaO	10.59	9.77	11.11	8.12	8.03	8.51	7.56	10.47	9.98	6.67	10.02	7.5	10.7
Na ₂ O	3.29	1.97	2.82	2.78	2.62	3.46	4.47	2.94	3.35	4.14	2.32	2.93	1.5
K ₂ O	0.97	0.89	0.48	0.45	0.62	1.87	2.83	0.14	0.16	0.09	1.98	1	0.4
P ₂ O ₅	0.27	0.44	0.14	0.29	0.3	0.42	0.3	0.72	0.5	0.16	0.3	0.27	0.36
H ₂ O	2.02	2.25	1.88	3.64	2.38	1.4	1.49	2.42	2.47	3.51	2.73	2.68	2.6
CO ₂	0.08	0.6	0.4	1.9	0.4	0.34	0.62	0.3	0.2	0.3	0.3	0.26	0.7
Cr ₂ O ₃	0.02	0.06	0.02	0.09	0.09	0.04	0.05	0.01	0.01	0.01	0	0.01	0.1
NiO	0.01	0	0	0	0	0.01	0.01	0	0	0	0	0	0.0
Tot	99.42	98.97	99.16	99.15	99.27	99.11	99.43	99.14	99.11	99.12	98.66	99.13	99.0
Nb	22	32	0	17	16	12	10	0	0	0	0	10	19.0
Zr	193	220	92	157	143	193	234	30	36	110	50	170	193
Y	31	24	26	20	20	33	35	19	16	20	10	29	21
Sr	211	445	405	277	190	273	228	544	527	372	441	245	149
U	0	0	0	0	0	0	0	0	0	0	0	0	0
Rb	11	19	16	13	13	120	208	6	6	4	20	35	4
Th	2	0	0	0	0	3	3	0	0	0	0	2	0
Pb	0	3	6	0	3	0	0	0	0	0	22	0	0
Ga	14	24	19	18	20	13	12	20	21	17	22	17	21
Zn	103	154	111	152	168	86	94	121	128	137	68	121	158
Cu	41	20	82	0	0	18	31	0	0	0	0	32	23
Ni	34	237	82	360	364	85	94	18	12	75	4	8	416
Co	49	97	71	75	84	39	34	68	56	61	40	52	94
Cr	127	461	189	739	729	253	293	43	51	71	28	47	714
V	274	314	307	255	262	239	181	299	301	177	158	390	309
Ce	47	64	27	45	46	64	66	35	30	22	29	44	59
Nd	29	31	11	27	20	39	41	19	10	15	5	25	31
Ba	166	333	2	63	328	255	221	0	0	0	576	166	0
La	22	31	7	16	20	22	24	10	11	7	14	92	29
S	181	113	107	64	181	110	244	57	86	0	104	2	135
Hf	0	5	2	5	3	0	0	1	2	3	1	2	4

Annex 3
Analytical tables of the
 $^{40}\text{Ar}/^{39}\text{Ar}$ incremental heating age determinations.
(phengite, biotite and glaucophane systems)

T (°C)	40Ar	39Ar	38Ar	36Ar	40Ar/39Ar(K)	39Ar(K)	%40Ar	Apparent age (Ma)
<i>KAW 415 - Arnad</i>								
	<i>External unit</i>			<i>J = 0.00503</i>	<i>wt. = 55.58 mg</i>	<i>phengite</i>		
750	1101.23 ± 39.38	193.564 ± 5.27	3.663 ± 0.519	0.5307 ± 0.0799	4.87 ± 0.28	6.26	85.65	43.7 ± 4.9
800	1374.25 ± 58.38	244.344 ± 8.42	3.499 ± 0.059	0.9792 ± 0.8089	4.43 ± 1.03	7.91	78.8	39.8 ± 9.1
850	3516.84 ± 147.94	608.945 ± 23.75	8.272 ± 0.263	1.307 ± 0.1912	5.13 ± 0.34	20.08	88.9	46 ± 3
900	2675.7 ± 91.34	523.802 ± 22.452	6.969 ± 0.463	0.1446 ± 0.0489	5.02 ± 0.28	16.95	98.3	45 ± 2.5
950	3319.92 ± 14.73	598.924 ± 3.182	8.12 ± 0.182	0.7249 ± 0.0828	5.18 ± 0.06	19.38	93.4	46.4 ± 0.5
1000	3288.14 ± 95.54	578.821 ± 14.555	7.97 ± 0.207	0.764 ± 0.0826	5.28 ± 0.22	18.73	93	47.3 ± 2
1150	1824.82 ± 51.54	314.225 ± 6.182	4.168 ± 0.068	0.3753 ± 0.1489	5.45 ± 0.24	10.17	93.8	48.8 ± 2.1
1350	158.65 ± 13.69	16.193 ± 0.494	0.223 ± 0.104	0.1976 ± 0.0596	6.18 ± 1.41	0.23	63.1	55.3 ± 12.4
fuse	243.68 ± 4.1	8.237 ± 0.22	0.106 ± 0.045	0.1378 ± 0.1658	24.63 ± 6.02	0.29	83.3	210.7 ± 48.6
Total fusion age = 46 Ma								
Weighted mean plateau age = (850-1000°C) = 46.4 ± 0.5 Ma								

<i>KAW 473 - Quassolo</i>								
	<i>Internal unit</i>			<i>J = 0.002639</i>	<i>wt. = 0.62 mg</i>	<i>phengite</i>		
650	300.83 ± 0.6	0.651 ± 0.007	0.203 ± 0.002	1.0089 ± 0.0056	8.82 ± 7.09	0.1	98.1	41.5 ± 33
800	99.72 ± 0.2	2.392 ± 0.027	0.072 ± 0.001	0.2168 ± 0.0027	15.21 ± 0.65	4.91	36.63	71 ± 3
850	207.04 ± 0.41	4.83 ± 0.043	0.157 ± 0.002	0.4586 ± 0.007	15.12 ± 0.63	9.91	35.19	70.6 ± 2.9
900	282.55 ± 0.57	7.788 ± 0.055	0.21 ± 0.003	0.5634 ± 0.007	15.15 ± 0.41	15.98	41.66	70.7 ± 1.9
950	486.03 ± 0.97	17.991 ± 0.042	0.381 ± 0.004	0.741 ± 0.0047	15 ± 0.12	36.91	55.39	70 ± 0.5
1000	324.61 ± 0.65	9.209 ± 0.046	0.25 ± 0.003	0.6283 ± 0.0031	15.32 ± 0.24	18.89	43.37	71.5 ± 1.1
1050	294.07 ± 0.59	5.932 ± 0.032	0.209 ± 0.003	0.6989 ± 0.0051	15.14 ± 0.43	8.04	30.47	70.7 ± 2
1100	90.86 ± 0.18	1.398 ± 0.014	0.063 ± 0.001	0.2399 ± 0.0021	14.83 ± 0.94	2.87	22.76	69.3 ± 4.3
1200	46.36 ± 0.47	0.767 ± 0.006	0.035 ± 0.001	0.1194 ± 0.0013	14.95 ± 0.99	1.57	24.68	69.8 ± 4.5
1550	46.33 ± 0.54	0.453 ± 0.009	0.009 ± 0.009	0.033 ± 0.002	14.14 ± 3.19	0.93	13.81	66.1 ± 14.1
Total fusion age = 71 Ma								
Weighted mean plateau age = (800-1050°C) = 70.4 ± 0.5 Ma								

<i>KAW 475 - Barne</i>								
	<i>External unit</i>			<i>J = 0.002637</i>	<i>wt. = 1.02 mg</i>	<i>phengite</i>		
750	44.82 ± 0.09	2.48 ± 0.005	0.057 ± 0.001	0.079 ± 0.0015	8.61 ± 0.19	3.5	47.73	40.7 ± 0.9
800	71.05 ± 0.14	4.7 ± 0.009	0.084 ± 0.001	0.085 ± 0.0015	9.77 ± 0.1	5.72	64.62	46.1 ± 0.5
850	42.49 ± 0.08	3.06 ± 0.006	0.053 ± 0.001	0.04 ± 0.0015	10.07 ± 0.15	3.72	72.53	47.5 ± 0.7
900	127.61 ± 0.26	10.19 ± 0.02	0.155 ± 0.001	0.075 ± 0.0015	10.34 ± 0.06	12.39	82.62	48.7 ± 0.3
950	323.14 ± 0.65	27.59 ± 0.055	0.396 ± 0.001	0.094 ± 0.0015	10.69 ± 0.04	33.55	91.33	50.4 ± 0.2
1000	266.56 ± 0.53	22.85 ± 0.046	0.326 ± 0.001	0.078 ± 0.0015	10.65 ± 0.04	28.12	91.29	50.2 ± 0.2
1050	92.2 ± 0.18	8.03 ± 0.016	0.117 ± 0.001	0.019 ± 0.0015	10.77 ± 0.06	9.76	93.82	50.7 ± 0.3
1100	21.21 ± 0.04	1.83 ± 0.004	0.028 ± 0.001	0.006 ± 0.0015	10.55 ± 0.24	2.23	91.01	49.7 ± 1.12
1250	11.21 ± 0.02	0.71 ± 0.001	0.017 ± 0.001	0.014 ± 0.0015	9.98 ± 0.62	0.87	63.49	47.1 ± 2.9
1570	7.46 ± 0.01	0.108 ± 0.001	0.008 ± 0.001	0.0244 ± 0.0015	2.3 ± 4.26	0.13	3.34	10.9 ± 20.2
Total fusion age = 49 Ma								
Weighted mean plateau age (950-1100°C) = 50 ± 0.2 Ma								

<i>KAW 476 - Gattinari</i>								
	<i>Intermediate unit</i>			<i>J = 0.002648</i>	<i>wt. = 1.02 mg</i>	<i>phengite</i>		
650	216.84 ± 0.43	2.395 ± 0.009	0.161 ± 0.002	0.6286 ± 0.0021	13.79 ± 0.57	1.62	15.19	64.7 ± 2.64
750	45.39 ± 0.43	1.995 ± 0.025	0.043 ± 0.001	0.0462 ± 0.0009	16.01 ± 0.39	1.35	70.19	74.91 ± 1.83
800	164.56 ± 0.33	8.93 ± 0.069	0.144 ± 0.002	0.0354 ± 0.0013	17.3 ± 0.15	6.05	93.67	80.8 ± 0.81
850	181.62 ± 0.36	9.786 ± 0.066	0.16 ± 0.002	0.0315 ± 0.0005	17.65 ± 0.13	6.64	94.9	82.43 ± 0.7
900	146.68 ± 0.29	7.813 ± 0.069	0.129 ± 0.001	0.0234 ± 0.0006	17.94 ± 0.17	5.3	95.3	83.7 ± 0.9
950	941.16 ± 1.88	49.38 ± 0.059	0.837 ± 0.002	0.1435 ± 0.0014	18.25 ± 0.05	33.48	95.52	85.14 ± 0.5
1000	920.11 ± 1.84	45.64 ± 0.07	0.773 ± 0.002	0.1312 ± 0.0002	19.35 ± 0.05	30.97	95.8	90.14 ± 0.5
1050	325.65 ± 0.65	15.439 ± 0.059	0.261 ± 0.002	0.042 ± 0.0016	20.34 ± 0.1	10.47	96.2	94.65 ± 0.6
1100	99.62 ± 0.2	4.647 ± 0.042	0.083 ± 0.001	0.0171 ± 0.0006	20.41 ± 0.2	3.15	94.98	95 ± 1
1150	29.96 ± 0.29	1.379 ± 0.017	0.023 ± 0.001	0.0069 ± 0.0008	20.31 ± 0.38	0.93	93.22	94.5 ± 1.8
1300	4.43 ± 0.09	0.049 ± 0.003	0.005 ± 0.0001	0.0142 ± 0.0007	5.47 ± 8.24	0.03	6.03	25 ± 38.8
Total fusion age = 87 Ma								
Weighted mean plateau age (800-1150°C) = 87.7 ± 0.25 Ma								

T (°C)	40Ar	39Ar	38Ar	36Ar	40Ar/39Ar(K)	39Ar(K)	%40Ar	Apparent age (Ma)
KAW 698 - Favaro								
	<i>Internal unit</i>		<i>J = 0.005049</i>		<i>wt. = 34.35 mg</i>	<i>phengite</i>		
550	269.28 ± 6.21	10.16 ± 0.229	0.742 ± 0.123	0.3904 ± 0.0823	15.144 ± 2.55	0.28	57.14	132.7 ± 21.58
650	738.00 ± 3.94	58.32 ± 0.159	0.916 ± 0.322	1.0309 ± 0.088	7.43 ± 0.45	1.62	58.69	66.32 ± 3.98
700	1247.17 ± 12.81	120.371 ± 0.727	2.196 ± 0.377	0.5219 ± 0.0791	9.074 ± 2.04	3.34	87.58	80.67 ± 2.04
750	1622.00 ± 25.8	164.39 ± 1.59	2.478 ± 0.475	0.5858 ± 0.0471	8.81 ± 0.2	4.56	89.27	78.39 ± 1.8
800	3025.3 ± 21.64	312.691 ± 1.592	4.009 ± 0.094	0.9031 ± 0.1537	8.81 ± 0.17	8.68	91.12	78.42 ± 1.5
850	4717.00 ± 121.88	488.631 ± 10.264	7.029 ± 0.157	1.3778 ± 0.0624	8.81 ± 0.32	13.56	91.29	78.4 ± 2.8
90	6483.5 ± 133.38	708.336 ± 13.444	9.909 ± 0.364	1.0714 ± 0.1422	8.7 ± 0.26	19.66	95.05	77.4 ± 2.3
950	7703.83 ± 24.52	822.577 ± 2.02	11.431 ± 0.292	1.6986 ± 0.1605	8.75 ± 0.07	22.83	93.4	77.8 ± 0.71
1000	6247.16 ± 11.56	664.469 ± 1.288	9.118 ± 0.053	0.9334 ± 0.0715	8.98 ± 0.04	18.44	95.5	79.87 ± 0.53
1150	835.35 ± 72.21	84.594 ± 4.289	1.651 ± 0.225	0.7046 ± 0.1114	7.4 ± 1.07	2.35	75.01	66.13 ± 9.39
1300	1444.77 ± 1.43	153.809 ± 0.108	2.084 ± 0.076	0.206 ± 0.0635	8.99 ± 0.12	4.27	95.72	79.9 ± 1.13
Total fr	212.04 ± 2.2	15.256 ± 0.064	0.487 ± 0.26	0.031 ± 0.1605	13.19 ± 3.11	0.42	95.64	117 ± 26.5
Total fusion age = 78 Ma Weighted mean plateau age (700-1000°C) = 79.1 ± 0.4 Ma								
KAW 700 - Isoello								
	<i>Northern intermediate unit</i>		<i>J = 0.004990</i>		<i>wt. = 34.52 mg</i>	<i>phengite</i>		
650	785.84 ± 2.88	103.637 ± 0.217	1.967 ± 0.193	0.4111 ± 0.2242	6.4 ± 0.64	2.64	84.46	56.75 ± 5.6
750	1951.38 ± 23.1	288.103 ± 2.237	4.153 ± 0.103	1.0181 ± 0.1433	5.72 ± 0.18	7.34	84.49	50.8 ± 1.6
850	6812.41 ± 94.75	1029.929 ± 12.181	14.217 ± 0.172	1.5602 ± 0.1333	6.16 ± 0.13	26.24	93.14	54.6 ± 1.1
900	10080.19 ± 114.65	1540.991 ± 15.831	21.236 ± 0.133	1.6365 ± 0.0823	6.22 ± 0.1	39.27	95.05	55.15 ± 1
950	2731.00 ± 20.39	414.766 ± 2.305	5.838 ± 0.103	0.6997 ± 0.0802	6.08 ± 0.08	10.57	92.34	53.93 ± 0.8
1000	2623.00 ± 11.32	398.229 ± 0.951	5.646 ± 0.116	0.4256 ± 0.0194	6.24 ± 0.04	10.15	95.12	55.55 ± 0.04
1100	774.6 ± 3.81	116.203 ± 0.247	1.981 ± 0.157	0.1785 ± 0.0366	6.2 ± 0.1	2.96	93.11	55.02 ± 0.91
1350	139.12 ± 0.95	17.264 ± 0.303	0.217 ± 0.101	0.0797 ± 0.1219	6.68 ± 2.09	0.44	83	59.22 ± 18.23
Fuse	150.42 ± 0.64	15.333 ± 0.625	0.263 ± 0.071	0.282 ± 0.0614	4.37 ± 1.27	0.39	44.54	38.9 ± 11.2
Total fusion age = 55 Ma Weighted mean plateau age (850-1350°C) = 55.2 ± 0.3 Ma								
KAW 702 - Ingria								
	<i>Intermediate unit</i>		<i>J = 0.005049</i>		<i>wt. = 43.52 mg</i>	<i>phengite</i>		
550	1718.08 ± 13.7	35.54 ± 0.784	2.344 ± 0.081	5.269 ± 0.2246	4.53 ± 2.39	0.11	9.36	40.7 ± 21.24
650	825.9 ± 2.2	95.155 ± 0.113	1.569 ± 0.077	1.083 ± 0.4586	5.31 ± 1.42	3	61.18	47.65 ± 12.62
750	2361.87 ± 70.06	312.036 ± 6.496	4.58 ± 0.201	1.3055 ± 0.1167	6.33 ± 0.3	9.83	83.59	56.63 ± 2.63
900	5462.00 ± 43.66	735.287 ± 3.387	10.017 ± 0.217	1.0202 ± 0.2392	7.01 ± 0.12	23.16	94.4	62.67 ± 1.08
950	6892.08 ± 266.93	954.642 ± 33.35	13.198 ± 0.651	1.5049 ± 0.1161	6.75 ± 0.38	30.07	93.47	60.32 ± 3.34
1000	5350.98 ± 64.21	779.548 ± 7.074	10.294 ± 0.103	0.9062 ± 0.1064	6.51 ± 0.11	24.55	94.91	58.28 ± 1.01
1050	844.7 ± 6.7	128.714 ± 0.373	1.731 ± 0.089	0.2426 ± 0.0722	6 ± 0.17	4.05	91.43	53.74 ± 1.57
1250	825.32 ± 4.44	110.349 ± 0.626	1.842 ± 0.14	0.324 ± 0.961	6.6 ± 0.26	3.48	88.32	59.08 ± 2.34
Fuse	490.34 ± 2.94	55.882 ± 0.086	0.978 ± 0.17	0.2877 ± 0.1131	7.25 ± 0.6	1.76	82.6	64.72 ± 5.28
Total fusion age = 59 Ma Weighted mean plateau age (750-1000°C) = 60.2 ± 0.7 Ma								
KAW 992 - Corio								
	<i>Southern internal unit</i>		<i>J = 0.005046</i>		<i>wt. = 44.39 mg</i>	<i>phengite</i>		
850	41.59.02 ± 97.47	616.823 ± 8.71	8.395 ± 0.634	1.7287 ± 0.2337	5.91 ± 0.22	16.68	97.63	52.94 ± 1.93
950	14604.33 ± 334.68	2196.51 ± 43.9	30.005 ± 0.64	3.4765 ± 0.2179	6.18 ± 0.2	59.41	92.88	55.29 ± 1.82
1050	4913.42 ± 54.53	735.632 ± 6.153	9.616 ± 0.288	0.7451 ± 0.1222	6.37 ± 0.11	19.99	95.43	57.04 ± 1
1150	639.69 ± 22.04	87.499 ± 1.565	1.44 ± 0.081	0.5129 ± 0.1142	5.57 ± 0.48	2.37	76.22	49.97 ± 4.25
1350	187.47 ± 6.26	23.603 ± 0.406	0.623 ± 0.087	0.1736 ± 0.1287	5.76 ± 1.64	0.64	72.57	51.66 ± 14.48
Fuse	291.02 ± 2.9	36.84 ± 0.208	0.985 ± 0.227	0.4741 ± 0.1238	4.09 ± 1	1	51.79	36.82 ± 8.89
Total fusion age = 55 Ma								
KAW 1424 - Fontainemore								
	<i>Internal unit</i>		<i>J = 0.005049</i>		<i>wt. = 39.58 mg</i>	<i>phengite</i>		
650	1131.97 ± 2.26	1.048 ± 0.08	0.802 ± 0.004	3.7557 ± 0.0061	32.17 ± 21.51	1.04	2.97	146.93 ± 54.88
750	72.97 ± 0.15	1.109 ± 0.01	0.055 ± 0.001	0.1876 ± 0.0041	16.35 ± 1.3	1.1	24.8	76.2 ± 5.98
800	93.61 ± 0.19	3.246 ± 0.013	0.072 ± 0.002	0.128 ± 0.0018	17.34 ± 0.21	3.23	59.99	80.7 ± 1.05
850	97.32 ± 0.19	4.789 ± 0.043	0.072 ± 0.001	0.0444 ± 0.0012	17.65 ± 0.21	4.76	86.64	82.1 ± 1.01
900	178.94 ± 0.36	8.802 ± 0.068	0.138 ± 0.002	0.0804 ± 0.0017	17.7 ± 0.17	8.75	86.83	82.3 ± 0.89
950	909.76 ± 1.82	47.335 ± 0.11	0.699 ± 0.003	0.2457 ± 0.002	17.74 ± 0.06	47.06	92.09	82.51 ± 0.5
1000	426.19 ± 0.85	22.179 ± 0.1557	0.33 ± 0.005	0.1162 ± 0.0019	17.72 ± 0.14	22.05	92	82.42 ± 0.77
1150	150.48 ± 0.3	8.078 ± 0.034	0.116 ± 0.002	0.0214 ± 0.0007	17.9 ± 0.09	8.03	95.81	83.2 ± 0.58
1300	57.96 ± 0.72	3.057 ± 0.038	0.05 ± 0.003	0.0127 ± 0.0019	17.79 ± 0.38	3.04	93.57	82.71 ± 1.78
Fuse	21.24 ± 0.14	0.927 ± 0.007	0.019 ± 0.001	0.0232 ± 0.0009	15.65 ± 0.37	0.93	68.1	72.97 ± 1.74
Total fusion age = 83 Ma Weighted mean plateau age (850-1000°C) = 82.4 ± 0.3 Ma								

T (°C)	40Ar	39Ar	38Ar	36Ar	40Ar/39Ar(K)	39Ar(K)	%40Ar	Apparent age (Ma)
<i>KAW 1425 - Ivory</i>		<i>Internal unit</i>		<i>J = 0.004570</i>	<i>wt. = 30.08 mg</i>	<i>phengite</i>		
650	524.96 ± 23.14	53.782 ± 0.904	1.477 ± 0.091	0.8403 ± 0.1263	5.14 ± 0.84	1.92	52.63	45.31 ± 7.28
750	2164.58 ± 21.5	269.364 ± 1.884	4.008 ± 0.08	0.9161 ± 0.1651	7.02 ± 0.21	9.62	87.42	61.67 ± 1.8
800	1874.36 ± 17.13	242.851 ± 1.63	3.361 ± 0.099	0.5952 ± 0.0583	6.99 ± 0.11	8.67	90.54	61.35 ± 1.02
850	3273.43 ± 30.24	424.482 ± 2.907	6.000 ± 0.083	0.8905 ± 0.1393	7.08 ± 0.13	15.16	91.89	62.19 ± 1.17
900	10655.24 ± 104.65	1381.733 ± 12.216	19.057 ± 0.175	1.8417 ± 0.1746	7.31 ± 0.11	49.35	94.82	64.14 ± 1
950	5318.23 ± 56.25	662.842 ± 5.641	9.689 ± 0.08	1.6099 ± 0.0242	7.3 ± 0.11	2.37	90.98	64.04 ± 1
1000	1612.82 ± 54.86	225.04 ± 3.371	4.523 ± 0.296	0.766 ± 0.1392	6.15 ± 0.32	8.04	85.87	54.14 ± 2.81
1150	1009.38 ± 14.2	127.813 ± 0.808	2.176 ± 0.111	0.3925 ± 0.1385	6.98 ± 0.34	4.56	88.44	61.31 ± 2.98
1350	85.88 ± 3.98	8.772 ± 0.415	0.517 ± 0.112	0.1931 ± 0.063	3.28 ± 2.24	0.31	33.49	29.04 ± 19.68

Total fusion age = 62 Ma

Weighted mean plateau age (750 -950°C) = 62.9 ± 0.5 Ma

<i>KAW 1432 - Fondo</i>		<i>Internal unit</i>		<i>J = 0.004980</i>	<i>wt. = 43.86 mg</i>	<i>phengite</i>		
650	521.66 ± 7.17	39.173 ± 0.428	0.714 ± 0.106	0.7596 ± 0.0703	7.58 ± 0.58	0.89	56.92	66.85 ± 5.05
750	2661.32 ± 10.08	242.928 ± 0.684	3.716 ± 0.065	1.6473 ± 0.0351	8.94 ± 0.07	5.51	81.66	78.63 ± 0.7
800	3212.59 ± 47.79	312.324 ± 3.946	4.509 ± 0.129	1.7195 ± 0.1129	8.65 ± 0.23	7.08	84.13	76.11 ± 2
850	9781.06 ± 145.09	996.275 ± 13.578	14.093 ± 0.193	3.3427 ± 0.1483	8.82 ± 0.2	22.58	89.84	77.55 ± 1.79
900	7381.06 ± 121.2	789.147 ± 11.446	11.188 ± 0.16	0.8652 ± 0.2527	9.02 ± 0.23	17.88	96.47	79.3 ± 1.98
950	5247.78 ± 58.28	542.998 ± 5.27	7.14 ± 0.706	1.6105 ± 0.0248	8.78 ± 0.14	12.31	90.87	77.22 ± 1.3
1050	11428.84 ± 56.4	1193.086 ± 5.452	16.796 ± 0.373	2.1158 ± 0.5731	9.05 ± 0.16	27.04	94.47	79.52 ± 1.4
1150	1862.73 ± 9.12	197.241 ± 0.747	2.732 ± 0.316	0.5597 ± 0.1194	8.6 ± 0.19	4.47	91.06	75.65 ± 1.66
1300	931.17 ± 4.09	99.186 ± 0.353	1.811 ± 0.533	0.0991 ± 0.0502	9.09 ± 0.16	2.25	96.79	79.85 ± 1.42

Total fusion age = 78 Ma

Weighted mean plateau age (750 -1050°C) = 78.3 ± 0.5 Ma

<i>KAW 1521 - Centovalli</i>		<i>External unit</i>		<i>J = 0.005049</i>	<i>wt. = 44.69 mg</i>	<i>phengite</i>		
550	426.59 ± 10.98	50.241 ± 0.409	1.405 ± 0.084	1.0694 ± 0.0427	2.19 ± 0.34	1.08	25.85	19.85 ± 3.1
650	342.41 ± 6.53	69.093 ± 0.481	1.015 ± 0.067	0.649 ± 0.0786	2.17 ± 0.35	1.49	43.87	19.66 ± 3.16
700	520.5 ± 14.28	139.055 ± 1.355	2.117 ± 0.094	0.5012 ± 0.1264	2.67 ± 0.29	3	71.39	24.16 ± 2.6
800	1117.00 ± 46.44	320.846 ± 6.715	4.745 ± 0.19	1.2838 ± 0.0427	2.29 ± 0.17	6.93	65.87	20.73 ± 1.52
900	2340.24 ± 35.38	806.672 ± 7.597	11.191 ± 0.18	1.1741 ± 0.0517	2.46 ± 0.06	17.41	84.98	22.28 ± 0.51
950	1635.01 ± 85.24	565.566 ± 18.762	8.109 ± 0.287	0.9223 ± 0.0687	2.4 ± 0.18	12.21	83.13	21.72 ± 1.64
1000	1252.29 ± 12.73	412.297 ± 2.155	5.47 ± 0.09	0.8973 ± 0.2029	2.39 ± 0.15	8.91	78.64	21.59 ± 1.35
1050	2289.75 ± 8.06	774.867 ± 1.38	10.413 ± 0.116	0.8956 ± 0.0528	2.61 ± 0.02	16.73	88.25	23.56 ± 0.24
1150	3933.93 ± 7.97	1425.408 ± 1.035	18.86 ± 0.042	0.7262 ± 0.096	2.6 ± 0.02	30.76	94.34	23.51 ± 0.22
1350	228.17 ± 2.06	68.956 ± 0.26	0.953 ± 0.048	0.2513 ± 0.1927	2.23 ± 0.83	1.49	67.28	20.13 ± 7.4

Total fusion age = 23 Ma

<i>SV9111C-Cavalcurt</i>		<i>Monometamorphic cover sequences</i>		<i>J = 0.0025525</i>	<i>wt. = 2.62 mg</i>	<i>phengite</i>		
800	0.86 ± 0.00	0.039 ± 0.000	0.001 ± 0.000	0.001 ± 0.0000	14.78 ± 0.14	0.45	67.01	66.8 ± 0.64
850	2.65 ± 0.01	1.51 ± 0.001	0.2 ± 0.000	0.0013 ± 0.0000	15.16 ± 0.09	72.75	85.84	68.5 ± 0.42
900	5.7 ± 0.01	0.367 ± 0.001	0.005 ± 0.000	0.0008 ± 0.0000	14.95 ± 0.05	7.59	95.84	67.51 ± 0.27
950	2.99 ± 0.01	0.197 ± 0.000	0.003 ± 0.000	0.0005 ± 0.0000	14.5 ± 0.06	7.59	95.08	65.58 ± 0.3
1000	1.09 ± 0.00	0.07 ± 0.000	0.001 ± 0.000	0.0003 ± 0.0000	14.36 ± 0.07	11.86	91.29	64.96 ± 0.35
1050	1.04 ± 0.00	0.066 ± 0.000	0.001 ± 0.000	0.0003 ± 0.0000	14.51 ± 0.07	3.48	92.28	65.59 ± 0.35
1150	2.77 ± 0.01	0.177 ± 0.000	0.001 ± 0.000	0.0005 ± 0.0000	14.87 ± 0.05	1.86	94.58	67.21 ± 0.29
1350	0.64 ± 0.00	0.028 ± 0.000	0.001 ± 0.000	0.0007 ± 0.0000	15.41 ± 0.23	1.86	67.01	69.62 ± 1.05

Total fusion age = 67 Ma

<i>SV9111F-Fontainemore</i>		<i>Internal unit</i>		<i>J = 0.0025365</i>	<i>wt. = 2.79 mg</i>	<i>phengite</i>		
700	0.5 ± 0.00	0.019 ± 0.000	0.000 ± 0.000	0.0005 ± 0.0000	18.18 ± 0.3	1	68.81	81.34 ± 1.31
800	0.18 ± 0.00	0.009 ± 0.000	0.000 ± 0.000	0.0001 ± 0.0000	17.18 ± 0.35	0.45	82.95	77 ± 1.55
850	25.85 ± 0.05	1.398 ± 0.003	0.2 ± 0.000	0.0059 ± 0.0000	17.33 ± 0.05	72.75	93.29	77.62 ± 0.3
950	2.66 ± 0.01	0.146 ± 0.000	0.002 ± 0.000	0.0006 ± 0.0000	17.24 ± 0.05	7.59	93.95	77.23 ± 0.29
1000	4.18 ± 0.01	0.228 ± 0.001	0.003 ± 0.000	0.0007 ± 0.0000	17.53 ± 0.07	11.86	95.13	78.5 ± 0.36
1050	1.27 ± 0.00	0.067 ± 0.000	0.001 ± 0.000	0.0003 ± 0.0000	17.99 ± 0.08	3.48	93.94	80.49 ± 0.39
1350	1.15 ± 0.00	0.036 ± 0.000	0.001 ± 0.000	0.0018 ± 0.0000	17.32 ± 0.018	1.86	53.61	77.56 ± 0.79
Fuse	5.12 ± 0.01	0.019 ± 0.000	0.03 ± 0.000	0.0161 ± 0.0001	24.18 ± 2.1	1	9.04	107.39 ± 9.06

Total fusion age = 78 Ma

Weighted mean plateau age (800-1000°C) = 77.6 ± 0.7 Ma

T (°C)	40Ar	39Ar	38Ar	36Ar	40Ar/39Ar(K)	39Ar(K)	%40Ar	Apparent age (Ma)
SV912T - Tavagnasco		Internal unit		J = 0.0025225	wt. = 2.72 mg	<i>phengite</i>		
700	1.31 ± 0.00	0.077 ± 0.000	0.001 ± 0.000	0.0006 ± 0.0000	14.88 ± 0.09	4.49	87.32	66.46 ± 0.43
800	1.20 ± 0.00	0.075 ± 0.000	0.001 ± 0.000	0.0002 ± 0.0000	16.82 ± 0.09	4.35	94.57	74.96 ± 0.42
850	0.43 ± 0.00	0.025 ± 0.000	0.000 ± 0.000	0.0000 ± 0.0000	17.06 ± 0.16	1.43	98.04	76.01 ± 0.72
900	5.06 ± 0.01	0.276 ± 0.000	0.004 ± 0.000	0.0006 ± 0.0000	17.77 ± 0.05	16.09	96.41	79.1 ± 0.3
950	12.00 ± 0.02	0.654 ± 0.000	0.009 ± 0.000	0.0010 ± 0.0000	18 ± 0.04	38.15	97.59	80.13 ± 0.3
1000	5.60 ± 0.01	0.300 ± 0.000	0.004 ± 0.000	0.0006 ± 0.0000	18.14 ± 0.05	17.51	96.8	80.72 ± 0.3
1050	4.26 ± 0.01	0.230 ± 0.000	0.003 ± 0.000	0.0003 ± 0.0000	18.22 ± 0.06	13.41	97.9	81.9 ± 0.3
1100	0.89 ± 0.00	0.048 ± 0.000	0.001 ± 0.000	0.0001 ± 0.0000	17.91 ± 0.11	2.82	96.77	79.74 ± 0.56
1350	0.45 ± 0.00	0.024 ± 0.000	0.000 ± 0.000	0.0001 ± 0.0000	18.63 ± 0.16	1.38	96.49	82.87 ± 0.72
Fuse	0.17 ± 0.00	0.006 ± 0.000	0.000 ± 0.000	0.0003 ± 0.0000	15.7 ± 0.83	0.36	56.38	70.09 ± 3.63

Total fusion age = 79 Ma

Weighted mean plateau age (9501050 °C) = 80.6 ± 0.5 Ma

T (°C)	40Ar	39Ar	38Ar	36Ar	40Ar/39Ar(K)	39Ar(K)	%40Ar	Apparent age (Ma)
SV913Q - Quincinetto		<i>Monometamorphic cover sequences</i>		J = 0.0025300	wt. = 2.51 mg	<i>phengite</i>		
700	2.86 ± 0.01	0.023 ± 0.000	0.002 ± 0.000	0.0088 ± 0.0000	13.56 ± 0.9	2.44	10.75	60.87 ± 3.97
800	1.22 ± 0.00	0.069 ± 0.000	0.001 ± 0.000	0.0008 ± 0.0000	14.56 ± 0.14	7.33	81.25	65.26 ± 0.65
850	1.43 ± 0.00	0.85 ± 0.000	0.001 ± 0.000	0.0007 ± 0.0000	14.62 ± 0.09	9.04	86.28	65.52 ± 0.41
900	3.9 ± 0.01	0.249 ± 0.000	0.004 ± 0.000	0.0012 ± 0.0000	14.3 ± 0.04	26.59	90.83	64.14 ± 0.23
950	2.73 ± 0.01	0.175 ± 0.000	0.002 ± 0.000	0.0006 ± 0.0000	14.73 ± 0.06	18.74	93.07	65.33 ± 0.31
1000	1.81 ± 0.00	0.113 ± 0.000	0.002 ± 0.000	0.0006 ± 0.0000	14.68 ± 0.05	12.02	90.89	65.79 ± 0.27
1150	3.44 ± 0.01	0.215 ± 0.000	0.003 ± 0.000	0.0011 ± 0.0000	14.661 ± 0.05	22.93	90.74	65.47 ± 0.27
1250	0.13 ± 0.00	0.008 ± 0.000	0.000 ± 0.000	0.0000 ± 0.0000	15.73 ± 0.51	0.87	99.45	70.42 ± 2.27
1350	0.01 ± 0.00	0.000 ± 0.000	0.000 ± 0.000	0.0000 ± 0.0000	29 ± 10.46	0.04	100	127.71 ± 44.49

Total fusion age = 66 Ma

Weighted mean plateau age (750-950 °C) = 65.2 ± 0.2 Ma

SV914B -Bonze - Monometamorphic cover sequences

J = 0.01602; wt. = 55.51 mg

650	726.25 ± 1.45	4.118 ± 0.005	0.626 ± 0.001	2.4609 ± 0.0063	1.58 ± 0.7	0	0.89	45.1 ± 19.83
750	67.84 ± 0.43	8.101 ± 0.067	0.156 ± 0.002	0.1512 ± 0.0043	2.92 ± 0.18	0	34.76	82.28 ± 5.08
800	60.88 ± 0.46	15.08 ± 0.115	0.221 ± 0.0003	0.0662 ± 0.0018	2.75 ± 0.06	3.84	68.06	77.76 ± 1.6
850	79.94 ± 0.16	23.047 ± 0.15	0.33 ± 0.003	0.0602 ± 0.0013	2.71 ± 0.03	57.16	77.85	76.44 ± 0.84
900	281.32 ± 0.56	90.451 ± 0.181	1.25 ± 7.000	0.1475 ± 0.0025	2.63 ± 0.001	57.16	84.49	74.43 ± 0.4
950	442.17 ± 0.88	161.146 ± 0.322	2.149 ± 0.01	0.0963 ± 0.0026	2.57 ± 0.01	8.29	93.43	72.65 ± 0.33
1000	790.13 ± 1.58	287.217 ± 0.574	3.865 ± 0.003	0.1792 ± 0.0013	2.57 ± 0.01	7.37	93.2	72.66 ± 0.3
1050	261.66 ± 0.52	89.568 ± 0.179	1.262 ± 0.07	0.0673 ± 0.0017	2.71 ± 0.01	10.05	92.43	76.44 ± 0.35
1150	108.71 ± 0.22	37.573 ± 0.156	0.542 ± 0.005	4.321 ± 0.83	2.74 ± 0.02	4.65	94.53	77.41 ± 0.46
1350	145.77 ± 0.29	49.861 ± 0.168	0.706 ± 0.003	0.0399 ± 0.0016	2.7 ± 0.02	8.68	92.09	76.22 ± 0.46
Fuse	7.3 0.08	0.507 0.004	0.012 0.001	0.0126 0.0007	6.99 0.46	8.68	48.9425	191.25 12.02

Total fusion age = 74 Ma

Weighted mean plateau age (850-1050 °C) = 74 ± 0.2 Ma

T (°C)	40Ar	39Ar	38Ar	36Ar	40Ar/39Ar(K)	39Ar(K)	%40Ar	Apparent age (Ma)
SV915M - Mombarone		<i>Monometamorphic cover sequences</i>		J = 0.0025705	wt. = 2.74 mg	<i>phengite</i>		
700	0.88 ± 0.00	0.045 ± 0.000	0.001 ± 0.000	0.0005 ± 0.0000	16.47 ± 0.14	0	84.06	74.8 ± 0.64
800	1.05 ± 0.00	0.06 ± 0.000	0.001 ± 0.000	0.0003 ± 0.0000	16.24 ± 0.1	3.84	93.04	73.77 ± 0.49
900	14.65 ± 0.03	0.899 ± 0.000	0.012 ± 0.000	0.0019 ± 0.0000	15.75 ± 0.04	57.16	96.2	71.58 ± 0.23
950	2.1 ± 0.00	0.13 ± 0.000	0.002 ± 0.000	0.0002 ± 0.0000	15.76 ± 0.06	8.29	96.89	71.64 ± 0.31
1000	1.9 ± 0.00	0.116 ± 0.000	0.002 ± 0.000	0.0002 ± 0.0000	15.84 ± 0.06	7.37	96.33	72.01 ± 0.32
1050	2.55 ± 0.01	0.158 ± 0.000	0.002 ± 0.000	0.0002 ± 0.0000	15.84 ± 0.03	10.05	97.79	72.02 ± 0.32
1150	1.19 ± 0.00	0.073 ± 0.000	0.001 ± 0.000	0.0001 ± 0.0000	15.82 ± 0.07	4.65	97.04	71.9 ± 0.37
1350	2.19 ± 0.00	0.136 ± 0.000	0.002 ± 0.000	0.0001 ± 0.0000	15.83 ± 0.05	8.68	98.32	71.95 ± 0.28

Total fusion age = 72 Ma

Weighted mean plateau age (800-1350 °C) = 71.8 ± 0.2 Ma

T (°C)	40Ar	39Ar	38Ar	36Ar	40Ar/39Ar(K)	39Ar(K)	%40Ar	Apparent age (Ma)
SV921D - Val Dolca		Internal unit		J = 0.0026645	wt. = 0.1602 mg	<i>phengite</i>		
650	7.1 ± 0.01	0.021 ± 0.002	0.005 ± 0.000	0.024 ± 0.0001	6.18 ± 40.91	1.07	1.79	29.47 ± 193
800	1.01 ± 0.00	0.048 ± 0.001	0.001 ± 0.000	0.0009 ± 0.0000	16 ± 0.26	2.46	74.99	75.31 ± 1.2
850	1.5 ± 0.00	0.081 ± 0.000	0.001 ± 0.000	0.0006 ± 0.0000	16.51 ± 0.09	4.17	88.44	77.69 ± 0.46
900	6.23 ± 0.01	0.348 ± 0.002	0.005 ± 0.000	0.0016 ± 0.0000	16.64 ± 0.1	18.02	92.5	78.24 ± 0.5
950	11.28 ± 0.02	0.66 ± 0.000	0.01 ± 0.000	0.004 ± 0.0000	16.47 ± 0.04	34.16	95.95	77.49 ± 0.26
1000	5.74 ± 0.01	0.331 ± 0.001	0.005 ± 0.000	0.0008 ± 0.0000	16.69 ± 0.07	17.12	95.72	78.49 ± 0.36
1100	4.38 ± 0.01	0.254 ± 0.000	0.004 ± 0.000	0.0006 ± 0.0000	16.64 ± 0.05	13.12	95.83	78.25 ± 0.3
1350	2.6 ± 0.01	0.152 ± 0.001	0.002 ± 0.000	0.0003 ± 0.0000	16.55 ± 0.07	7.88	96.32	77.86 ± 0.39
Fuse	0.7 ± 0.00	0.039 ± 0.000	0.001 ± 0.000	0.0002 ± 0.0000	16.64 ± 0.22	2	91.43	78.28 ± 1.05

Total fusion age = 77 Ma

T (°C)	40Ar	39Ar	38Ar	36Ar	40Ar/39Ar(K)	39Ar(K)	%40Ar	Apparent age (Ma)
SV921DZ - Donnaz		Intermediate unit		J = 0.0025325	wt. = 2.52 mg	phengite		
700	2.45 ± 0.00	0.037 ± 0.000	0.002 ± 0.000	0.0066 ± 0.0000	14.17 ± 0.58	2.25	21.47	63.59 ± 0.256
800	1.29 ± 0.00	0.043 ± 0.000	0.001 ± 0.000	0.0023 ± 0.0000	14.54 ± 0.31	2.62	48.84	65.27 ± 1.38
850	2.45 ± 0.00	0.107 ± 0.000	0.002 ± 0.000	0.0032 ± 0.0000	14.38 ± 0.11	6.42	62.18	64.53 ± 0.51
900	4.5 ± 0.01	0.291 ± 0.001	0.000 ± 0.000	0.0013 ± 0.0000	14.23 ± 0.06	17.55	91.74	63.88 ± 0.31
950	10.5 ± 0.02	0.708 ± 0.000	0.01 ± 0.000	0.0015 ± 0.0000	14.26 ± 0.03	42.67	95.7	64.01 ± 21
1000	3.8 ± 0.01	0.254 ± 0.001	0.003 ± 0.000	0.0006 ± 0.0000	14.32 ± 0.05	15.3	95.18	64.26 ± 0.25
1050	1.91 ± 0.00	0.126 ± 0.000	0.002 ± 0.000	0.0003 ± 0.0000	14.47 ± 0.06	7.61	95.38	64.94 ± 0.29
1100	1.11 ± 0.00	0.07 ± 0.000	0.001 ± 0.000	0.0003 ± 0.0000	14.69 ± 0.08	4.24	92.78	65.92 ± 0.37
1350	0.17 ± 0.00	0.01 ± 0.000	0.000 ± 0.000	0.0001 ± 0.0000	14.46 ± 0.21	0.62	89.57	64.88 ± 0.92
Fuse	0.61 ± 0.00	0.012 ± 0.000	0.000 ± 0.000	0.0015 ± 0.0000	15.94 ± 0.71	0.73	31.17	71.38 ± 3.1

Total fusion age = 64 Ma

T (°C)	40Ar	39Ar	38Ar	36Ar	40Ar/39Ar(K)	39Ar(K)	%40Ar	Apparent age (Ma)
SV923P - Perlioz		Intermediate unit		J = 0.0026635	wt. = 2.91 mg	phengite		
700	2.04 ± 0.00	0.023 ± 0.000	0.001 ± 0.000	0.0054 ± 0.0000	20.088 ± 0.98	1.04	22.47	94.03 ± 4.47
800	0.66 ± 0.00	0.024 ± 0.000	0.001 ± 0.000	0.0006 ± 0.0000	20.63 ± 0.34	2.13	74.62	96.49 ± 1.57
850	1.6 ± 0.00	0.066 ± 0.000	0.001 ± 0.000	0.0006 ± 0.0000	21.7 ± 0.1	3	89.33	101.37 ± 0.52
900	2.78 ± 0.01	0.115 ± 0.000	0.002 ± 0.000	0.0009 ± 0.0000	22.01 ± 0.08	5.21	90.39	102.76 ± 0.45
950	19.94 ± 0.04	0.828 ± 0.002	0.014 ± 0.000	0.0055 ± 0.0000	22.23 ± 0.07	37.62	91.93	103.77 ± 0.4
1000	11.07 ± 0.02	0.458 ± 0.000	0.007 ± 0.000	0.003 ± 0.0000	22.38 ± 0.05	20.79	92.11	104.44 ± 0.35
1050	5.74 ± 0.01	0.235 ± 0.000	0.004 ± 0.000	0.0015 ± 0.0000	22.76 ± 0.06	10.65	92.62	106.2 ± 0.37
1150	5.28 ± 0.01	0.213 ± 0.000	0.003 ± 0.0013	0.0000 ± 0.0000	23.14 ± 0.08	9.68	92.89	107.89 ± 0.43
1350	3.9 ± 0.01	0.162 ± 0.000	0.003 ± 0.000	0.001 ± 0.0000	22.5 ± 0.08	9.68	92.84	105 ± 0.44
Fuse	0.32 ± 0.00	0.079 ± 0.000	0.001 ± 0.000	0.0002 ± 0.0000	3.36 ± 0.06	7.34	81.17	16.06 ± 0.31

Total fusion age = 101 Ma

Weighted mean plateau age (900-1000 °C) = 104.0 ± 0.3 Ma

T (°C)	40Ar	39Ar	38Ar	36Ar	40Ar/39Ar(K)	39Ar(K)	%40Ar	Apparent age (Ma)
SV923Q - Quincinetto		Monometamorphic cover sequences		J = 0.0025225	wt. = 2.90 mg	phengite		
700	0.99 ± 0.00	0.035 ± 0.000	0.001 ± 0.000	0.0012 ± 0.0000	18.48 ± 0.28	0	65.06	82.2 ± 1.25
800	1.21 ± 0.00	0.0055 ± 0.000	0.001 ± 0.000	0.0008 ± 0.0000	17.91 ± 0.21	3.84	80.44	79.71 ± 0.92
850	1.24 ± 0.00	0.06 ± 0.000	0.001 ± 0.000	0.0006 ± 0.0000	17.62 ± 0.12	57.16	85.68	78.46 ± 0.56
900	5.28 ± 0.01	0.292 ± 0.000	0.004 ± 0.000	0.0016 ± 0.0000	16.6 ± 0.06	57.16	91.35	74.02 ± 0.32
950	6.49 ± 0.01	0.376 ± 0.000	0.005 ± 0.000	0.001 ± 0.0000	16.55 ± 0.04	8.29	95.37	73.78 ± 0.25
1000	4.6 ± 0.01	0.257 ± 0.000	0.004 ± 0.000	0.001 ± 0.0000	16.91 ± 0.05	7.37	93.83	75.34 ± 0.29
1050	2.13 ± 0.00	0.115 ± 0.000	0.002 ± 0.000	0.0006 ± 0.0000	17.09 ± 0.09	10.05	92.06	76.14 ± 0.43
1100	0.55 ± 0.00	0.029 ± 0.000	0.003 ± 0.000	0.0002 ± 0.0000	16.68 ± 0.15	4.65	89.48	74.4 ± 0.7
1350	3.39 ± 0.01	0.193 ± 0.000	0.003 ± 0.000	0.0006 ± 0.0000	16.69 ± 0.06	8.68	94.5	74.39 ± 0.3

Total fusion age = 76 Ma

Weighted mean plateau age (900-1000 °C) = 74.5 ± 0.2 Ma

T (°C)	40Ar	39Ar	38Ar	36Ar	40Ar/39Ar(K)	39Ar(K)	%40Ar	Apparent age (Ma)
SV925VC - Tallorno		Monometamorphic cover sequences		J = 0.0025430	wt. = 2.64 mg	phengite		
700	0.49 ± 0.000	0.024 ± 0.000	0.000 ± 0.000	0.0004 ± 0.0000	15.63 ± 0.22	2.65	75.69	70.34 ± 0.99
800	0.63 ± 0.00	0.035 ± 0.000	0.000 ± 0.000	0.0003 ± 0.0000	16.05 ± 0.16	3.9	87.82	72.16 ± 0.71
850	0.86 ± 0.00	0.048 ± 0.000	0.001 ± 0.000	0.0003 ± 0.0000	16.17 ± 0.13	5.37	90.53	72.68 ± 0.59
900	3.65 ± 0.01	0.218 ± 0.000	0.0003 ± 0.000	0.0007 ± 0.0000	15.91 ± 0.04	24.18	71.55	71.55 ± 0.24
950	4.51 ± 0.01	0.276 ± 0.000	0.004 ± 0.000	0.0006 ± 0.0000	15.79 ± 0.05	30.81	96.16	71.04 ± 0.27
1000	2.86 ± 0.01	0.17 ± 0.001	0.002 ± 0.000	0.0004 ± 0.0000	16.13 ± 0.07	18.96	95.47	72.51 ± 0.34
1050	0.52 ± 0.00	0.031 ± 0.000	0.000 ± 0.000	0.0001 ± 0.0000	16.03 ± 0.18	3.48	95.07	72.08 ± 0.81
1150	1.2 ± 0.00	0.07 ± 0.000	0.001 ± 0.000	0.0003 ± 0.0000	16.06 ± 0.07	7.83	93.71	72.23 ± 0.35
1350	0.5 ± 0.00	0.025 ± 0.000	0.000 ± 0.000	0.0001 ± 0.0000	18.42 ± 0.12	2.82	92.92	82.56 ± 0.58

Total fusion age = 72 Ma

126/91 - Savenca - Internal unit

J = 0.0026404; wt. = 1.29 mg

650	570.88 ± 1.14	5.576 ± 0.017	0.401 ± 0.002	1.2899 ± 0.0063	34.84 ± 0.55	5.56	33.94	158.8 ± 2.4
800	178.21 ± 2.16	29.255 ± 0.050	0.683 ± 0.003	0.2072 ± 0.0014	34.88 ± 0.1	29.18	94.38	158.9 ± 0.4
850	1688.52 ± 3.38	47.993 ± 0.033	1.151 ± 0.001	0.2042 ± 0.0008	34.05 ± 0.08	47.86	96.51	155.3 ± 0.3
900	567.21 ± 1.13	15.536 ± 0.014	0.458 ± 0.001	0.1389 ± 0.0006	34.04 ± 0.08	15.49	92.96	155.3 ± 0.4
950	316.48 ± 0.63	8.084 ± 0.015	0.213 ± 0.002	0.0691 ± 0.0008	36.77 ± 0.11	8.06	93.66	167.2 ± 0.5
1000	185.77 ± 0.37	4.645 ± 0.042	0.110 ± 0.002	0.0233 ± 0.0011	38.63 ± 0.38	4.63	96.33	175.2 ± 1.6
1100	216.29 ± 0.43	5.975 ± 0.047	0.129 ± 0.002	0.0144 ± 0.0010	35.58 ± 0.3	5.96	98.04	162 ± 1.3
1250	105.62 ± 0.04	3.005 ± 0.036	0.650 ± 0.001	0.0085 ± 0.0009	34.4 ± 0.44	3	97.64	156.9 ± 1.9
1350	2.53 ± 0.13	0.102 ± 0.005	0.005 ± 0.001	0.0073 ± 0.0013	3.13 ± 4.16	0.101	16.55	19.6 ± 19.6

Total fusion age = 158 Ma

Weighted mean plateau age (800900 °C) = 156 ± .8 Ma

T (°C)	40Ar	39Ar	38Ar	36Ar	40Ar/39Ar(K)	39Ar(K)	%40Ar	Apparent age (Ma)
-----------	------	------	------	------	--------------	---------	-------	----------------------

mb1k/91 -Savenca - Internal unit

J = 0.0026295; wt. = 1.58 mg

650	699.90 ± 1.40	1.200 ± 0.005	0.505 ± 0.002	2.2184 ± 0.0083	42.76 ± 4.38	1.19	7.3	192.2 ± 18.7
800	689.80 ± 1.38	14.524 ± 0.028	0.293 ± 0.002	0.1121 ± 0.0018	45.35 ± 0.14	14.48	95.25	203.3 ± 0.6
900	600.07 ± 1.20	13.477 ± 0.032	0.248 ± 0.001	0.0275 ± 0.0004	44.05 ± 0.14	13.44	98.67	197.7 ± 0.6
950	573.08 ± 1.15	13.594 ± 0.005	0.384 ± 0.001	0.1573 ± 0.0008	39.1 ± 0.09	13.55	92.13	176.5 ± 0.4
1000	293.99 ± 0.59	6.489 ± 0.046	0.119 ± 0.003	0.0289 ± 0.0010	44.11 ± 0.34	6.47	97.11	198 ± 1.43
1050	142.85 ± 0.29	2.987 ± 0.023	0.055 ± 0.002	0.0152 ± 0.0009	46.45 ± 0.39	2.98	97.79	207.9 ± 1.7
1150	626.37 ± 1.25	14.313 ± 0.021	0.250 ± 0.002	0.0392 ± 0.0003	43.08 ± 0.11	14.27	98.18	193.7 ± 0.5
1300	43.28 ± 0.47	0.980 ± 0.016	0.016 ± 0.002	0.0036 ± 0.0009	43.2 ± 0.92	0.97	97.56	194.1 ± 3.9
1540	8.02 ± 0.13	0.160 ± 0.005	0.009 ± 0.001	0.0168 ± 0.0004	19.53 ± 2.02	0.159	38.81	90.4 ± 9.1

Total fusion age = 194 Ma

KAW 998 -Mucrone - Internal unit

J = .005049; wt. = 41.09 mg

500	1870.00 ± 9.00	36.500 ± 0.300	3.600 ± 0.100	3.5700 ± 0.2800	35.02 ± 12.56	33.4	62.54	293.6 ± 97.2
650	16977.00 ± 157.00	570.000 ± 5.100	28.600 ± 0.400	9.3500 ± 0.5500	29.21 ± 2.94	553.19	95.2	248 ± 23.4
750	34105.00 ± 244.00	1433.800 ± 7.800	69.500 ± 0.300	4.4200 ± 0.3200	23.1 ± 0.34	1431.4	96.95	199 ± 2.78
850	40844.00 ± 110.00	1707.000 ± 6.000	826.000 ± 0.900	43.8000 ± 0.1700	23 ± 0.33	1709	96.24	198.2 ± 2.7
950	17085.00 ± 102.00	706.500 ± 4.600	34.200 ± 0.200	1.8700 ± 0.36	22.75 ± 0.44	709.77	94.5	196.1 ± 3.6
1050	7965.00 ± 11.00	357.700 ± 1.200	15.700 ± 0.100	1.2900 ± 0.2900	22.05 ± 0.78	355.45	98.38	190.4 ± 6.41
1150	14086.00 ± 6.90	560.700 ± 0.320	28.100 ± 0.400	1.93 ± 0.0800	20.16 ± 2.44	576.9	82.52	174.9 ± 20.5
1250	5905.50 ± 12.70	230.305 ± 0.710	11.722 ± 0.065	0.8275 ± 0.0932	24.57 ± 0.15	230.3	95.84	231.3 ± 9.4

Total fusion age = 202 Ma

Weighted mean plateau age (700-1150 °C) = 198 ± 2 Ma

Plate I - The Polycyclic Basement Complex



PHOTO 1.1. View of the southern face of the Cima di Bonze and of the upper Scalario valley. The monometamorphic cover sequences outcrop in the shaded cliffs and in upper-right sector of the Photo. They can be recognised by alternating blue-green lithologies (metabasalts) interbedded with leucocratic gneisses (impure quartzites and gneiss pipernoïdes)



PHOTO 1.2. Mylonitised and refolded basement composed of strongly deformed high grade parashists and pre-Alpine meta-aplites. The amphibolitic assemblages are generally completely transformed by Alpine parageneses, although relics of dark-blue high temperature quartz can still be seen.



PHOTO 1.3. Northern side of the C. Cavalcourt 2210 m. alt. Polymetamorphic marble of the polycyclic basement complex. This lithology is characterized by an highly transposed decimetric alternation of calcite-rich and silicate-rich levels. Quincinetto, private area of ENEL Idroelectric Power

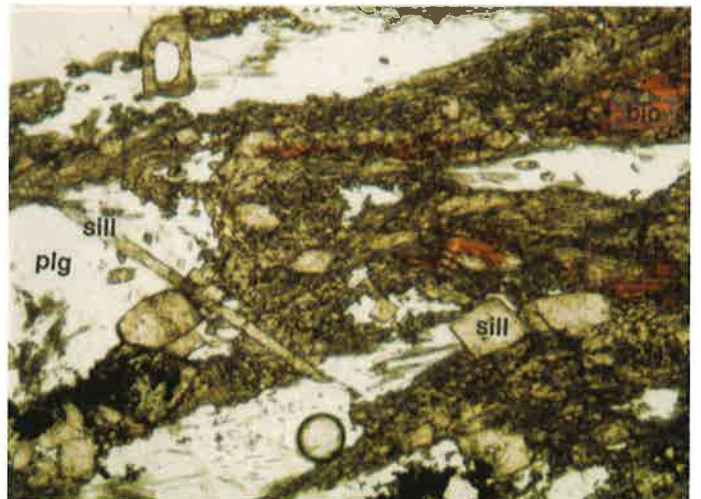


PHOTO 1.4. Photomicrograph of a pre-Alpine garnet, biotite, sillimanite, plagioclase and quartz-bearing assemblage (kinzigitites) in transformed metakinzigitites; the sillimanite is replaced by kyanite, the biotite is replaced by Alpine garnet and the plagioclase is completely saussuritised. Southern side of the

Plate II/a - The Monometamorphic Cover Complex and the pre-Alpine high grade basement Complex



PHOTO 2.1. The south-eastern sector of the Cima di Bonze (2360-2480 m). The top of the cliff is composed of metabasalts and related metasediments. A ten meter-thick level of calcschists and yellow-white dolomitic marbles underlies the mafic rocks. At the base of the sequence a strongly mylonitised basem



PHOTO 2.2. Decametric tight F2 folds in impure quartzites of the monometamorphic cover sequence. The metabasalts form the upper part of the cliff. Interbedded between the mafic rocks and the quartzites there is a metric level of dolomitic limestones. Northern face of Colletto Bonze 1950 m.

Plate II/b - The Monometamorphic Cover Complex and the pre-Alpine high grade basement Complex



PHOTO 2.3. Well-preserved garnet granulate in the pre-Alpine high grade basement complex, outcropping in the upper Fert valley (southern side of the lower Aosta valley). Northern face of Colle Finestra, 2250 m.



PHOTO 2.4. Pre-Alpine centimetric garnets rimmed by Alpine glaucophane. A fine grained zoisite and phengite matrix replaces the pre-Alpine plagioclase. Pre-Alpine high grade basement complex, upper Fert Valley, 2160 m.

Plate III - Glaucophane-eclogites and related metasediments



PHOTO 3.1. Relics of pillow lava textures in within basaltic levels from the upper Bonze valley. The matrix of the pillows comprises white mica, zoisite and quartz. Colletto Bonze, 2260 m.



PHOTO 3.2. Decimetric blocks of a metabasaltic breccia within a zoisite-rich matrix. Upper Bonze valley, 2340 m.



PHOTO 3.3. Alternance of Mn-rich garnet and glaucophane layers within the transformed metabasalts of the monometamorphic cover complex. Upper Succinto valley, Alpi Solanger, 2245 m.



PHOTO 3.4. Quartzitic and zoisite-rich metasediments related to the metabasalts of the monometamorphic cover sequences. The mafic blocks within the metasediments show the same chemical pattern as the metabasalts. South face of Bec delle Strie, 2300 m.

Plate IV - Eo-Alpine fabric of glaucophane eclogites

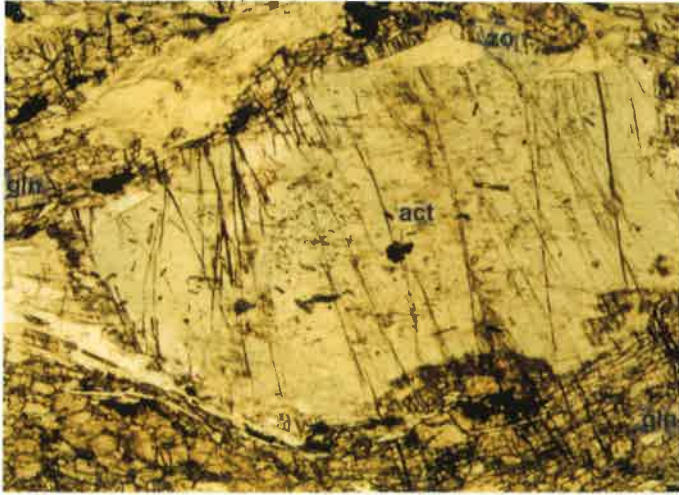


PHOTO 4.1. Photomicrograph of an actinolite porphyroblast. The foliation is defined by zoisite, glaucophane and minor Mg-chlorite. MB16, plane



PHOTO 4.2. Prograde mylonitic glaucophanic foliation cut by omphacite and garnet veins. Eastern face of Cima di Bonze, upper Scalario valley, 2400 m

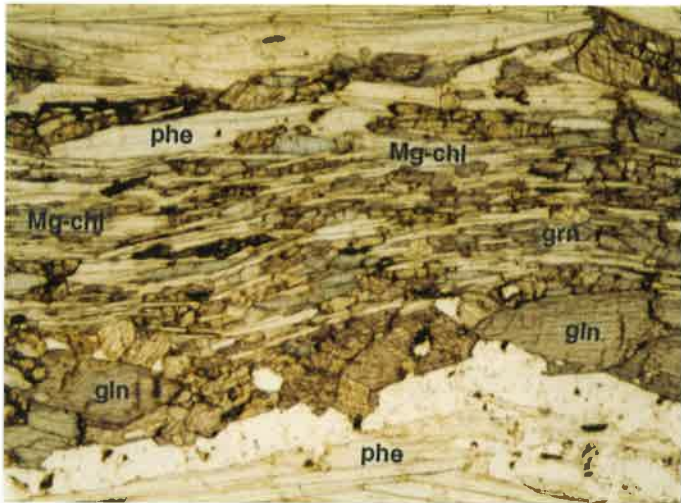


PHOTO 4.3. Photomicrograph of the Alpine prograde foliation defined by Mg-chlorite (Mg-chl), glaucophane (gln), first generation of garnet (grn) and phengite (phe) Sv919b, plane polarized light, 6X

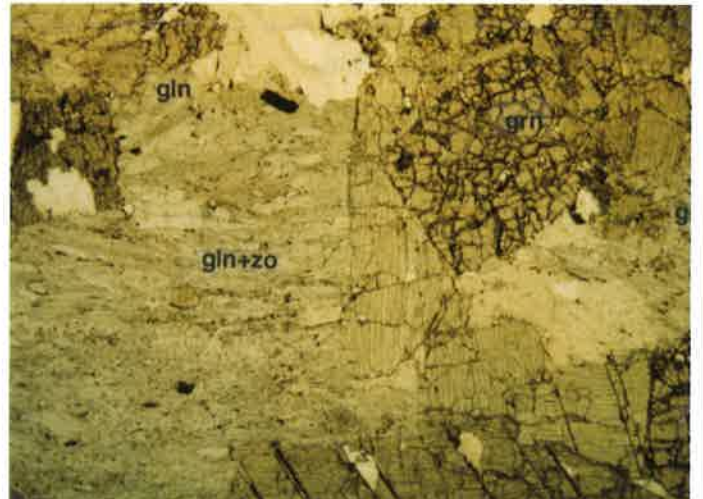


PHOTO 4.4. Photomicrograph of mylonitic prograde foliation crosscut by omphacite and garnet porphyroblasts. gln = glaucophane, zo = zoisite grn = garnet. MB24, plane polarized light, 20X

Plate V/a - Blastomylonitic metagabbros



PHOTO 5.1. Mylonitic metagabbros with scattered relics of magmatic hornblende (dark spots within the sample) (sample sv914b) South face of Cima di Bonze, upper Scalario valley, 2370 m.



PHOTO 5.2. Mylonitic metagabbro with a preserved magmatic texture. The primary assemblage is partially replaced by Alpine high pressure phases. Alpe Moriondo superiore, upper Succinto valley, 2160 m.

Plate V/b - Blastomylonitic metagabbros

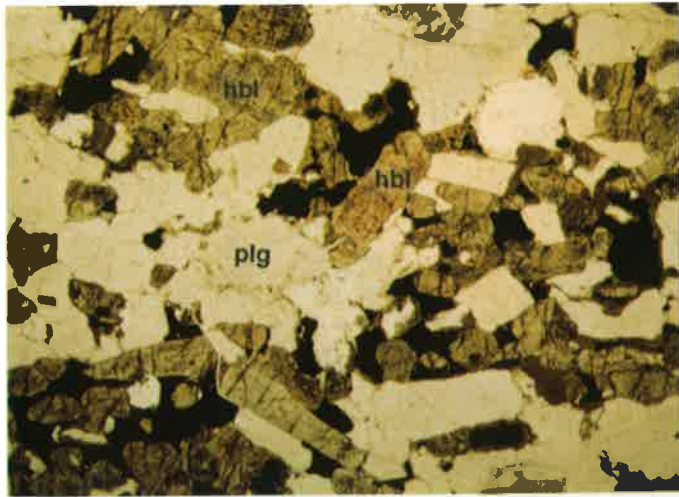


PHOTO 5.3. Photomicrograph of the Sermenza valley gabbro. Magmatic minerals are perfectly preserved. This sample provided the zircons dated by F. Bussy. (see conclusions). plg = plagioclase; hbl = hornblende Sermenza valley, middle Anzasca valley.

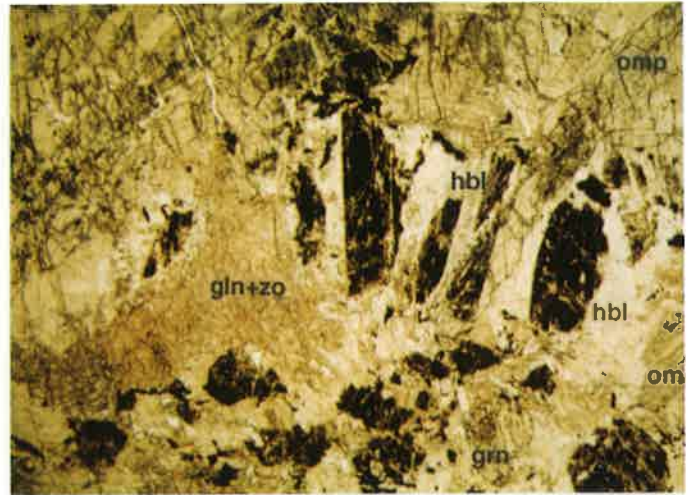


PHOTO 5.4. Magmatic hornblende relics within a mylonitic metagabbro. The dark colour is given by sagenitic rutile. The hornblende is partially replaced by Ca-actinolite and glaucophane. hbl = hornblende; gln+zo = glaucophane + zoisite; grn = garnet; omp = omphacite

Plate VI - Dolomitic marbles



PHOTO 6.1. Metric dolomitic marble in contact with the metabasalts of the monometamorphic cover sequences. Balma Nera, Scalero valley,



PHOTO 6.2. Metric-scale interbedding of dolomitic marbles and glaucophanic metabasalts. The lithologic repetition, whereas strongly transposed, of these two lithologies could be interpreted as the result of mafic doleritic intrusions in the dolomitic marbles. Upper Bonze valley, 2160 m .



PHOTO 6.3. Folded dolomitic marble in the Mombarone lake area. Northern side of the lower Aosta valley, 2350 m .



PHOTO 6.4. Refolded dolomitic marble in the Cavalcourt area within a leucocratic gneiss. Southern side of the lower Aosta valley, 2350 m .

Plate VII - Quartz -rich marbles and calcschists



PHOTO 7.1. Decimetric outcrop of gray calcschists and impure marbles alternating with impure dolomitic marbles Quincinetto region



PHOTO 7.3. Strongly deformed and refolded layers of dolomitic marbles within the calcschists of the monometamorphic cover sequences Balma Nera,



PHOTO 7.2. Metric transition from impure quartzites to calcschists. The lithologic boundary is marked by a change in colour due to a differential alteration. Upper Scalario valley, Cavalcourt region 2275 m.



PHOTO 7.4. Decimetric brownish clasts of pre-Alpine basement paragneisses within the detritic calcschists of Col Fênêtre. Croix Courma region, northern side of Col Fênêtre, 1690 m.

Plate VIII/a - Mn-rich calcschists and conglomeratic calcschists **Plate IX- Quartzites, impure quartzites, mesocratic gneisses and metaconglomerates**



PHOTO 8.1. Mn-rich calcschist. Dark spots represent a spessartine-calcite±phengite assemblage. Cima di Bonze region



PHOTO 8.2. Dolomitic marble breccias in the calcschists of the monometamorphic cover sequences Middle Chiuella valley Colle del Prà 2416 m.

Plate VIII/b - Mn-rich calcschists and conglomeratic calcschists **Plate IX- Quartzites, impure quartzites, mesocratic gneisses and metaconglomerates**



PHOTO 8.3. Spessartine-calcite boudins within the calcschists of the monometamorphic cover sequences Calvalcort region 2210 m .

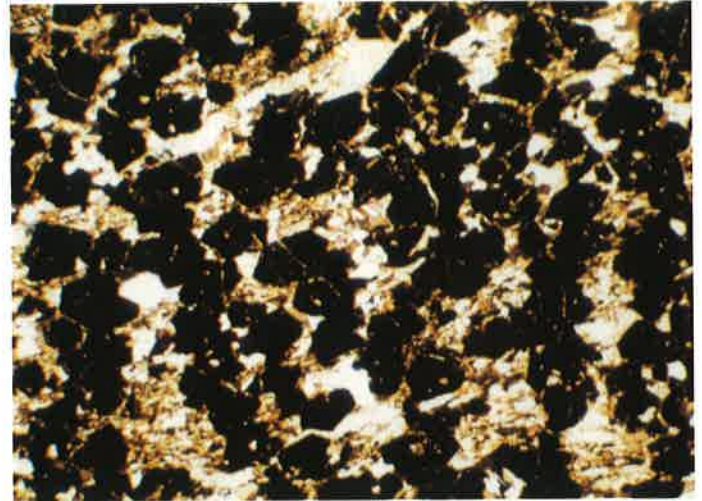


PHOTO 8.4. Photomicrograph of the spessartine-calcite levels in the calcschists of the monometamorphic cover sequences Cross nicols light, 20X (sv9115vc)

Plate IX- Quartzites, impure quartzites, mesocratic gneisses and metaconglomerates



PHOTO 9.1. Metric alternance of pure quartzites (white levels), impure quartzites (yellowish horizons) and graphitic metapelites. This sequence underlies metric to decametric-quartz-rich marbles and calcschists. North face of Cima di Bonze upper Bonze valley, 2360 m.



PHOTO 9.2. Elongated centimetric quartzite boudins or clasts within a mesocratic gneissic matrix probably derived from a conglomerate. South-western face of Croix Courma lower Aosta valley, 1650 m.



PHOTO 9.3. Metric-scale alternance of mafic levels, impure quartzites and yellow dolomite-ankerite marbles within the mesocratic gneisses (gneiss pipernoïdes) Cavalcort area, 2180 m. (stop 2 of par. 2.6.2)



PHOTO 9.4. Decimetric clasts of metagranites within supposed Permo-Triassic metaconglomerates. South face of Croix Courma, east of Verale, lower Aosta valley, 1810 m.

Plate X - BSE microphotographs of zoned amphiboles, garnets and pyroxenes

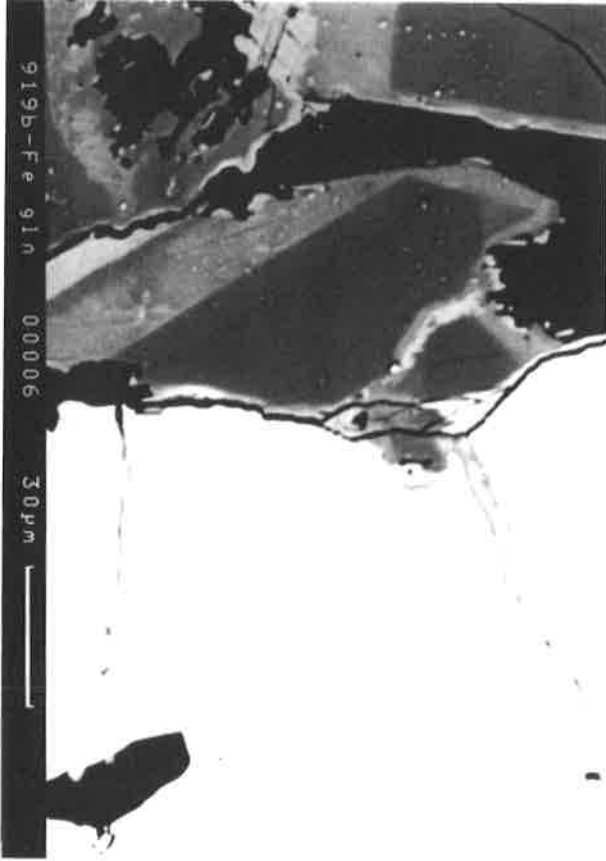


PHOTO 10.1. Small-grained glaucophane in contact with a garnet. The pale rim of the amphibole results from a relative Fe²⁺ enrichment. The garnet-amphibole geothermometer was calculated using the composition of the core of the glaucophane. Sample sv919b

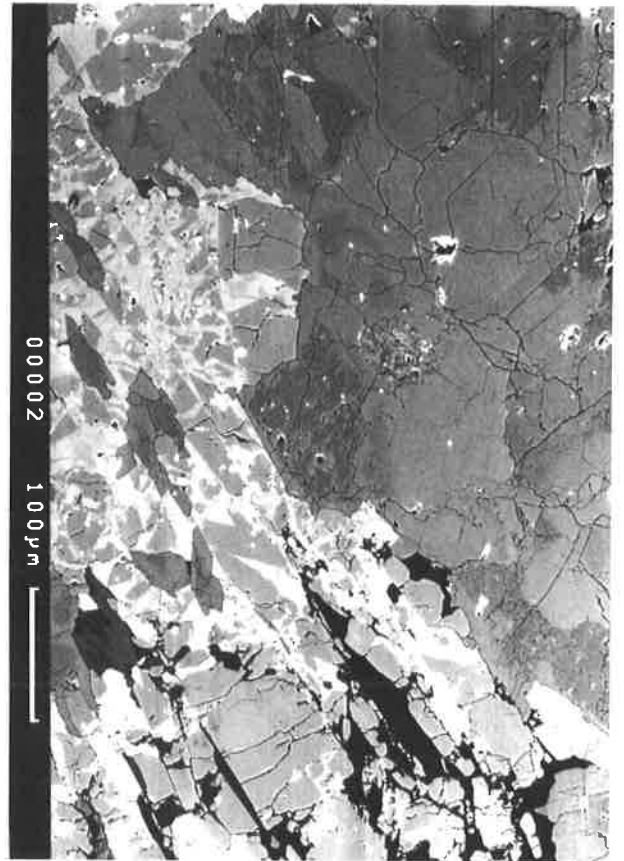


PHOTO 10.2. BSE photograph of a porphyroblast of actinolite surrounded by a foliated aggregate of glaucophane and zoisite/clinozoisite. Light colours indicate iron-rich phases. The actinolite (in the left-upper part of the photo) contains regions partially enriched in Ca (deep gray regions). The glaucophane defining the foliation is weakly zoned, and zoisite is always rimmed by clinozoisite. (sample MB16)

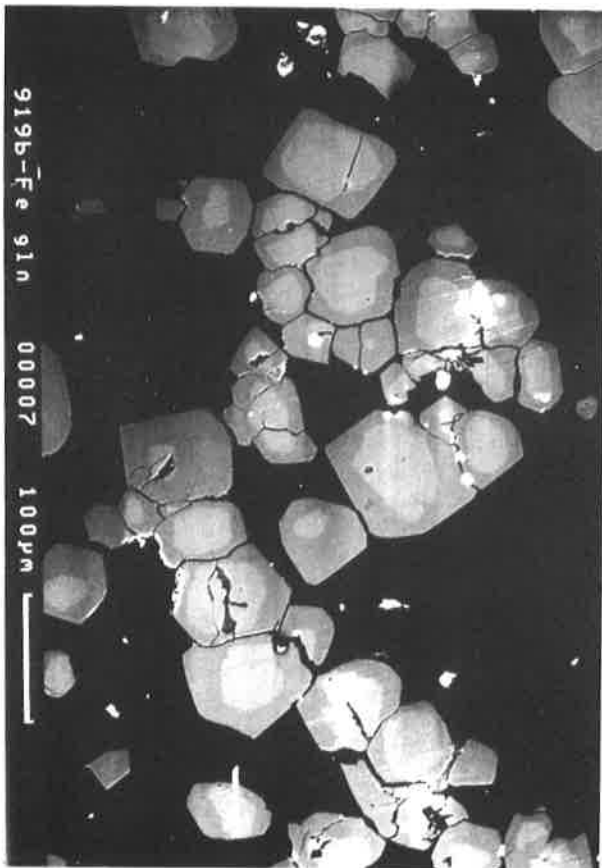


PHOTO 10.3. Zoned garnets characterised by Fe-rich core and a Ca-rich edge. This zonation is inverted, according to Spear and Sliverstone (1983). The dark matrix is composed of glaucophane, zoisite and mica. (Sample sv919b)



PHOTO 10.4. The zoned edge of an omphacite (dark phase in the upper part of the photo) at its contact with an almandine-rich garnet. The core of the pyroxene is characterised by an enrichment in the jadeite component. (Sample sv915q)

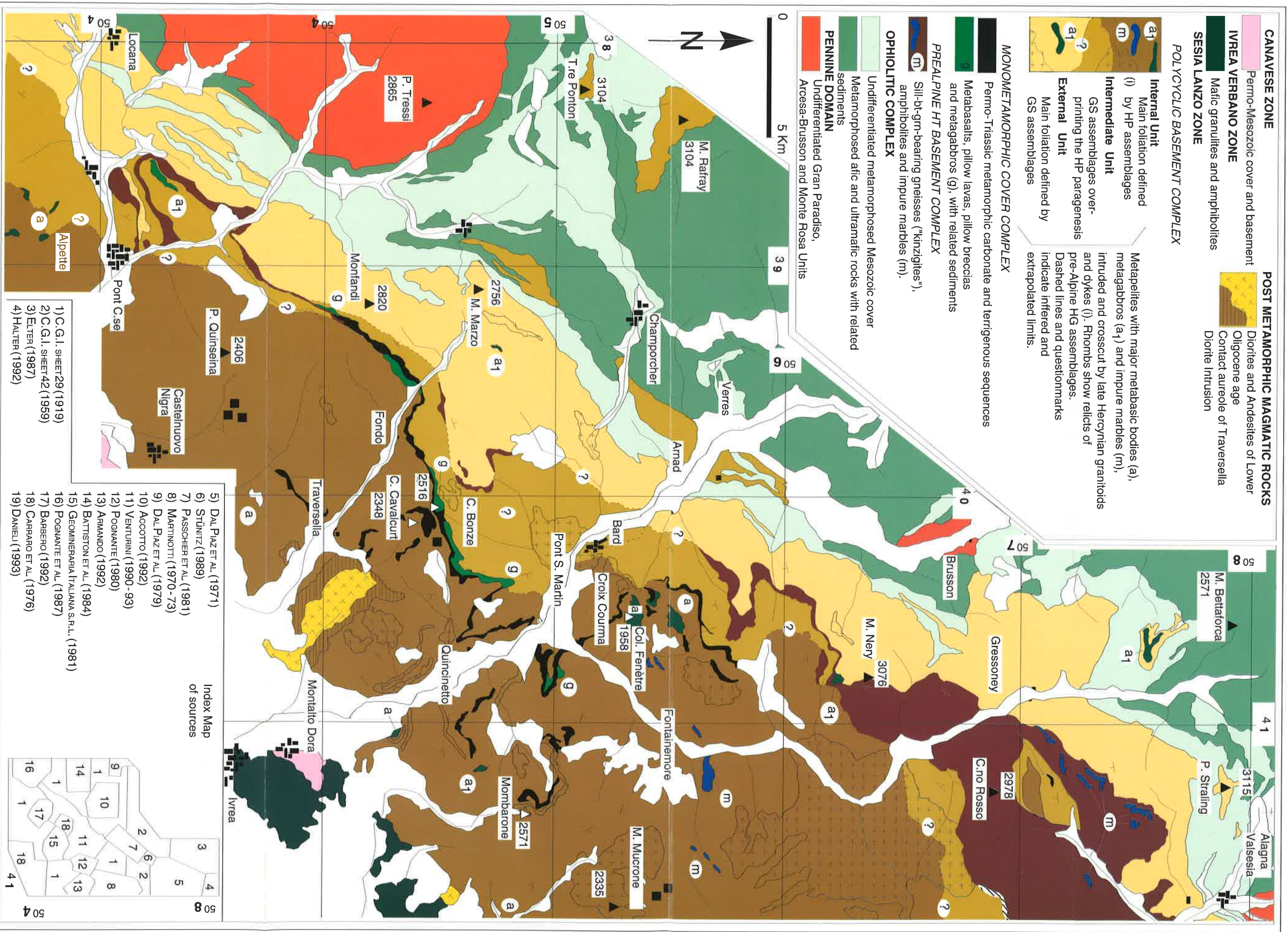


Plate 1 - Geological interpretative map of the central Sesia zone (modified after Venturini et al., 1994).

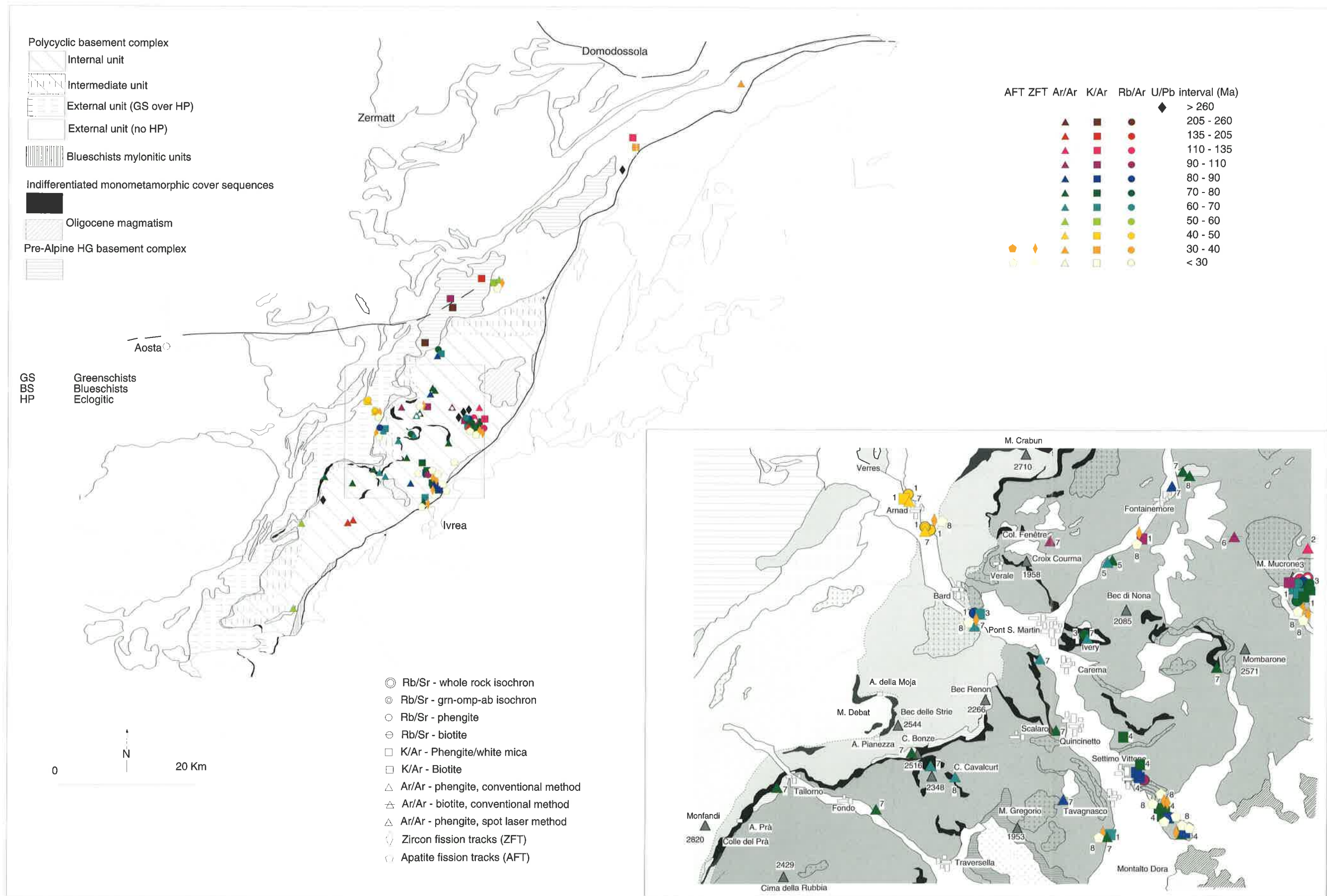


Plate 2a - Compilation of the available geochronological data for the Sesia zone. Data from Hunziker (1974), Hy (1984) Oberhänsli et al., (1985), Stöckhert et al. (1986), Stöckhert (1989), Hurford et al. (1991), Hunziker et al. (1992), Ruffet et al., (1993; 1994), Kelly et al. (1994), Inger and Cliff (1994), Venturini et al., (1994b, this work). Plate 2b- Available geochronological data for the lower Aosta valley sector of the Sesia zone. Source of data: 1) Hunziker (1974), 2) Hy (1984), 3) Oberhänsli et al., (1985), 4) Stöckhert et al. (1986), 5) Ruffet et al., (1993; 1994), 6) Kelly et al. (1994), 7) Venturini et al., (1994b, this work), 8) Hurford et al. (1991), 9) Inger and Cliff (1994).

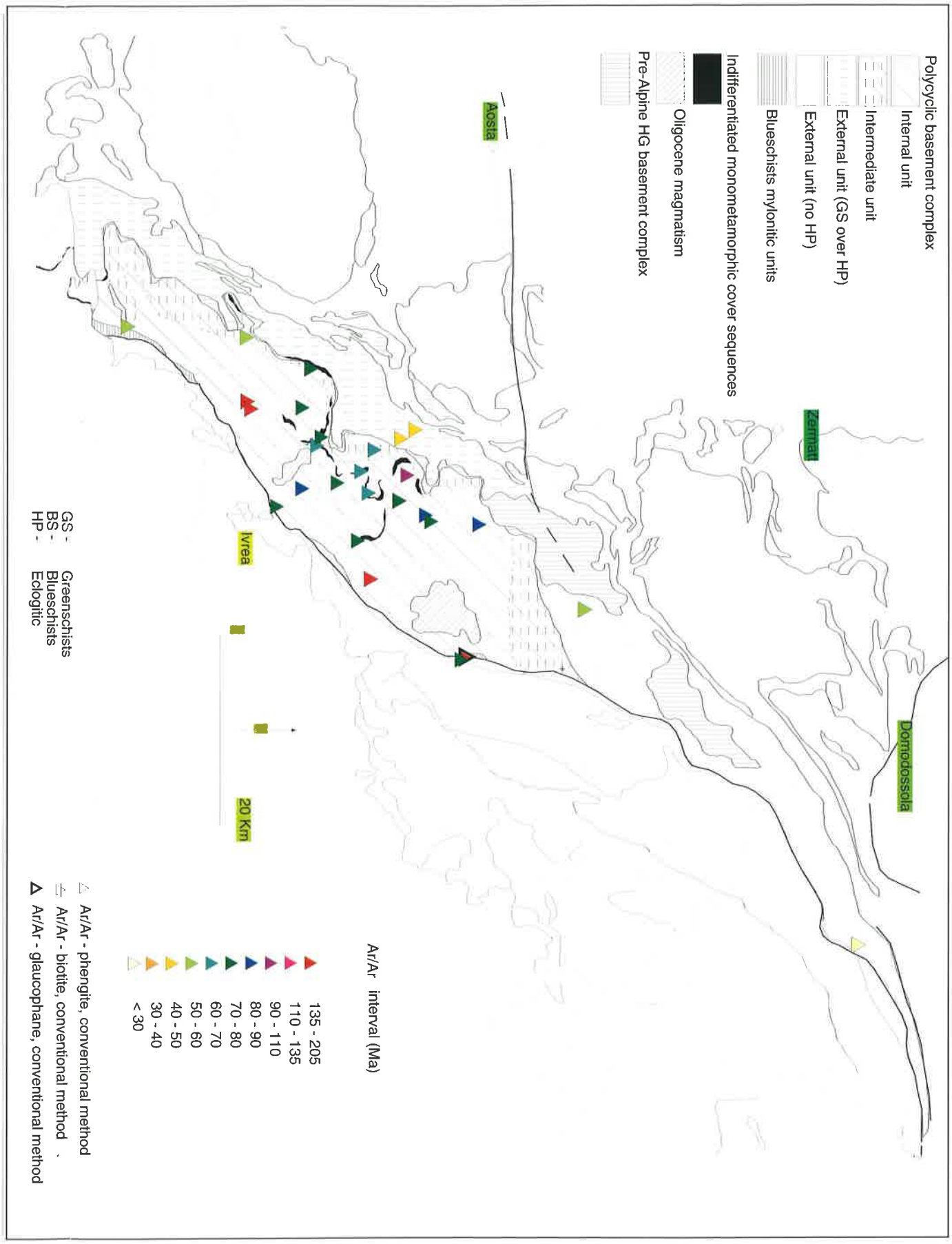
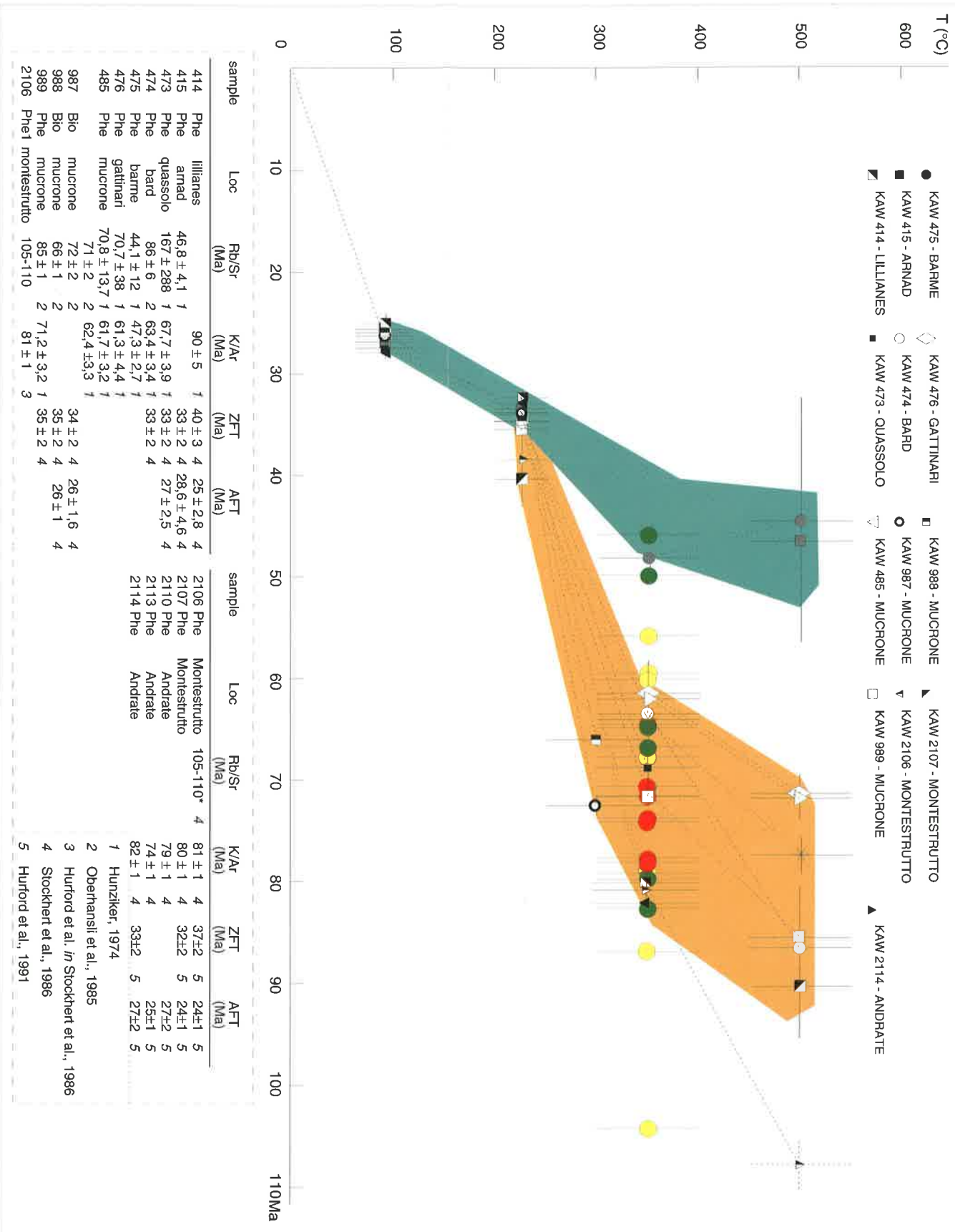


Plate3a - Location of the $^{40}\text{Ar}/^{39}\text{Ar}$ age determinations carried out in this work. Samples labelled KAW where collected by J.C. Hunziker, while samples SV where collected during this study. Plate3b - Different cooling paths from the internal and external units of the Sesia zone reconstructed on the basis of the available data. Coloured circles represent the $^{40}\text{Ar}/^{39}\text{Ar}$ age determinations carried out in this work, which are superposed to the previous K/Ar ages. Red circles = reliable ages; green circles = reasonable ages; yellow circles = possible ages. Deep gray = cooling trajectory of the internal Sesia zone; Slight gray = cooling path of the external Sesia zone.



Mémoires de Géologie (Lausanne)

- No. 1 BAUD A. 1987. Stratigraphie et sédimentologie des calcaires de Saint-Triphon (Trias, Préalpes, Suisse et France). 202 pp., 53 text-figs, 29 pls.
- No. 2 ESCHER A., MASSON H. and STECK A. 1988. Coupes géologiques des Alpes occidentales suisses. 11pp., 1 text-figs, 1 map.
- No. 3 STUTZ E. 1988. Géologie de la chaîne de Nyimaling aux confins du Ladakh et du Rupshu (NW-Himalaya, Inde) - évolution paléogéographique et tectonique d'un segment de la marge nord-indienne. 149 pp., 42 text-figs, 11 pls.
- No. 4 COLOMBI A. 1989. Métamorphisme et géochimie des roches mafiques des Alpes ouest-centrales (géoprofil Viège-Domodossola-Locarno). 216 pp., 147 text-figs, 2 pls.
- No. 5 STECK A., EPARD J.-L., ESCHER A., MARCHANT R., MASSON H. and SPRING L. 1989. Coupe tectonique horizontale des Alpes centrales. 8 pp., 1 map.
- No. 6 SARTORI M. 1990. L'unité du Barrhorn (Zone Pennique, Valais, Suisse). 140 pp., 56 text-figs, 3 pls.
- No. 7 BUSSY F. 1990. Pétrogenèse des enclaves microgrenues associées aux granitoïdes calco-alcalins: exemple des massifs varisque du Mont-Blanc (Alpes occidentales) et miocène du Monte Capanne (Ile d'Elbe, Italie). 309 pp., 177 text-figs.
- No. 8 EPARD J.-L. 1990. La nappe de Morcles au sud-ouest du Mont-Blanc. 165 pp., 59 text-figs.
- No. 9 PILLLOUD C. 1991. Structures de déformation alpines dans le synclinal de Permo-Carbonifère de Salvan-Doréaz (massif des Aiguilles Rouges, Valais). 98 pp., 59 text-figs.
- No. 10 BAUD A., THÉLIN P. and STAMPFLI G. (Eds) 1991. Paleozoic geodynamic domains and their alpidic evolution in the Tethys. IGCP Project No. 276. Newsletter No. 2, 155pp.
- No. 11 CARTER E. 1993. Biochronology and Paleontology of uppermost Triassic (Rhaetian) radiolarians, Queen Charlotte Island, British Columbia, Canada. 132 pp., 15 text-figs, 21 pls.
- No. 12 GOUFFON Y. 1993. Géologie de la «nappe» du Grand St-Bernard entre la Doire Baltée et la frontière suisse (Vallée d'Aoste - Italie). 147 pp., 56 text-figs, 3 pls.
- No. 13 HUNZIKER J. C., DESMONS J. and HURFORD, A.J. 1992. Thirty-two years of geochronological work in the Central and Western Alps: a review on seven maps. 59 pp., 18 text-figs, 7 pls.
- No. 14 SPRING L. 1993. Structures gondwaniennes et himalayennes dans la zone tibétaine du Haut Lahul-Zaskar oriental (Himalaya indien). 148 pp., 66 text-figs, 1 pls.
- No. 15 MARCHANT R. 1993. The Underground of the Western Alps. 137 pp., 104 text-figs.
- No. 16 VANNAY J. C. 1993. Géologie des chaînes du Haut-Himalaya et du Pir Panjal au Haut-Lahul (NW Himalaya, Inde). 148 pp., 44 text-figs, 6 pls.
- No. 17 PILLEVUIT A. 1993. Les Blocs Exotiques du Sultanat d'Oman: Evolution paléogéographique d'une marge passive flexurale. 249 pp., 138 text-figs, 7 pls.
- No. 18 GORICAN S. 1994. Jurassic and Cretaceous radiolarian biostratigraphy and sedimentary evolution of the Budva Zone (Dinarides, Montenegro). 120 pp., 20 text-figs, 28 pls.
- No. 19 JUD R. 1994. Biochronology and systematics of Early Cretaceous radiolaria of the Western Tethys. 147 pp., 29 text-figs, 24 pls.
- No. 20 DI MARCO G. 1994. Les terrains accretés du sud du Costa Rica. Evolution tectonostratigraphique de la marge occidentale de la plaque Caraïbe. 166 pp., 35 text-figs, 73 pls.
- No. 21 O'DOGHERTY L. 1994. Biochronology and paleontology of middle Cretaceous radiolarians from Umbria-Marche Apennines (Italy) and Betic Cordillera (Spain). 415 pp., 35 text-figs, 73 pls.
- No. 22 GUEX J. and BAUD A. (Eds) 1994. Recent developments on Triassic Stratigraphy. 184 pp.
- No. 23 INTERRAD, Jurassic-Cretaceous Working Group. BAUMGARTNER P.O. et al. (Eds) 1994. Middle Jurassic to lower Cretaceous Radiolaria of Tethys: occurrences, Systematics, Biochronology. env 900 pp., 400 pls.
- No. 24 REYMOND B. 1994. Three-dimensional sequence stratigraphy offshore Louisiana, Gulf of Mexico (West Cameron 3D seismic data). 215 pp.
- No. 25 VENTURINI G. 1995. Geology, Geochemistry and Geochronology of the inner central Sesia Zone (Western Alps - Italy). 183 pp., 57 text-figs, 12 pls.

Order from **Institut de Géologie et Paléontologie,**
Université de Lausanne, BFSH-2. CH-1015, SWITZERLAND.
Bank Transfer: Banque Cantonale Vaudoise 1002 Lausanne
Account Number: **C.323.52.56** Institut de Géologie, rubrique: Mémoires

Price \$20 or CHF 30 per volume (volume 23: price on request) includes postage and handling.
Payment in U.S. Dollars or Swiss Francs

- Please do not send check -